Dissertation

Submitted to the

Combined Faculties of Natural Sciences and Mathematics

of the Ruperto-Carola University of Heidelberg, Germany

For the degree of

Doctor of Natural Sciences

Presented by:

Mareike Grees (M.Sc.)

Born in Essen, Germany

Oral examination: 21st July 2017

Improved dendritic cell vaccination for combined melanoma immune therapy

Referees:

Apl. Prof. Dr. Viktor Umansky

PD Dr. Adelheid Cerwenka

Declaration according to § 8 (3) b) and c) of the doctoral degree regulations:

b) I hereby declare that I have written the submitted dissertation myself and in this process have used no other sources or materials than those expressly indicated,

c) I hereby declare that I have not applied to be examined at any other institution, nor have I used the dissertation in this or any other form at any other institution as an examination paper, nor submitted it to any other faculty as a dissertation.

Heidelberg,

Name (Mareike Grees)

The work described in this thesis was started in January 2014 and completed in May 2017 under the supervision of Prof. Dr. Viktor Umansky at the Research Group “Clinical Cooperation Unit Dermato-Oncology“ of the German Cancer Research Center (DKFZ), Heidelberg and the University Medical Center Mannheim.

I. Publications

OncoImmunology, Vol.5, Issue 6, April 2016

mRNA-based dendritic cell immunization improves survival in ret transgenic mouse melanoma model

Adi Sharbi-Yunger*, Mareike Grees* (shared first authorship), Jochen Utikal, Viktor Umansky, Lea Eisenbach

Conference presentations:

04/2017 **CITIM Conference, Prague, Czech Republic**

Poster presentation

"Combined melanoma immunotherapy using dendritic cell vaccination and paclitaxel in preclinical mouse models"

Mareike Grees, Adi Sharbi Yunger, Lea Eisenbach, Viktor Umansky, Jochen Utikal

02/2017 **EMBL-Cancer Core Europe Conference, Heidelberg, Germany**

Poster presentation

"Novel tumor antigens for dendritic cell vaccination in pre-clinical mouse models"

Mareike Grees, Adi Sharbi Yunger, Lea Eisenbach, Viktor Umansky

05/2016 **CIMT Conference, Mainz, Germany**

Poster presentation

"Melanoma immunotherapy using dendritic cell vaccination in ret-tg mouse model"

Mareike Grees, Adi Sharbi Yunger, Lea Eisenbach, Viktor Umansky

04/2015 **CITIM Conference, Ljubljana, Slovenia**

Poster presentation

" Improving Dendritic cell vaccines for melanoma immunotherapy

Mareike Grees, Adi Sharbi Yunger, Lea Eisenbach, Viktor Umansky"

II. Table of Contents

III. Zusammenfassung

Das maligne Melanom der Haut gehört zu den bösartigsten Tumoren des Menschen, die sich immer noch sehr schwer behandeln lassen. Trotz der intrinsischen Immunogenität, kann das maligne Melanom sehr immunsuppressiv wirken und sich dadurch dem Immunsystem entziehen. Darüber hinaus kann die Entwicklung von Melanom-spezifischen Effektor-T-Zellen durch unzureichende Tumorantigen-Aufnahme, Verarbeitung und Präsentation von Dendritischen Zellen behindert werden. Eine effiziente MHC-Peptid-Komplex Expression auf der DC-Zelloberfläche bestimmt das Ausmaß und die Qualität der T-Zell-Antwort und die maximale Menge an präsentierten Antigenen ist somit ein wichtiger Parameter bei der Konstruktion von DC-basierten Krebsimpfstoffen. Wir haben vor kurzem die Herstellung von Konstrukten, die für die Haupthistokompatibilitätskomplex (MHC), Klasse I-Moleküle kodieren und die Peptidpräsentation mit der Aktivierung von DC koppeln, hergestellt. Diese Modalität war sehr effizient bei der Hemmung des Tumorwachstums und der Verbesserung des Überlebens sowohl bei transplantierbaren als auch bei spontanen präklinischen Melanom Modellen.

Das Ziel dieser Studie war es, einen neuartigen und stärkeren DC-Impfstoff für die Melanom-Immuntherapie auf der Grundlage der kürzlich entwickelten bi-funktionellen Klasse von genetischen mRNA-Krebs-Impfstoffen zu erzeugen. Um die Antitumor-Immunantwort zu erhöhen, weisen diese modifizierten DCs unterschiedliche chimäre MHC-Klasse-I- und MHC-Klasse-II-Rezeptoren auf, um ein multivalenter DC-Impfstoff zu werden, der bei einer gleichzeitigen Präsentation verschiedener Melanom-assoziierter Antigene eine Induktion von CD8+ zytotoxischen- und CD4+ T-Helfer Zellen ermöglicht. Ausgewählte Klasse I und Klasse II Antigene, die von TRP-1 und Tyr abgeleitet wurden, konnten eine starke Immunantwort von CD8+ zytotoxische T-zellen- und CD4+ T-Helfer Zellen hervorrufen. Darüber hinaus haben wir ausgewählte TRP-1 / Tyr-Klasse I und Klasse-II-Rezeptoren auf ihre Fähigkeit hin untersucht, eine *in vivo* Antitumor-Immunantwort in zwei verschiedenen Melanom-Mausmodellen (ret transgen und BRAF) zu induzieren. Überraschenderweise führte eine Co-Elektroporation von MHC-I- und MHC-II-chimären Konstrukten zu keiner Verbesserung des Überlebens bei Melanomen in *ret*-tg-Mäusen. Zusätzlich wurde eine erhöhte Aktivität antigenspezifischer Tregs gemessen, deren Einfluss auf die Immunantwort in weiteren Studien untersucht werden soll.

Im Gegensatz zu diesen Ergebnissen haben wir auch gezeigt, dass bei der Behandlung mit einem mehrwertigen β2m-basierten-DC-Impfstoff, Melanom tragende Mäuse (Ret-tg und BRAF) eine Tumorregression erfahren und das Überleben signifikant verbessert haben. Die Impfung mit chimärem TRP-1 und Tyr-Klasse-I-DC-Impfstoff und insbesondere der Mix

(TRP-1/Tyr)-Impfstoff, hauptsächlich aufgrund seiner multivalenten Eigenschaften, zeigte eine erhöhte Häufigkeit von IFNg+ CD8+ T-zellen, ergänzt durch eine erhöhte, systemische Aktivität von CD8+ T-zellen, sowie eine Erhöhung der CD8+ -Effektor-Gedächtnis-T-Zellen. Wichtig ist, dass diese immunstimulatorischen Effekte keinen stimulierenden Reaktionen auf immunsuppressive Tregs und MDSC gezeigt haben. Schließlich konnten wir Anzeichen von Autoimmunität (Vitiligo) in 3 ret-tg-Mäusen, die mit dem TRP-1 / Tyr-Klasse-I-Mix-DC-Impfstoff behandelt wurden, nachweisen, was einen weiteren Beweis für eine hoch aktivierte Immunantwort darstellt. Unsere Daten deuten darauf hin, dass die Immuntherapie mit einem multivalenten, β2m-basierten-DC-Impfstoff das Überleben von Tumor-tragenden Mäusen signifikant verbessern kann, insbesondere durch die Erhöhung des MAA-Repertoires der DCs. Besonders bei der Kombination mit sehr niedrigen, nicht zytotoxischen Dosen von Paclitaxel wurde die T-Zell-Immunantwort erhöht und durch eine gleichzeitige systemische Reduktion der immunsuppressiven Aktivität von MDSC und Treg noch weiter gesteigert. Diese Ergebnisse deuten auf weitere Vorteile für die kombinierte Immuntherapie, die sich mit unserem verbesserten DC-Impfstoff bietet und in weiteren Studien eingehender untersucht werden soll.

IV. Abstract

Malignant melanoma is known for its fast progression and poor response to current treatments. Despite melanoma immunogenicity, tumor escape could be due to a profound immunosuppression in the melanoma microenvironment. Moreover, the development of melanoma-specific effector T cells may be hampered by insufficient tumor antigen delivery, processing and presentation of dendritic cells (DCs). Efficient MHC-peptide complex expression on the DC cell surface determines the degree and quality of the T cell response and the maximal amount of presented antigenic peptides is thus a key parameter in the design of DC-based cancer vaccines. We have recently established the production of constructs encoding the major histocompatibility complex (MHC) class I molecules that couples the peptide presentation and activation of DC. This modality was highly efficient in inhibiting tumor growth and improving survival, both in transplantable and spontaneous preclinical melanoma models.

The goal of this study was to generate a novel and more potent DC vaccine for melanoma immunotherapy based on the recently developed bi-functional class of genetic mRNA cancer vaccines. To enhance the anti-tumor response, these modified DC present different chimeric MHC class I and MHC class II receptors, in order to become a multivalent DC vaccine allowing a simultaneous presentation of different melanoma associated antigens (MAA) of choice for induction of $CD8^+$ CTL and $CD4^+$ Th, respectively. Selected class I and class II restricted antigens derived from TRP-1 and Tyr were able to elicit a potent $CD8^+$ CTL and $CD4^+$ Th response. Furthermore, we studied selected TRP-1/Tyr- class I and class II receptors for their *in vivo* capacity to induce antitumor immune response in two different melanoma mouse models (*ret* transgenic and BRAF). Unexpectedly, co- electroporation of MHC-I and MHC-II chimeric constructs did not improve survival in melanoma bearing ret tg mice, probably due to increased activity of antigen-specific Tregs, which will be investigated in further studies.

In contrast to these results, we also demonstrated that melanoma-bearing mice (*ret*-tg and BRAF) experienced tumor regression and significantly improved survival upon treatment with multivalent β2m-based-DC vaccine. Vaccination with chimeric TRP-1 and Tyr class I- β 2m DC vaccine and in particular the Mix-(TRP-1/Tyr)- β2m DC vaccine, mainly due to its multivalent properties, demonstrated increased frequency of IFNγ producing $CD8^+$ T cells, complemented by increased, systemic CD 8^+ T cell activity as well as an increase of $CD8^+$ effector memory T cells. Importantly, these immune-stimulatory effects were found without any stimulatory effects on immunosuppressive Tregs and MDSC. Finally, we could detect signs of autoimmunity (vitiligo) in 3 *ret*-tg mice treated with TRP-1/Tyr class I-Mix DC

vaccine, providing further evidence of increased immune stimulation. Our data suggest that immunotherapy with multivalent β2m-based-DC vaccine can significantly improve the survival of tumor bearing mice, especially by increasing the MAA-repertoire presented by the DCs. Notably, upon combination with ultra-low dose of paclitaxel T cell dependent immunity was even further enhanced by concomitant systemically reduction of immunosuppressive activity of MDSC and Treg, further providing rational for advantages in combined immunotherapy with our improved DC vaccine which will be investigated in more detail in future studies.

1 Introduction

1.1 The immune system

The immune system consists of cells, tissues and organs and is responsible for the detection and protection of various foreign pathogens like viruses, bacteria, fungi, parasites and tumors. It distinguishes between own healthy tissue and non-self or altered self-structures. The defense mechanism of the immune system is based on detecting structural features of the invading pathogens. It recognizes attacks and kills pathogen, which can adapt in order to escape the immune system. Parts of the immune system also play a role in case of auto-immune and cancer diseases and allergy[1]. In vertebrates, there are two arms of the immune system: the innate immune system, which is responsible for a broad spectrum of unspecific, pathogen structures, and the adaptive immune system, which is specific for particular non-self-antigens[2].

1.1.1 The innate immune system

The innate immune system is naturally hereditary and serves as the first defense against pathogens with the epithelial barrier. This part of the system does not need a sensitization to antigens. The innate immune system consists of the following cells: granulocytes, macrophages, dendritic cells, natural killer cells and plasma proteins called the complement system.

The recognition of an infectious agent is based on germline-encoded receptors. These receptors are called pattern recognition receptors (PRR) and recognize pathogen-associated molecular patterns (PAMPS). These PAMPS are conserved repeating patterns from microorganisms, e.g. lipopolysaccharide (LPS) of gram-negative bacteria, lipoteichoic acid (LTA) of gram-positive bacteria, mannose and glycan of fungi, bacterial CpG DNA or double-stranded viral RNA. The best characterized PRRs are toll-like receptors (TLR)[3–5]. Their activation leads to pathogen uptake by phagocytic cells. As a result of the uptake, the phagocytic cells secret pro-inflammatory cytokines and chemokines which are important for the recruitment of other immune cells[5]. The most efficient phagocytic cells are dendritic cells (DCs). After pathogen uptake they mature, migrate to the local lymph nodes where they secret factors that are important for the innate immune response and induce the adaptive immune response. So they connect the innate with the adaptive immune system[6,7].

1.1.2 **The adaptive immune system**

The adaptive immune system needs to be activated by the innate immune system. It is categorized in the cellular and humoral immunity. Cellular immunity consists of T cells with antigen-specific TCR that recognize short antigen fragments bound to MHC molecules. The humoral immunity consists of B cells that express antigen-specific receptors that recognize antigenic determinants. The receptors of T cells and B cells are random products of somatic gene rearrangement during maturation[8].Extracellular pathogens are recognized by B cells that originate from the bone marrow (BM). During the maturation they express membrane bound immunoglobulins (B cell receptor, BCR). After activation they differentiate into either memory or antibody-secreting plasma cells. Intracellular pathogens are detected by T cells via cell-mediated immune response. T cells are generated in the BM and migrate to the thymus for their maturation. T cell receptors recognize peptides only when they are presented by MHC molecules. $CD8^+$ T cells can bind to MHC class I, whereas $CD4^+$ T cells bind to MHC class II. For the complete activation, T cells need costimulatory signals from antigen presenting cells (APC). The effectors cells then undergo either apoptosis or built the immunological memory that is responsible for a rapid reinduction of the memory cells after the reentering of the same pathogen[9]. This immunological memory is often a long lasting or lifelong protection against diseases[9].

1.2 Dendritic cell biology

As previously mentioned, DCs are antigen-presenting cells of the mammalian immune system and act as messengers between the innate and the adaptive immune systems[10]. DCs are present in those tissues that are in contact with the external environment, such as the skin and the inner lining of the nose, lungs, stomach and intestines[7]. They can also be found in an immature state in the blood. Once activated, they migrate to the lymph nodes where they interact with T cells and B cells to initiate and shape the adaptive immune response[6]. DCs arise from hematopoietic progenitors of the BM and circulate through the blood, peripheral tissues and lymphoid tissues The majority of DCs are derived from $CD34^+$ myeloid progenitors which differentiate into myeloid DC (mDCs) (also referred to as conventional DCs), while the rest of them from lymphoid progenitors, which differentiate into plasmacytoid DC (pDCs)[11–13]. DCs express several PRR (e.g. TLR), which endow them with the capacity to recognize PAMPs of microbial products. pDCs are mainly responsible for the recognition of viruses or host-derived nucleic acid-containing complexes via TLR7 and TLR9, producing large amounts of type I Interferons (IFN). On the other hand, mDCs express TLR2 and TLR4 on their surface, which bind several bacteria-derived products, producing high amounts of IL-12[6].

Circulating immature DCs are characterized by high endocytic and phagocytic capacity, which is needed for efficient capture of invading pathogens or their constituents (**Fig.1**)[14]. Upon antigen recognition, DCs maturate and release a variety of pro-inflammatory and anti-viral cytokines, leading to migration and activation of several cell subsets of the innate immunity at the site of infection[15]. Additionally, mature DCs overexpress MHC class I and II, costimulatory molecules like CD80, CD86, and CD40, as well as adhesion molecules (e.g. CD54 and CD58) on their surface, which are crucial for efficient priming of antigen-specific T cells and their differentiation into effector cells at the local draining lymph nodes (LNs)[7]. Matured DCs also start expressing the chemokine receptor CCR7, which drives their migration towards regional LNs in response to chemotactic gradients of its ligands CCL19 and CCL21 that are expressed by lymphatic vessels and lymph node (LN)-residing cells[7,13]. Of note, the particular TLRs that are engaged at the DC surface polarize the ensuing adaptive response toward the T_h1, T_h2, T_h17 or the regulatory T cell subsets. For instance, ligation of TLR4 leads to secretion of IFN-γ, TNF, and IL-12, inducing strong T_h1 responses[164]. In addition to their role in polarizing T helper cell immune responses, they are also crucial in regulating NK and B cell functions, but also in controlling the balance between immunity and tolerance, as shown in **Fig.2**[10]. DCs are therefore considered to be the most important and potent APCs, representing a bridge between the innate and adaptive immunity and orchestrating the immune responses [6,17,18].

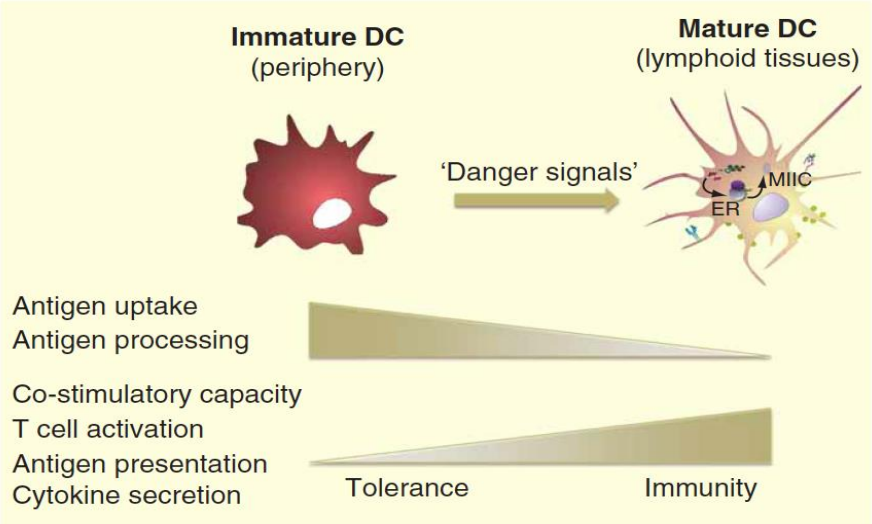

Fig. 1: Main characteristics of immature and mature dendritic cells[14]

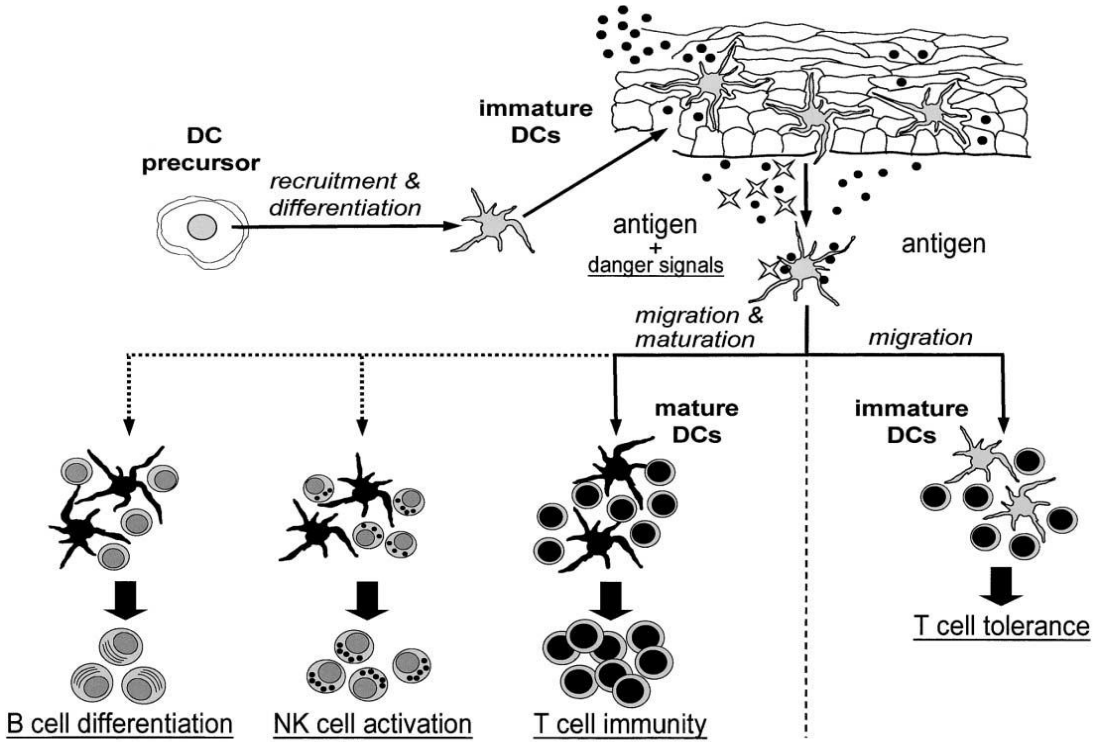

Fig. 2: Integrated view of DC immunobiology. DCs are derived from either myeloid or lymphoid bone marrow progenitors through intermediate DC precursors and they differentiate into immature DCs. After antigen uptake in the presence of maturation signals associated with inflammation or infection, immature DCs are activated by TLRs, IFNs, or members of TNF-R family and undergo a complex maturation process, accompanied by their CCR7-driven migration towards lymphoid organs, where they present antigen-derived peptides to antigen-specific T cells and direct their differentiation into T effector or memory cells. Furthermore, mature DCs can induce NK cell activation, as well as B cell differentiation into antibody-producing cells. On the other hand, antigen capture in the absence of activation stimuli may lead to the induction of T cell tolerance, due to antigen presentation by immature DCs in the absence of costimulation.[10]

Antigens presented by DCs can be either endogenous or exogenous, depending on how they enter into the cells (**Fig.3**). Exogenous antigens are taken up and processed in endosomes followed by presentation of generated peptides on the cell surface bound to MHC II molecules, activating antigen-specific $CD4^+$ T cells. Intracellular endogenous antigens are produced in the cytoplasm of DCs and degraded into peptides in the cytosol followed by presentation of the peptides on DC surface bound to MHC I molecules, activating antigen-specific $CD8^+$ T cells. However, DCs have also the ability to present exogenous antigens (such as from apoptotic or necrotic tumor cells) on MHC I molecules via cross-presentation to activate antigen-specific $CD8^+$ T cells, which is important for the induction of anti-tumor cytotoxic T cell immune responses [18–20]

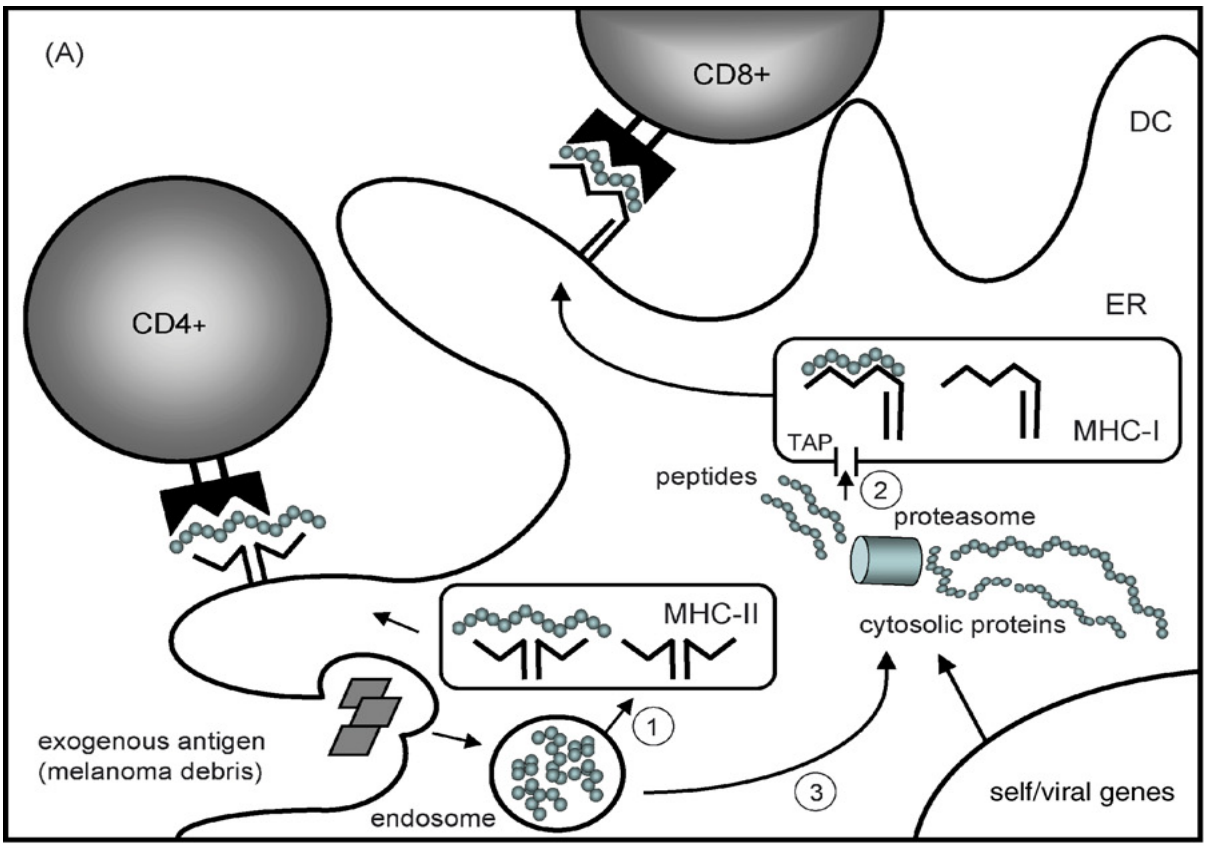

Fig. 3: Mechanisms of antigen processing by the DC. Exogenous antigens are internalized by DCs and enter the endocytic pathway in which they are targeted to lysosome-related MHC class II-rich compartments. In these compartments the antigens are degraded and loaded onto MHC class II molecules. During maturation of the DC the MHC-peptide complexes are released to the surface, thus making the cell ready for antigen presentation to $CD4^+$ T helper cells (route 1 in the figure). Intracellular endogenous antigens, such as unstable self-proteins or viral proteins, are cleaved into peptides in the proteasome and subsequently translocated into the lumen of the endoplasmatic reticulum (ER) by transporters associated with antigen processing (TAP), where stable MHC class I-peptide complexes are assembled. Upon binding of the peptide, the complex is released from the endoplasmatic reticulum and transferred to the cell surface (route 2 in the figure), where it is presented to $CD8^+$ cytotoxic T cells. Lastly, DC have the unique capacity to present exogenous antigens, such as necrotic or apoptotic tumor cells, in MHC class I to cytotoxic T cells, a process referred to as cross presentation (route 3 in the figure)[19].

1.3 Malignant Melanoma

Malignant melanoma is an aggressive malignancy of transformed melanocytes that is resistant to standard therapy, e.g. chemo- or radiotherapy. In the United States, melanoma is the fifth and sixth most common type of cancer in males and females expected to be diagnosed in 2016[21]. Only 5 % of all skin cancers account for melanoma, but it is responsible for 90 % of skin cancer deaths. In terms of incident, malignant melanoma is the most rapidly increasing malignancy in Western population[22] due to improved life standard, e.g. travelling to sunny resorts and get tanned and due to the higher life average of the people. Mostly effected are young and middle-aged Caucasians triggered by solar UV radiation, fair skin, red or blond hairs, blue eyes or family history of melanoma[23]. Melanoma arises from the transformation of melanin-producing melanocytes in the skin and rarely in non-cutaneous melanocytes like retina or mucosal surfaces. Patients suffering from melanoma can be divided into different groups according to the TNM classification. This classification considers the size of the tumor, the affection of LN and metastasis[22]. Stage I is an invasive melanoma and tumor cells spread in situ. In stage II, when the tumor size is 1.5 mm or bigger, patients have a 5-year survival rate of 45-79%. When the tumor starts to metastasize into regional LN and the skin, patients are in stage III. Stage IV is classified when the tumor cells from distant metastases spread through the peripheral blood, and lymphatic system into the brain, lung, liver, skin and BM[22,24].If melanoma is diagnosed early (stages I or II), most patients have a good prognosis, albeit with a significant risk of relapse. On the other hand, treatment options for metastatic disease are still limited and the prognosis of advanced melanoma remains very poor with a median survival of less than one year. After the standard therapy of stage III and IV melanoma, there is a 50–90% risk of recurrence in clinically disease-free patient[25].

There are some gene mutations involved in melanoma development. Mutations in BRAF or NRAS genes promote the proliferation of melanoma cells since these genes are important for the MAP-kinase signaling pathway. Approximately 40-60% of melanomas contain a mutation in the gene that encodes BRAF that leads to constitutive activation of downstream signaling in the MAP kinase pathway. In 80-90% of these cases, the activating mutation consists of the substitution of glutamic acid for valine at amino acid 600 (V600E)[24,26]

1.4 Immunogenicity versus immunosuppression in melanoma

Melanoma is one of the most immunogenic solid malignancies, inducing both innate and adaptive immune responses since it is often found to be heavily infiltrated by immune cells[27,28] One offered explanation of the immunogenicity of melanoma is due to the overexpression of several melanocyte differentiation antigens such as melanoma-associated antigen 1 (MAGE-1), gp100, tyrosinase (Tyr), tyrosinase related protein-1 (TRP-1), TRP-2, and MART-1/MelanA, which are the main target of spontaneous anti-melanoma immune responses (**Fig.4**).[2930] Therefore, melanoma has been considered as a prime target for immunotherapeutic approaches. However, despite the exceptionally high immunogenicity of melanoma leading to an early enrichment and activation of melanoma-specific $CD8^+$ and $CD4^+$ T cells, it displays a remarkable ability to evade immune responses through a variety of mechanisms, resulting in a rapid progression of the disease and limiting the efficacy of immunotherapy[31–33].

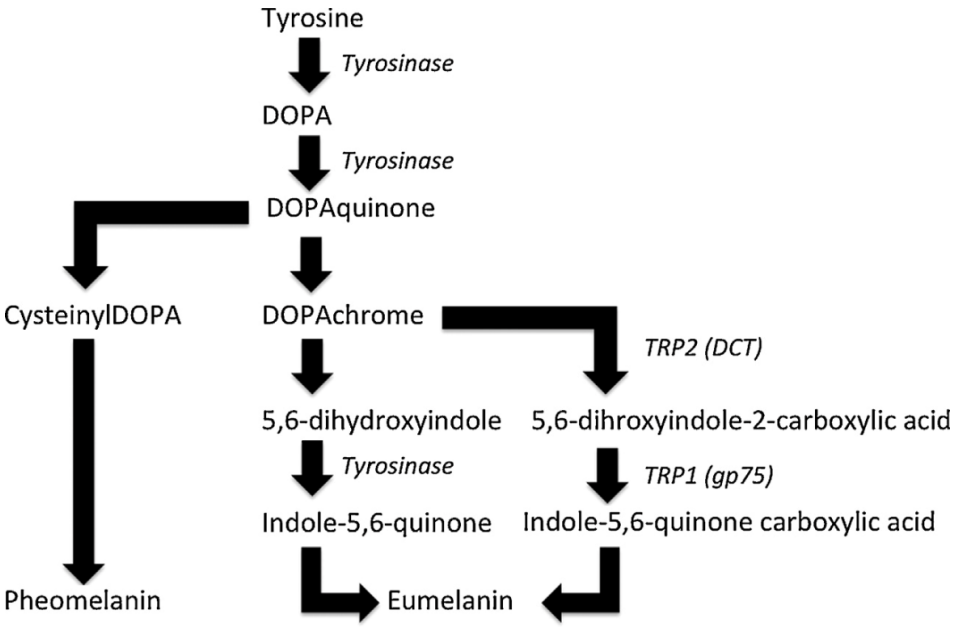

Fig. 4: The melanogenesis pathway. Enzymes involved in the pathway that act as differentiation antigens and consist of melanoma-associated antigens are indicated with *italics*[29]

Several tumor escape mechanisms are nowadays under investigation[34–36]. These “hallmarks of cancer” were first described by Hanahan and Weinberg in 2002, including two new hallmarks of cancer in 2011, such as “Avoiding of immune destruction”[37]. The process of tumot immunoediting is composed of three phases: elimination, equilibrium and escape. In the first phase, immune cells fight against arising tumors[37]. The tumor is either eradicated or persists and enters equilibrium. The second phase is the stage of immune mediated latency. The cancer and immune cells stay in balance. Incomplete tumor destruction and escape

result in an immune resistant tumor growth. When the tumor increases and metastasis develop, the escape phase is reached. [38]

One reason why tumor cells can escape T cell recognition is the modulation of the presentation or processing of antigens. [39] Downregulation of MHC class I and class II molecules in melanoma cells has been shown. Several mechanisms that alter the MHC molecules in human (called human leukocyte antigen (HLA)) are described such as a defect of beta (2)-microglobulin synthesis, loss of genes encoding or downregulation of HLA heavy chain, defect of regulatory mechanism that control HLA expression and an alteration of antigen processing machinery[40]. In some tumor cases, expressions of tumor antigens (e.g., MART-1, Melan-A) are downregulated. Furthermore, mutations can result in the escape from tumor recognition by T cells[34].

Another reason why immunotherapeutic clinical studies often fail is the development of immunosuppressive tumor microenvironment[35,41–44]. T cells, for example, are able to infiltrate the tumor but they are often inhibited by immunosuppressive network and are unable to attack cancer cells, leading finally to the tumor progression. There are several negative regulation mechanisms that are suggested in cancer patients: (1) expansion of immune suppressor cells, (2) expression of co-inhibitory molecules and (3) production of immunosuppressive cytokines or other suppressive factors[45,46].

1.4.1 **Regulatory T cells**

$CD4^+CD25^+Foxp3^+$ regulatory T cells (Treg) play a crucial role in self-tolerance and homeostasis of the immune system by suppressing many physiological and pathological immune responses. They represent one important immunosuppressive cell population that is highly enriched in melanoma microenvironment as well as several other tumor entities. They are considered to be important for suppressing anti-tumor T cell-mediated immune responses and hurdling tumor immunotherapy[31,37,43,47–50]. During cancer disease as they are able to inhibit the activity of $CD4^+$ and $CD8^+$ T cells, B cells, DCs and NK cells[51]. There are various mechanisms of Treg-mediated suppression. Treg produce inhibitory cytokines such as TGF-β and IL-10. They can directly induce cytolysis in a granzyme A/B or perforin-dependent manner. Furthermore, Treg express CD25 and thus compete with effector T cells (Teff) for IL-2. The deprivation of IL-2 hampers Teff in their proliferation. The expression of the inhibitory co-receptor CTLA-4 on Treg and the binding of this molecule with the co-stimulatory molecules B7-1 and B7-2 on DC results in an upregulation of IDO which inhibits T cell activation and function[52]. Additionally, they express inhibitory molecules such as CTLA-4 that inhibit the interaction of APCs with cytotoxic T lymphocytes (**Fig. 5**).[53]. Recently, the role

of CD73 and CD39 ectonucleotidases in T cell differentiation were described since they are involved in generation of extracellular adenosine through ATP hydrolysis, thus tilting the balance towards immunosuppressive microenvironments (ref.). Interestingly, CD39 and CD73 ectonucleotidases are highly expressed on murine CD4+Foxp3+ Treg and have been extensively used as activity markers of this T-cell subpopulation[54]. An increased ratio of $CD8^+$ T cells to Tregs in the tumor microenvironment correlates with favorable clinical outcome and survival in melanoma patients, rendering them a useful prognostic marker[55–57].

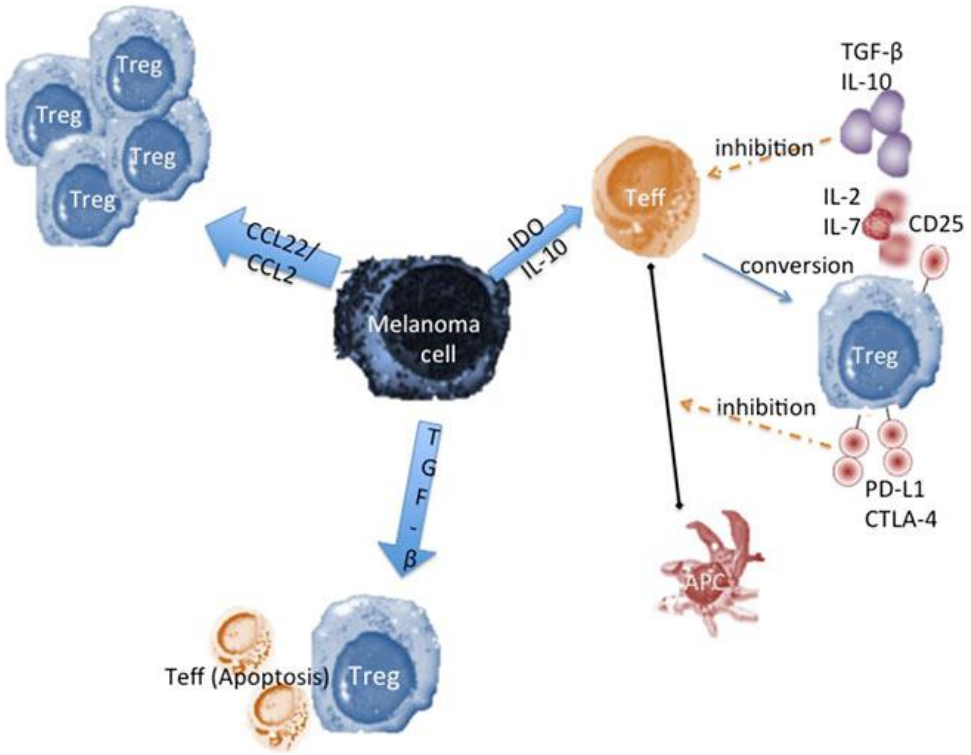

Fig. 5: Mechanisms of local accumulation of regulatory T cells and the main mechanisms Tregs apply to induce immunosuppression. Mechanisms contributing to the aggregation of Tregs in tumor microenvironment include the following: (1) secretion of CCL2/CCL22 and other chemokines by melanoma cells induces Treg migration; (2) Secretion of IDO and IL-10 promotes conversion of Teffs into Tregs; (3) Local anti-inflammatory cytokines such as TGF-β selectively induce Teff apoptosis while having little impact on Tregs. Mechanisms Tregs used to induce immune escape include the following: (1) secretion of immunosuppressive cytokines (TGF-β and IL-10) blunts the anti-tumor response of cytotoxic T cells and other immune cells; (2) Overexpression of CD25 sinks anti-tumor cytokines such like IL-2 and IL-7; (3) Expression of inhibitory molecules including CTLA-4 and PD-1 inhibits the interaction of APCs with Teffs[53].

1.4.2 **Tumor associated macrophages (TAMs)**

Accumulating evidence suggests TAMs actively promote tumor growth and development[58–66]. Several experiments on animal tumor models suggest that TAMs stimulate tumor progression and angiogenesis by producing pro-angiogenic cytokines (e.g., TNF alpha, IL-1). TAMs isolated from tumors are generally less efficient in presenting antigens as there are unable to produce IL-12 needed for anti-tumor responses mediated by NK cells and T cells.

In addition, TAMs are shown to produce immunosuppressive cytokine IL-10 and TGF–β and to express programmed death ligand (PD-L)-1[62,67].

1.4.3 **MDSC**

MDSC represent a heterogeneous population of immature myeloid cells (IMC)[33,39,46,68–70]. Only several years ago, MDSC contribution to the negative regulation of immune responses during pathological conditions was demonstrated[71]. All MDSC have in common their myeloid origin, the immature state and their ability to suppress T cell responses. Under pathological conditions, e.g chronic inflammation, traumata or tumor development, myeloid precursor cells are converted into MDSC in the tumor microenvironment[33,39,46,68–71].

Mouse MDSC are characterized by the coexpression of CD11b and the lineage differentiation antigen Gr-1[72]. Gr-1 contains the Ly6C and Ly6G epitopes, which enable discrimination between two morphological and functional distinct MDSC subpopulations: monocytic MDSC (Mo-MDSC) ($CD11b^{+}Ly6C^{high}Ly6G^{-}$) with monocytic phenotype and polymorhonuclear MDSC (PMN-MDSC) ($CD11b^{+}Ly6C^{low}Ly6G^{+}$) that morphologically resemble polymorphonuclear granulocytes[45,73–75]. CD11b+Gr-1+ Mo-MDSC and PMN-MDSC subsets have been found in tumor-bearing mice[47,70,73,76,77]. Both subsets are able to inhibit T cells; however, MDSC have more potent suppressive activity in tumor than in peripheral lymphoid organs[78]. Studies in tumor-bearing mice have shown that MDSC inhibit T cell function and stimulate the development of Treg in and IFN-γ and IL-10 dependent way[78].

1.4.4 **MDSC expansion and suppressive functions under chronic inflammation**

MDSC are produced in response to the tumor inflammatory microenvironment and to various tumor-derived cytokines**.** They were found to be enriched and activated in the melanoma microenvironment, inhibiting anti-tumor immune responses via several mechanisms, leading to the tumor progression (**Fig.6**) [70].

There are several factors that influence the expansion, activation and accumulation of MDSC in tumors[43]. Soluble factors, which are responsible for the expansion of MDSC, are mostly secreted by tumor cells and inhibit the maturation of IMC like prostaglandins, stem-cell factor (SCF), macrophage-stimulating factor (M-CSF), IL-6, granulocyte/macrophage colony-stimulating factor (GM-CSF) and vascular endothelial growth factor (VEGF) [45]. Most of these factors are inducers for the Janus kinase (JAK) and signal transducer and activator of transcription (STAT) 3 signaling pathways involved in the survival, proliferation and differentiation of myeloid progenitor cells. A permanent activation of the STAT3 pathway in

myeloid progenitor cells leads to higher production of S100 calcium-binding protein A8 (S100A8) and S100 calcium binding protein A9 (S100A9), resulting in the inhibition of the MDSC differentiation and promoting their expansion in the spleen of tumor bearing mice [69,79]. Since S100A8 and S100A9 play a critical role in the induction of inflammation and could induce MDSC expansion, these molecules connect the inflammation with immune suppression in cancer.

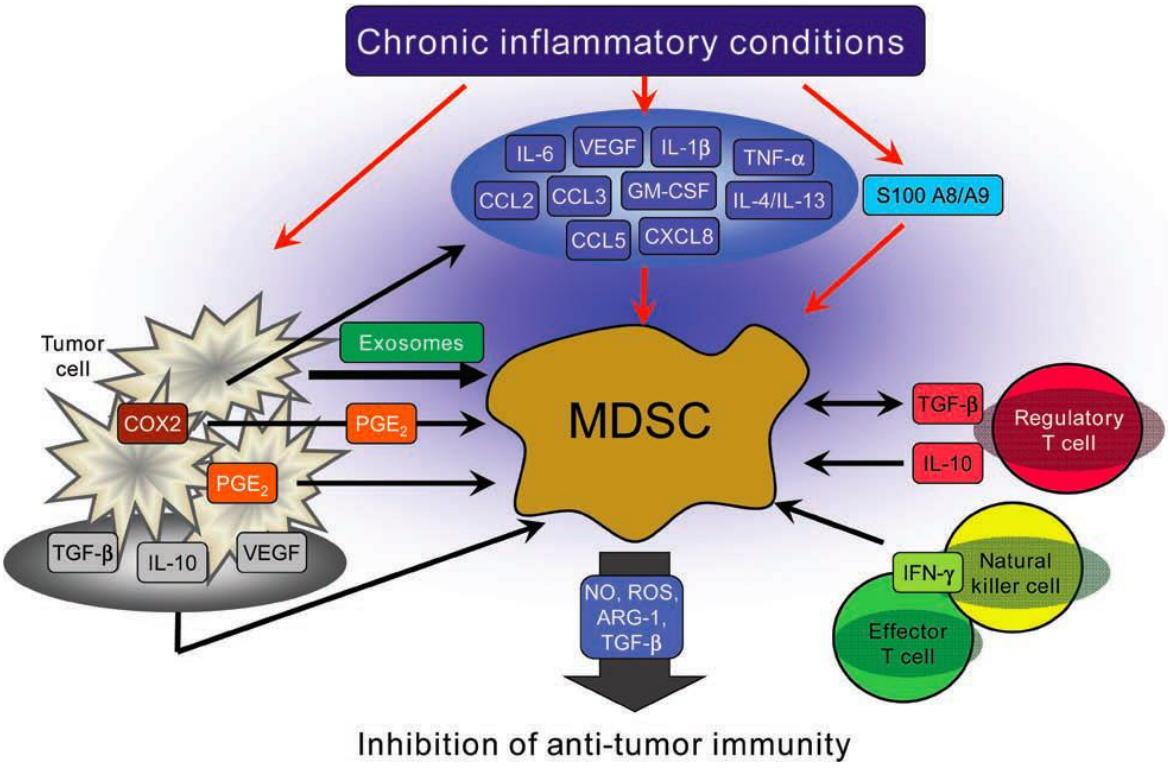

Fig. 6: Induction of MDSC recruitment and activation in the melanoma microenvironment under chronic inflammatory conditions. Soluble mediators of chronic inflammation (such as IL-1β, IL-6, TNF-α, CCL2, TGF-β, VEGF, GM-CSF etc.) secreted by melanoma and stroma cells can induce the migration and stimulation of MDSCs. Activated MDSCs, producing NO, ROS, TGF-ß and expressing increased amounts of arginase (ARG)-1, inhibit anti-tumor immune responses mediated by effector T and NK cells[70]

The second group of factors stimulating MDSC is mainly produced by immune cells and fibroblasts such as IFN-γ, TLRs, IL-13, IL-4, TGF-β and IL-1β. Without these factors, MDSC would not be able to exert their immunosuppressive function[70]. They induce STAT6, STAT1 and nuclear factor kappa B (NF-κB). STAT1 is activated by IFN-γ and IL-1β and leads to the upregulation of arginase-1 (ARG-1) and inducible nitric oxide synthase (iNOS) expression [69,80]. Therefore, STAT1 deficient mice fail to suppress T cell proliferation[81]. In addition, signaling via CD124 has been reported to induce STAT6, as well as ARG-1 and iNOS expression[80]. Moreover, both IL-4 and IL-13 can upregulate ARG-1 activity in MDSC and enhance their immunosuppressive function[68].

Several studies indicate that tumor-infiltrating MDSC can convert into tumor-associated macrophages (TAM) under hypoxia in the tumor microenvironment [82,83]. MDSC can also skew macrophages towards an M2 phenotype [63,84]. High levels of TAM correlate with a bad prognosis in different cancer types[64,85]. It has been shown that MDSC stimulate the expansion and activation of Treg [43,69]. Treg induction is based on IL-10 and TGF-β production by MDSC[84].

In addition to the morphological and phenotypical distinctions, MDSC subsets use different approaches to suppress anti-tumor immunity (**Fig7**) [46,86]. It was found that MDSC suppress T cell proliferation and T cell cytokine production through enhanced expression of ARG-1, iNOS and the elevated production of reactive oxygen species (ROS)[78] .This is associated with the loss or reduced expression of the TCR ζ-chain[87], inhibition of T cell activation, inhibition of IFN-γ production by CD8+ T cells, blocking the development of CTL[78,88]. The suppressive activity of MDSC was associated with the degradation of L-arginine. L-arginine is metabolized by iNOS leading to nitric oxide (NO) production and by ARG-1 converting L-arginine into urea and L-ornithine[35,43,46,68,69]. Both enzymes are highly activated in MDSC and lead to the suppression of T cell proliferation[68]. When MDSC deplete L-arginine from the T cell microenvironment, ζ-chain expression is reduced and T cells are not able to transmit the required signals for their activation[34,88]. NO induces T cell apoptosis and is responsible for the inhibition of MHC class II gene expression [89].

ROS production can be detected in MDSC from tumor bearing mice and in cancer patients[45,86]. Increased ROS production by MDSC is associated with an enhanced NADPH oxidase NOX2 activity [90]. Peroxynitrite leads to the nitrosylation of the TCR of CD8+ T cells and prevents interactions with peptide-MHC complex [43]. This leads to the inhibition of antigen-specific T cell responses through the downregulation of ζ-chain expression in tumor-bearing mice. [88]. The tumor-induced ROS production by MDSC can stimulate MDSC proliferation and block differentiation into APC [81]. In vitro studies showed that the inhibition of ROS in MDSC isolated from mice or patients inhibit the suppressive function of MDSC. Treg in melanoma bearing mice were described to stimulate MDSC to express PD-L1 and to produce IL-10. Hypoxic conditions inside the tumor upregulate PD-L1 expression on tumor-infiltrating MDSC resulting in more potent suppressive activity as compared to splenic MDSC[91].

Moreover, MDSC have been reported to deplete cysteine from the T cell environment[83]. Cysteine is essential for the activation, differentiation and proliferation of T cells[68,80]. Under normal conditions, APC provide T cells with cysteine by importing cysteine, converting it into cysteine and then exporting it with ASC transporters[92]. MDSC compete with T cells for

cysteine thus preventing the generation of cysteine on their own. This leads to the depletion of cysteine from the tumor microenvironment and the inhibition of T cell activation and function[92,93].

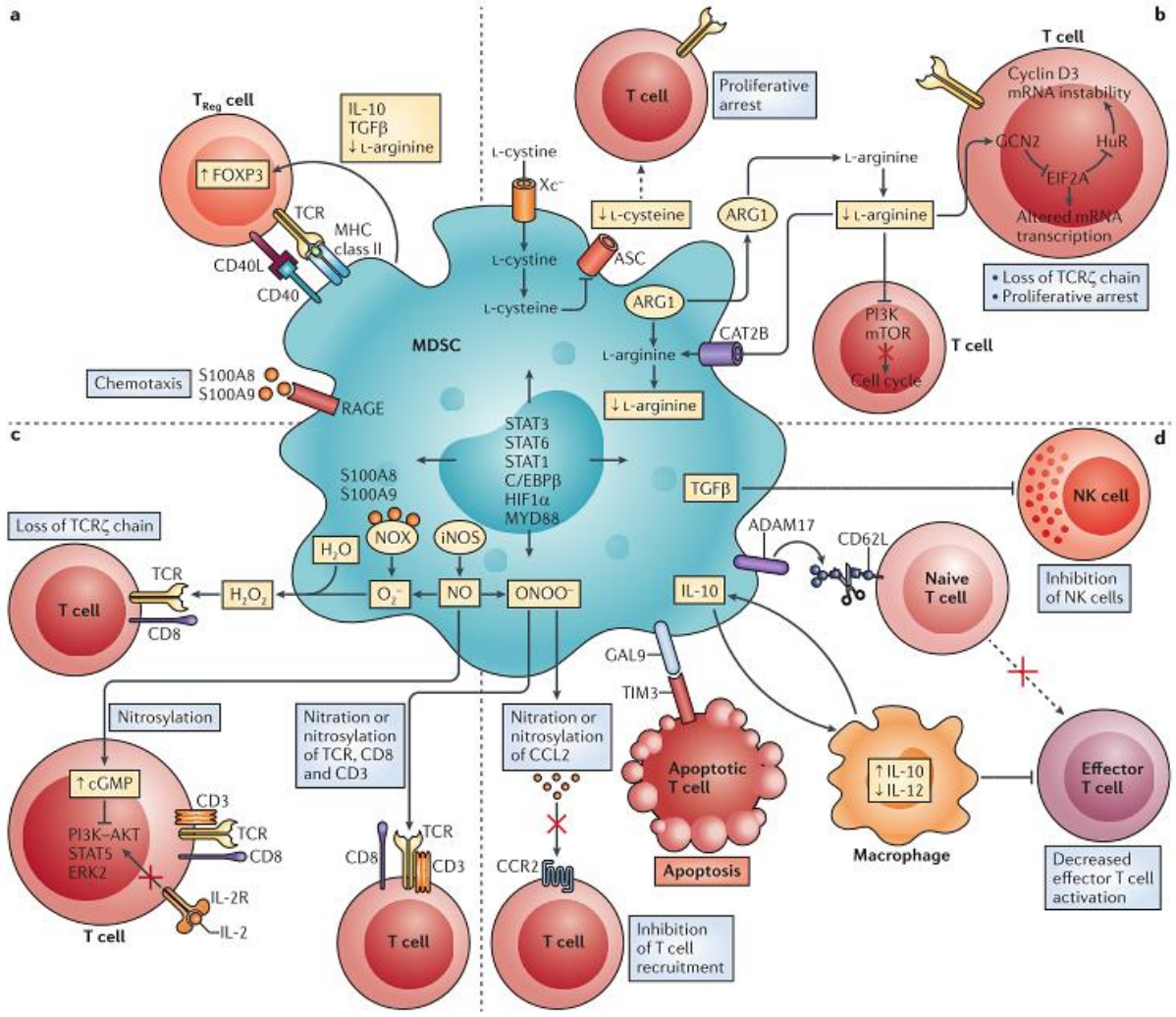

Fig. 7: Mechanisms of MDSC-dependent inhibition of T cell activation and proliferation. MDSCs can inhibit efficient anti-tumor T cell responses through a number of mechanisms. (a) Tumor-associated MDSCs induce the development of Tregs or expand existing Tregs. (b) Tumor-associated myeloid cells deprive T cells of amino acids that are essential for their growth and differentiation, such as cyteine. (c) Tumor-associated myeloid cells release oxidizing molecules, such as hydrogen peroxide (H_2O_2) and peroxynitrite ($ONOO^-$). Peroxynitrite causes nitration and nitrosylation of components of the TCR signaling complex, and H_2O_2 causes the loss of the TCR ζ-chain, thereby inhibiting T cell activation through the TCR. (d) Tumor-associated myeloid cells can also interfere with T cell migration and viability. The metalloproteinase ADAM17 cleaves CD62L, which is necessary for T cell migration to draining lymph nodes, and galectin 9 (GAL9) can engage T cell immunoglobulin and mucin domain-containing protein 3 (TIM3) on T cells to induce apoptosis. As the induction of the immunosuppressive pathways that are depicted in the figure is regulated by common transcription factors, these pathways can operate in more than one myeloid cell type[45]

1.5 Melanoma therapy

1.5.1 Conventional therapies

The standard procedure for localized melanoma with adequate margins is surgical excision and the assessment of metastasis with short-term and long-term follow-ups[94] Patients with non-resectable metastasis or advanced melanoma are treated with radiotherapy[95]. This method is still in use after tumor dissection to treat left tumor tissue. Conventional chemotherapeutics such as Dacarbazin and Temozolomid were shown to not have a significant increase in the overall survival of patients and the number of responding patients is very low [96]. Therefore, novel treatment strategies are urgently needed.

1.5.2 Targeted therapies

40 – 60 % of cutaneous melanoma patients have a mutation in BRAF that constitutively activate the MAP kinase pathway[24,97,98]. Thereby, the most frequent mutation is V600E. In 2011, Vemurafinib, a BRAFV600 kinase inhibitor was approved for patients carrying the V600E mutation with unresectable or metastatic melanoma. The disadvantage of this therapy is the short-term duration of clinical response and drug resistance [99,100]. Since the approval of a Vemurafinib, this treatment is the standard therapy except patients without the BRAF mutation.[26]

Other therapeutics approved for the treatment of late stage melanoma BRAF mutated patients are Trametinib and Cobimetinib, two inhibitors of MEK, a kinase downstream to BRAF in the MAPK pathway. Combination of BRAF and MEK inhibitors showed a delayed resistance development[101].

1.5.3 Negative checkpoint inhibitors

Since standard therapies are not efficient and a lot of tumor-associated antigens for the immunogenic melanoma are already known, new therapies that target immune regulatory pathways had been developed. Antibodies against so called immune checkpoint molecules help to keep tolerance to self-molecules and stimulate or block an immune response.

Cytotoxic T-lymphocyte-associated protein 4 (CTLA-4) is expressed on T cells and competes with CD28 for the ligands CD80 and CD86 on APC thereby leading to an inhibition of T cell activation. Ipilimumab is a human monoclonal antibody that binds and blocks the extracellular domain of CTLA-4, which enhances T cell activation and function and thus promote anti-tumor immunity[102]. CTLA-4 blockage leads to a downregulation of pathways

involved in T cell activation and the therapy with Ipilimumab results in an enhanced antitumor immune response in melanoma patients[103 104] and an increased overall survival in melanoma patients[105]. Ipilimumab was approved in 2011 by FDA.

PD-1 is another immune checkpoint molecule that is upregulated upon T cell activation. Once PD-1 binds to PD-L1 (B7-H1) and PD-L2 (B7-H2), which are mainly expressed by tumor cells, T cell activity is blocked[106,107]. Pembrolizumab, PD-1 inhibitor, was approved for the treatment of melanoma patients after Ipilimumab treatment. The blockade of the interaction between PD-1 and PD-L1 potentiates the immune response and mediates anti-tumor activity[106,107].

1.5.4 **Cancer vaccines**

Another approach to elicit potent anti-tumor immune responses without side effects is the immunization with whole tumor cells, tumor specific peptides, recombinant viruses, DC, and naked DNA combined with different adjuvants [59,61,108–111]. The aim is to stimulate innate and adaptive immunity to recognize and eliminate tumor cells. Although therapeutic cancer vaccines showed an impressive anti-tumor activity in numerous animal models, their clinical benefit in cancer patients leaves much to be desired. Multiple clinical trials have achieved only low overall survival with rare complete responders[30,112,113], which could be due to the immunosuppressive tumor microenvironment and other tumor escape mechanisms previously described in Chapter 1.4.

1.5.5 **Combined treatment strategies**

Although there have been significant advances in melanoma treatment over the past several years, monotherapies have significant limitations, e.g. partial responses with subsequent tumor relapses or development of resistance to current (mono-) therapies, such as chemotherapy, BRAF inhibitors or anti-PD-1 treatment[11499]. Thus, there is an increasing interest to using these strategies in combination[18,115,116]. However, it is not yet completely clear how to best incorporate targeted, immune-targeted therapies or chemotherapy into combination regimens for melanoma patients. The influences of each of these monotherapies and potential synergistic effects of designed immunotherapy-based combination regiments on the host anti-tumor immune response and host anti-response (e.g. autoimmune and toxicity) must be taken into consideration[102]. Therefore, there is a increasing need for preclinical studies further illuminating pro and contra indications upon combinatorial treatments, before starting phase I clinical trials in humans.

Several preclinical studies are already underway. For instance, combination of targeted therapy with immune therapy, such as a triple combination therapy of BRAF and MEK inhibitors and adoptive therapy in melanoma mouse models was described. This strategy resulted in an increased MHC I molecule expression and T cell infiltration into the tumor, leading to complete tumor regression[117].

Furthermore, there are several ongoing clinical trials based on the combination of immune checkpoint inhibitors with immunotherapies and combination of radiotherapy or chemotherapy with immunotherapy [102,118,119].

With regards to combination of immunotherapy with chemotherapy, modulation of the immune cell activities by ultra-low doses of agents, designed as chemo-immunomodulation has been recently described [120]. The approach involves an application of chemotherapeutics in ultra-low doses without any cytotoxic effects on tumor or host cells. Application of ultra-low doses of paclitaxel, gemcitabine and 5-fluorouracil was able to stimulate maturation and function of human and murine dendritic cells[121]. Furthermore, it was shown that paclitaxel promotes differentiation of MDCS into DCs in vitro in a TLR-4-independent manner[122]. In addition, ultra-low dose of paclitaxel improved the efficiency of therapeutic TRP2-peptide vaccination in healthy mice[123] as wells as therapeutic efficacy of a recombinant adenovirus against several murine cancers[124]. Overall, these promising preclinical studies suggest further investigation of potential combinatorial approaches in a preclinical setting in order to overcome current melanoma treatment limitations, such as partial responses and development of resistance.

1.6 Dendritic cell-based immunotherapy

1.6.1 Dendritic cells in tumor-specific T cell responses

DCs can process and present tumor-derived peptides to $CD4^+$ and $CD8^+$ T cells and are pivotal for priming, proliferation, activation and differentiation of specific T-cell subsets as (see **Chapter 1.2**). These features are making autologous DC-based vaccines an attractive and promising tool to elicit anti-tumor T cell immune responses, resulting in tumor cell eradication (**Fig. 8**)[125].The realization of the dominant role of DCs in the initiation of immune response and specifically in T cell priming has pushed numerous efforts to harness DCs for the immunotherapy of cancer[1710842]. **Fig. 9** summarizes the DC-based vaccination approaches used for cancer immunotherapy[14]. The primary goal of using DCs as tumor vaccine is to elicit a strong and long lasting $CD8^+$ T cell-specific antitumor immune response. Such tumor specific $CD8^+$ T cells should be able to: i. Become tumor specific with high avidity; ii. Penetrate the tumor microenvironment, and iii. Overcome the tumor immunosuppressive surrounding[126]. In order to achieve these goals, DC vaccination must be accompanied by the induction of $CD4^+$ T helper (Th) cells, elimination of Treg and the reversal of the tumor immunosuppressive environment[127].The first clinical study of DC-based vaccine immunotherapy was published in 1996, in which autologous antigen-pulsed DCs were vaccinated in patients with follicular B cell lymphoma[128] Until today, more than 150 clinical trials have been conducted for a variety of cancer types, including phase III clinical trials in melanoma, prostate cancer, glioblastoma, and renal cell carcinoma[20,42,108,109,129,130]

Even though tumor-specific cytotoxic T lymphocyte (CTL) and Th1 responses and occasional tumor regressions have been reported in many patients, the clinical impact of DC vaccines has been scarce so far. Sipuleucel-T (Provenge; Dendreon Corporation, Seattle, WA) is the first and so far the only DC-based vaccine approved for the treatment of metastatic, hormone-refractory prostate cancer. A small number of individuals who respond favorably to DC vaccinations indicates the need for developing more immunogenic DC vaccines and understanding the reasons for highly variable clinical responses[19,131,132]. Previous findings have highlighted several mechanisms that contributed to DC vaccine efficiency including higher IL-12 production, efficient co-stimulatory signals, and stronger induction of antigen-specific Th1 responses or lower Treg numbers in the tumor tissue[19,131,132]. Other parameters, such as the site of injection, the number of injected DCs or the number of DCs reaching the T cell zone of lymph nodes are also critical for DC vaccine efficiency[19,131,132]. It has been shown that only a small fraction of the injected DCs reached the draining lymph node and increasing DC mobility improved survival in gliobastoma patients.[133]

One of the main reasons why DC vaccines have not been so successful for melanoma immunotherapy is the poor presentation of tumor-derived peptides, resulting in limited antitumor $CD8^+$ T cell immune responses[15]. In addition, the elevated levels of Tregs found in melanoma microenvironment impair DC functions[15]. Moreover, it has been shown that melanoma cells secret factors such as IL-10, which directly inhibit DC functions and convert them into tolerogenic DCs, promoting anergy of melanoma-specific T cells[19,30]. Given the role of impaired DC function in melanoma pathogenesis, several improvements need to be considered regarding the preparation and administration of the DC vaccines, such as the source and *ex vivo* manipulation of DCs, the type and form of the antigen to be loaded, the antigen-loading strategy, the origin, subset and number of DCs to inject as well as the amount, frequency, route and the site of administration so that tumor-specific cytotoxic T cell and Th1 immune responses could be enhanced[30,42].

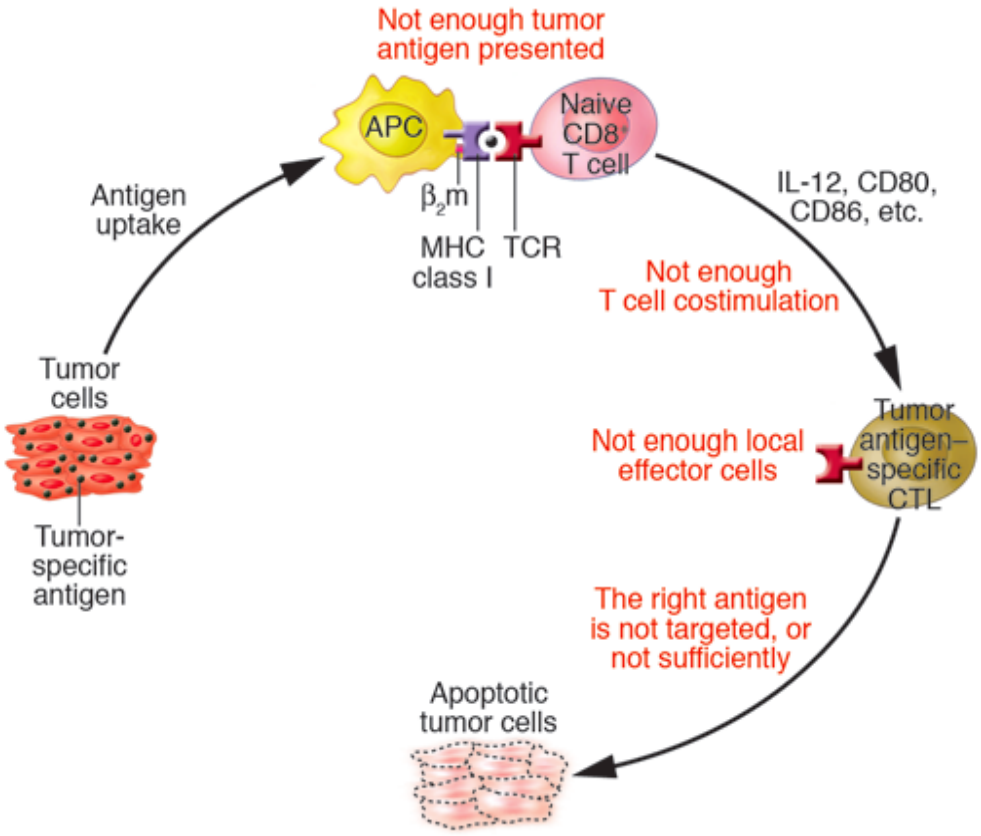

Fig. 8: Role of dendritic cells in tumor-specific T cell responses. APCs such as DCs capture antigens from tumor cells. Antigen-loaded APCs then prime naïve T cells to become anti-tumor CTLs through soluble mediators such as IL-12 and/or co-signaling molecules such as CD80 or CD86. Failure to elicit protective immunity is seen as a lack of sufficient quantity or quality of one of these events (indicated in red text). This model predicts that augmenting numbers or quality of a specific component will suffice as a clinical strategy.[125]

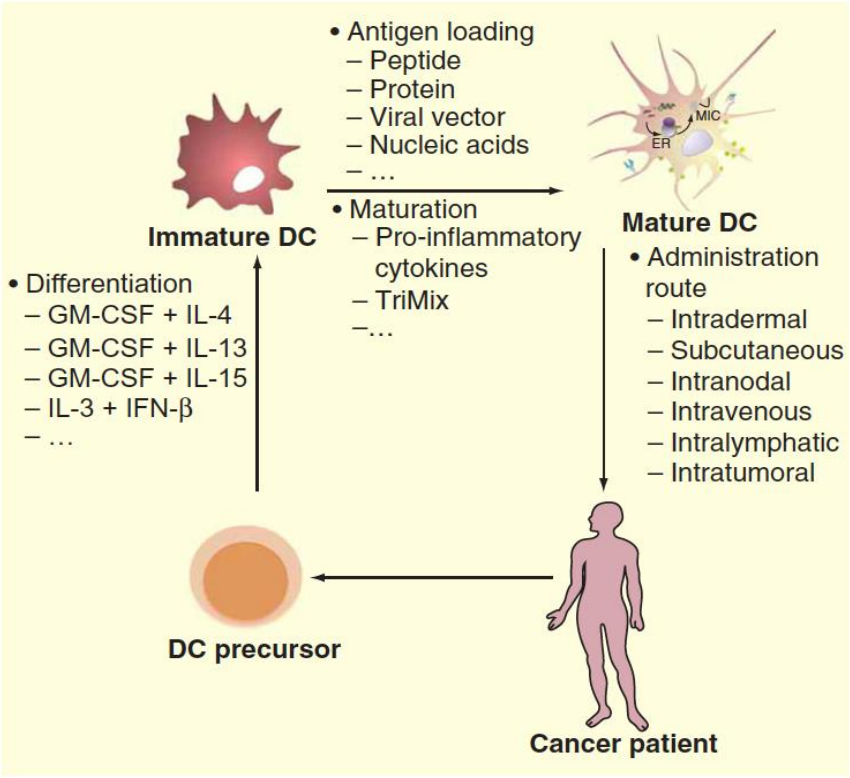

Fig. 9: DC-based immunotherapy in cancer patients. DCs are generated from DCs are generated from precursors and differentiated by various stimuli, followed by antigen loading and/or maturation. Mature DCs are re-administered into the patient[14]

1.6.2 Peptide-loaded dendritic cell vaccines

Matured DCs *ex vivo* pulsed with synthetic antigenic peptides are among the most widely used in DC-based vaccination clinical studies[20,134]. Antigen processing represents a bottleneck in antigen presentation, whereas synthetic peptides exogenously loaded can simply bind the groove of the MHC molecules liberally displayed on the surface of matured DCs for presentation to T cells. Additionally, in contrast to full-length antigens, this approach has an advantage of monitoring peptide-specific T-cell responses in patients using a variety of methods such as CTL assays, tetramer staining, ELISpot and intracellular cytokine staining[135].

However, in this approach synthetic peptides exogenously loaded have to compete with peptides that are already bound to MHC molecules on the cell surface. Additionally, this approach has the prerequisite of preselected and well-defined tumor-specific peptides, however immunogenic cytotoxic as well as helper peptides from tumor-associated proteins have not been defined for all tumor entities[13]. Moreover, this approach is MHC-restricted; hence the patient's MHC haplotype should be identified. Furthermore, one peptide can bind

either MHC I or MHC II, thus in contrast to whole tumor antigens where multiple epitopes are presented in both MHC class I and II, peptide-pulsed DC vaccines cannot activate both $CD4^+$ and $CD8^+$ T cell immune responses, limiting their clinical efficacy[20]. Finally, the half-life of peptide-MHC complexes (pMHC) is usually short[15134]. This is an important disadvantage of peptide-loaded DC vaccines since prolonged presentation of MHC-peptide complexes results in enhanced immunogenicity[136].

1.6.3 **mRNA-based dendritic cell vaccines**

Induction of tumor-associated antigen (TAA) expression in DCs via RNA transfection has arisen as a novel antigen-loading technique. TAAs can be delivered in DCs in the form of tumor-derived RNA or synthetic *in vitro* transcribed RNA encoding for specific TAA[19]. mRNA-based DC vaccines overcome many limitations of the peptide-loaded DC vaccines summarized in **Table 1**. mRNA encoding tumor antigens and immune modulating proteins can be efficiently delivered to DCs, offering more prolonged presentation of the antigen compared to peptide-loading which appears to be short-lived[19]. mRNA is a chemically well-defined, polyvalent and safe molecule that can be easily and inexpensively generated at high purity, ensuring reproducible manufacturing and activity[14]. Additionally, RNA is advantageous and safer than naked DNA or viral transfection due to the fact that RNA induces transient but sufficiently long and high protein expression without the risk of integrating into the host genome[136].

RNA can be delivered alone or coated with liposomes (lipofection), through electroporation, gene guns, nucleofection, sonoporation recombinant viral vectors or recombinant bacterial vectors[137–139]. RNA encoding for tumor antigens is much easier to isolate or synthesize than tumor peptides or proteins[14,140]. The last few years increasing interest has been observed in delivering the mRNA to DCs through electroporation. mRNA-electroporation has turned to be a very efficient way for delivering TAA to DCs, and it is superior to other RNA methods in generating immunostimulatory DCs for DC-based immunotherapies, resulting in stronger anti-tumor T cell responses[141–144].

Table 1: Main advantages of mRNA-based over peptide-loaded dendritic cell vaccines

mRNA	Peptide-loaded
Undefined neo epitopes can be presented	Prior identification of antigenic peptides
MHC restriction of the patients	No MHC restriction of the patients
Prolonged antigen presentation	Short half-life of peptide/MHC complex
Mechanisms of intrinsic antigen processing by the DC is partly bypassed	Peptide loading onto MHC class I or II molecules are depending on affinity

1.6.4 **Novel DC vaccines based on membrane attached β2-microglobulin**

Efficient MHC-peptide complex expression on the cell surface determines the degree of T cell responsiveness. The maximal yield of presented peptides derived from encoded proteins is thus a key parameter in the design of cancer vaccines[129,145]. This rationale has prompted attempts to enhance the level of peptide presentation by APCs through genetic manipulations aimed at elevating the actual number of pre-selected MHC-I-peptide and MHC-II-peptide complexes on the cell surface[146]. Moreover, in the last few years, increasing interest has been observed in using mRNA-electroporated DCs for immunotherapy[147]. Cafri et al.[147] have developed a genetic platform based on membrane-anchored β2-microglobulin (β2m) linked to the antigenic peptide of interest at its N-terminus and to the transmembrane and intracellular signaling domain of toll-like receptor (TLR)-4 C-terminally. Human (h)β2m was employed to enable the detection of the protein product on the surface of transfected mouse BM-derived DCs (BMDCs) with flow cytometry. Their aim was to ameliorate the priming of peptide-specific $CD8^+$ T cell responses by APCs, which requires both effective antigen presentation on MHC class I products and co-stimulatory signaling. Electroporation of DCs with *in vitro* transcribed mRNA encoding for such genetic platforms resulted in an exceptionally efficient peptide-specific T cell recognition and conferred a constitutively activated phenotype on the transfected cells. Their findings provided evidence that these encoded peptide-β2m-TLR polypeptides could link peptide presentation to cellular activation and DC maturation through constitutive TLR signaling, resulting in a cytokine and chemokine secretion as well as costimulatory molecule upregulation. DC maturation strongly supports the initiation of immune response and pro-inflammatory conditioning, being prerequisites for efficient vaccination. In that way, the use of adjuvants is precluded, avoiding any adverse effects[114,118,119].

Using this allele-independent platform, presentation does not depend on proteasomal degradation, is transporter for antigen presentation (TAP)-independent, and no additional peptide trimming is required, making antigen presentation very efficient[145]. Importantly, these recombinant bi-functional peptide-hβ2m-TLR4 polypeptides were found to be superior to peptide-loaded mature BM-derived DCs in presenting antigenic peptides, in accordance with previous findings showing that membrane-anchored β2m stabilizes the MHC-I molecules and prolongs the peptide presentation[144,146,148]. They could also show that BMDCs were able to induce efficient peptide-specific T cell activation indicated by an elevated cytokine production by effector $CD8^+$ T cells[144,149]. Moreover, these DCs prompted efficient peptide-specific target cell killing *in vivo*, demonstrating that they are potent inducers of CTLs. In addition, mRNA-electroporated BMDCs vaccination induced antigen-specific effector memory $CD8^+$ T cells, protected mice from tumor progression following the administration of B16F10.9 melanoma

cells and suppressed the tumor growth of pre-established B16F10.9 tumors[144], prolonging the survival of mice[144,149].

Recently, BMDCs electroporated with the chimeric peptide-hβ2m-TLR4 platform were also injected into *ret* transgenic mice, which spontaneously develop malignant skin melanoma that closely resembles human melanoma regarding histopathology, clinical development and MAAs expression[150,151]. It was shown that this vaccination resulted in the prolonged survival of tumor-bearing mice, increased frequency of $CD62L^{+}CD44^{hi}$ central and $CD62L^{-}CD44^{hi}$ effector memory $CD8^{+}$ T cells without any stimulatory effect on immunosuppressive Tregs and MDSCs, suggesting that this DC immunization could be efficiently employed for melanoma immunotherapy[149,152].

1.6.5 **Chimeric peptide-hβ2m receptor platform for CTL induction**

According to the method developed in the Weizmann Institute of Science (WIS, Rehovot, Israel), genetic constructs were designed to induce specific CTL response. This was achieved by converting invariant chain of human ß2-microglobulin (hß2m) into an integral membrane protein and the genetic linking of an antigenic peptide to its N terminus (**Fig.10**)[147]. This modality prompts exceptionally efficient peptide presentation on MHC-I molecules[144,147,153] by:

1. Directly targeting ß2m/peptide to the ER through the leader peptide, uncoupling presentation from proteasomal degradation and TAP-mediated translocation.
2. Obviating the need for N-terminal peptide trimming at the ER Facilitating full MHC-I complex assembly.
3. Yielding abundance of peptide available for de-novo complex formation at the cell membrane.
4. Representing the most stable expression of the MHC-class I- hß2m-peptide on DCs.
5. Replacing the transmembranal and cytosolic domains of H-2Kb with the intact transmembranal and cytosolic domains of native TLR4 (as TLR4 anchor).

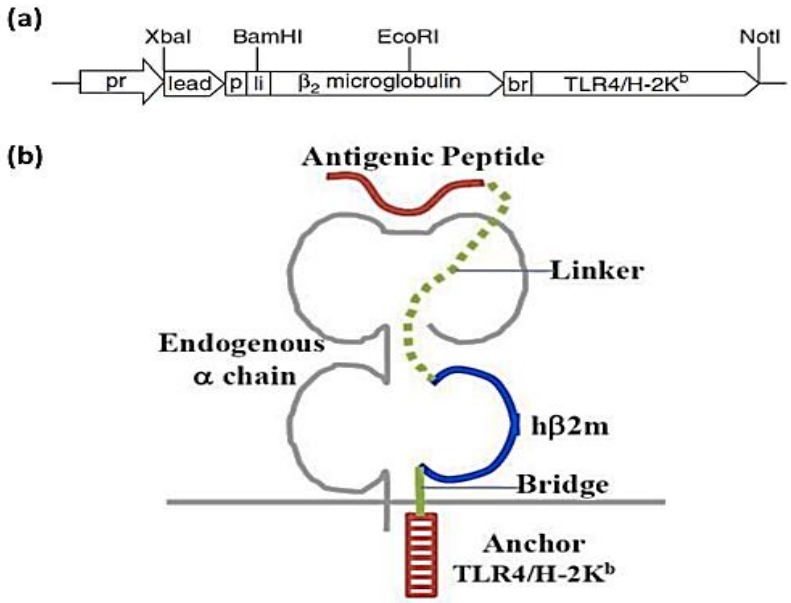

Fig. 10: Scheme of the h2m-based bi-functional constructs. (a) Genetic design. Major restriction sites are shown. Abbreviations: pr, promoter; lead, leader peptide; p, antigenic peptide; li, linker peptide; br, bridge; **(b)** Anticipated configuration of the polypeptide products with a linked antigenic peptide in the context of an MHC-I heavy chain [144].

1.6.6 Chimeric MHC-class II as a platform for CD4 T cells induction

To address the challenge of inducing a significant immune response to specific antigens by CD4+ T cells, the group of Prof. Lea Eisenbach (Department of Immunology, WIS) designed a single chain chimeric MHC-II molecule (**Fig.11**). The molecule comprises three main components:

1. An MHC class II restricted antigenic peptide.
2. MHC-II I-Ab alpha and beta chains.
3. Anchor sequence, stabilizing peptide presentation on dendritic cell surface.

The CD40 anchor was selected, according to earlier results of best MHC class II stabilization and kinetic membrane expression (unpublished data, Prof. Lea Eisenbach).

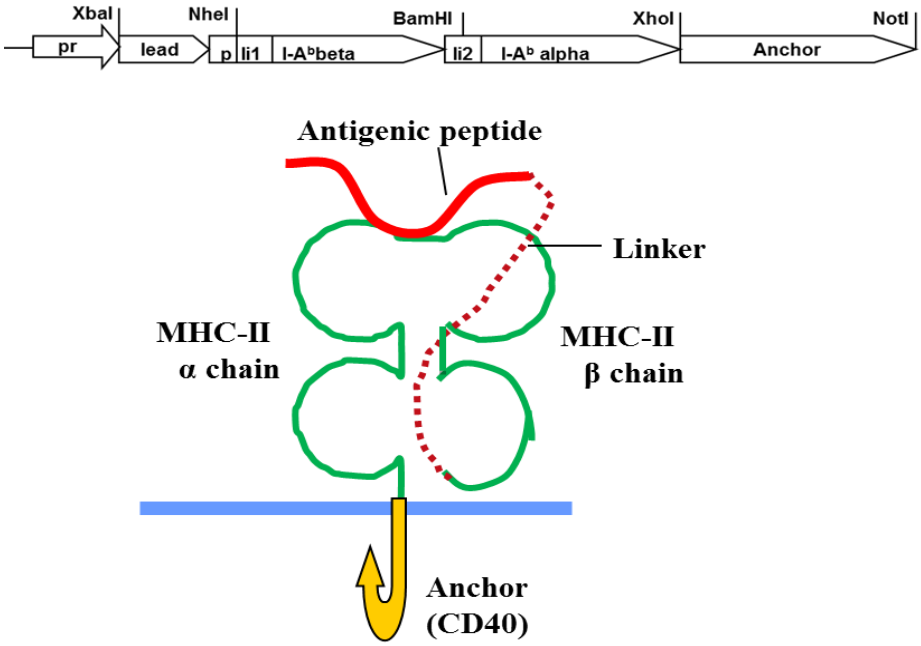

Fig. 11: Scheme of the MHC-II-H2-IAb restricted genetic constructs. (a) Genetic design. Major restriction sites are shown. Abbreviations: pr, promoter; lead, leader peptide; p, antigenic peptide; li, linker peptide; br, bridge; **(b)** Anticipated configuration of the polypeptide products with a linked antigenic peptide linked to the MHC-II ß chain. The cytosolic part was modified by CD40 domain for stabilization (unpublished data, department of immunology, WIS, Rehovot, Israel).

1.6.7 Class II-Associated Invariant Chain Peptide (CLIP)-construct

MHC class II molecules present endogenous or exogenous peptides on the surface of APC to select or activate $CD4^+$ T cells in the thymus or periphery[6]. MHC Class II restricted antigen presentation is dependent on the release of CLIP and exchange with antigenic peptides usually sampled in endosomal compartments. Murine leukocyte antigen H-2M (murine analog to the human HLA-DM) in the endosomes promotes the dissociation of the CLIP peptide as a place holder from MHC class II, which then catalyzes peptide exchange of CLIP with endosomal peptides, favoring more stable peptide–MHC class II complexes, presented on the APC surface[6,154].

Therefore, the experimental idea of the 'CLIP construct' presented in this study was to use CD74, also known as invariant chain, as a platform for direct class II antigenic peptide delivery into APC by electroporation. Invariant chain is a universal, allele-independent platform for CD4 T cell induction, whereas the previously described I-Ab construct is restricted to the use in C57BL/6 mice[155,156]. An expression vector (plasmid) containing the human Ii cDNA, in which the CLIP-coding sequence can be easily replaced by other sequences was kindly provided by Prof. Lea Eisenbach, Weizmann institute of Science, Israel. **CLIP** coding sequence (22aa): PKSAKPVSQMRMATPLLMRPMS was replaced by either **mTRP1$_{111\text{-}128}$** peptide sequence (18aa): GTCRPGWRGAACNQKILT or **mTYR$_{99\text{-}117}$**

peptide sequence (19aa): NCGNCKFGFGGPNCTEKRV, repsectively. The respective CLIP mRNA construct represents a universal, alleel independant platform for MHC class II restricted antigenic peptide delivery in APC (e.g. autologous DC) and subsequent CD4 T cell induction.

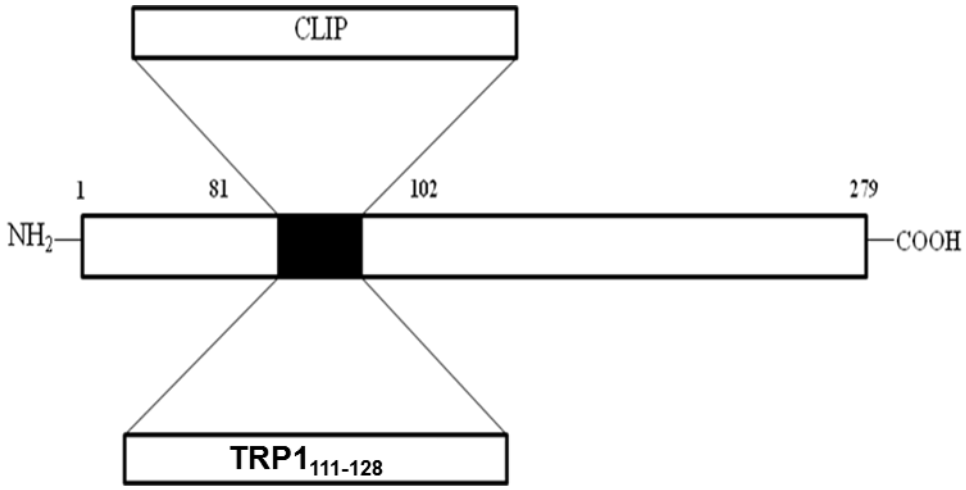

Fig. 12: Scheme of the experimental MHC-II restricted genetic invariant chain construct platform. Anticipated configuration of the polypeptide products, in which the CLIP coding sequence is exchanged by an MHC class II restricted antigenic peptide of choice (unpublished data, department of immunology, WIS, Rehovot, Israel). Upon electroporation of respective mRNA, further H-2M processing in the endosomes of DC occur and the antigenic peptide of choice is released and loaded onto the MHC class II molecule under physiological conditions and presented (via MHC class II) on the DC cell surface.

1.7 Preclinical mouse melanoma models

Murine cancer models designed to capture the complexities of human cancers currently offer the most advanced preclinical opportunity for navigating diverse mechanisms that provide rationale for therapeutic development[157].

1.7.1 BRAF mouse model

This genetic model recapitulates key pathophysiological aspects of the human melanoma, in which 40 – 60 % of cutaneous melanoma patients have a BRAF V600E mutation that constitutively activate the MAP kinase pathway[97]. This mouse model is based on the Cre/lox recombination system to generate inducible, tissue-specific genetic modifications. The $Braf^{CA}$, Tyr::CreER and $Pten^{lox4-5}$ mouse developed by McMahon and Bosenberg[158] is a tri-allelic mouse model, which develops induced malignant melanomas following intradermal application of Tamoxifen/4-hydroxytamoxifen (4-OHT). It has CreERT2 fusion protein directed by mouse tyrosinase promoter/enhancer specifically in melanocytes and also contains loxP-flanked sequences for Pten exons 4 and 5. Tamoxifen induces a Cre-mediated recombination, resulting in deletion of the floxed sequences (Pten exon 4 and 5) and expression of the BRAF proto oncogene and leading to an accumulation of BRAF V600E mutation in melanocytes. Finally, the development of melanoma similar to patients carrying the BRAFV600E mutation will be observed[158].

The prevention and therapy of BRafV600E-induced melanomas by pharmacological inhibition of MEK1/2 and mTorc1 was investigated with this mouse model by using specific and selective inhibitors of MEK1/2 (PD325901) or mTorc1 (rapamycin), which are downstream of BRafV600E or PI3-kinase, respectively[159]. In addition, it was shown that induced melanomas highly overexpressed several TAAs such as tyrosinase (Tyr), tyrosinase related protein 1 (Trp1), Trp2, gp100, which makes it applicable for novel immunotherapies targeting these melanoma anigens[158,159].

1.7.2 Spontaneous ret transgenic mouse melanoma model

In transplantable models, like B16 melanoma model, tumor cells are transplanted intradermal for 5-10 days so that the interaction of the tumor cells with the immune system is not comparable to the clinical situation. To get more insights in the tumor microenvironment and study melanoma immunotherapies in more detail, Kato et al.[125] engineered a transgenic mouse model, in which melanoma lesions develop spontaneously. The lesions in mice resemble human melanoma with regards to tumor genetics, histopathology and clinical development. In this model, the human *ret* recombinant oncogene was fused with a

methallothioneine-I promotor[125]. This leads to an overexpression in melanocytes under the control of methallothionein promotor-enhancer. An activation of the kinase also leads to the activation of downstream signaling molecules like mitogen-activated protein kinase (MAPK), Erk2 and c-Jun. The activation of *ret* promotes malignant transformation of melanocytes and tumor development[125]. Melanoma emerges at head, neck, back, and tail and metastasizes in LN, BM, liver, brain and lungs[150,151]. Melanoma lesions show characteristic melanoma morphology and express melanoma-associated antigens like S100, tyrosinase, tyrosinase related protein (TRP)-1, TRP-2 and gp100[152]. The metastatic profile is similar to the metastatic pattern in patients with malignant melanoma[24,160]. Although the mutation of *ret* has not been detected yet in melanoma patients the activation of the MAP-kinase signaling pathway is routinely seen in human melanoma[123]. It was previously shown that immunosuppressive cells like MDSCs and Tregs accumulate during tumor progression in skin tumor and metastatic lymph nodes [77,161,162]. Furthermore, MDSC were shown to inhibit T cell response that allows a rapid tumor progression and metastasis[32,77]. The administration of the phosphodiesterase-5 inhibitor sildenafil neutralized the MDSC immunosuppressive activity, which leads to an increased survival of melanoma-bearing mice[67]. Furthermore, various inflammatory factors driving MDSC activation, expansion and migration were found at the site of tumor [32,87]. This complex immunosuppressive network in the tumor microenvironment could be one reason that conventional melanoma therapies are not successful.

2 Aim of the project

The goal of this study was to generate a novel and more potent DC vaccine for melanoma immunotherapy based on the recently developed bi-functional class of genetic mRNA cancer vaccines. These modified DC present different chimeric MHC class I and MHC class II receptors, in order to become a multivalent DC vaccine allowing a simultaneous presentation of different melanoma associated antigens (MAA) of choice for induction of $CD8^+$ CTL and $CD4^+$ Th, respectively. We tested several class I and class II restricted MAA derived from TRP-1 and Tyr for their capability to elicit a potent $CD8^+$ CTL and $CD4^+$ Th responses. Afterwards, we investigated selected TRP-1/Tyr-β2m-TLR4/Kb and TRP-1/Tyr-β2m-class II receptors (H2-IAb and CLIP) for their *in vivo* capacity to induce antitumor immune response in two different melanoma mouse models (*ret* transgenic and BRAF). To this end, we studied melanoma-bearing mice for tumor regression and survival and performed analyses of immune cell subsets in skin tumor and lymphoid organs (LN, spleen and BM) upon the treatment with multivalent DC vaccine. Finally, the most potent DC vaccine was applied in combination with ultra-low dose of paclitaxel to further promote T cell dependent immunity and to overcome immunosuppression.

3 Materials and Methods

3.1 Materials

3.1.1 Mice

6 to 12 weeks-old **C57BL/6** (H-2b) as well as **B6.SJL** (CD45.1 /H-2b) mice were purchased from Charles River laboratories (Sulzfeld, Germany).

Braf mice. The $Braf^{CA}$, $Tyr::CreER^{T2}$ and $Pten^{lox4-5}$ were kindly provided by Dr. Rienk Offringa, DKFZ Heidelberg with previous consent by Martin McMahon, University of California, San Francisco,USA and Marcus Bosenberg, Yale University, USA. This tri-allelic mouse model with a melanocyte-specific Cre-Lox recombination develops induced malignant melanomas with Bra V600E mutation following intradermal application of tamoxifen. Small, local palpable tumor usually appear 25-30 day after induction. The mice were monitored every second day.

***Ret* transgenic mice**. These mice have C57BL/6 background expressing the human ret transgene in melanocytes under the control of mouse metallothionein-I promotor-enhancer were provided by Dr. I. Nakashima (Chubu University, Aichi, Japan) (Kato et al., 1998). These mice overexpress the human Ret proto-oncogene in melanocytes under the control of mouse metallothionein-I promoter-enhancer. The tumor develops spontaneously approximately 30-35 day after birth. The mice were monitored every second day.

Mice were crossed and kept under pathogen-free conditions in the animal facility of the German Cancer Research Center (Heidelberg, Germany). Experiments were performed in accordance with government and institutional guidelines and regulations.

3.1.2 Cell lines

DC2.4. A murine dendritic cell line, were kindly provided by Dr. Kenneth Rock (University of Massachusetts Medical Center, Worcester, MA). Cells were grown in complete media comprised of RPMI (GibcoBRL, Grand Island, NY), supplemented with 10% FBS (Hyclone, Logan, UT), 10 mM HEPES, 2mM L-glutamine and 50 □M 2-mercaptoethanol. DC2.4 cells were maintained at 37 0C in a humidified incubator with 5% CO2. B3Z. An OVA257–264-specific, H-2Kb-restricted CTL hybridoma, which expresses the NFAT-LacZ reporter gene, was a kind gift from Dr. N. Shastri (University of California, Berkeley, CA). Cells were grown in complete media comprised of RPMI (GibcoBRL, Grand Island, NY), supplemented with 10% FBS (Gibco®), 10mM HEPES, 2mM L-glutamine and 50 uM 2-mercaptoethanol.

B16-MO5 (MO5). B16 melanoma cells stably transfected with OVA were cultured in DMEM with 10% FBS, 2 mM glutamine, 1 mM pyruvate, 50 µM 2-ME, combined antibiotics and 800 µg/ml G418. Cells were kindly provided by Prof Lea Eisenbach (WIS, Israel).

B16-F10.9. A highly metastatic clone of the B16-F10 melanoma line that expresses low levels of MHC class-I antigens was cultured in DMEM with 10% FBS, 2 mM glutamine, 1 mM pyruvate, 50 µM 2-ME and combined antibiotics. Cells were kindly provided by Prof Lea Eisenbach, Weizmann institute of science, Rehovot, Israel.

D122. High-metastatic, low-immunogenic D122 clone of the 3LL carcinoma Reference and the carcinogen-induced T cell lymphoma. Cells were kindly provided by Prof Lea Eisenbach, Weizmann institute of science, Rehovot, Israel.

EL4 cells (H-2b) were grown in DMEM (Invitrogen) containing 10% FCS, 2mM L-glutamine, 1mM sodium pyruvate, 1% nonessential amino acids, 1% Penicillin-Streptomycin combined antibiotics. Cells were kindly provided by Prof Lea Eisenbach, Weizmann institute of science, Rehovot, Israel.

RET-cells were isolated from skin melanoma developed in *ret* transgenic mice (Zhao F. et al., 2009, Clin Cancer Res.) and cultured in RPMI (Invitrogen) containing 10% FCS, 2mM L-glutamine, 1% nonessential amino acids and 1% Penicillin-Streptomycin.

YAC cells. Orginally induced by inoculation of Moloney leukaemia virus into a new-born A/Sn mouse. Sensitive to the cytoxic activity of naturally occurring killer cells in mice (NK cells). Often used as target cells in NK assays. Cells were kindly provided by Prof Lea Eisenbach, Weizmann institute of science, Rehovot, Israel.

RMA-S cells. Rauscher virus-transformed lymphoma cell line of C57BL/6 (H-2b) origin, and RMA-S is a RMA TAP-deficient mutant cell line.re grown in RPMI 1640 medium, supplemented with 10% heat-inactivated FCS, 2 mM L-glutamine, and 50 uM β2-mercaptoethanol.

3.1.3 **Cell culture products**

Product	Company	Catalog No.
96-well flat bottom with lid	TPP®	92096
96-well U-bottom with lid	Sigma Aldrich	M9436-100EA
24-well flat bottom with lid	Greiner bio-one	622160
12-well flat bottom with lid	BD	353043
6-well flat bottom with lid	Thermo Scientific	140675
50 ml conical tubes	Falcon	352070
15 ml conical tubes	Falcon	352096
5 ml round-bottom polypropylene test tubes	BD	352008

5 ml round-bottom polypropylene test tubes w. cell strainer	BD	352235
serological pipettes: 5, 10 and 25 ml, sterile	Greiner bio-one	606180 607180 760180
40 µm cell strainer	BD	
Cryovial, 2 ml sterile	Sigma Aldrich	V5760-500EA
Freezing Container, "Mr. Frosty"		
Safe lock tubes: 0.5, 1.5 and 2 ml	Eppendorf	
Filter tips: 20, 200, 1000 µl	Steinbrenner	SL-GPS-L10, L250, L1000
Neubaur Zählkammer		
Cell culture flasks T75	Sigma Aldrich	C7231-120EA
Syringe 1 ml	BD	
LeucoSep tubes	Greiner Bio-one	

3.1.4 **Cell culture media**

Product	Company	Catalog No.
HEPES Buffer (1M)	Sigma Aldrich	H0887
MEM NEAA (100x)	Gibco	11140-035
UltraPure™ EDTA (0.5M, pH 8.0)	Gibco	15575
sodium pyruvate (100 mM)	Gibco	11360-039
2-βMercaptoethanol (50 mM)	Gibco	31350
RPMI Medium 1640 (1x) + GlutaMAX™	Gibco	61870-010
DPBS (1x), without Mg^{2+}/Ca^{2+}	Gibco	14190-094
MEM-α Medium (1x)	Gibco	22561-021
X-Vivo 20	Lonza	BE04-448Q
Ficoll	Sigma Aldrich	
Fetal Bovine Serum	PAN Biotech GmbH	3702-P260718
Bovin serum albumin	Sigma	7030-50G
Penicillin/ Streptomycin	PAA	P11-010
Dimethylsulfoxid (DMSO)	Merck	109678
0.4 % Trypan blue solution	Sigma Aldrich	T8154
Dimethylsulphoxide Hybrid Max (DMSO)	Sigma Aldrich	472301-100ML

3.1.5 **Kits**

Product	Company	Catalog No.
BCA™ Protein Assay Kit	Thermo Scientific	23225
Bioplex cytokinbe reagent kit		
Bioplex®Cell lysis kit	Bio-Rad	171-304011
Bioplex® TGF-β1 Set	Bio-Rad	171-V4001M
Bioplex® TGF-β Standard	Bio-Rad	171-X40001
Bioplex , mouse 23-Plex Panel	Bio-Rad	M60-009RDPD
FoxP3/ Transcription Factor Fixation/ Permeabilisation Concentrate and Diluent	eBioscience	00-5521-00
Perm/Wash Buffer (10x)	eBioscience	00-8333-56
Cellscript T7 mScript™ Standard mRNA Production System	Cellscript	C-MSC100625

3.1.6 **Antibodies**

Primary antibodies	Fluorochrom	Clone	Company	Catalog. NO
CD11b	APC Cy7	M1/70	BD	557657
CD11b	APC	M1/70	BD	553312
Gr-1	PE Cy7	RB6-8C5	BD	552985
Ly6C	FITC	AL-21	BD	553104
Ly6C	APC	AL-21	BD	560595
PD-L1	APC	MIH5	BD	564715
PD-L1	BV421	MIH5	BD	564716
CD45.2	PerCp Cy5.5	1O4	BD	552950
CD3	PerCp Cy5.5	145-2C11	BD	551163
CD4	PE cCy7	RM4-5	BD	552775
CD8	APC Cy7	53-6.7	BD	557654
CD8	APC Cy7	YTS156.7.7	Biolegend	126620
CD25	APC Cy7	PC61	Biolegend	102026
CD25	APC	PC61	BD	557192
FoxP3	FITC	FJK-16s	eBioscience	11-5773-82
TCR/ CD247	PE	K25-407.69	BD	558448
PD-1/ CD279	BV421	J43	BD	562584
CD69	APC	H1.2F3	BD	560689

3.1.7 **Human/mouse reagents**

Primary antibodies	Fluorochrom	Clone	Company	Catalog No.
NOS Detection Kit	FITC-channel (488 nm)	production of chemical reaction	cell technologies	NOS200-2
anti-h/m Arginase 1	APC	MAB58681	R&D	IC5868A
FcR Blocking Reagent			Miltenyi	130-059-901

3.1.8 **Chemicals and biological reagents**

Product	Company	Catalog No.
7-AAD	BD	51-68981E
recombinant murine GM-CSF	Prospec	Cyt-222
Carboxyfluorescein succinimidyl ester (CFSE)	Biolegend	423801
Heparin-Natrium-25000 Units	Ratiopharm	PZN-3029843
Isofluran		
RBC Lysis Buffer (10x)	Biolegend	420301
Fetal bovine serum (FBS),	Gibco	10082147
Freund's Adjuvant, Complete	Sigma	F5881

3.1.9 **Solutions**

Solution	Ingredients
Freezing medium 1	60 % FBS 40 % X-VIVO 20
Freezing medium 2	75 % FBS 25 % DMSO
MACS buffer	1x PBS 1% FCS 0.5 mM EDTA
Primary cell culture medium	1x RPMI 10 % FCS 100 U/ml Penicillin, 100 µg/ml Streptamycin 1mM Sodium pyruvate 1x Non-essential amino acids 0.5 mM ß-Mercaptoethanol
FACS buffer	1x PBS 2% FBS 0,2 % NaN_3 2mM EDTA

3.1.10 **Routine laboratory material**

Product	Company	Catalog No.
Needle (27G)	neolab	194210020
Needle (23G)	BD	300800
Needle (25G)	BD	300400
6.5 mm Transwell® with 3.0 µm Pore Polycarbonate Membrane Insert	Corning	3415
Pipets: 2-20 µl, 20-200 µl, 200-1000 µl	Rainin	L-20XLS+, L-200XLS+, L-1000XLS+
Object carrier Superfrost plus	R. Langenbrinck	03-0060

3.1.11 **Laboratory equipment**

Equipment	Name	Company
Cell culture incubator	Hera Cell	Heraeus
Centriguges		
	Laborfuge 400R	
	Laborfuge 40R	Heraeus
	Biofuge primo R	
	Varifuge K	
Microplate Reader	Tecan infinite M200	Tecan
Flow cytometer	FACS Canto II, 8 colours	BD
Laminar flow hood	Hera safe	Thermo Electron Cooperation
Refrigerator (-20 °C)	Premium	Liebherr
Refrigerator (-80 °C)	HeraFreeze	Heraeus
Fridge		Liebherr
Ice machine		
Magnetic stirrer	RCT basic	IKA Werke
Microscope	DMIL	Leica
N2 tank		
pH meter	766	Calimatic
Vortexer	REAX top	Heidolph
Vortexer	Vortex Genie 2	Scientific Industries
Balance	BP 3100P	Sartorius
Water bath	DC3	HAAKE, GFL

3.1.12 **Software for data analysis**

Product	Company
Flow Jo (Version 7.6.1)	Tree Star, Inc., Ashland, USA
GraphPad PRISM (Version 5)	GraphPad Software, Inc., San Diego, USA

3.2 Methods

3.2.1 Determination of cell numbers

To distinguish dead from live cells, an aliquot of cell suspension was diluted 1:10 with trypan blue. Cell numbers were determined by using a Neubauer counting chamber and the total number of cells per mL was calculated by the formula:

(Counted cell number / number of counted chambers) x 10^4 x dilution factor.

3.2.2 Organ preparation and single cell suspension

Mice were sacrificed by cervical dislocation for organ preparation. Cell suspensions from spleens, BM, LNs and skin tumor were prepared and adjusted to 1x10^6cells/100µL in cell culture medium or respective buffer according to the assay.

Spleen (SP)

Mouse spleens were collected in a 15 mL falcon tube with 5 mL PBS. Single cell suspension was prepared by smashing the spleen with a plunger through a 40 µm cell strainer. Single cell suspension was washed with PBS at 1400 rpm for 7 min. Erythrocytes were depleted with 2 mL lysis buffer followed by 3 min of incubation at RT. To stop the reaction cells were washed with 10 ml PBS before cells were counted and resuspended in cell culture medium or 1x PBS dependent on the following assay.

Bone marrow (BM)

Femur and tibiae from the same mouse were cut at both ends. BM was flushed out with PBS using a syringe with a 23G needle. Cells were filtered through a 40 µm cell strainer and washed with PBS at 1400 rpm, for 7 min. Red blood cells were lysed with 2 mL lysis buffer for 3 min at room temperature (RT). PBS was used to stop the reaction and cells were washed at 1400 rpm for 7 min. Pellet was resuspended in appropriate buffer for further analysis.

Lymph nodes (LN)

Lymph nodes from the inguinal, axillary and head region were extracted. LN were smashed between two object slides and filtered through a 40 µm cell strainer. The strainer was then washed with PBS to collect all cells. The cells were washed with PBS at 1400 rpm, 7 min and resuspended in PBS for flow cytometry.

Skin tumor (Tu)

The isolated skin tumors from melanoma-bearing mice were weight and then smashed through a 40 µm cell strainer by a plunger into a 50 mL falcon tube. After the depletion of the erythrocytes, cells were washed with PBS at 1400 rpm for 7 min and resuspended in an appropriated buffer for further analysis.

3.2.3 Flow cytometry analysis

Mice were sacrificed 10 days after the last vaccination. Cell suspensions from SP, BM, LN and skin tumor were prepared and adjusted to $1x10^6$cells/100ul in staining buffer (PBS with 0.5% BSA and 0.1% sodium azide). Fluorochrome-conjugated antibodies were added for 30 minutes at 4C in the dark. Acquisition was performed by eigh-color flow cytometry using FACS Canto II with FACSDiva software (both from BD Biosciences). The compensation control was performed with BD CompBeads set (BD Biosciences) using the manufacturer's instruction. FlowJo software (Tree Star, Ashland, OR) was used to analyze at least 200,000 events. Data were expressed as dot plots.

3.2.4 Surface staining

$1x10^6$ cells were transferred into a 96 flat-bottom plate and centrifuges at 1000 rpm for 7 min. The supernatant was discarded and the pellet was resuspended in FACS buffer with Fc-blocking reagent for 10 min at 4 °C. Cells were washed with 100 µl FACS buffer and centrifuged (1000 rpm, 7 min). The pellet was stained with fluorochrom-conjugated monoclonal antibodies against surface antigens. After incubation of 30 min at 4 °C cells were centrifuged (1000 rpm, 7 min), washed twice with 200 µL FACS buffer and measured with FACSCanto II (BD) using the BD Diva Software V.6.1.1. At least 200,000 events for $CD3^+$ in Sp, LN, BM were acquired and at least 200,000 for $CD45^+$ leukocytes in tumor cell suspensions, respectively. FlowJo software 7.6.1 (Tree Star) was used for dot plots or histograms.

3.2.5 Intracellular staining

For intracellular staining cells were incubated in 100 µl of Fixation/ Permeabilization solution (1:4 dilution) (eBioscience) for 45 min at 4 °C and subsequently washed twice with 200 µl 1x Perm/ Wash buffer (ebioscience) before fluorescently labeled antibodies against intracellular antigens were added. After 30 min incubation at 4 °C, cells were washed with 1x Perm/ Wash buffer resuspended in 100 µl of FACS buffer and measured by flow cytometry (FACSCanto II from BD Biosciences). FlowJo software 7.6.1 (Tree Star) was used for data analysis and shown as dot plots and histograms.

3.2.6 **Tetramer staining**

The class II and Class I MHC tetramers listed below were kindly provided by NIH tetramer core facility, NIH Tetramer Core Facility; Emory University; 954 Gatewood Road; Atlanta, GA, USA.

Class II MHC biotinylated monomers were delivered by NIH and further treated with streptavidin-APC (PJ27S; from Prozyme) for tetramerization, directly prior to use. According to NIH protocols, 17.4 µL Streptavidin-APC (1 mg/mL) was added to 100ug of monomer solution every 10 min for a total of 10 times. In addition, a human CLIP peptide as negative control reagent was provided. Tetramer staining was performed by incubating collected and washed *in vitr*o restimulated cells with 1:200 dilution of assembled tetramer, and incubated either at 37°C or RT for 2 hours. Afterwards, cells were washed once with PBS and then surface markers CD4- PE-Cy and CD8-APC Cy7 were stained for 30 min on ice. 7-Amino-Actinomycin D (7-AAD) was added for 10 more minutes for exclusion of nonviable cells in flow cytometric analysis.

Class II MHC biotinylated monomers:

1. TRP-$1_{(111\text{-}128):}$ H2-I-Ab: CRPGWRGAACNQKI
2. $Tyr_{(99\text{-}117)}$ H2-I-Ab: NCGNCKFGFGGPNCTEKRV

MHC Class I –PE labelled tetramers:

1. H-2D(b) KVPRNQDWL –PE labelled
2. H-2D(b) AAPDNLGYM- PE labelled PE
3. H-2D(b) SSMHNALHI- PE labelled PE
4. H-2K(b) SVYDFFVWL – PE labelled PE

3.2.7 **Bioplex protein array Luminex**

For the detection of multiple cytokines and chemokines in the lysates of skin tumor and Luminex assay (23-Plex Panel, Cat # M60-009RDPD, Bio-Rad) was performed. Bio-Plex Multiplex immunoassays use Luminex magnetic beads for the quantification of biologically relevant target. Luminex assay is based on capture antibodies that are directed against the antigen and conjugated with beads. The reaction is detected by antibodies coupled to horseradish peroxidase. The advantage of this method is that several factors can be measured simultaneously in the same sample.

Skin tumors and metastatic LN were isolated and one small piece (3 mm^2) of the tumor was snap frozen in liquid nitrogen. To prepare lysates of the tissue, 250 µL lysis buffer for tumor was added to the frozen samples. The tissue was mechanically smashed in an Eppendorf

tube then frozen at -80 °C for 10 min. Lysates were thawed on ice and the rest of the tissue was broken down in the ultrasonic bath for 20 min at 4 °C. Lysates were again frozen at -80 °C for 20 min and thawed on ice before they were centrifuged at 1300 rpm for 20 min at 4 °C. Supernatant was transferred into a new Eppendorf tube and protein concentration was determined by BCA assay. Samples were diluted with Bioplex Sample Diluent to a concentration of 1 mg/ml total protein. 23 different cytokine and chemokine concentration were finally determined with a Bioplex Protein Array according to the manufacturer´s instructions. Bio-Plex Manager™ software (Version 6.0) was used for the acquisition and data analysis.

3.2.8 **Statistical analysis**

Statistical analyses were performed using GraphPad Prism software Statistical analysis was conducted with 1-way ANOVA or an unpaired two-tailed Student's t test. Significance of the differences was assessed by Bonferroni multiple comparison posttest. Survival curves were generated using the product limit (Kaplan-Meier) method and comparisons were conducted using the log-rank (Mantel-Cox) test. A value of $P < 0.05$ was considered statistically significant. (*, $p< 0.05$; **, $p< 0.01$; ***, $p<0.001$).

3.2.9 **Ultra-low dose treatment of paclitaxel**

Taxol stock-infusion solution (6mg/ml) was diluted 1:60, in sterile 1XDPBS. A dose of 1mg/kg per mouse was injected i.p. three times with 7 days interval.

3.2.10 **In-vivo killing assay**

BMDCs were washed twice with PBS. Cells were re-suspended at $2.5x10^6$/100 μL in BIO-RAD electroporation (EP) buffer. Cells were mixed with mRNA (5 ug/$2.5x10^6$) and EP at 400V, 0.9 ms using BTX ECM 830 instrument. Following EP, cells were transferred to 10ml DCs medium containing 20 ng/mL GM-CSF. Control groups were washed once with Opti-MEM, resuspended in 2 mL of Opti-MEM and incubated for 2 hours with 30 μg/ml peptide. For vaccination, cells were washed 3 times with PBS, resuspended at 0.5x106/200 μL in PBS and injected I.P. ($0.5x10^6$ per mice) 3 times in 7 days intervals. Ten days following last vaccination, target cells consisting of splenocytes from B6.SJL (CD45.1+) mice, labeled with CFSE at various concentrations give concentrations, loaded with specific peptides and injected intravenously (I.V.) $20x10^6$/mice at 1:1:1 ratio. 14-18 hours later, spleens were excised, washed twice with PBS and suspended in 2ml FACS buffer (PBS-/-, 0.1% sodium azide, 0.5% BSA). Cells ($4x10^6$) were transferred into FACS tubes, labeled with anti CD45.1

Ab and analyzed by flow cytometry for specific killing. The specific killing in % was calculated as: 1-[(CFSEHigh/low/CFSEint)] x100.

3.2.11 **In vitro killing assay**

^{35}S labeled methionine is incorporated into melanoma tumor /target cells and released into the supernatant by lysis of tumor-specific T killer cells upon co-culture. The amount of ^{35}S labeled methionine release into the supernatant by lysed tumor cells (measured in CPM by Beta-counter) correlates with the specific killing capacity of the CTLs. The specific killing in % was calculated as: [(CPM of sample- CPM spontaneous release/CPM total release – spontaneous release)] x100.

3.2.12 **MHC binding assay**

Culture of the murine lymphoma mutant cell line RMA-S at reduced temperature (19-33 degrees C) promotes assembly of MHC class I , and results in a high level of cell surface expression of H-2/beta 2-microglobulin complexes that do not present endogenous antigens, and are labile at 37C. They can be stabilized at 37C by exposure to specific peptides known to interact with H-2K^b or D^b. Candidate MHC class I restricted peptides were tested for H-2K^b or D^b binding and subsequent MHC stabilization on RMA-S cells as previously described with minor changes. Briefly, RM-s cells were suspended in ~20ml RPMI medium (Gibco +garamycin (no serum)) in a 50ml tube, incubate at 26C for 1.5hr in incubator (on shaker, loose 50ml lid). Candidate peptides (H-2 Db- and Kb-restricted peptides) were diluted at different concentrations in OptiMEM medium in 96 well plates. Afterwards, 100ul of pre-incubated RMA-s cells were seeded (2x10^5 cells/well) into 96 well plate with prediluted peptides. After 16-20 of incubation at 37°C, 5% CO2 cell incubator, cells were stained with Anti mouse MHC Class I (H-2Kb)-APC (eBioscience 17-5958, 0.06ug/sample, 0.3ul), and Anti Anti mouse MHC Class I (H-2Db)-FITC (eBioscience 11-5999, 0.25ug/sample, 0.5ul) and analyzed by flow cytometry.

3.2.13 **Proliferation assay**

MHC class II–restricted MAAs were tested in vitro proliferation assay for antigen specific CD4+ T cell induction. Therefore, C57/BL/6 mice were vaccinated with respective peptide emulsified in complete Freund's adjuvant (CFA, Sigma-Aldrich). Briefly, emulsion was prepared by mixing respective peptide diluted to 1 mg/ml in PBS -/- (without Ca and Mg) and mixed with CFA at ratio of 1:1. Each emulsion was stored at 4°C until further use.

3 mice per peptide/CFA emulsion were immunized intra footpad (in both hind legs) with 50ul of emulsion (25ug peptide) in each footpad. 11 days later draining lymph nodes (popliteal lymph nodes) were excised and re-stimulated in vitro with 30ug/ml of peptide or irrelevant class-II peptide $OVA_{(323-339),}$ respectively. Following incubation for 72 hours, cells were pulsed with ^{3}H-thymidine for 18 hours. Specific peptide proliferation was detected by the thymidine uptake.

3.2.14 **Restriction-free (RF) cloning**

It is a simple, universal method to precisely insert a DNA fragment into any location within a circular plasmid, independent of restriction sites, ligation, or alterations in either the vector or the gene of interest. The technique uses a PCR fragment encoding a gene of interest as a pair of primers in a linear amplification reaction around a circular plasmid. In contrast to QuickChange™ site-directed mutagenesis, which introduces single mutations or small insertions/deletions, RF cloning inserts complete genes without the introduction of unwanted extra residues. The absence of any alterations to the protein as well as the simplicity of both the primer design and the procedure itself makes it suitable for high-throughput expression and ideal for structural genomics[163–165]

Detailed information of gene assembly and cloning of the template MHC class I-hß2m chimeric construct (with H2kb and TLR4 anchor, respectively) and MHC class II chimeric IAb construct assembling were described in detail elsewhere[144,146–148]. Shortly, constructs were embedded in pGEM-4Z vector backbone. An XbaI-BamHI fragment encoding the full leader peptide of human-ß2m, the human-gp100 (25-33) peptide and the 5' part of the flexible linker $Gly4Ser(Gly3Ser)^2$ was cloned essentially as described[145] For creating the intact constructs encoding peptide-hb2m-anchor, all corresponding fragments were modularly cloned in a single step.

Template constructs such as the hgp100-Kb anchor- and hgp100-TLR4 anchor construct and class II–OVA-IAb constructs were kindly provided by Prof. Lea Eisenbach. For this study, the OVA peptide DNA-sequences of the template constructs were exchanged with MAA-candidate DNA-sequences by the restriction free (RF) cloning. Megaprimers, encoding for whole length of respective MAA sequence and additional 25bp of plasmid vector sequence were designed and ordered from Sigma Aldrich. Restriction free cloning method was performed according to already established and previously published method[163–165]. Obtained DNA-construct sequences were verified by sequencing.

3.2.15 **Chimeric MHC class I- β2m-bi-functional constructs**

pGEM-T easy polymerase chain reaction (PCR) cloning vector was purchased from PROMEGA. pGEM-4Z 5'UT-eGFP-3'UT-A64 (pGEM-4Z) vector was kindly provided by Dr Eli Gilboa. This plasmid contains a 741-bp eGFP fragment from peGFP-N1 (Clontech, Westburg, Leusden, the Netherlands) flanked by the 5' and 3' UTRs of Xenopus laevis β-globin and 64 A–T bp. mRNA Transcription is controlled by a bacteriophage T7 promoter.

The β2m-TLR4 and β2m-Kb backbones were covalently linked to the tumor-associated peptides as previously described[146–148]. Briefly, the mouse TLR4 (mTLR4) sequence (GenBank accession number AF 110133) was aligned with the human TLR4 (hTLR4) transmembranal and cytoplasmic domains (GenBank NM 138554) to identify, by similarity, the mTLR4 TC domains. The TC portions of mTLR4 were cloned by RT-PCR from mRNA of RAW cells with the forward primer-5’ CCG TCG ACC ACC TGT TAT ATG TAC AAG ACA ATC 3’ and the reverse primer- 5’ CGC GCG GCC GCA CTG GGT TTA GGC CCC AG 3’. The full length human β2m (hβ2m) was previously cloned in our lab from Jurkat cells by RT-PCR. All products, together with the peptide sequence were cloned in a single step into pGEM-4Z plasmid.

3.2.16 **In-vitro mRNA transcription**

Appropriate plasmids were linearized using SpeI restriction enzyme. One µg of linear plasmid was used to transcript in-vitro mRNA using AmpliCap-MaxTM T7 High Yield Message Maker Kit (EPICENTRE Biotechnologies, Madison, U.S.A.). The concentration and quality of the mRNA were assessed by spectrophotometry and agarose gel electrophoresis

3.2.17 **Generation of DC from murine BM cells**

Generation of murine bone marrow derived DC was described by Lutz et al.[166,167] and used with minor modifications. Briefly, bone marrow cells from femurs and tibiae of 4-6 weeks old C57Bl/6, female mice were cultured in RPMI medium supplemented with 10% heat-inactivated FCS, 50 uM 2-mercaptoethanol, 2 mM L-glutamine, combined antibiotics and 200 U/ml rmGM-CSF (Prospec, Israel). On day 8 non - adherent cells were harvested and further cultured in fresh medium containing 100 U/ml rmGM-CSF for 24 hours. DCs were matured by addition of 1ug/ml of lipopolysaccharide (LPS, Sigma, Saint Louis, MI) for another period of 24 hours. Non-adherent cells were analyzed by FACS and found to express typical characteristics of immature and mature DCs ($CD11c^+$, $CD80^+$, $CD86^+$, MHC class II^+).

3.2.18 **mRNA electroporation of DC**

Cells (DC2.4 or BMDCs) were harvested, centrifuged at 1000 rpm and 18°C for 10 minutes, washed twice with Opti-MEM medium Reduced Serum Medium (Cat. No.: 31985070, Gibco - Life Technologies) and counted. Cell titer was adjusted to $16.67X10^6$ cells/ml in Opti-MEM. 150 µl of cell suspension ($2,5X10^6$ cells) were transferred into 0.2 cm–gap Gene Pulser/MicroPulser Electroporation Cuvettes (Cat. No.: 1652086, Bio-Rad) and electroporated with 5 µg of mRNA per construct, with one pulse of 400 mV and 1 msec, using the Gene Pulser Xcell Eukaryotic System electroporator (Cat. No.: 1652661, Bio-Rad). Immediately after electroporation, cells were transferred into 50 ml CELLSTAR polypropylene tubes containing 5 ml warm complete growth medium composed of RPMI-1640 (Cat. No.: 11875093, Gibco - Life Technologies) supplemented with 10% heat inactivated FBS (Cat. No.: 10082147, Gibco - Life Technologies) and incubated at 37°C for 6 hours under shaking. After incubation, cells were washed with 1X DPBS and centrifuged at 1000 rpm and 18°C for 10 minutes. Cells were then resuspended in 1 ml 1X DPBS (final cell concentration $2,5X10^6$ cells/ml) and used for mouse vaccination.

In order to assess the constructs expression and the quality of the generated DC vaccines, 100 µl of each vaccine were stained at 4°C for 30 minutes with 1 µg/ml PE-anti-human β2-microglobulin (clone 2M2, Cat. No.: 316306, BioLegend, San Diego, CA, USA), 2 µg/ml APC-anti-mouse MHC class II (I-A/I-E) (clone M5/114.15.2, Cat. No.: 17-5321-82, eBioscience, San Diego, CA, USA), 2 µg/ml PE-Cy7-anti-mouse CD86 (clone GL1, Cat. No.: 560582, BD Pharmingen), 5 µg/ml FITC-anti-mouse CD80 (clone 16-10A1, Cat. No.: 11-0801-82, eBioscience, San Diego, CA, USA), and 2 µg/ml APC/Cy7-anti-mouse CD11c (clone N418, Cat. No.: 117324, Biolegend, San Diego, CA, USA). After incubation, 500 µl of 1X DPBS were added and cells were centrifuged at 1000 rpm and 4°C for 10 minutes. Cell pellets were resuspended in 200 µl of 1X DPBS and samples were analyzed using the BD FACSCantoTM II and FACSDiva software (both from BD Biosciences). Flow cytometry results were analyzed using FlowJo v8.7 (Tree Star, Ashland, OR). Data were expressed as histograms.

3.2.19 **Peptides**

Synthesized and HPLC purificated peptides were kindly provided by Prof. Stefan Eichmüller, GMP & T cell Therapy Unit, DKFZ, Heidelberg, Germany.

MHC Class I peptides

- H2-SYFPEITHI Kb/Db-prediction

Peptides	Sequence	Designation
mTRP-1 $_{455-463}$ –variant 1	*TAPDNLGYM	H2-Db
mTRP-1 $_{455-463}$ –variant 2	*AAPDNLGYM	H2-Db
mTRP-1 $_{455-463}$ –native	*TAPDNLGYA	H2-Db
#6: mTyr $_{360-368}$	**SSMHNALHI**	**H2-Db**
#7: mTyr $_{255-264}$	**RHPENPNLL**	**H2-Db**
#8: mTyr $_{118-126}$	**LIRRNIFDL**	**H2-Db**
#9: mTyr $_{445-452}$	LGYDYSYL	H2-Kb
#10: mTyr $_{133-140}$	KFFSYLTL	H2-Kb

*Sequence published by Dougan *et al* , *Cancer Immunol Res 2013*

MHC Class II peptides

- IEDB MHC class II-H2-I-Ab-prediction

Peptides	Sequence	Designation
#122: mTRP1 $_{111-128}$	*GTCRPGWRGA ACNQKILT	H2-IAb
#123: mTRP-1 $_{110-129}$	*CGTCRPGWRG AACNQKILTV	H2-IAb
#129: mTYR $_{403-422}$	RHRPLLEVYPEA NAPIGHNR	H2-IAb
#130: mTYR $_{99-117}$	NCGNCKFGFGG PNCTEKRV	H2-IAb
#175: hTRP-2 $_{88-102}$	**RKFFHRTCKC TGNFA	H2-IAb

*Sequence published by Muranski *et al*, *BLOOD, 2008*

**Sequence published by Kianizad *et al*, *Cancer research, 2013*

3.2.20 **Peptide loading of DC**

LPS-maturated BMDCs were harvested, centrifuged at 1000 rpm and 18°C for 10 minutes, washed twice with Opti-MEM Reduced Serum Medium and counted. Cell titer was adjusted to 25X10^6 cells/ml in Opti-MEM medium. 100 µl of cell suspension (2,5X10^6 cells) were transferred into 50 ml CELLSTAR polypropylene tubes containing 5 ml of Opti-MEM medium, and were pulsed with 30 µg/ml of peptides Trp-1$_{455-463}$ (AAPDNLGYM), Tyr$_{360-368}$ (SSMHNALHI), the combination of Trp-1 and Tyr (Mix), and OVA$_{257-264}$ (SIINFEKL), at 37°C for 2-3 hours under shaking. After incubation, cells were washed with 1X DPBS and centrifuged at 1000 rpm and 18°C for 10 minutes. Cells were then counted (final cell concentration 2.5X10^6 cells/ml), resuspended in 1 ml 1X DPBS and used for the mice vaccinations.

3.2.21 **Immunization of mice (DC vaccination)**

BMDCs were either electroporated with 5ug mRNA (per respective construct) or loaded with 30µg/mL of respective peptides for 2 h at 37°C. Cells were washed three times with PBS and resuspended at 2.5x10^6/ml in PBS. In all experiments, mice were vaccinated intraperitoneal (I.P.) using 200 µl cell suspension containing either 1 x10^6 DC or 0.5 x10^6 DC; three times with 7 days intervals.

4 Results

4.1 Selection process of potential MHC class I and class II restricted melanoma associated antigens (MAAs)

Tyrosinase (Tyr), tyrosinase-related protein 1 (TRP-1) and tyrosinase-related protein 2 (TRP-2) overexpressed in malignant melanoma were chosen as candidate proteins for this study. Eight MHC class I restricted peptides were selected for further testing after literature research and SYFPEITHI database H2-Kb/H2-Db binding prediction. Similarly, five class II candidates were selected after literature research and IEDB database MHC class II-IAb binding prediction (**Table 3**).

Table 2: Summary of candidate peptides: Eight MHC class I restricted MAA candidate peptide sequences and 5 MHC class II restricted candidate peptides

MHC Class I peptides

- H2-SYFPEITHI Kb/Db-prediction

Peptides	Sequence	Designation
mTRP-1 $_{455-463}$ –variant 1	*TAPDNLGYM	H2-Db
mTRP-1 $_{455-463}$ –variant 2	*AAPDNLGYM	H2-Db
mTRP-1 $_{455-463}$ –native	*TAPDNLGYA	H2-Db
#6: mTyr $_{360-368}$	**SSMHNALHI**	**H2-Db**
#7: mTyr $_{255-264}$	**RHPENPNLL**	**H2-Db**
#8: mTyr $_{118-126}$	**LIRRNIFDL**	**H2-Db**
#9: mTyr $_{445-452}$	LGYDYSYL	H2-Kb
#10: mTyr $_{133-140}$	KFFSYLTL	H2-Kb

*Sequence published by Dougan *et al* , *Cancer Immunol Res 2013*

MHC Class II peptides

- IEDB MHC class II-H2-I-Ab-prediction

Peptides	Sequence	Designation
#122: mTRP1 $_{111-128}$	*GTCRPGWRGA ACNQKILT	H2-IAb
#123: mTRP-1 $_{110-129}$	*CGTCRPGWRG AACNQKILTV	H2-IAb
#129: mTYR $_{403-422}$	RHRPLLEVYPEA NAPIGHNR	H2-IAb
#130: mTYR $_{99-117}$	NCGNCKFGFGG PNCTEKRV	H2-IAb
#175: hTRP-2 $_{88-102}$	**RKFFHRTCKC TGNFA	H2-IAb

*Sequence published by Muranski *et al*, *BLOOD, 2008*

**Sequence published by Kianizad *et al*, *Cancer research, 2013*

4.1.1 Testing of MHC Class I restricted candidate peptides

CTL in vivo assay

First, MHC class I candidate MAA-peptides were tested for their capacity to elicit a specific CTL response *in vivo* and *in vitro*. Therefore, mice were vaccinated 3 times (in weekly intervals) with respective MAA-peptide loaded onto bone marrow-derived DCs. 10-11 days later CTL *in vivo* killing assay and CTL *in vitro* killing assay were performed. **Figure 13** shows results of CTL *in vivo* killing assay. Vaccination of peptide loaded BMDCs resulted high specific killing for TRP1 variant 1, TRP1 variant 2 and Tyr #6, indicating that these

candidate MHC class I restricted peptides are able to elicit a specific CTL response in vaccinated C57BL/6 mice. TRP1.3 native and Tyr #9 showed moderate *in vivo* killing.

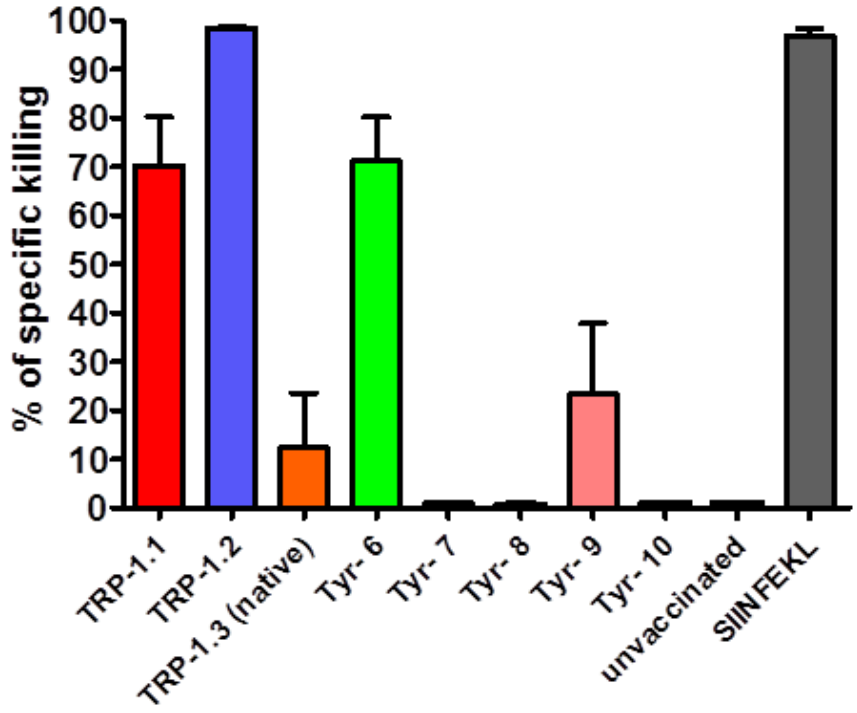

Fig. 13: CTL *in vivo* assay. Mice were injected i.p. with peptide loaded BMDCs (2 mice per group, 30µg/ml peptide, $1x10^6$ cells in 0.2 mL, 3 times, weekly intervals). 11 days after last vaccination, 30µg/ml of respective peptide was loaded onto splenocytes of B6/SJL mice, cells were CFSE labeled, and i.v. injected into vaccinated mice. 18 h later, splenocytes from vaccinated mice were isolated and checked for *in vivo* killing by FACS analysis (CD45.1 positive cells). Bar chart shows specific *in vivo* killing of respective peptide loaded CFSE-labeled splenocytes.

CTL in vitro killing assay

To ensure that induced CTLs in vaccinated mice are also able to specifically target and kill tumor cells, which overexpress MAAs such as TRP-1 and Tyr, CTL *in vitro* assay was performed. As specific target cells, the melanoma cell line B16F10.9, B16 melanoma cell line stably transfected with OVA (B16MO5) and the melanoma cell line established from skin tumors of *ret* transgenic mice (Ret) were used. Lewis lung carcinoma cells (D122), which do not express MAAs, were used as a negative control. For CTL *in vitro* assay, mice were vaccinated i.p. with peptide loaded bone marrow-derived DCs. 11 days later; CTL in vitro assay was performed. Afterwards supernatant was removed and specific target cell lysis by ^{35}S methionine release (with ß-counter) was calculated. Results of CTL *in vitro* assay (**Fig. 14**) revealed that respective CTLs (produced by vaccinated mice) of all three TRP-1 candidate peptides showed high specific killing of target tumor cells when compared with D122-negative control. Both Tyr peptides showed lower but still detectable specific lysis of

tumor cell line compared to D122 negative control. However, specific lysis after the stimulation with Tyr #9 peptide was slightly lower than that of Tyr #6 one. Therefore, the Tyr #9 peptide was excluded from further studies.

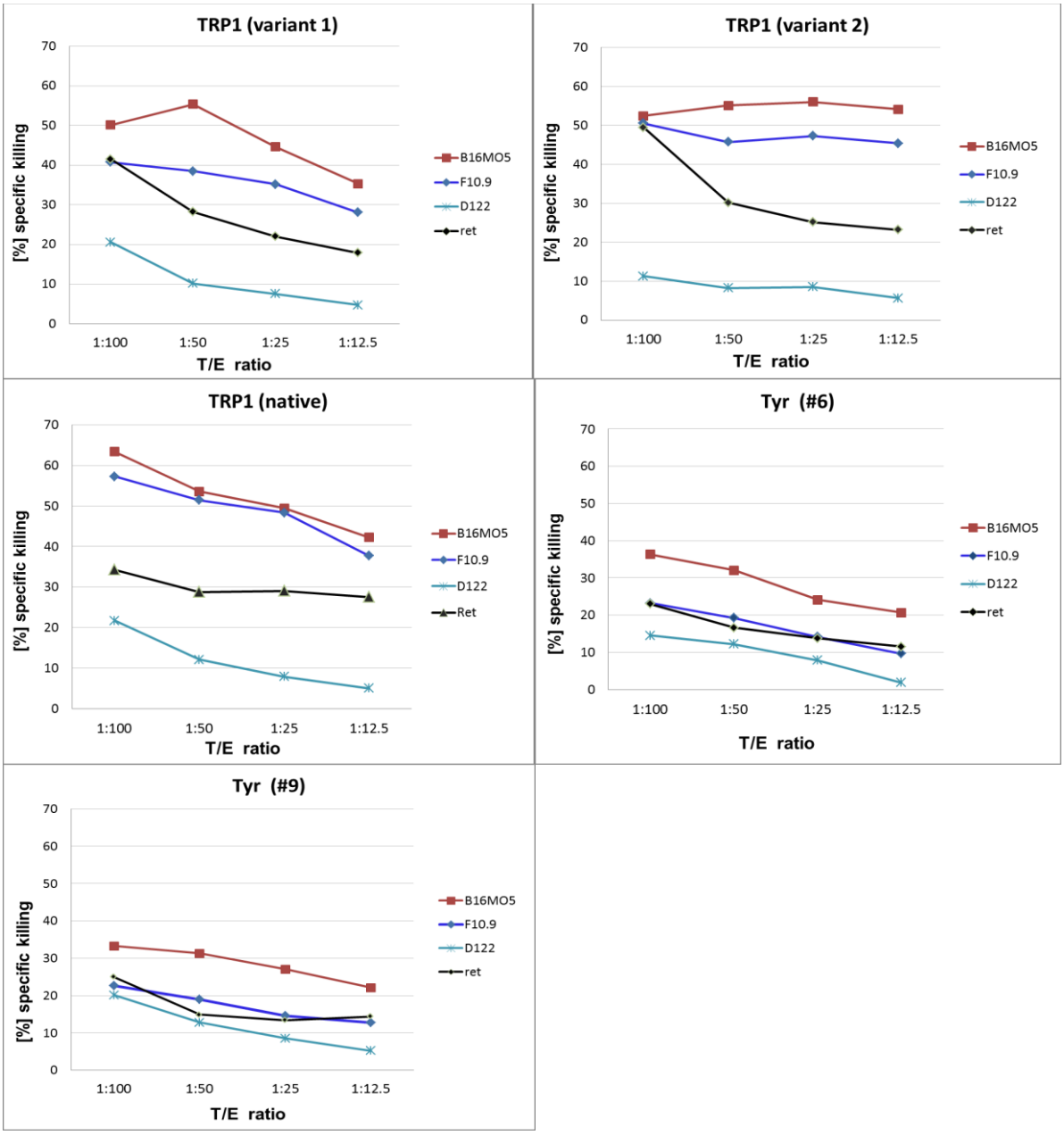

Fig. 14: CTL *in vitro* assay. Mice were vaccinated i.p. with peptide loaded BMDCs (3 mice per group, 30µg/ml peptide, $1x10^6$ cells in 0.2 mL) 3 times in weekly intervals. 10 days later, splenocytes from vaccinated mice were isolated and *in vitro* sensitized by peptide for 4 days at 37°C. Target tumor cell lines (B16MO5, B16F10.9, Ret and D122), were labeled for 10-12 hours with ^{35}S methionine. Afterwards supernatant was removed and specific target cell lysis by ^{35}S methionine release (with ß-counter) was calculated. Assay was repeated 2 times giving similar results.

4.1.2 MCH class II candidate peptide testing

Proliferation assay

Five MHC class II restricted peptides were tested for their ability to elicit a specific $CD4^+$ T cell response (**Table 3**) by *in vitro* proliferation assay. Therefore, wild type C57/BL6 mice were injected intro food pad (i.f.p) with complete Freund's adjuvant (CFA) /peptide emulsion and after 10 days, draining lymph nodes (popliteal LN) were excised and lymphocytes were tested for specific $CD4^+$ T cell proliferation after 72 h *in vitro* re-stimulation with specific (or irrelevant) peptide. As shown in **Fig.15**, class II restricted peptides TRP1 (122), TRP1 (123) and Tyr (130) and TRP2 (175) peptide were able to induce a specific T cell proliferation *in vitro*. Specific proliferation was detected by ^{3}H-labelled thymidine uptake, resulting in strong elevation of CPMs compared to control. These candidate peptides were then further subjected to the restriction free (RF) cloning to produce the respective IAb and CLIP constructs. Peptide Tyr (129) did not induce antigen specific proliferation and subsequent elevated CPM levels and was therefore excluded from further studies.

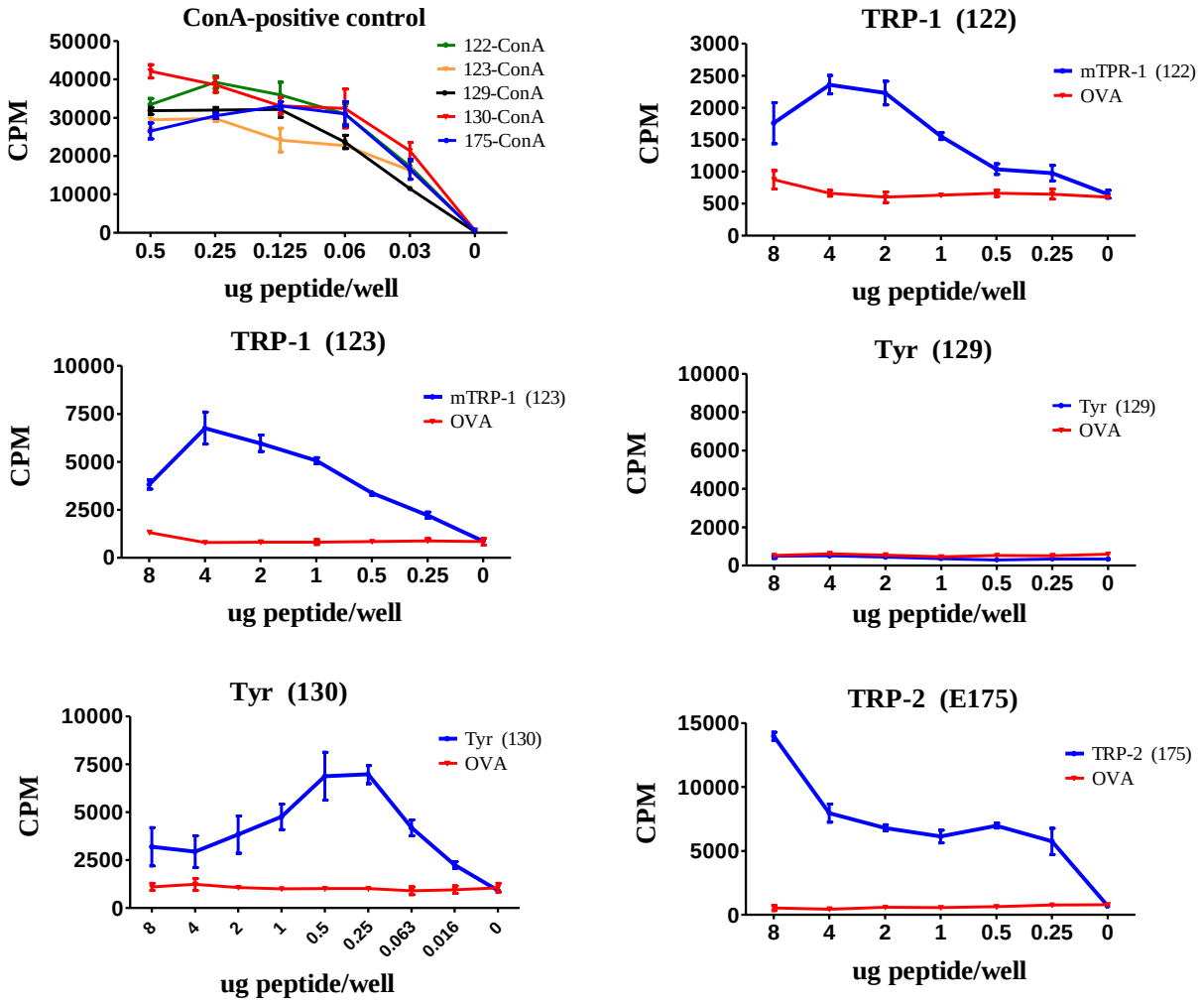

Fig. 15: MHC class II–restricted melanoma associated antigens were tested by in-vitro proliferation assay. C57BL/6 mice were vaccinated with peptide emulsified in complete Freund's

adjuvant. Ten days later, the draining lymph nodes were excised and lymphocytes were re-stimulated in-vitro with 30ug/ml of peptide $Tyr_{(99-117)}$ or irrelevant class-II peptide $OVA_{(323-339)}$, respectively. Following incubation of 72 hours, cells were pulsed with ^{3}H-labeled thymidine for 18 hours. Specific proliferation was detected by thymidine uptake, resulting in strong elevation of CPMs (blue curve) compared to irrelevant $OVA_{(323-339)}$ (red). Assay was repeated 3 times with similar results.

.

4.2 MHC class I and II chimeric construct expression kinetics

Cytoplasmic expression system based on mRNA electroporation (EP) was used to efficiently insert the class I (hß2m-peptide-Kb-anchor and hß2m-peptide-TLR4 anchor) and class II (IA-b-peptide-CD40 anchor) encoding polypeptide into DC2.4 (dendritic cell line). In vitro transcription was performed with T7 mScript Standard mRNA Production System (CellScript, Madison, WI 53713 USA). DC2.4 cells were washed twice with PBS and then adjusted to a cell concentration of 16.67 x 10^6 cells/mL. 150 µL cell suspension was mixed with 10 µg of in vitro transcribed mRNA and transferred into 2 mm gap electroporation cuvette and pulsed once for 0.9 ms. Afterwards, cells were immediately transferred into 5 ml culture medium and further cultured in cell incubator. Beta-2m-expression **(Fig. 16**) and I-Ab expression kinetics (**Fig.17**) were assessed after several time points by flow cytometry.

All selected class I constructs showed elevated surface expression levels for at least 48 h for Kb-anchor constructs and for at least 36 h for TLR4-anchor sequences, indicating slightly more stable expression kinetics of native Kb anchor.

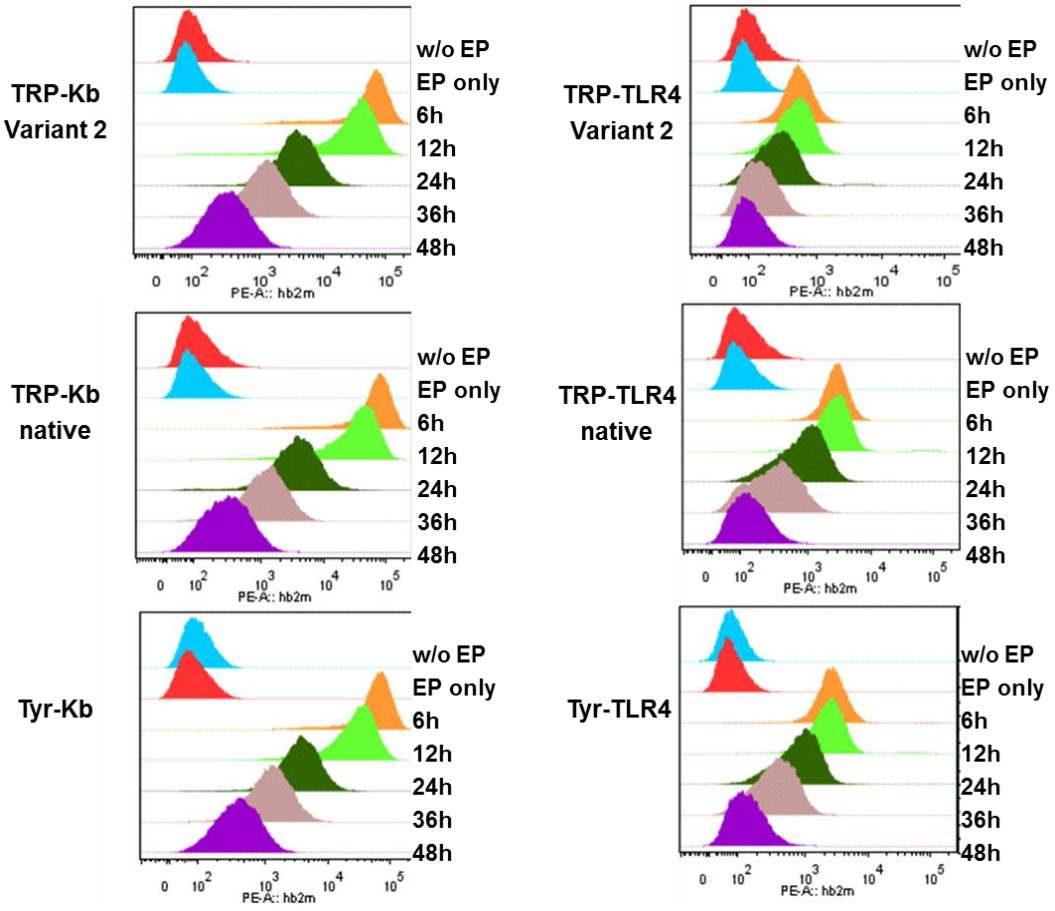

Fig. 16: Class I construct expression kinetics on DC2.4 cells. DC2.4 cells were washed twice with PBS and adjusted to a cell concentration of 16.67 x 10^6 cells/ml. 150 µL cell suspension was mixed with 10 µg of *in vitro* transcribed mRNA and transferred into 2 mm gap electroporation cuvette and pulsed once for 0.9 ms. Afterwards, cells were immediately transferred into 5 ml culture medium and

further cultured in cell incubator. Hb2m-expression were assessed after 6, 12, 24, 36 and 48 h by flow cytometry. All Kb anchor constructs showed elevated expression levels for at least 48 h. All TLR4 anchor constructs showed elevated cell surface expression for at least 36h

Class II constructs showed stable surface expression levels for TPP1 (122) IAb-construct and Tyr (130)–IAb-construct (**Fig.17**). TRP-2–IAb (175) and TRP1 (123)-IAb constructs did not show an elevation in IAb expression after the electroporation of DC2.4 cells even after several repeats of sequence verification, mRNA transcription and subsequent electroporation. These peptides were therefore excluded from further studies.

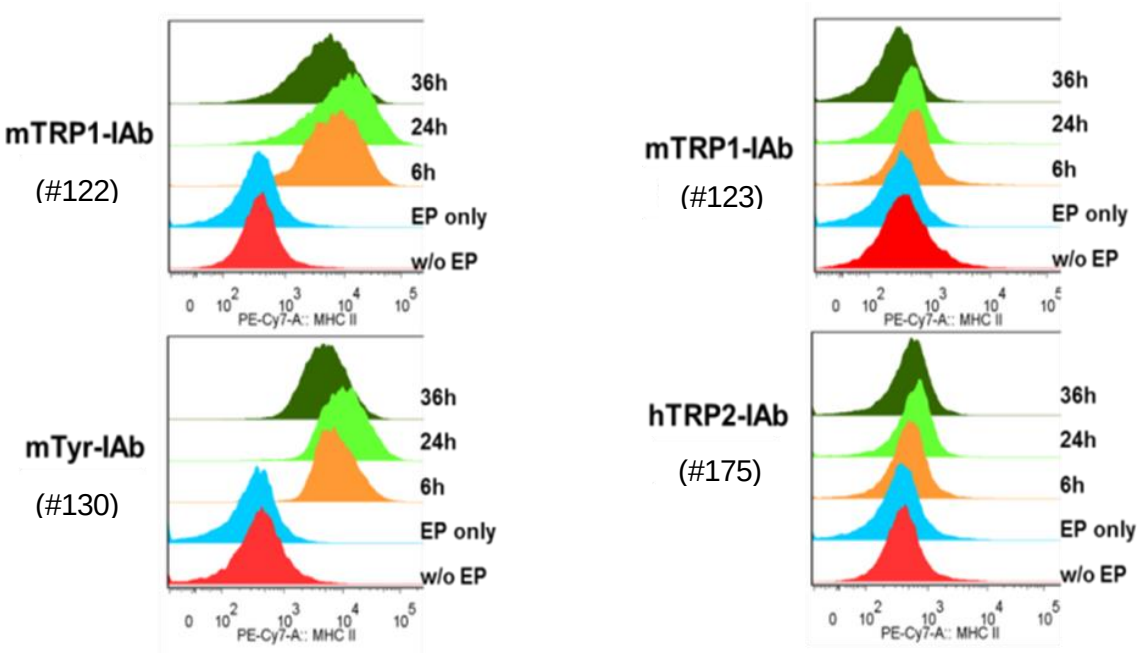

Fig. 17: Class II construct expression kinetics on DC2.4 cells. DC2.4 cells were washed twice with PBS and then adjusted to a cell concentration of 16.67 x 10^6 cells/mL. 150 µL cell suspension was mixed with 10 µg of in vitro transcribed mRNA and transferred into 2 mm gap electroporation cuvette and pulsed once for 0,9 ms. Then cells were immediately placed into 5 ml culture medium and further cultured in cell incubator. IAb-expression was assessed by flow cytometry after 6, 24 and 36 h.

4.3 *In vivo* and *in vitro* testing of selected constructs as mRNA-based-DC vaccines

4.3.1 Class I mRNA –based DC cell vaccine

Selected hb2m-Kb and -TLR constructs were tested for their capacity to elicit a specific CTL response in vivo and in vitro. Mice were vaccinated 3 times weekly with 1:1 mixture of hß2m-Kb and –TLR constructs (5 µg each) electroporated into BMDCs. CTL in-vivo killing assay and CTL in-vitro killing assay were performed 10 days later. **Fig. 18** shows results of CTL in vivo killing assay (3 mice per group). Vaccination with mRNA electroporated DCs resulted in high specific killing of CFSE-labelled and i.v. injected SJL- splenocytes for TRP-1 variant 2-vaccine (44/86/88% killing), for TRP-1 variant 2 vaccine (60/51/49% killing). A moderate killing was demonstrated for Tyr #6 vaccine (28/18/0% killing). These results indicate that tested MHC class I hß2m mRNA construct expression is long-lasting and able to elicit a specific CTL response in vaccinated C57BL/6 mice

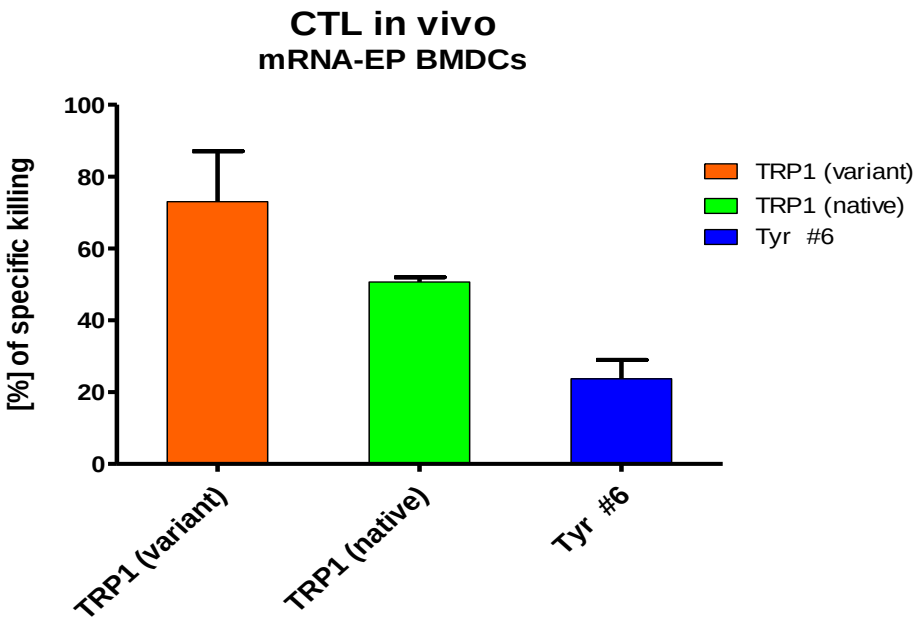

Fig. 18: CTL in vivo assay with mRNA electroporated BMDCs. Mice were i.p. injected with mRNA electroporated DCs (3 mice per group, 0,5 x10^6 cells in 0.2ml, 3 times, weekly intervals). 11 days after last vaccination, splenocytes of B6 /SJL mice were loaded with 30 µg/mL of respective peptide, labeled with CFSE and injected i.v. into vaccinated mice. 18 hours later, splenocytes from vaccinated mice were isolated and checked for in vivo killing by FACS analysis. Bar chart shows specific in vivo killing of respective peptide loaded CFSE-labeled splenocytes.

Previous results of CTL *in vitro* assay revealed that respective CTLs stimulated by both TRP-1 vaccines (**Fig. 19** (a,b) and Tyr vaccine (**Fig. 19** c) showed highly increased specific killing

of target tumor cells when compared to D122-negative control. Interestingly, the TRP-1 mRNA construct presenting the native TRP-1 MHC class I restricted sequence induced even higher CTL tumor cell killing capacity (B16-F10 (32%), MO5 (37%) and Ret (29%)) than TRP-1 variant 2 vaccine (B16-F10 (18%), MO5 (22%) and Ret (20%)). Tyr class I vaccine induced similar CTL tumor cell killing capacity (B16-F10 (18%), MO5 (26%) and Ret (20%)). Additionally, a possible killing induced by natural killer (NK) cells in the splenocyte cell population of vaccinated mice was analyzed by NK cell-dependent YAC-1 cell lysis. As shown in **Fig. 19** d the lysis of YAC-1 cells was similar to irrelevant control cell line (D122), indicating that there are almost no lysis mediated by NK cells.

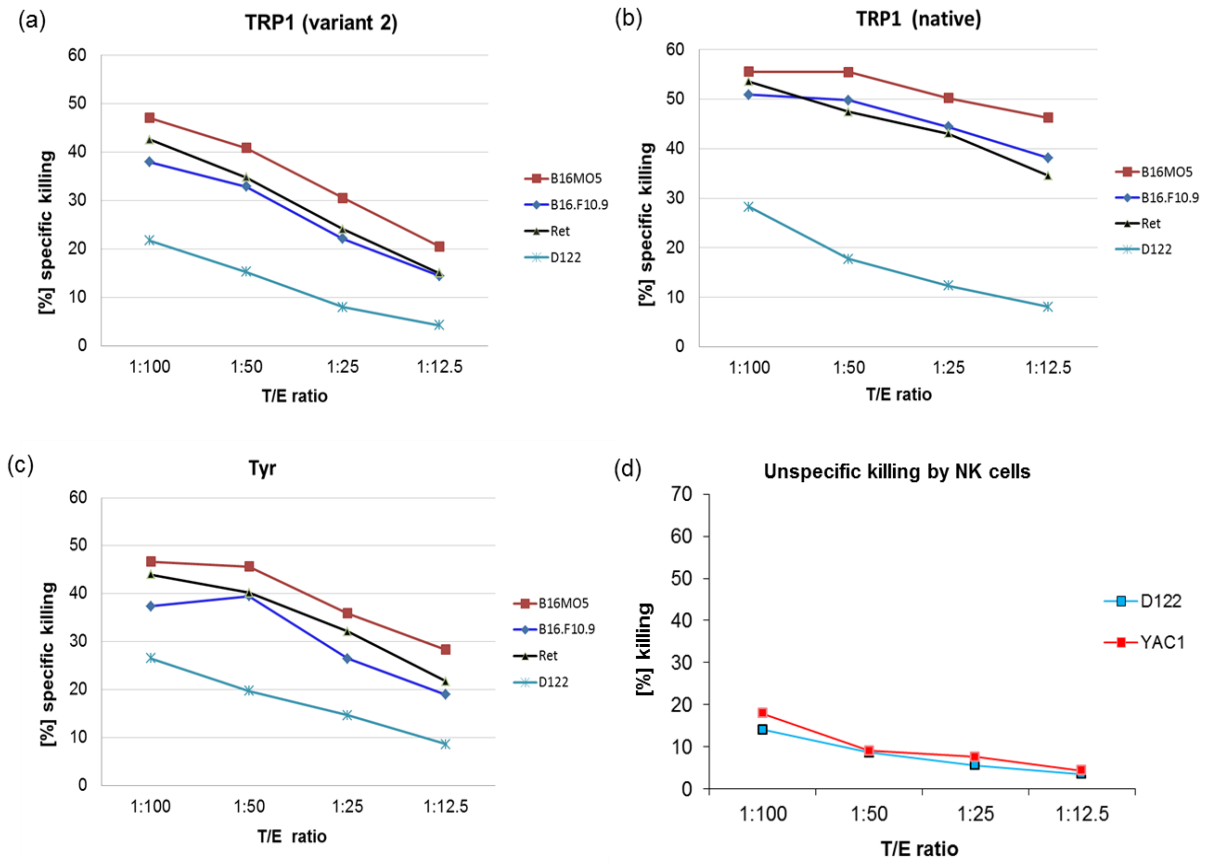

Fig. 19: CTL in vitro assay. Mice were vaccinated i.p. with mRNA electroporated DCs (3 mice per group, 0.5x106 cells in 0.2 mL) 3 times weekly. 10 days later, splenocytes of vaccinated mice were isolated and in vitro sensitized by peptide for 4 days at 37°. Target tumor cell lines (B16MO5, B16F10.9, Ret and D122), were labeled for 10-12 hours 35S methionine. Afterwards, target tumor cells and sensitized splenocytes were co-incubated at different ratios for 5 h at 37°C. Then supernatant was removed and specific target cell lysis by 35S methionine release was calculated. Graphs represent the mean percentage of specific killing of tumor cells by CTL induced after vaccination with respective class I-DC vaccine, namely (a) vaccination with Class I -Trp1 (variant) construct, (b) vaccination with Class I -Trp1 (native) construct and (c) vaccination with Class I -Tyr (variant) construct, respectively. (d) Graph shows a percentage of unspecific killing induced by either spontaneous lysis of irrelevant control cell line (D122) or by naturally occurring killer cells (NK cells) in vaccinated mice, indicated by NK cell sensitive YAC-1 cell lysis. Assay was repeated once with similar results.

4.4 Tetramer staining of CD4$^+$ T cells after proliferation assay

Class II IAb-constructs were tested for their ability to elicit a specific CD4$^+$ T cell response. C57BL/6 mice were injected intra footpad (i.f.p) with CFA/peptide emulsion. 11 days later, lymphocytes from draining popliteal lymph nodes were tested for specific CD4$^+$ T cell proliferation after 72h *in vitro* restimulation with the construct containing specific or irrelevant peptide- sequence at different DC: T cell ratios. As shown in **Figure 20,** a specific CD4$^+$ T cell proliferation to Tyr and TRP-1 peptides was significantly increased as compared to irrelevant OVA$_{(323-339)}$. Importantly, no specific CD8$^+$ T cell response was detected.

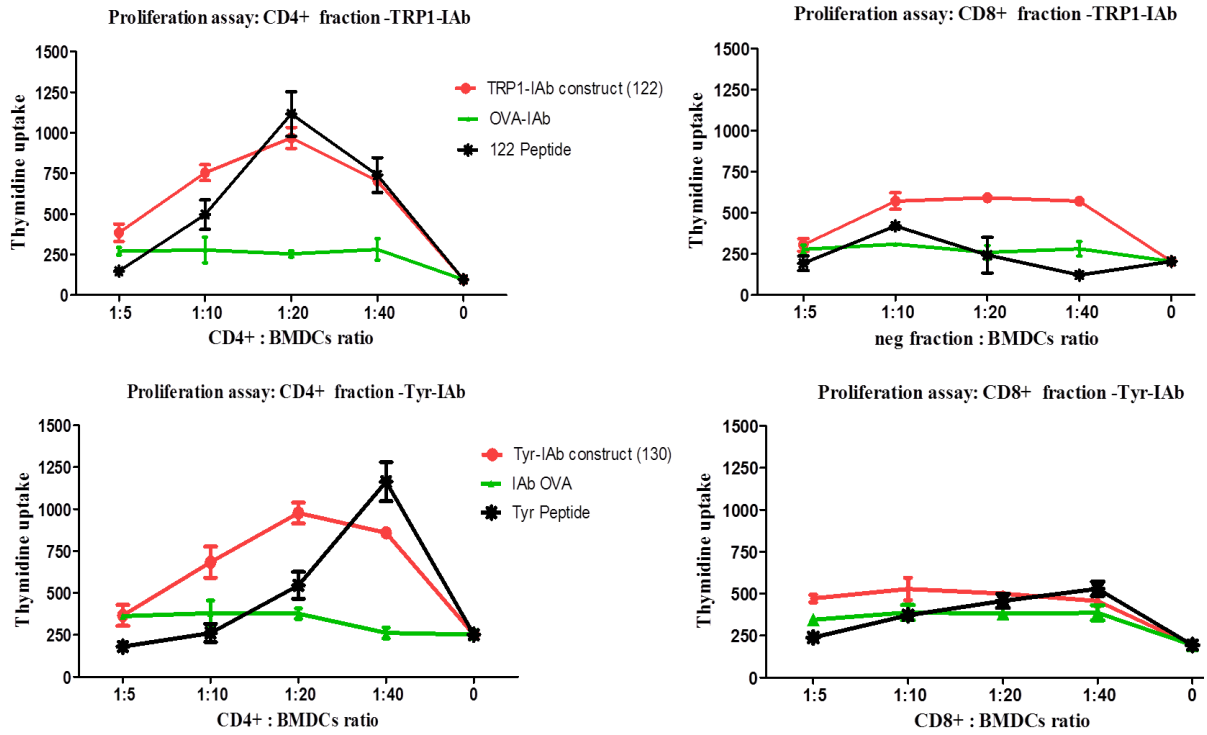

Fig. 20: *In vitro* proliferation assay for Class II IAb-constructs. C57/BL6 mice were vaccinated with peptide in complete Freund's adjuvant. Eleven days *later*, CD4+ and CD8+ T lymphocytes from draining lymph nodes were separated by IMag^{TM} particles and re-stimulated *in vitro* with DCs electroporated with 10 ug IAb consruct (IAb-Tyr$_{99-117}$ or irrelevant class-II construct IAb-OVA$_{323-339}$). DCs loaded with the Tyr$_{99-117}$ peptide were used as a control. Following incubation for 72 hours, cells were pulsed with ^{3}H thymidine for 18 h. Specific CD4$^+$ cell proliferation was assessed by the thymidine uptake. Results are presented as mean +/- SD. The assay was repeated 2 times.

In two additional *in vitro* proliferation assay experiments, cells were harvested 80 h after *in vitro* restimulation with respective class II peptide and subjected to tetramer staining in order to confirm presence of antigen specific CD4$^+$ T cells. Tyr and TRP1 Class II-I-A^b biotinylated monomers, as well as respective negative control monomers were kindly provided by NIH tetramer core facility (Emory University, Atlanta, GA, USA) and are listed in **Table 4**.. As shown in **Figure 21** , TRP1-I-A^b tetramer staining of cells upon *in- vitro* restimulation at room

temperature (RT) and 37°C with relevant peptide revealed elevated levels of $CD4^+$ T cell that were also tetramer positive (4.5 % and 1.4%), providing evidence of antigen-specific $CD4^+$tetramer$^+$ cells. Importantly, TRP1-I-A^b tetramer staining of $CD8^+$ T cell did not show elevated tetramer levels, indicating $TRP1_{(111-128)}$ specific $CD4^+$ T cell proliferation after immunization and *in-vitro* restimuation with $TRP1_{(111-128)}$ peptide. Similarly, Tyr-I-A^b Tetramer staining of cells upon *in- vitro* restimulation at RT and 37°C with Tyr-IA^b peptide revealed elevated levels of $CD4^+$ and Tyr-IAb-tetramer$^+$ (2.7 % and 1.6%), also providing evidence of $Tyr_{(99-117)}$ specific $CD4^+$ tetramer$^+$ T cells.

To summarize, tetramer staining provided further evidence that selected MHC class II restricted candidate peptides $TRP1_{(111-128)}$ and $Tyr_{(99-117)}$ are able to induce an antigen specific $CD4^+$ T helper cell response. Experiment was repeated one more time showing similar results for both peptides (data not shown).

Table 3: MHC class II restricted monomers used for tetramer staining following in vitro proliferation assay

#	Name	Peptide sequence	Concentration
1	Trp-$1_{455-463}$ – I-Ab	CRPGWRGAACNQKI	2mg/ml
2	TYR_{99-117} – I-Ab	NCGNCKFGFGGPNCTEKRV	2mg/ml
3	Clip-negative control	PVSKMRMATPLLMQA	2mg/ml

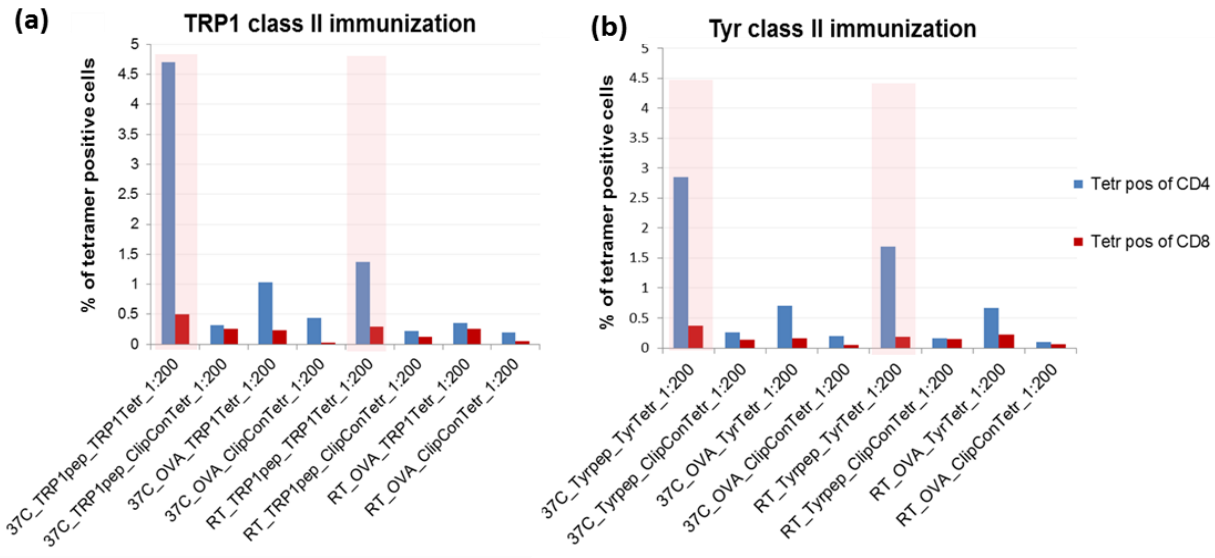

Fig. 21: I-Ab tetramer staining after *in-vitro* proliferation assay. 11 days after CFA/class II-peptide i.f.p. injection with $TRP1_{(111-128)}$ (a) and $Tyr_{(99-117)}$ (b) , *in-vitro* restimulation with specific peptide or irrelevant control ($OVA_{323-339}$) was performed. 80 hours later cells were collected and analyzed by flow cytometry for tetramer+ cells among $CD4^+$ cell (blue) and $CD8^+$ cell subsets (red). Tetramer staining was performed with 1:200 tetramer dilution at RT and 37°C, respectively.

4.5 Analysis of peptide-loaded versus class I mRNA-electroporated DC immunization

4.5.1 Immunization with mRNA-electroporated DCs is superior in inducing antigen-specific CD8$^+$ T cell immune responses

In this set of experiments, the potential of mRNA-electroporated DCs and peptide-loaded DCs to elicit antigen-specific immune responses was compared. We utilized a mixture of mRNA encoding for the MHC Class I constructs (Trp-1$_{455-463}$ Tyr$_{360-368}$) linked to β2m-TLR4 and β2m-Kb backbones). BMDCs were electroporated with Trp1-Kb/TLR4, Tyr- Kb/TLR4 transcribed mRNAs followed by 6 h of incubations at 37°C. In addition, LPS-maturated BMDCs were loaded with 30 µg/mL synthetic peptides of peptides Trp-1$_{455-463}$, Tyr$_{360-368}$, or the combination of Trp-1 and Tyr (Mix) for 2-3 hours at 37°C. C57BL/6 mice were immunized i.p. with the generated DC vaccines three times in 7 days intervals (0.5X10^6 cells per mouse), and 10 days after the last vaccination, LNs were harvested and analyzed for the induction of peptide-specific CD8$^+$ by intracellular staining (ICS) for IFN-γ and TNF-α. Cells were in in vitro re-stimulated using Trp-1$_{455-463}$ and Tyr$_{360-368}$ peptides or their combination (1:1), and their intracellular levels of IFN-γ and TNF-α were measured.

Our results indicated that all three mRNA-electroporated DC vaccines were more potent in inducing peptide-specific CTL immune responses than the corresponding peptide-loaded DC vaccines (**Fig.22**). This is evident from the fact that in both lymph nodes and spleens the frequency of IFN-γ and TNF-α secreting CD8$^+$ T-cells was found to be significantly higher in mice vaccinated with mRNA-electroporated vaccines. In LNs of mice immunized with mRNA-electroporated DC vaccines, the frequency of CD8$^+$ T cells secreting both IFN-γ and TNF-α was significantly higher than in mice received the corresponding peptide-loaded DC vaccines.

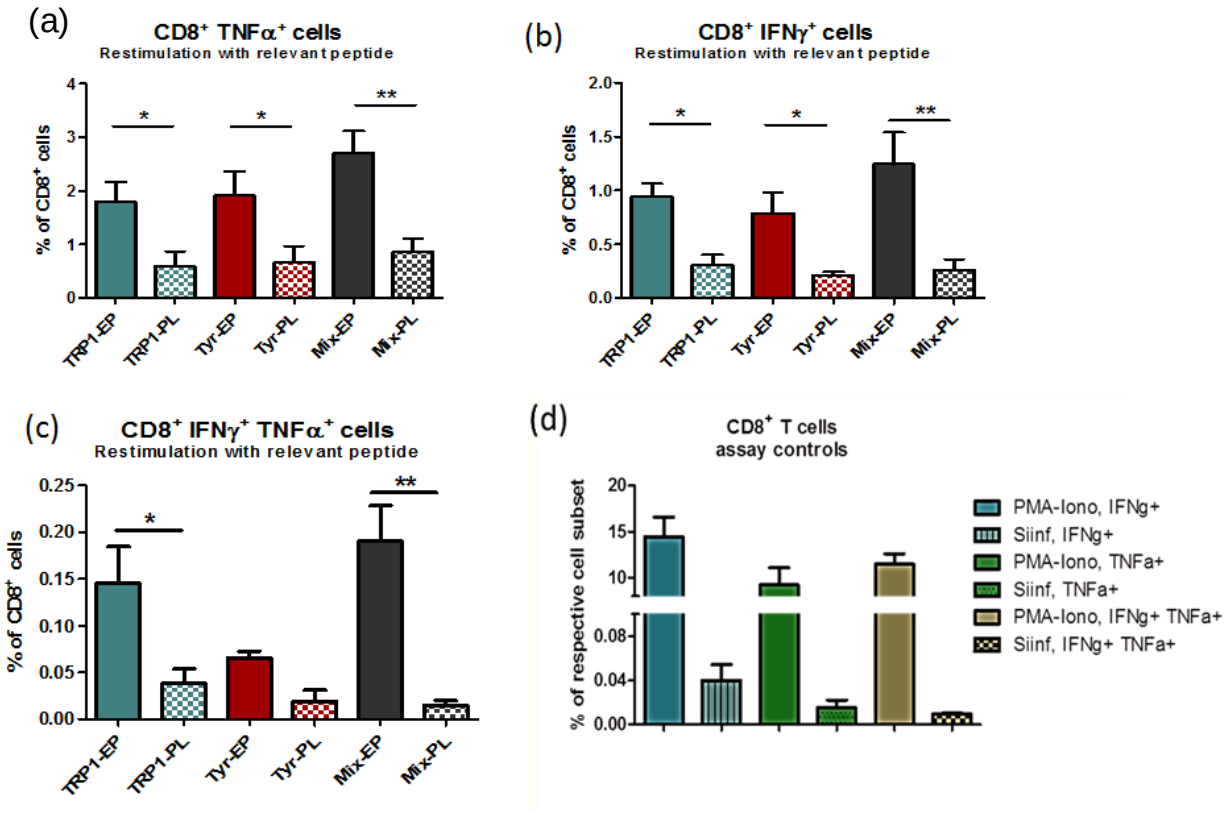

Fig. 22: Analysis of CD8+ T-cell antigen-specific immune responses in the lymph nodes following vaccination with mRNA-electroporated and peptide-loaded DCs. C57BL/6 mice (n=3) were vaccinated intraperitoneally 3 times using BMDCs electroporated with Trp1-Kb/TLR4, Tyr-Kb/TLR4, or the combination (Mix) mRNAs, as well as BMDCs peptide-loaded with Trp-$1_{455-463}$, $Tyr_{360-368}$, or the combination of the two peptides. Ten days after the last vaccination lymph nodes were harvested and analyzed for the induction of peptide-specific CD8+ T cells by ICS for IFN-γ and TNF-α, following 6 h re-stimulation with the relevant peptide according to the group (Trp-$1_{455-463}$, $Tyr_{360-368}$ or their combination) in the presence of 3ug/ml Golgi-plug. As assay controls, unspecific stimulation with 2ug/ml PMA/ 20ug/ml ionomycine was performed as positive control and as negative control in vitro restimulation with irrelevant peptide (SIINFEKL) was performed. Bar graphs represent the percentages of CD8+ INFγ+ (a), CD8+ TNF-α+ (b), CD8+ INFγ+ TNFα+ (c) and respective assay controls (d) for lymph nodes. Results are presented as mean ± standard deviation (SD), (*P ≤ 0.05; **P ≤ 0.01; ***P ≤ 0.001; mRNA-electroporated versus peptide-loaded DCs; unpaired student's t-test).

4.6 Vaccination with mRNA-electoporated DC induces memory T cells

Splenocytes and LN cells isolated from C57BL/6 mice immunized with mRNA-electroporated or peptide-loaded DCs were also used to assess the activation status of T lymphocytes, by cell-surface expression of CD44 and CD62L. Vaccination with mRNA-electroporated DC vaccines induced a significant reduction in the frequency of naïve $CD8^+$ T-cells in LN and in spleen (**Fig.23**). mRNA-electroporated DC vaccines induced elevation in the central memory (CM) $CD8^+$ T cell population in both spleens and lymph nodes. Statistically significant changes were observed in the effector-memory (EM) $CD8^+$ T cell population in spleens and lymph nodes upon vaccination with Mix-EP vaccine and Tyr-EP vaccine, which resulted in a higher frequency of EM $CD8^+$ T cell population in LNs compared to the respective peptide-loaded DC vaccine (**Fig.23**).

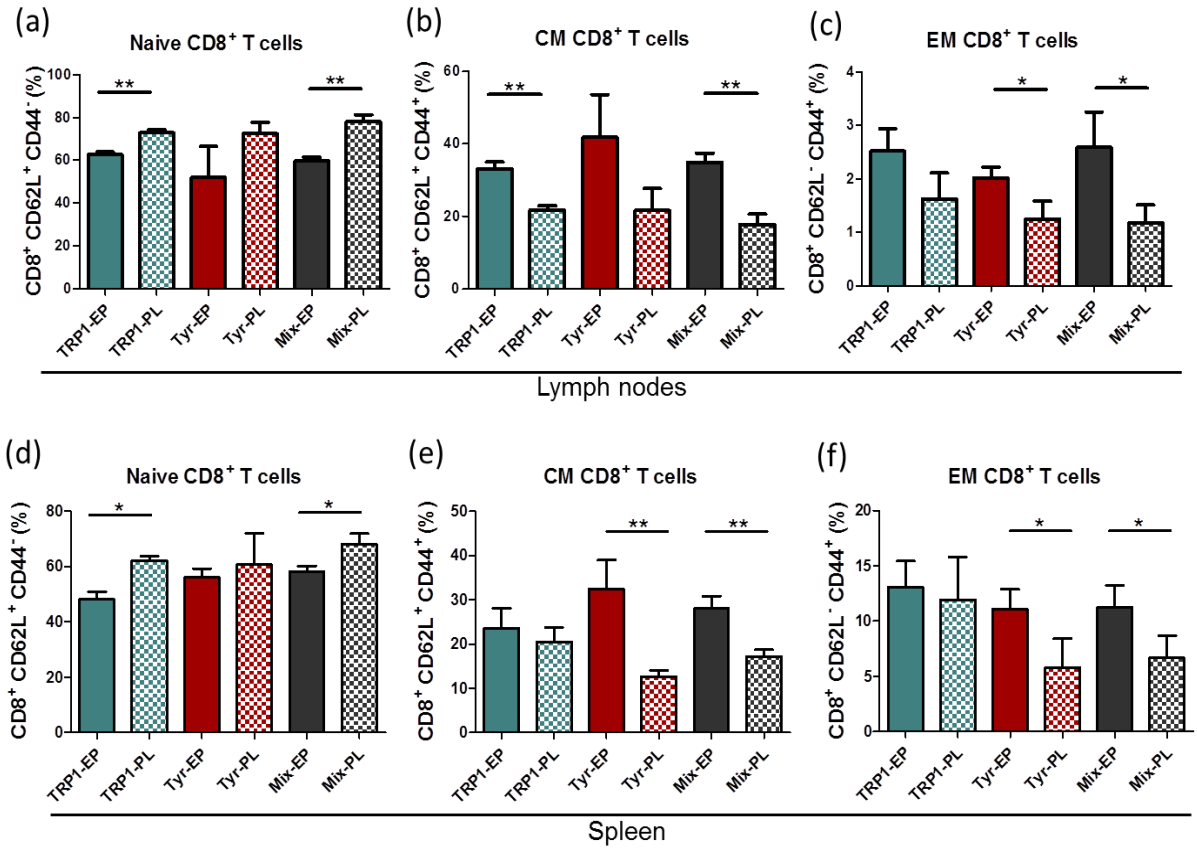

Fig. 23: Frequency of naïve, central memory and effector-memory peptide specific $CD8^+$ T cells in mice vaccinated with mRNA-electroporated and peptide-loaded DCs. C57BL/6 mice (n=3) were vaccinated intraperitoneally 3 times using BMDCs electroporated with Trp1-K^b/TLR4, Tyr-K^b/TLR4, or the combination (Mix) mRNAs, as well as BMDCs peptide-loaded with Trp-$1_{455-463}$, $Tyr_{360-368}$, or the combination of the two peptides. Ten days after the last vaccination spleens and LNs were harvested and the activation status of T lymphocytes was assessed by expression of CD44 and CD62L analysis. Bar graphs representing the percentage of naïve ($CD62L^+$ $CD44^-$) (a, d), central memory (CM; $CD62L^+$ $CD44^+$) (b, e), and effector-memory (EM; $CD62L^-$ $CD44^+$) (c, f) $CD8^+$ T-cells, for both lymph nodes (a-c) and spleen (d-f) are shown. Results are presented as mean ± standard deviation (SD) (*P ≤ 0.05; **P ≤ 0.01; ***P ≤ 0.001; mRNA-electroporated versus peptide-loaded DCs; student's t-test)

4.7 *In vivo* target cell killing upon immunization

CTL in vivo killing assay was performed in order to test if mRNA electroporated BMDCs are superior to peptide-loaded, LPS-matured BMDCs in inducing specific CTL killing in vivo. 3 C57BL/6 mice were vaccinated intraperitoneally (i.p.) three times at 7 day intervals using BMDCs were electroporated with either Trp1-Kb/TLR4 or Tyr-Kb/TLR4 mRNA as well as their combination (Mix). Mice were also immunized with BMDCs peptide-loaded with Trp-$1_{455-463}$, $Tyr_{360-368}$, or the combination of the two peptides. Mice vaccinated with SIINFEKL-loaded DCs served as positive control for assay performance. Ten days later mice were injected with CFSE-labeled, C57/BL6-Ly5.1 (CD45.1+) derived splenocytes loaded with Trp-$1_{455-463}$, $Tyr_{360-368}$, Trp-$1_{455-463}$/$Tyr_{360-368}$, or $OVA_{257-264}$ (SIINFEKL) peptides as target cells and sacrificed 14-18 hours later. As seen in **Fig. 24**, all three mRNA-electroporated DCs were able to elicit very effective CTL responses *in vivo*. Additionally, they were significantly more efficient in inducing peptide-specific cytolysis *in vivo* as compared to the respective peptide-loaded ones.

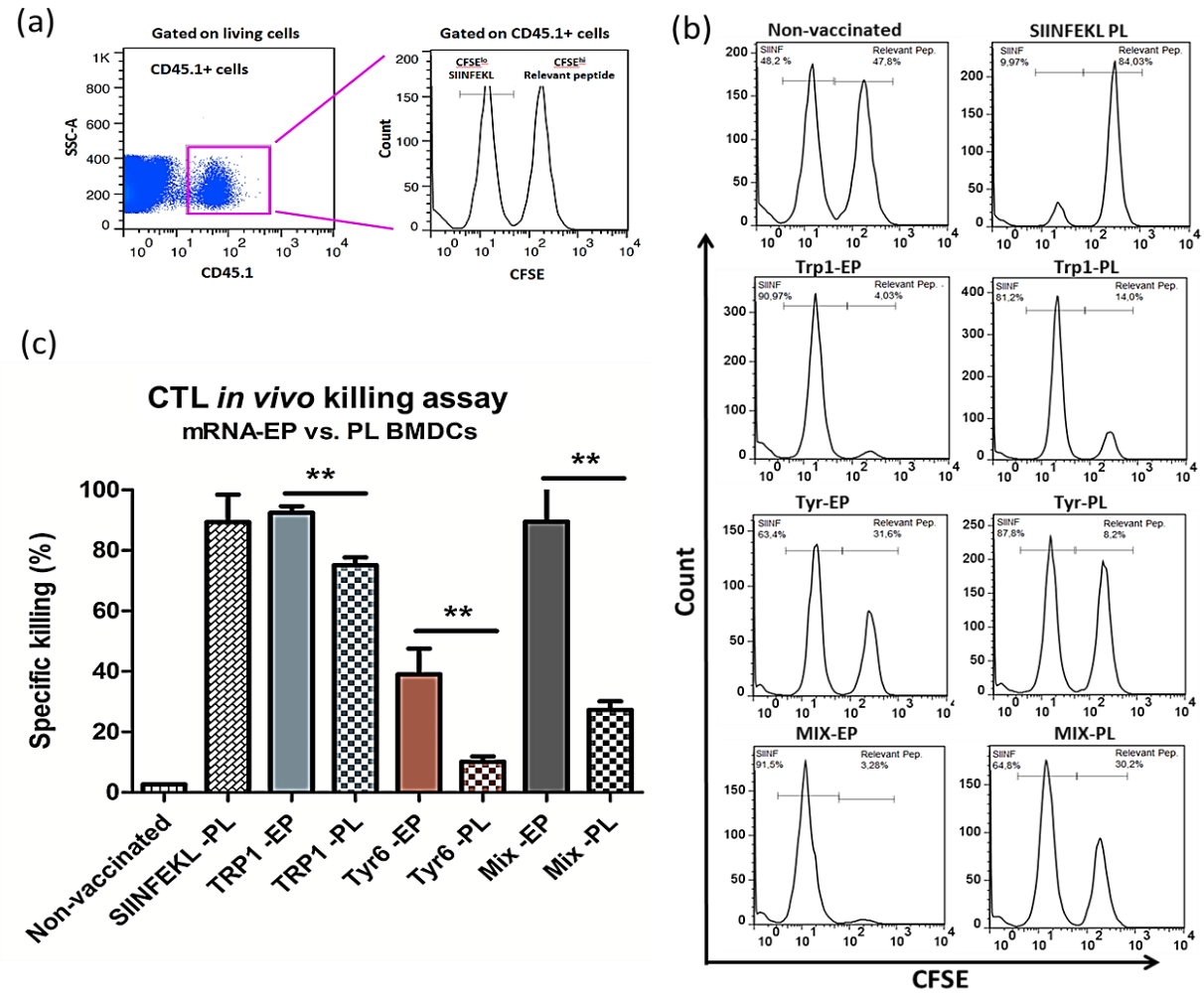

Fig. 24: *In-vivo* target cell killing in mice vaccinated with mRNA-electroporated and peptide-loaded DCs. C57BL/6 mice (n=3) were vaccinated intraperitoneally three times using BMDCs

electroporated with Trp1-K^b/TLR4, Tyr- K^b/TLR4, or the combination (Mix) mRNAs, as well as BMDCs peptide-loaded with Trp-$1_{455-463}$, $Tyr_{360-368}$, or the combination of the two peptides. Mice vaccinated with SIINFEKL-loaded DCs were used as control. Ten days after the last vaccination splenocytes from C57/BL6-Ly5.1 ($CD45.1^+$) mice donors were pulsed with Trp-$1_{455-463}$, $Tyr_{360-368}$, Trp-$1_{455-463}$/$Tyr_{360-368}$, and $OVA_{257-264}$ (SIINFEKL) peptides. (a) Splenocytes loaded with specific peptides (target cells) were labeled with 1.5 µM CFSE ($CFSE^{Hi}$), while SIINFEKL-loaded splenocytes with 0.15 µM CFSE ($CFSE^{Lo}$). (b) Target and control cells are injected intravenously into vaccinated C57BL/6 mice at 1:1 ratio. Fourteen to eighteen hours later, splenocytes from the vaccinated mice were stained with CD45.1 antibody and analyzed by flow cytometry for presence of the differentially labeled peptide-loaded C57/BL6-Ly5.1 splenocytes and are presented at individual histograms (c) Bar graph represents the percentage of specific killing in the different groups. Results are presented as mean ± standard deviation (SD) (*P ≤ 0.05; **P ≤ 0.01; ***P ≤ 0.001; mRNA-electroporated versus peptide-loaded DCs; unpaired student's t-test)

To summarize, tested class I -mRNA electroporated BMDCs stimulated specific $CD8^+$ T cell response. Induced CTLs were also able to mediate a specific cytolysis of relevant tumor cells *in vitro.* Importantly, mRNA-electroporated DCs could elicit the effective CTL responses *in vivo*. These DCs were significantly more efficient in inducing specific cytolysis *in vivo* as compared to the respective peptide-loaded ones.

4.8 Effect of DC vaccination on melanoma development in mice

4.8.1 Immunotherapy of melanoma bearing *ret* transgenic mice

5-week old melanoma-bearing *ret* transgenic (*ret*-tg) mice were immunized intraperitoneally i.p. with mRNA-electroporated BMDCs three times every week. In an additional experiment, melanoma-bearing mice were vaccinated in parallel with peptide loaded, LPS maturated BMDCs. Mice treated with electroporated, but empty BMDC were used as a control group. Mice were closely monitored in regular intervals for at least 80 days to assess survival benefits upon respective treatment. In some experiments 4 mice of respective treatment groups were sacrificed 10 days after last vaccination, and flow cytometry analyses of different immune cell subsets in BM, SP, LN and tumor were performed.

The scheme of DC vaccination is shown in **Figure 25**. MHC class I and MHC class II vaccine composition and treatment groups are shown in **Table 5**.

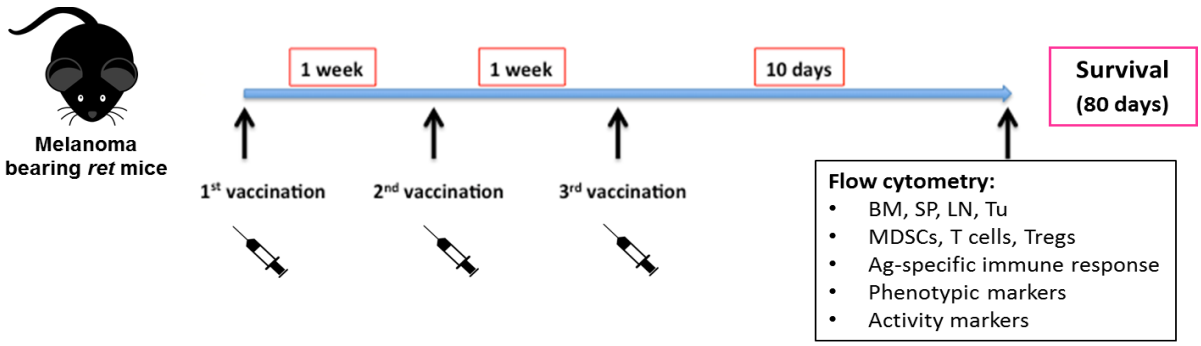

Fig. 25: Dendritic cell vaccination scheme for melanoma immunotherapy. 5 week old melanoma bearing ret mice, 6-12 mice per group, were immunized i.p. three times in 7 days intervals with DC vaccine ($0.5x10^6$ cells per mouse). Ten days after last vaccination, 4 mice of respective treatment groups were sacrificed and flow cytometry analyses were performed. Remaining mice of respective groups were kept and closely monitored for survival analysis for at least 80 days.

Table 4: Designations of the MHC restricted constructs and peptides used for immunizations

#	MHC class I –Vaccine Construct's Composition	Designation
1	Variant – Trp1-hβ2m-K^b / Variant Trp-1-hβ2m-TLR4	Class I –Trp1 (variant)
2	Trp-$1_{455-463}$-hβ2m-K^b / Trp-1-hβ2m-TLR4	Class I –Trp1 (native)
3	Tyr-hβ2m-K^b / Tyr-hβ2m-TLR4	Class I –Tyr
4	Trp-1 (#1) / Tyr (#3)	Class I –Mix
5	Trp-$1_{455-463}$ / $Tyr_{360-368}$ peptide mix	Class I –Mix–PL

#	MHC class II -Vaccine Construct's Composition	Designation
6	Trp-$1_{455-463}$ - H2-I-A^b	Class II –Trp1-I–A^b
7	TYR_{99-117} - H2-I-A^b	Class II –Tyr-I–A^b
8	TRP1- H2-I-A^b / Tyr- H2-IA^b (#6 and #7)	Class II –Mix- I–A^b
9	Trp-$1_{455-463}$ - CLIP	Class II –Trp1–CLIP
10	TYR_{99-117} - CLIP	Class II –Tyr–CLIP
11	TRP1- CLIP / Tyr- CLIP (#9 and #10)	Class II –Mix–CLIP
12	Trp-$1_{455-463}$ / TYR_{99-117} peptide mix	Class II –Mix–PL

4.8.2 **Survival analysis**

Fig. 26 shows survival curve of *ret*-transgenic mice treated with BMDCs electroporated with Trp1-K^b/TLR4, Tyr- K^b/TLR4, or the combination (Class I-Mix) mRNAs. We found a significantly improved survival rate of melanoma bearing mice after treatment with DCs electroporated with Class I–Mix mRNA and Trp1-mRNA (variant) as compared to control group. Importantly, vaccination with Class I–Mix mRNA electroporated DC was superior over vaccination with DCs loaded with Class I peptide mix. To confirm results, most beneficial treatments were repeated in a second immunotherapy experiment with similar results.

In addition, both class II-IA^b and CLIP vaccines were tested as a single treatment and in combination, analogous to the class I–DC vaccination and was compared to control group.

In contrast to DCs electroporated with Class I –mRNA, none of the groups treated with DCs electroporated Class II-IA^b –mRNA or CLIP–mRNA showed any significant survival benefit upon vaccination **Figure 27** shows survival curve of ret-transgenic mice treated with BMDCs electroporated with Class II -Trp1-I-A^b; Class II Tyr-I-A^b; or the combination (Class II-Mix I-A^b) **Figure 28** Class II-Tyr-CLIP, Class II-Trp1-CLIP, or the combination (Class II-Mix-CLIP). Median survival (in days) for each treatment group are summarized in **Table 6.** Results were confirmed in a second immunotherapy experiment with the same treatment groups, except for treatment #2 (data not shown).

Table 5: Summary of median survival of each therapy after 80 days (n=6-12)

#	MHC class I –Vaccine	Median survival (days)
1	Class I –Trp1 (variant)	43.5
2	Class I –Trp1 (native)	33.0
3	Class I –Tyr	36.0
4	Class I –Mix	51.0

#	MHC class II -Vaccine Construct's Composition	Median survival (days)
6	Class II –Trp1-I–A^b	40.5
7	Class II –Tyr-I–A^b	36.5
8	Class II –Mix- I–A^b	42.5
9	Class II –Trp1–CLIP	42.0
10	Class II –Tyr–CLIP	41.0
11	Class II –Mix–CLIP	39.5
13	Control (DC only)	35.5

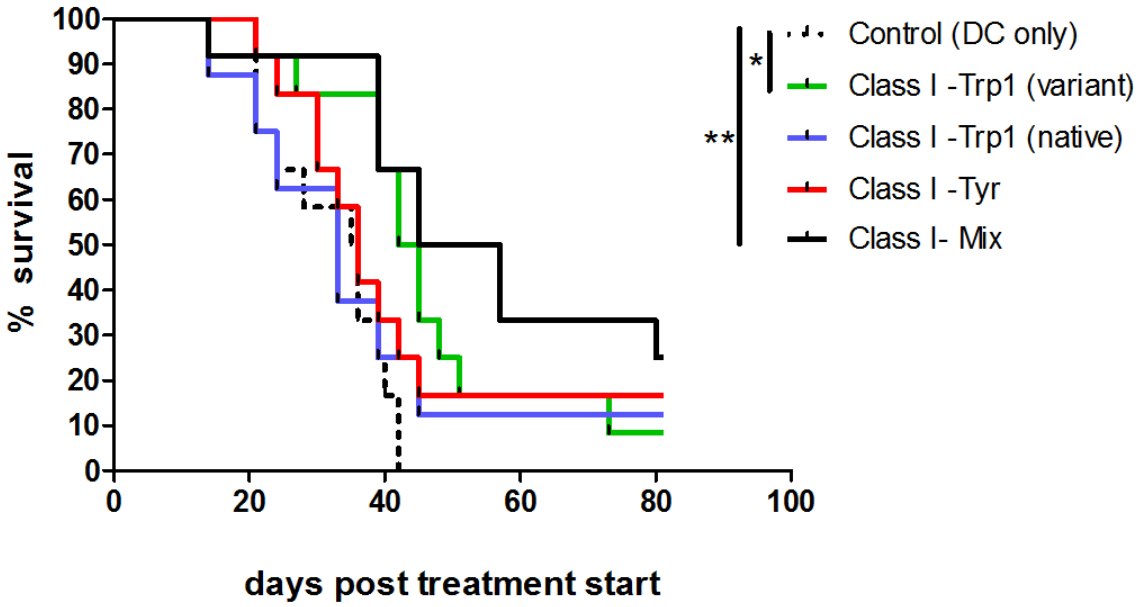

Fig. 26: Survival proportions of melanoma bearing *ret* tg mice following vaccination with class I mRNA-electroporated DCs. Melanoma bearing *ret* transgenic mice were vaccinated i.p. three times using BMDCs electroporated with Trp1-K^b/TLR4, Tyr- K^b/TLR4, or the combination (Mix) mRNAs. Mice vaccinated with electroporated but unloaded DCs were used as control (DC only). Mice (n=6-12/ group) were closely monitored for at least 80 days after the first vaccination. Survival curves of each treatment group are shown. Results are presented as percent of surviving mice (*P ≤ 0.05; **P ≤ 0.01; ***P ≤ 0.001; generated using, product limit (Kaplan-Meier) method, comparison of survival curves; Log-rank (Mantel-Cox) test)

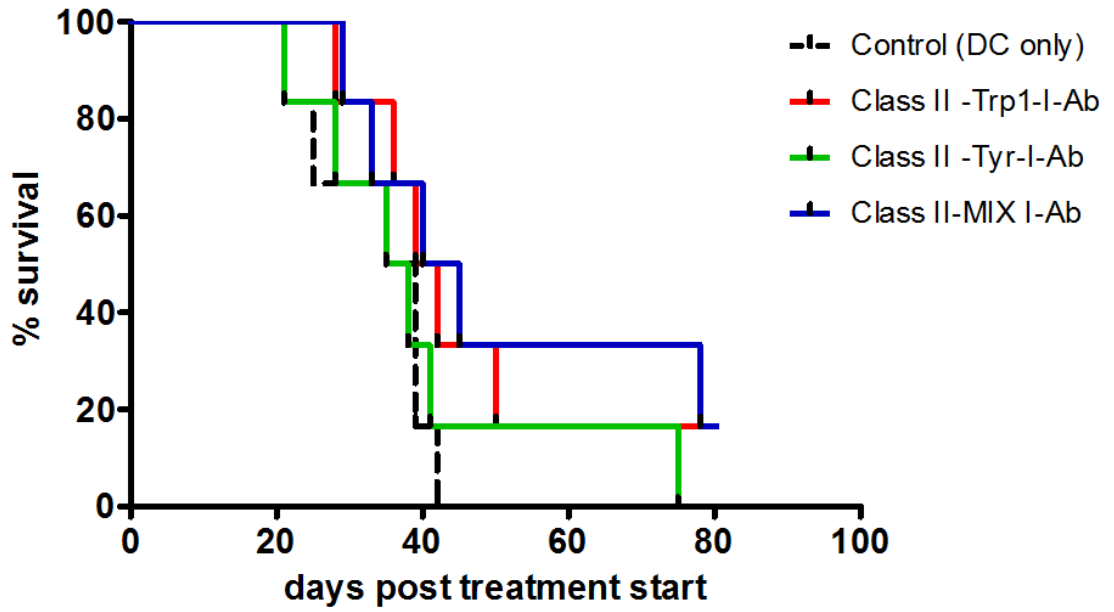

Fig. 27: Survival proportions of melanoma bearing *ret* tg mice following vaccination with class II-IAb mRNA-electroporated DCs. Melanoma bearing *ret* transgenic mice were vaccinated i.p. three times using BMDCs electroporated with Class II -Trp1-I-Ab, Class II -Trp1-I-Ab, or the combination (Mix) mRNAs. Mice vaccinated with electroporated but unloaded DCs were used as control. Mice (n=6/group) were closely monitored for 80 days after the first vaccination. Survival curves of each treatment group are shown. Results are presented as percent of surviving mice (*P ≤ 0.05; **P ≤ 0.01; ***P ≤ 0.001; generated using, product limit (Kaplan-Meier) method, comparison of survival curves; Log-rank (Mantel-Cox) test). Experiment was repeated with similar results.

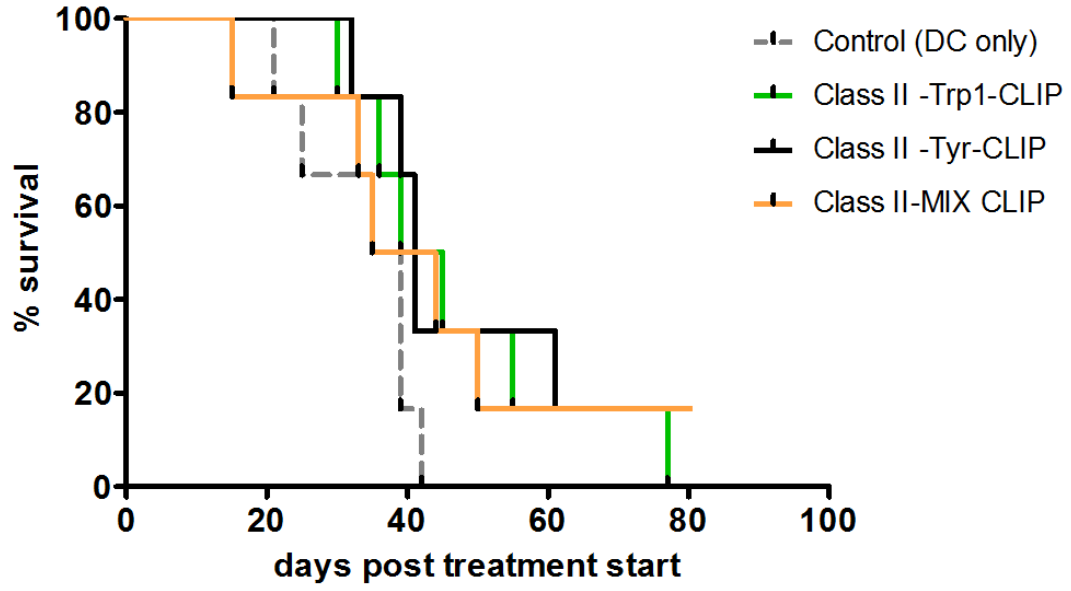

Fig. 28: Survival proportions of melanoma bearing *ret* tg mice following vaccination with class II -CLIP mRNA-electroporated DCs. Melanoma bearing *ret* transgenic mice were vaccinated i.p. three times using BMDCs electroporated with Class II -Trp1-CLIP, Class II -Trp1-CLIP, or the combination (Mix) mRNAs. Mice vaccinated with electroporated but unloaded DCs were used as control. Mice (n=6/group) were closely monitored for 80 days after the first vaccination. Survival curves of each treatment group are shown. Results are presented as percent of surviving mice (*P ≤ 0.05; **P ≤ 0.01; ***P ≤ 0.001; generated using, product limit (Kaplan-Meier) method, comparison of survival curves; Log-rank (Mantel-Cox) test). Experiment was repeated with similar results

4.8.3 mRNA-electroporated DC versus peptide loaded DC vaccination

In an additional experiment, comparative survival analysis of melanoma bearing *ret-tg* mice following vaccination with class I mRNA-electroporated DCs Trp1/-Kb/TLR4 + Tyr- Kb/TLR4 (Class I Mix-EP) mRNAs and DCs peptide-loaded with Trp-$1_{455-463}$/$Tyr_{360-368}$ (Class I Mix-PL), was performed. Melanoma bearing mice vaccinated with electroporated but unloaded DCs were used as control. As described before, melanoma bearing *ret*-tg mice were vaccinated i.p. three times in seven day intervals and monitored for at least 80 days after first vaccination. Survival curves of each treatment group are shown in **Fig. 29**. and demonstrate significantly higher survival rates in group vaccinated with Mix of class I mRNA-electroporated DCs (Class I Mix-EP) than in group vaccinated with Mix of class I peptides loaded onto DC (Class I Mix-PL).

Furthermore, we performed a survival analysis of melanoma bearing mice following vaccination with class II mRNA-electroporated DCs, Trp1/TYR-IAb-Mix (Class II-Mix-IAb), Trp1/TYR-CLIP-Mix (Class II Mix-CLIP) mRNAs and DCs peptide-loaded with Trp-$1_{455-463}$/$Tyr_{360-368}$ (Class I Mix-PL). Melanoma-bearing mice vaccinated with electroporated but unloaded BMDCs were used as a control. Interestingly, none of the class II vaccinated groups significantly increased survival of melanoma bearing *ret*-tg mice compared to control group (**Fig. 30**).

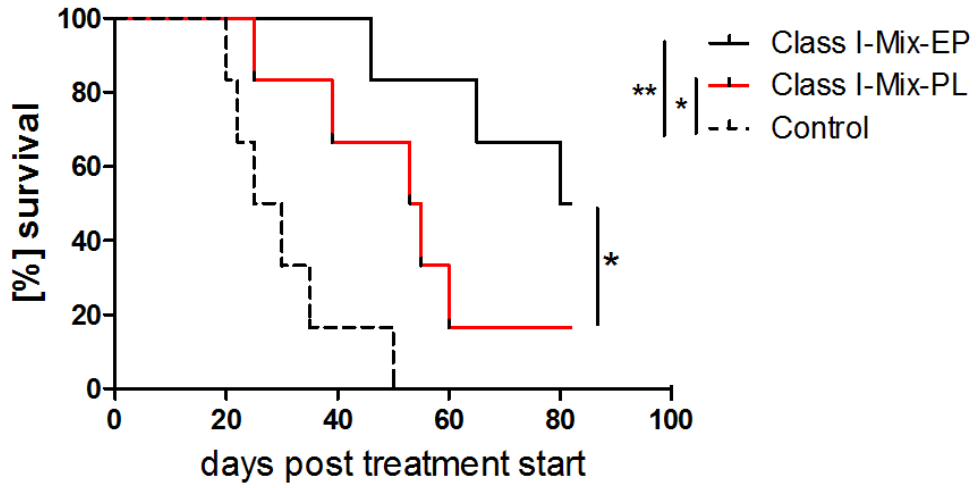

Fig. 29: Survival of melanoma-bearing mice following vaccination with class I Mix mRNA-electroporated DCs or vaccinated with DCs loaded with mix of class I peptides. Melanoma bearing *ret* transgenic mice were vaccinated i.p. three times using BMDCs electroporated with Trp1-K^b/TLR4, Tyr- K^b/TLR4, or the combination (Mix) mRNAs. Mice vaccinated with electroporated but unloaded DCs were used as a control (DC only). Mice (n=6/group) were monitored for 80 days after the first vaccination. Survival curves of each treatment group are shown Results are presented as a percentage of surviving mice (*P ≤ 0.05; **P ≤ 0.01; ***P ≤ 0.001; generated using, product limit (Kaplan-Meier) method, comparison of survival curves; Log-rank (Mantel-Cox) test)

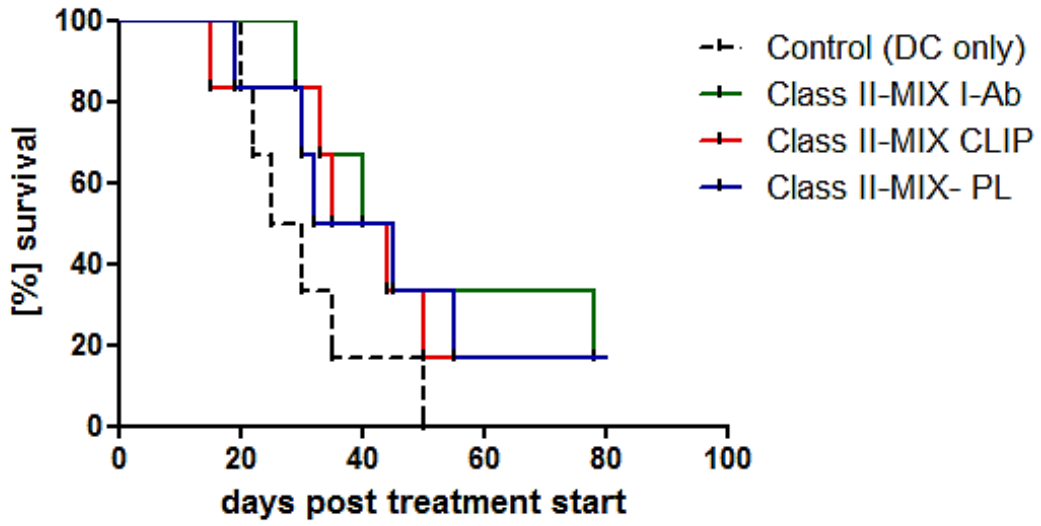

Fig. 30: Survival of melanoma bearing mice following vaccination with class I Mix mRNA-electroporated DC or vaccinated with DC loaded with mix of class I peptides. Melanoma bearing *ret* transgenic mice were vaccinated i.p. three times using BMDCs electroporated with Trp1-K^b/TLR4, Tyr- K^b/TLR4, or the combination (Mix) mRNAs. Mice vaccinated with electroporated but unloaded DCs were used as control (DC only). Mice (n=8-12) were closely monitored for 80 days after the first vaccination. Survival curves of each treatment group are shown Results are presented as a percentage of surviving mice (*P ≤ 0.05; **P ≤ 0.01; ***P ≤ 0.001; generated using, product limit (Kaplan-Meier) method, comparison of survival curves; Log-rank (Mantel-Cox) test).

To summarize, bivalent Trp1/Tyr–class I–mRNA-based DC-vaccine (Class I-Mix) showed superior anti-tumor properties upon vaccination of melanoma bearing *ret* trasngenic mice as compared to groups vaccinated with respective monovalent mRNA-based-DC vaccine or with peptide loaded DCs respectively. Moreover, monovalent as well as bivalent mRNA-based-DC class II IAb–DC vaccines, Class II-IAb and Class II-CLIP did not improve survival rates of treated melanoma bearing mice.

4.8.4 **Immune cell analyses after DC vaccination**

To further analyze the underlying mechanism of action in *ret*-tg mice, which were treated with mRNA-based DC vaccine, 4 mice of each treatment group were used for mechanistic analyses of immune cells subsets 10 days after last vaccination. Although Class II-mRNA-based DC vaccination did not improve survival of melanoma bearing ret-tg mice, 4 mice of each Class II-IAb–group was included into analyses. Results of two experiments were combined to increase number of mice per group. Mice were sacrificed and flow cytometry analyses of immune cell subsets from bone marrow (BM), spleen (SP), lymph nodes (LN) and skin tumor were performed. Respective phenotypic and activity markers analyzed by flow cytometry are summarized in the following:

MDSC: $CD11b^+$, $Gr1^+$

- activity markers: PD-L1, arginase-1, NO production

T cells: $CD3^+$, **$CD4^+$**, $FoxP3^-$ or $CD3^+$, **$CD8^+$**, $FoxP3^-$

- Activity: TCR-zeta chain expression, PD-1, CD69
- Memory phenotype: CD44, CD62L
- Intra cellular staining (ICS): TNF-α and IFN-γ production of antigen-specific $CD4^+$ and $CD8^+$ T cells after *in-vitro* restimulation.

T regs: $CD3^+$, $CD4^+$, $CD25^+$ $FoxP3^+$

- Activity: Ki-67, CD39

Treatment of melanoma bearing mice with DC vaccines did not significantly alter frequency of MDSC within LN, skin tumors (**Fig. 31**), BM and spleen (**Appendix 1**). However, the expression of activity markers in MDSCs from LNs and skin tumors was strongly diminished upon Class I–DC vaccination (solid symbols), indicated by significantly reduced arginase-1 **(Fig.31 b**) and PD-L1 expression (**Fig. 31 d**) and decreased NO production (**Fig. 31 c**). Similar changes but not as prominent as in LN and skin tumor were also observed in SP and BM (**Appendix 1**). No statistically significant changes in MDSC frequency and activity were observed in the groups of mice treated with either Class II–DC vaccine (empty symbols) as compared to control group. Interestingly, vaccination with Class I–DC vaccines resulted in significantly lower expression levels of PD-L1 on MDSC and lower production levels of arginase-1 and NO in MDSCs compared to the groups of mice treated with Class II-IAb vaccine.

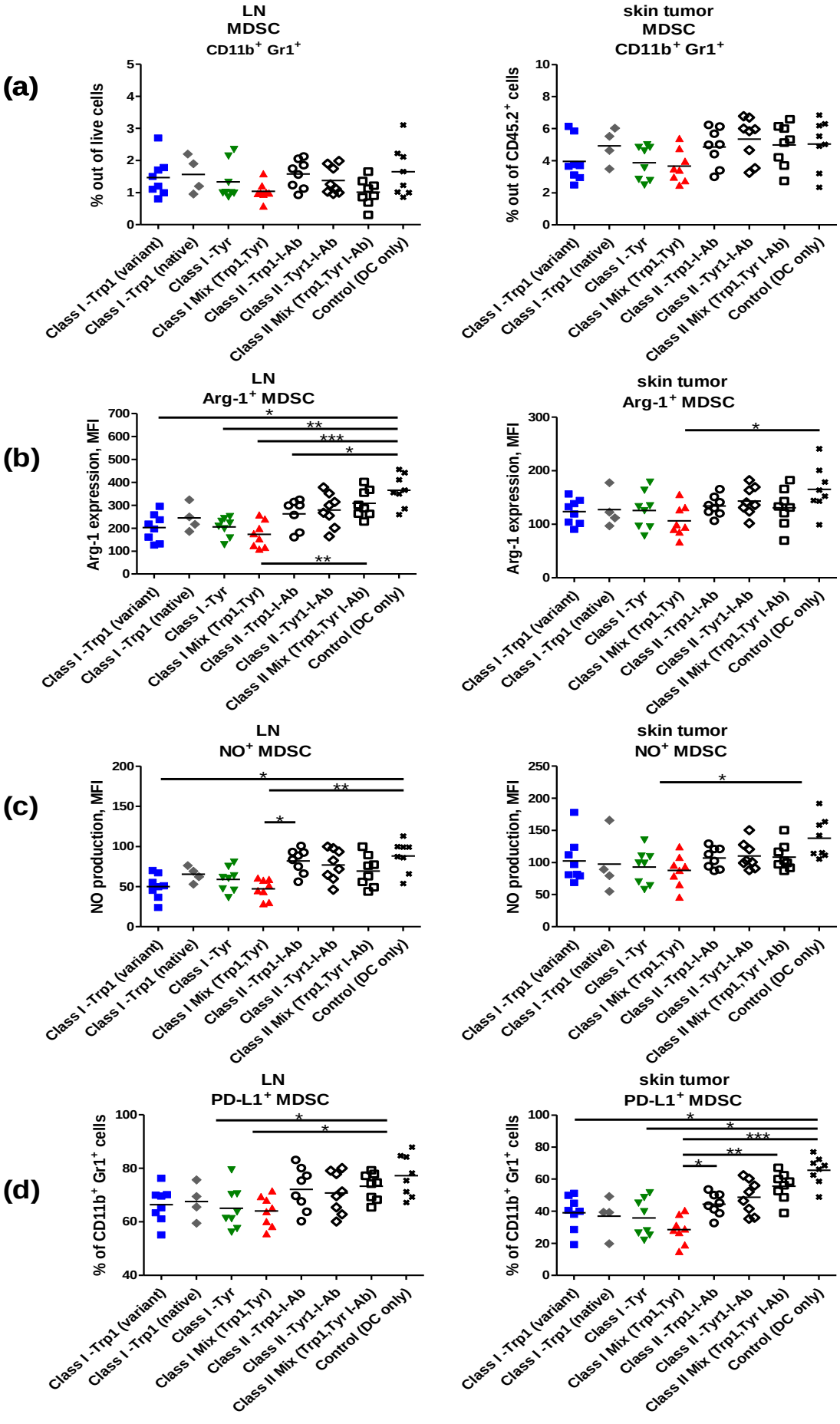
(a)
LN
MDSC
CD11b+ Gr1+
% out of live cells
skin tumor
MDSC
CD11b+ Gr1+
% out of CD45.2+ cells
(b)
LN
Arg-1+ MDSC
Arg-1 expression, MFI
skin tumor
Arg-1+ MDSC
Arg-1 expression, MFI
(c)
LN
NO+ MDSC
NO production, MFI
skin tumor
NO+ MDSC
NO production, MFI
(d)
LN
PD-L1+ MDSC
% of CD11b+ Gr1+ cells
skin tumor
PD-L1+ MDSC
% of CD11b+ Gr1+ cells
Class I -Trp1 (variant)
Class I -Trp1 (native)
Class I -Tyr
Class I Mix (Trp1,Tyr)
Class II -Trp1-I-Ab
Class II -Tyr1-I-Ab
Class II Mix (Trp1,Tyr I-Ab)
Control (DC only)

Fig. 31: Class I –Mix DC-vaccine but not Class II DC vaccines diminished MDSC activity within LN and skin tumors of *ret* tg mice. 4-5 week old melanoma bearing mice were vaccinated with class I -Trp1 (variant), class I –Tyr, class I –Mix (solid symbols) and with class II -Trp1-I-Ab and class II-Tyr-I-Ab and class II –Mix (empty symbols), respectively (empty symbols). (a) MDSC frequency was phenotypically analyzed by flow cytometry 10 days after last vaccination. MDSC activity was assessed by their Arginase-1 production (b), NO-production (c) and PD-L1 surface expression (d) upon vaccination with respective DC vaccine. Results are presented as individual values on scatter plot, mean value of each group is also presented. (*P ≤ 0.05; **P ≤ 0.01; ***P ≤ 0.001; one-way analysis of variance, the differences were assessed by Bonferroni multiple comparison post-test).

In addition, memory T lymphocytes in BM, SP, LN and skin tumors of *ret* tg mice were measured by the expression of CD44 and CD62L. Upon vaccination with class I- Mix mRNA-electroporated DC vaccine, we observed a strong reduction in the frequency of naive $CD62L^+$ $CD44^-$ $CD8^+$ T-cells in LN and skin tumors of tumor bearing mice (**Fig 32,**) as wells as in SP and BM (**Appendix 2**). Furthermore, we found a significant elevation of $CD62L^-$ $CD44^+$ $CD8^+$ EM T cells population in the LN and skin tumor as compared to the control group or to class II vaccinated groups. Interestingly, no statistically significant changes were observed in $CD8^+$ EM cells after vaccination with either Class II –DC vaccine. With regards to CD4+ T memory cell analysis in LN and skin tumor, a significant reduction in the frequency of naive $CD4^+$ T-cells and an increase in $CD4^+$ EM cells was observed after class II mRNA electroporated DC vaccination but not after class I mRNA electroporated DC vaccination. Similar changes were found in SP and BM upon respective vaccination (**Appendix 3**) but to a much lesser extent than in LNs and skin tumors.

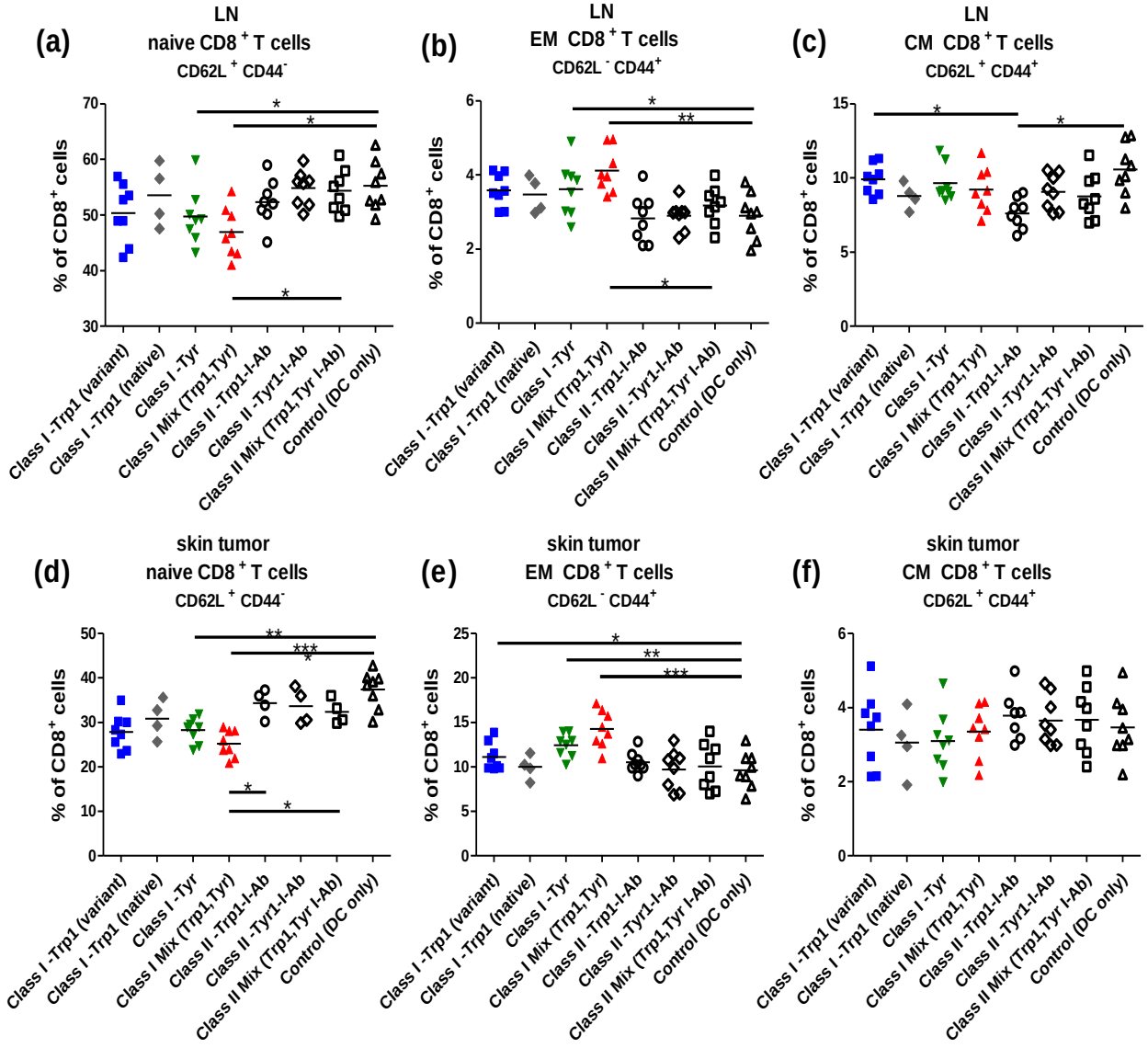

Fig. 32: mRNA-based- DC-vaccine elicits CD8+ T memory response in LN and skin tumors of *ret* tg mice. 4-5 week old melanoma bearing mice were vaccinated with class I -Trp1 (variant), class I –Tyr, class I –Mix (solid symbols) and with class II -Trp1-I-Ab and class II-Tyr-I-Ab and class II –Mix (empty symbols), respectively (empty symbols). 10 days after last vaccination frequency of naïve, central memory and effector-memory was phenotypically determined by CD62L and CD44 expression T lymphocytes. Graphs represent the percentage of naïve ($CD62L^+$ $CD44^-$) (a, d), central memory (CM; $CD62L^+$ $CD44^+$) (b, e), and effector-memory (EM; $CD62L^-$ $CD44^+$) (c, f) for $CD8^+$ T. Results are presented as individual values on scatter plot, mean value of each group is also presented (*P ≤ 0.05; **P ≤ 0.01; ***P ≤ 0.001; one-way analysis of variance, the differences were assessed by Bonferroni multiple comparison post-test).

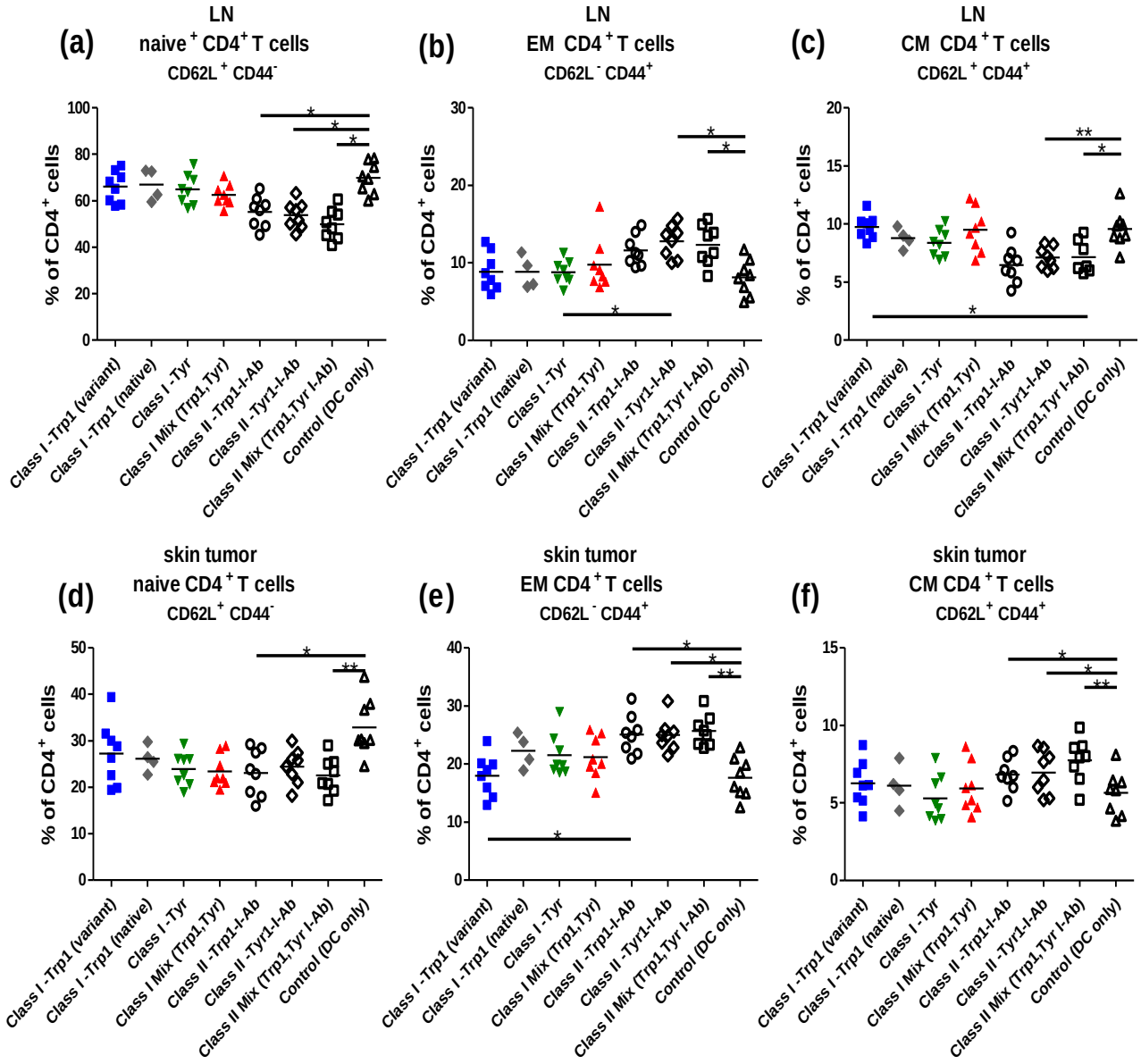

Fig. 33: mRNA-based- DC-vaccine elicits CD4$^+$ T memory response in LN and skin tumors of *ret* tg mice. 4-5 week old melanoma bearing mice were vaccinated with class I -Trp1 (variant), class I –Tyr, class I –Mix (solid symbols) and with class II -Trp1-I-Ab and class II-Tyr-I-Ab and class II –Mix (empty symbols), respectively (empty symbols). 10 days after last vaccination frequency of naïve, central memory and effector-memory was phenotypically determined by CD62L and CD44 expression T lymphocytes. Graphs represent the percentage of naïve (CD62L$^+$ CD44$^-$) (a, d), central memory (CM; CD62L$^+$ CD44$^+$) (b, e), and effector-memory (EM; CD62L$^-$ CD44$^+$) (c, f) CD4$^+$ T cells. Results are presented as individual values on scatter plot, mean value of each group is also presented (*P ≤ 0.05; **P ≤ 0.01; ***P ≤ 0.001; one-way analysis of variance, the differences were assessed by Bonferroni multiple comparison post-test).

Furthermore, we measured frequencies and activity of T cells upon vaccination. CD8 and CD4 T cell frequency in metastatic LNs, tumors, BM and SP was phenotypically analyzed by flow cytometry. T cell activity was assessed by CD69 expression, PD-1 expression and intensity of TCR ζ -chain expression on respective subsets.

Vaccination with either mRNA-based DC vaccines did not significantly alter the frequency of $CD8^+$ T cells in LNs, SP, tumors (**Fig. 34**) and in BM (**Appendix 4**). However, upon vaccination with Class I –Mix vaccine and we observed significantly elevated frequencies of CD69+ CD8+ T cells in LN, SP and skin tumors, in which the elevation was even more profound. Furthermore, upon Class I-Mix vaccination, but not after Class II– DC vaccination, we observed an increase in TCR ζ -chain expression in these organs (**Fig. 34**). In contrast, vaccination with Class I DC vaccine did not alter $CD4^+$ Tell frequency and activity markers, in all studied organs of tumor-bearing mice. However, significant differences in $CD4^+$ T cell activity were observed in vaccinated groups with either class II DC vaccine compared to control or class I vaccinated groups. We demonstrated also elevated frequencies of $CD69^+$, PD-1+ cells and increased TCR ζ -chain expression levels, in $CD4^+$ T cells from LNs and skin tumors. No significant changes were observed in SP and BM of treated mice (**Appendix 5**).

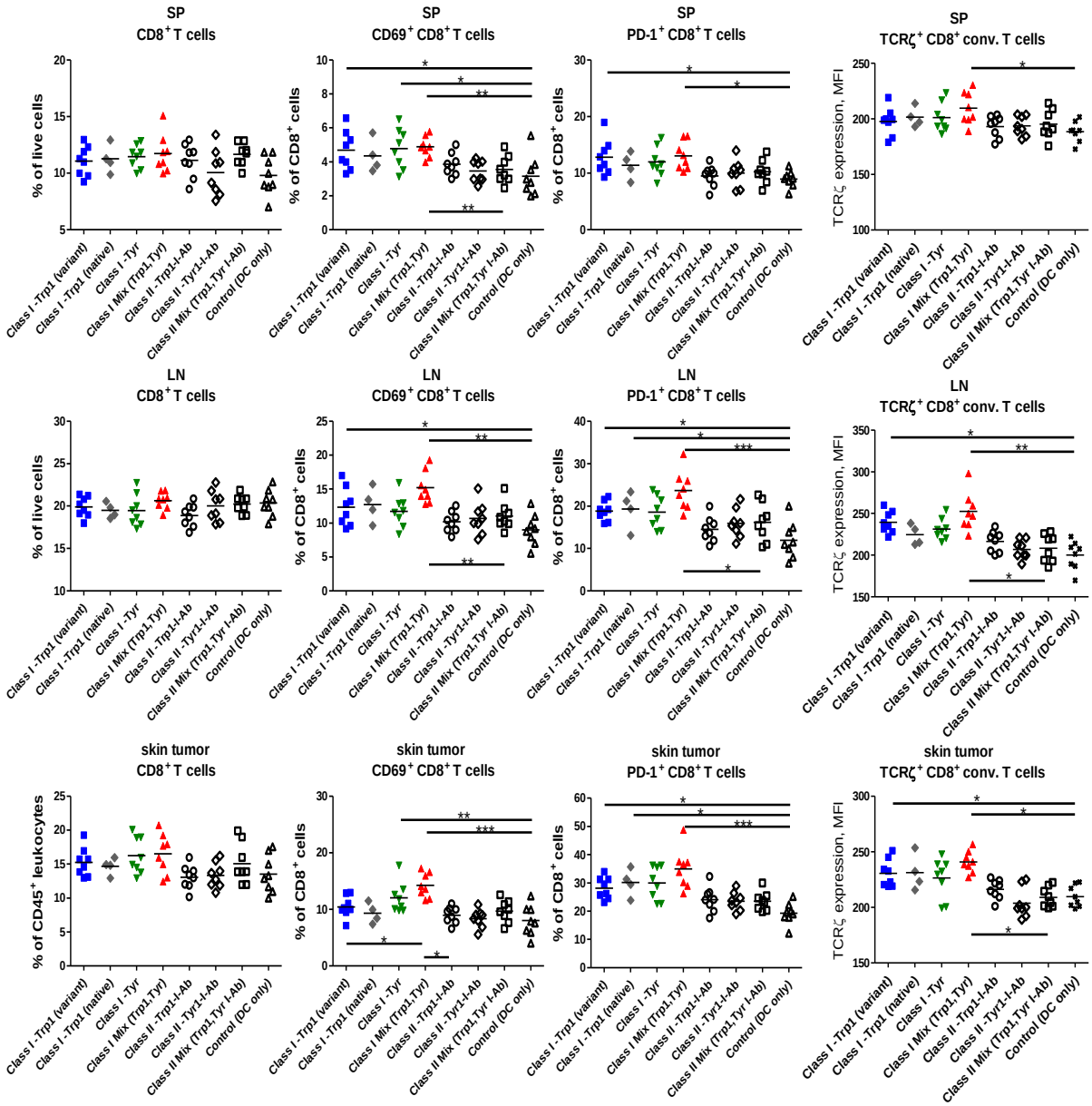

Fig. 34: mRNA-based- DC vaccination improves CD8+ T cell activity in ret tg mice. According to respective treatment group 4-5 week old melanoma bearing mice were vaccinated with class I -Trp1 (variant), class I –Tyr, class I –Mix (solid symbols) and with class II -Trp1-I-Ab and class II-Tyr-I-Ab and class II –Mix (empty symbols), respectively (empty symbols). 10 days after last vaccination CD8+ T cell frequency within the tumor was phenotypically analyzed by flow cytometry (a, d). CD8+ T cell activity was assessed by CD69, PD-1 and TCR ζ-chain expression (b, e). Results are presented as individual values on scatter plot, mean value of each group is also presented (*P ≤ 0.05; **P ≤ 0.01; ***P ≤0.001; one-way analysis of variance, the differences were assessed by Bonferroni multiple comparison post-test).

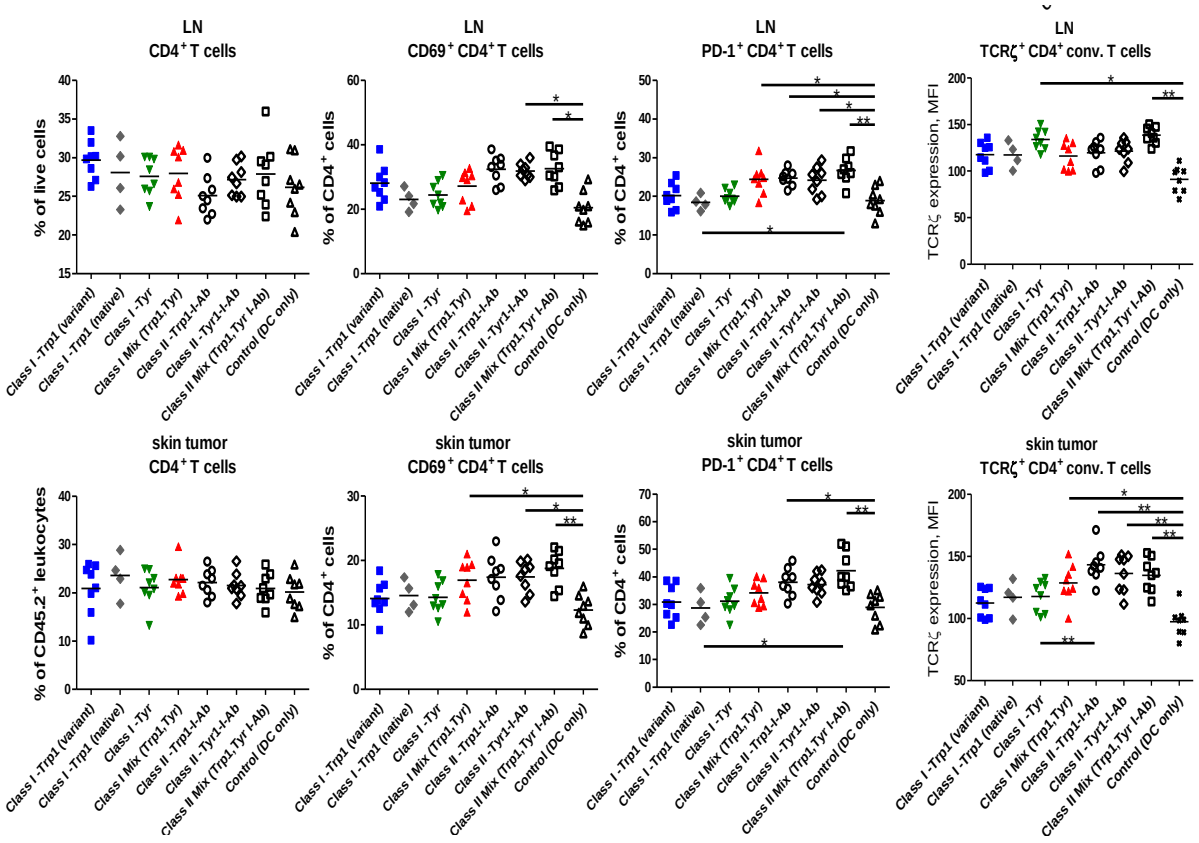

Fig. 35: mRNA-based- DC-vaccine improves CD4$^+$ T cell activity in *ret* tg mice. According to respective treatment group 4-5 week old melanoma bearing mice were vaccinated with class I -Trp1 (variant), class I –Tyr, class I –Mix (solid symbols) and with class II -Trp1-I-Ab and class II-Tyr-I-Ab and class II –Mix (empty symbols), respectively (empty symbols). 10 days after last vaccination CD4+ and CD8+ T cell frequency within the tumor was phenotypically analyzed by flow cytometry (a, d). T cell activity was assessed by intensity of TCRzeta-chain expression (b, e), and % of Ki67+ T cells (c, f) upon respective treatment. Results are presented as individual values on scatter plot, mean value of each group is also presented (*P ≤ 0.05; **P ≤ 0.01; ***P ≤0.001; one-way analysis of variance, the differences were assessed by Bonferroni multiple comparison post-test).

To further characterize the T cell populations following vaccination, we tested the frequency of Treg measured by the expression of CD4, CD25 and FoxP3. In addition, their activity was assessed by the CD39 and Ki-67 expression. Furthermore, the frequency of CD4+ CD25+ FoxP3- activated conventional T cells (Tcons) was measured. Statistically significant differences in the frequency of Tregs were seen exclusively in BM and LN upon treatment with class I mix DC vaccine (**Fig. 36**). We found significantly reduced frequencies of CD39$^+$ and Ki67$^+$ Tregs from SP, LNs and tumors as compared to control group and vaccinated groups with class II-DC vaccine. These results indicated lower immunosuppressive function and lower proliferation capacity of Tregs after Class I -Mix vaccination. Moreover, vaccination with TRP1 (variant) and Class I -Mix resulted in elevated levels of activated T cons in LNs and tumors of *ret* transgenic mice. Interestingly, vaccination with either class II-DC vaccine did not lead to statistically significant reduction of Treg activity upon vaccination. However,

we detected significantly elevated levels of CD39 and Ki 67 expressing Tregs in skin tumors and SP upon class II Mix vaccination. No significant changes in Treg activity in the BM was measured upon the treatment (**Appendix 6).**

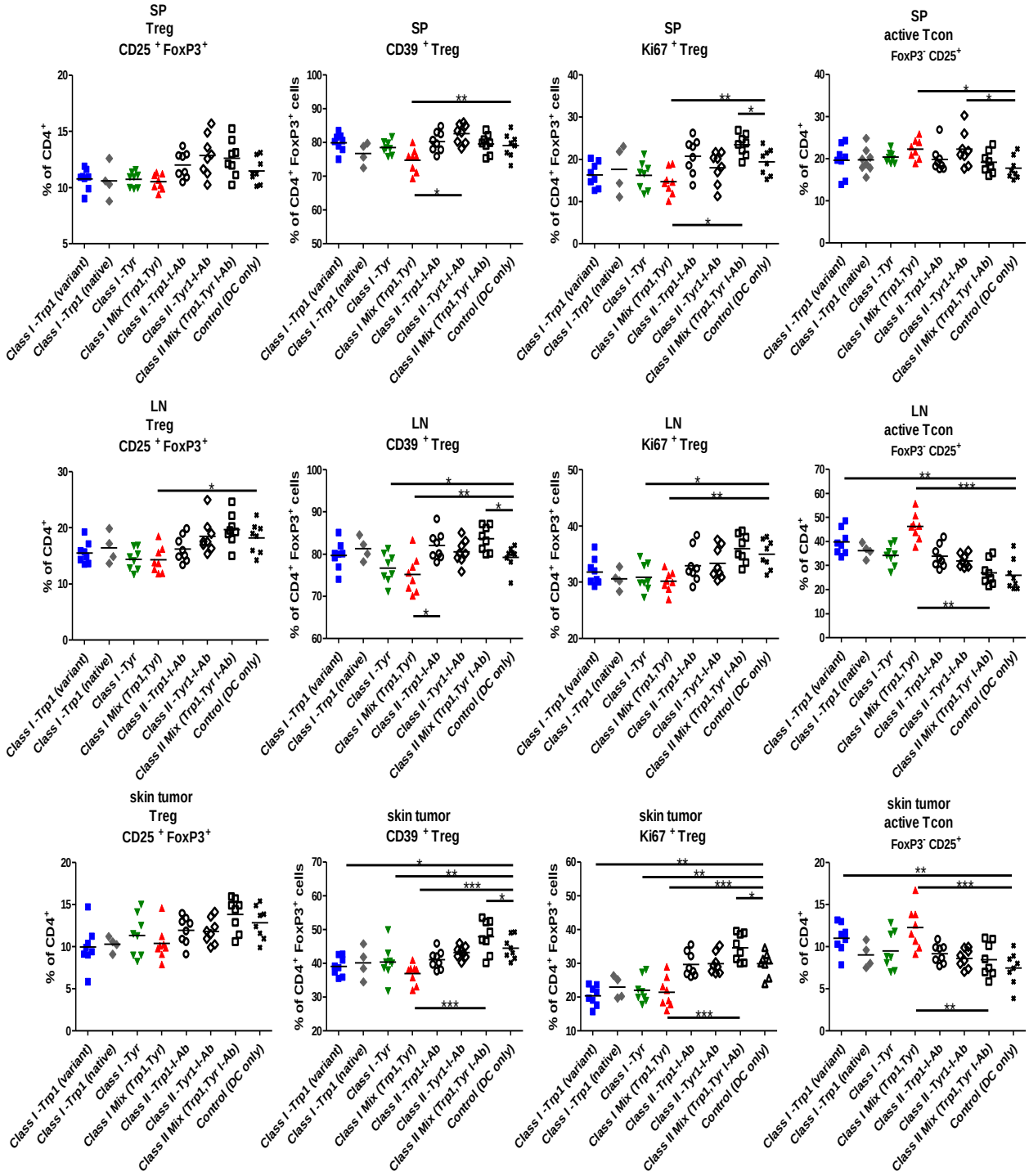

Fig. 36: mRNA-based- DC-vaccine alters T reg and T con frequencies and Treg activity in SP, LN and skin tumors of ret tg mice. 4-5 week old melanoma bearing mice were vaccinated with class I -Trp1 (variant), class I –Tyr, class I –Mix (solid symbols) and with class II -Trp1-I-Ab and class II-Tyr-I-Ab and class II –Mix (empty symbols), respectively (empty symbols 10 days after last vaccination frequency of Treg as well as Treg activity was determined by flow cytometry. Graphs represent the percentage of T reg (a), $CD39^+$ (b) and $Ki67^+$ (c) expression on Treg surface. In addition, a percentage

of activated Tcons ($CD4^+CD25^+FoxP3^-$) was assessed. Results are presented as individual values on scatter plot, mean value of each group is also presented (*P ≤ 0.05; **P ≤ 0.01; ***P ≤ 0.001; one-way analysis of variance, the differences were assessed by Bonferroni multiple comparison post-test)

Furthermore, the potential of the different DC vaccines to elicit antigen-specific immune responses was evaluated. After the treatment, tumors and LNs were analyzed for the induction of peptide-specific $CD4^+$ and $CD8^+$ T cells by ICS for IFN-γ and TNF-α following the re-stimulation with the relevant peptide. Our results indicated an elevated frequency of IFN-γ and TNF-α producing $CD8^+$ T cells. Such elevated levels were not detected in CD4+ T cells, indicating the specificity of Class I vaccination. (**Fig. 37**). In contrast, increased frequency of IFN-γ and TNF-α producing $CD4^+$ T cells were exclusively detected in skin tumor and LN upon vaccination with class II Mix (**Fig. 37** and **Appendix 7)**.

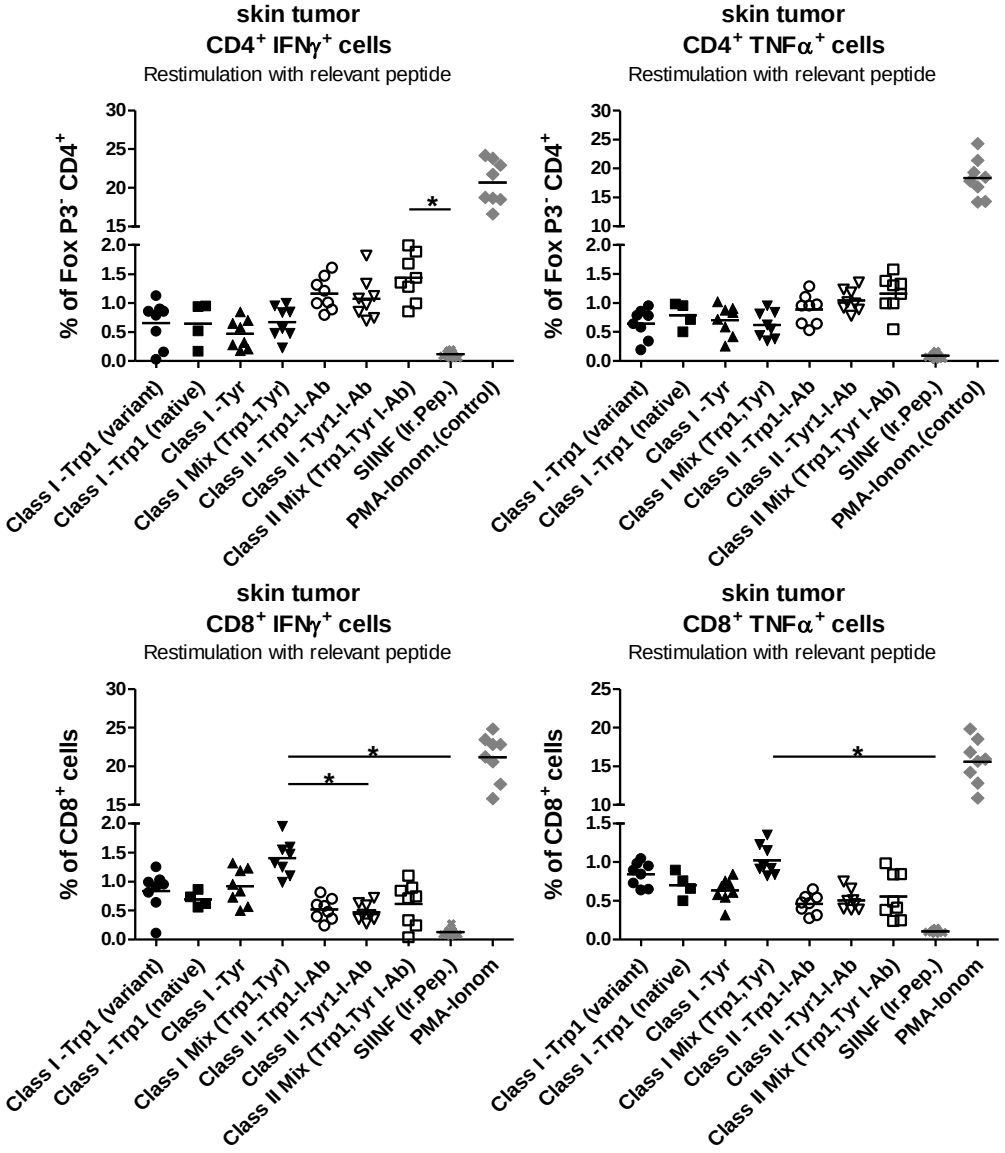

Fig. 37: Analysis of T-cell antigen-specific immune responses in skin tumors of ret tg mice following vaccination with class I or class II mRNA-electroporated DCs. Tumor bearing ret mice

were vaccinated intraperitoneally 3 times using BMDCs electroporated with class I constructs Trp1-Kb/TLR4, Tyr- Kb/TLR4, the combination (Mix) mRNA, or class II constructs Trp1-I-Ab, Tyr-I-Ab respectively. Ten days after the last vaccination spleens and lymph nodes were harvested and analyzed for the induction of peptide-specific $CD4^+$ and $CD8^+$ T cells by ICS for IFN-γ and TNF-α, following re-stimulation with the relevant peptide according to the group ($Trp\text{-}1_{455\text{-}463}$, $Tyr_{360\text{-}368}$ or their combination or $Trp\text{-}1_{455\text{-}463}$ I-Ab, $Tyr_{99\text{-}117}$ I-Ab). Restimulation with irrelevant peptide (SIINFEKL) was used for as negative control and 50ng/mlPMA-2μg/mL Ionomycine restimulation as positive control. Graphs represent the percentages of $CD4^+$ $INF\gamma^+$ and $TNF\text{-}\alpha^+$ (upper row), and $CD8^+$ $IFN\gamma^+$, and $TNF\text{-}\alpha^+$ cells (lowe row). Results are presented as individual values on scatter plot, mean value of each group is also presented (*P ≤ 0.05; **P ≤ 0.01; ***P ≤ 0.001; one-way analysis of variance, the differences was assessed by Bonferroni multiple comparison post-test)

To summarize, we showed that vaccination with mRNA based Class I DC vaccines stimulated a strong, systemic CD8 T cell response indicated by induction of antigen specific IFN-γ producing and memory $CD8^+$ T cells in skin tumors, LNs and SP. In addition, these cells showed increased levels of activity markers (CD69, PD-1 and TCR ζ-expression). Moreover, effects of vaccination with bivalent DCs, simultaneously expressing the Class I Mix (Tyr and TRP1) revealed a more profound effect on the CD8 T cell response as compared to monovalent class I DC vaccines. This was correlating with significant improved survival rates or melanoma bearing mice that were vaccinated with Class I Mix. Importantly, suchsystemic CD8 T cell response was not induced upon vaccination with any Class II DC vaccine. In contrast, a specific CD4+ T cells response (measured by increased PD-1, CD69 and TCR ζ expression) was elicited in LNs and skin tumors exclusively upon vaccination with class II vaccines. However, a significant induction of several Treg activity markers (Ki67, CD39) was also observed. Finally, the vaccination with class II constructs alone did not significantly improve survival rate of tumor bearing mice.

4.9 Combined melanoma treatment with low-dose paclitaxel and dendritic cell vaccination

According to previous studies in our lab, application of paclitaxel in low, non-cytotoxic doses supported vaccination with melanoma-specific peptides in normal mice[168]. This effect was strongly associated with a significant reduction in frequencies of IMC (as a counterpart of MDSC in healthy mice) and Treg. Thus, in the following experiments the impact of mRNA-based DC vaccination on melanoma bearing *ret* transgenic mice were assessed by treating the mice with low-dose paclitaxel in combination with bivalent Class I –Mix-DC vaccine and Class I & Class II (IAb)-Mix as a multivalent DC vaccine (**Table 7**). The reason for combination of class I and class II mRNA constructs for DC vaccination was to stimulate both systemic CD8 and CD4 T cell responses since exclusive class II vaccination did not lead to improved overall survival of treated mice (Chapter 6.1).

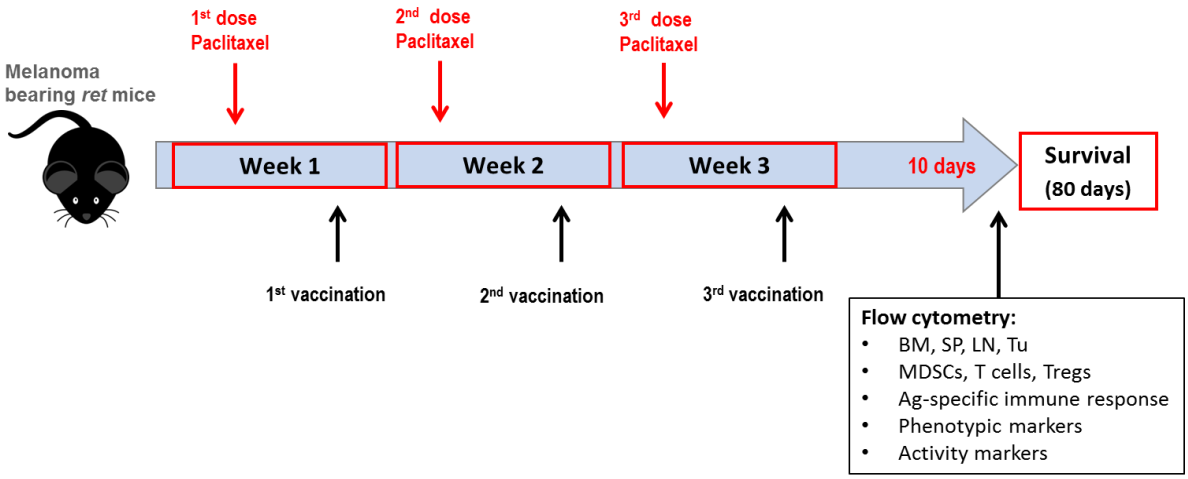

Fig. 38: Combined melanoma treatment strategy for paclitaxel and dendritic cell vaccination. In order to compare the effects of combined melanoma immunotherapy, 4-5 weeks old melanoma bearing ret tg mice were treated i.p. with ultra-low dose of Paclitaxel (1mg/kg) three times in 7 days intervals. 3-4 days later respective mice were vaccinated i.p. with mRNA-electroporated DCs ($0.5X10^6$ cells per mouse) three times in 7 days intervals. Ten days after last vaccination, 4 mice of each treatment group were sacrificed and flow cytometry analyses, was performed. Remaining mice of each group were kept for survival analysis and monitored for at least 80 days in regular intervals

Table 6: Treatment groups for melanoma immunotherapy experiment combined with paclitaxel

#	Treatment
1	Class I –Mix (mTrp-$1_{455-463}$/ mTyr$_{360-368}$-hβ2m-K^b / TLR-4)
2	Class I –Mix + Paclitaxel (1mg/kg)
3	Class I –Mix + Class II Mix (Trp-$1_{455-463}$ / TYR$_{99-117}$-I-Ab)
4	Class I –Mix + Class II Mix + Paclitaxel (1mg/kg)
6	Paclitaxel (1mg/kg)
7	Control (DC only)

4.9.1 Survival analysis

Fig. 38 shows survival curves of treated tumor bearing mice 80 days after the start of the treatment with paclitaxel and Class I–Mix DC vaccine. In line with previous results, we found a significantly improved survival of mice treated with DCs electroporated with Class I–Mix DC vaccine compared to control group (P <0.01). Importantly, an addition of paclitaxel further improved the survival of mice (P <0.001). **Fig. 39** presents survival of tumor bearing mice 80 days upon the treatment with paclitaxel and Class I Mix + Class II-IAb-Mix. The treatment with Class I–Mix + Class II–Mix showed improved survival rate of melanoma bearing mice compared to control group (P < 0.05), whereas paclitaxel treatment did not further improved mouse survival (P < 0.05) (**Fig. 40**).

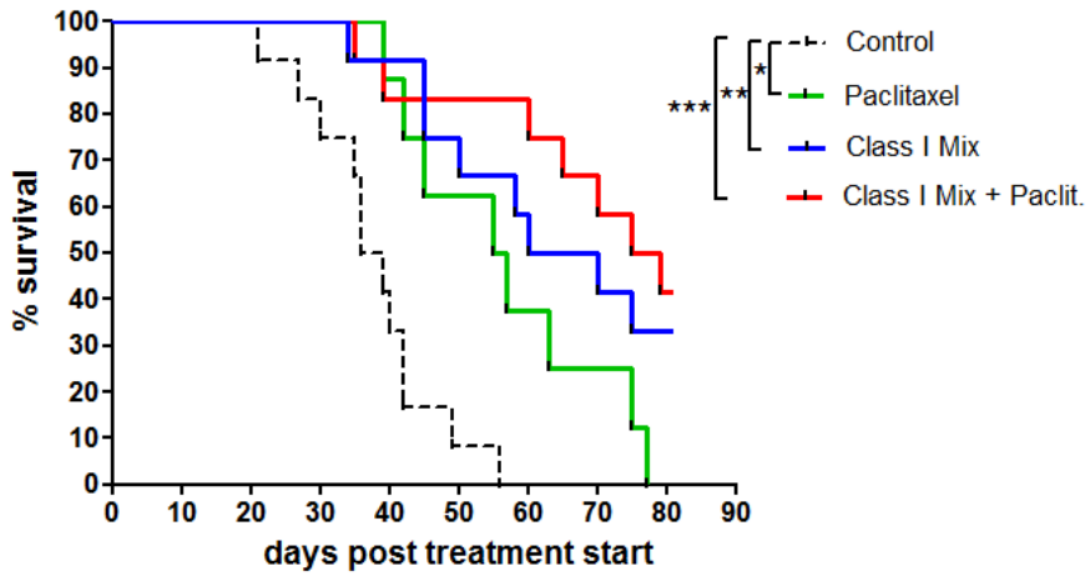

Fig. 39: Survival proportions of melanoma bearing *ret* mice following vaccination with class I mRNA-electroporated DCs in combination with low dose of paclitaxel. Melanoma bearing ret tg mice were treated i.p. with ultra-low dose (ld) of Paclitaxel (1mg/kg) three times in 7 days intervals. 3-4 days later respective mice were vaccinated i.p. ,three times in 7 days intervals with mRNA-electroporated DCs ($0.5X10^6$ cells per mouse; according to groups). Mice vaccinated with electroporated but unloaded DCs were used as control. Mice (n=6-12) were monitored for 80 days after the first vaccination. Survival curves of each treatment group are shown results are presented as percent of surviving mice (*P ≤ 0.05; **P ≤ 0.01; ***P ≤0.001; generated using, product limit (Kaplan-Meier) method, comparison of survival curves; Log-rank (Mantel-Cox) test).

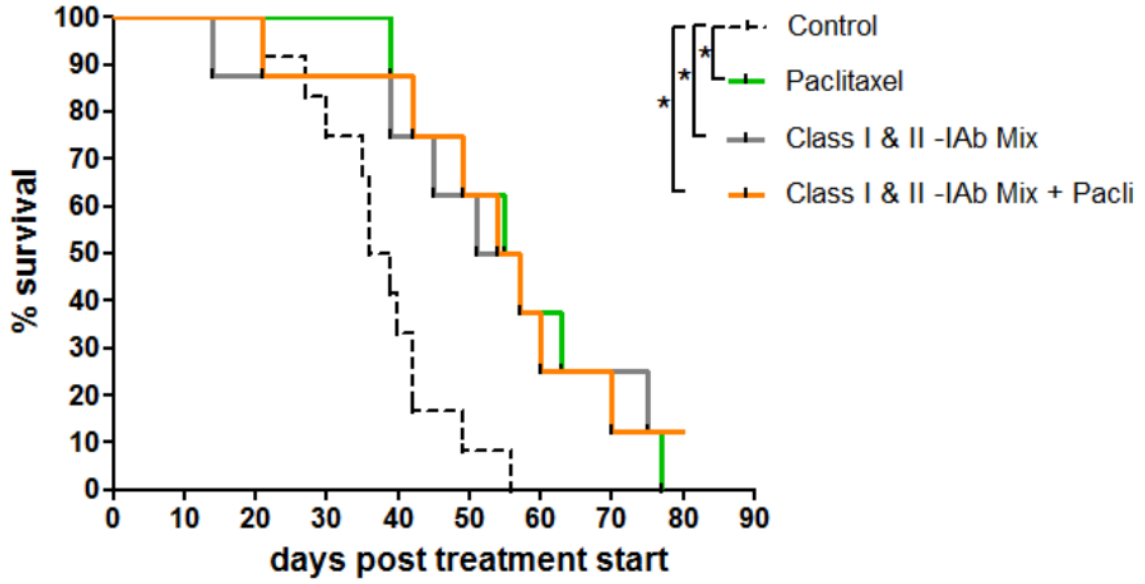

Fig. 40: Survival proportions of melanoma bearing *ret* mice following vaccination with class Mix of class I and II mRNAelectroporated DCs in combination with low dose of paclitaxel. Melanoma bearing ret tg mice were treated i.p. with ultra-low dose (ld) of Paclitaxel (1mg/kg) three times in 7 days intervals. 3-4 days later respective mice were vaccinated i.p. ,three times in 7 days intervals with mRNA-electroporated DCs ($0.5X10^6$ cells per mouse; according to groups). Mice vaccinated with electroporated but unloaded DCs were used as control. Mice (n=6-12) were monitored for 80 days after the first vaccination. Survival curves of each treatment group are shown Results are presented as percent of surviving mice (*P ≤ 0.05; **P ≤ 0.01; ***P ≤0.001; generated using, product limit (Kaplan-Meier) method, comparison of survival curves; Log-rank (Mantel-Cox) test).

4.9.2 Immune cell analyses after DC vaccination combined with paclitaxel treatment

We found that the combination of Paclitaxel and Class I-Mix DC vaccine decreased the frequency of tumor-infiltrating MDSCs (**Fig. 41**). In addition, MDSC activity in LNs, SP and the skin tumor was diminished upon Class I–Mix DC vaccination. This effect was even more profound after the combination with paclitaxel treatment indicated by a significant decrease of arginase-1 and PD-L1 expression as well as NO production.

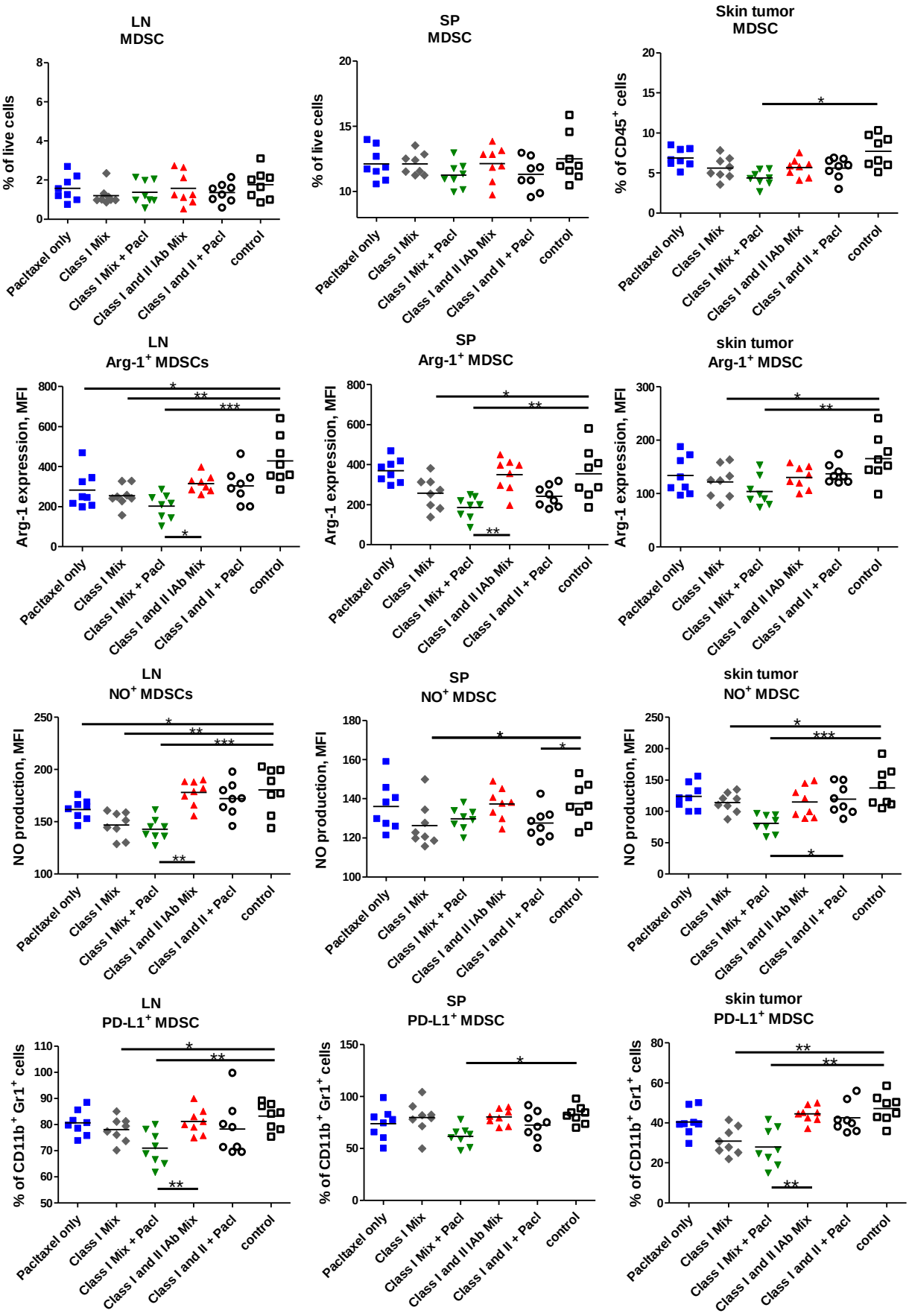

Fig. 41: In combined therapy, paclitaxel increases class I –Mix DC-vaccine effect in diminishing MDSC activity in combined therapy within LN, SP and skin tumors of *ret* tg mice. According to

respective treatment group, 4-5 week old melanoma bearing mice were injected with low-dose of paclitaxel (1mg/kg) and/or vaccinated with class I –Mix or class I –Mix + class II -Mix, respectively. MDSC frequency within the tumor was phenotypically analyzed by flow cytometry 10 days after last vaccination. MDSC activity was assessed by their Arginase-1 production, NO-production and PD-L1 surface expression upon vaccination with respective DC vaccine. Results are presented as individual values on scatter plot, mean value of each group is also presented (n= 8; *P ≤ 0.05; **P ≤ 0.01; ***P ≤0.001; one-way analysis of variance, the differences were assessed by Bonferroni multiple comparison post-test).

Furthermore, we measured frequencies and activity of T cells. Vaccination with DCs did not significantly alter frequency of $CD4^+$ T cells within LN, SP and skin tumors (**Fig. 42**). as the frequency of CD8+ T cells in skin tumors was found to be significantly increased as compared to control upon Class I DC vaccination combined with paclitaxel. Moreover, we observed elevated intensities of TCR ζ chain expression and increased frequencies PD-1+ cells within $CD4^+$ T cells, in LNs and skin tumors after Class I–Mix + Class II–Mix vaccination or combinatorial treatment with Paclitaxel as compared to the control group. In contrast, upon class I DC vaccination, we observed no significant changes on CD4+ T cells frequencies or activity markers. However, Class I DC vaccination significantly affected $CD8^+$ T cells activity after Class I–Mix vaccination (**Fig. 43**). We detected a strong increase of TCR ζ chain expression as well as PD-1 expression in CD8+ T cells in LN, SP and skin tumors of treated mice as compared to control group or class I Mix + class II mix vaccinated group. Moreover, these tendencies were even more profound when class I DC vaccination was combined with low dose of Paclitaxel. These results clearly revealed that Paclitaxel increased DC vaccination effect by restoring the activity of tumor-infiltrating $CD8^+$ and $CD4^+$ T cells.

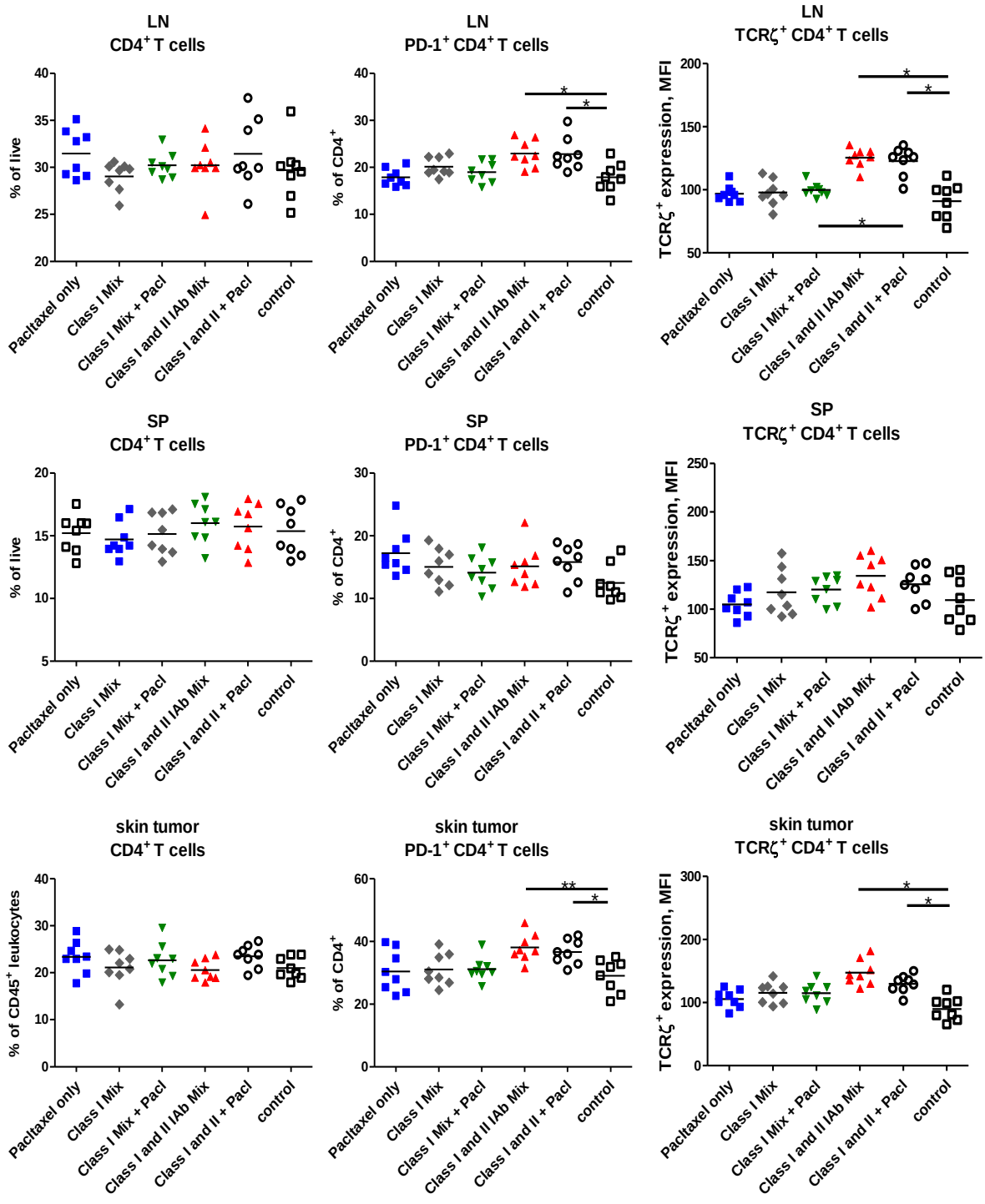

Fig. 42: In combined therapy, paclitaxel increases class I –Mix DC-vaccine effect by restoring T cell activity within skin tumors of *ret* tg mice. According to respective treatment group, 4-5 week old melanoma bearing mice were injected with paclitaxel (1mg/kg) and/or vaccinated with class I –Mix or class I –Mix + class II -Mix, respectively. 10 days after last vaccination CD4+ and CD8+ T cell frequency within the tumor was phenotypically analyzed by flow cytometry (a, d). T cell activity was assessed by intensity of TCRζ-chain expression (b, e), and % of Ki67+ T cells (c, f) upon respective treatment. Results are presented as individual values on scatter plot, mean value of each group is also presented (n= 8; P ≤ 0.05; **P ≤ 0.01; ***P ≤0.001; one-way analysis of variance, the differences were assessed by Bonferroni multiple comparison post-test)

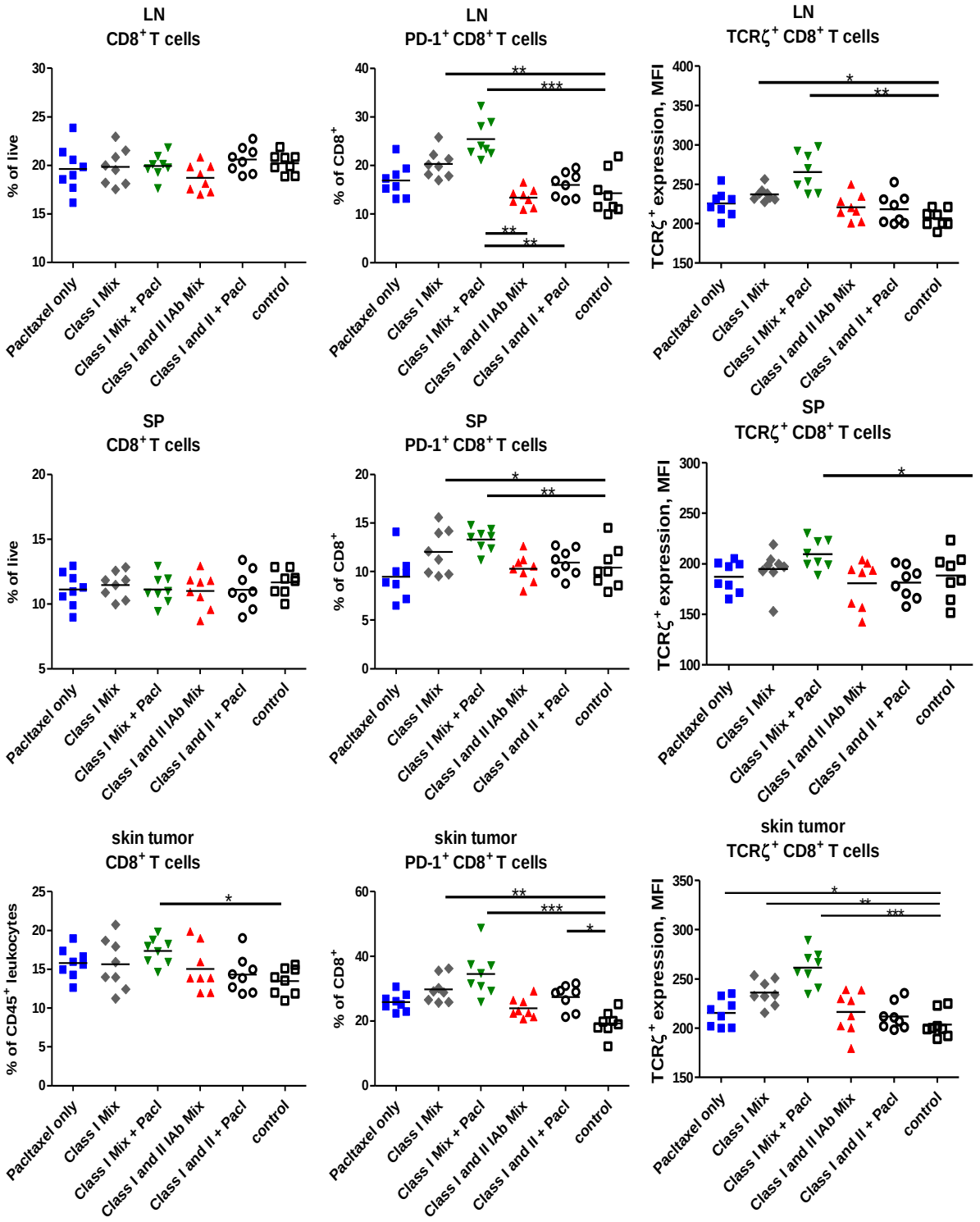

Fig. 43: In combined therapy, paclitaxel increases class I –Mix DC-vaccine effect by restoring T cell activity within skin tumors of *ret* tg mice. According to respective treatment group, 4-5 week old melanoma bearing mice were injected with paclitaxel (1mg/kg) and/or vaccinated with class I –Mix or class I –Mix + class II -Mix, respectively. 10 days after last vaccination CD4+ and CD8+ T cell frequency within the tumor was phenotypically analyzed by flow cytometry (a, d). T cell activity was assessed by intensity of TCR ζ-chain expression (b, e), and % of Ki67+ T cells (c, f) upon respective treatment Results are presented as individual values on scatter plot, mean value of each group is also presented (n= 8; *P ≤ 0.05; **P ≤ 0.01; ***P ≤0.001; one-way analysis of variance, the differences were assessed by Bonferroni multiple comparison post-test)

In addition, we measured systemic memory T lymphocyte induction upon treatment of *ret* tg mice d by expression of CD44 and CD62L. upon vaccination with Class I–Mix + Class II–Mix DC vaccine, a significant reduction in the frequency of naive and CM $CD4^+$ T cells, along with a significant elevation of EM $CD4^+$ T cell were observed in LNs, SP and skin tumors of *ret* tg mice compared to the control, paclitaxel only or to class I vaccinated groups, respectively (**Fig. 44**). Combination with Paclitaxel augmented this effect. Vaccination with Class I–Mix DC vaccine significantly reduced the frequency of naive $CD8^+$ T cells and elevated the frequency of EM ($p<0.05$) and CM $CD8^+$ T cells ($P<0.05$) in LN and skin tumors of *ret* tg mice compared to control or Paclitaxel only treated group (**Fig. 45**). Importantly, combination with Paclitaxel further augmented this effect indicated by an increased frequency of EM $CD8^+$ T cells as compared to Class I–Mix DC vaccination alone ($P<0.01$). These results showed that combinatorial treatment with low dose paclitaxel could enhance systemic memory T cell induction.

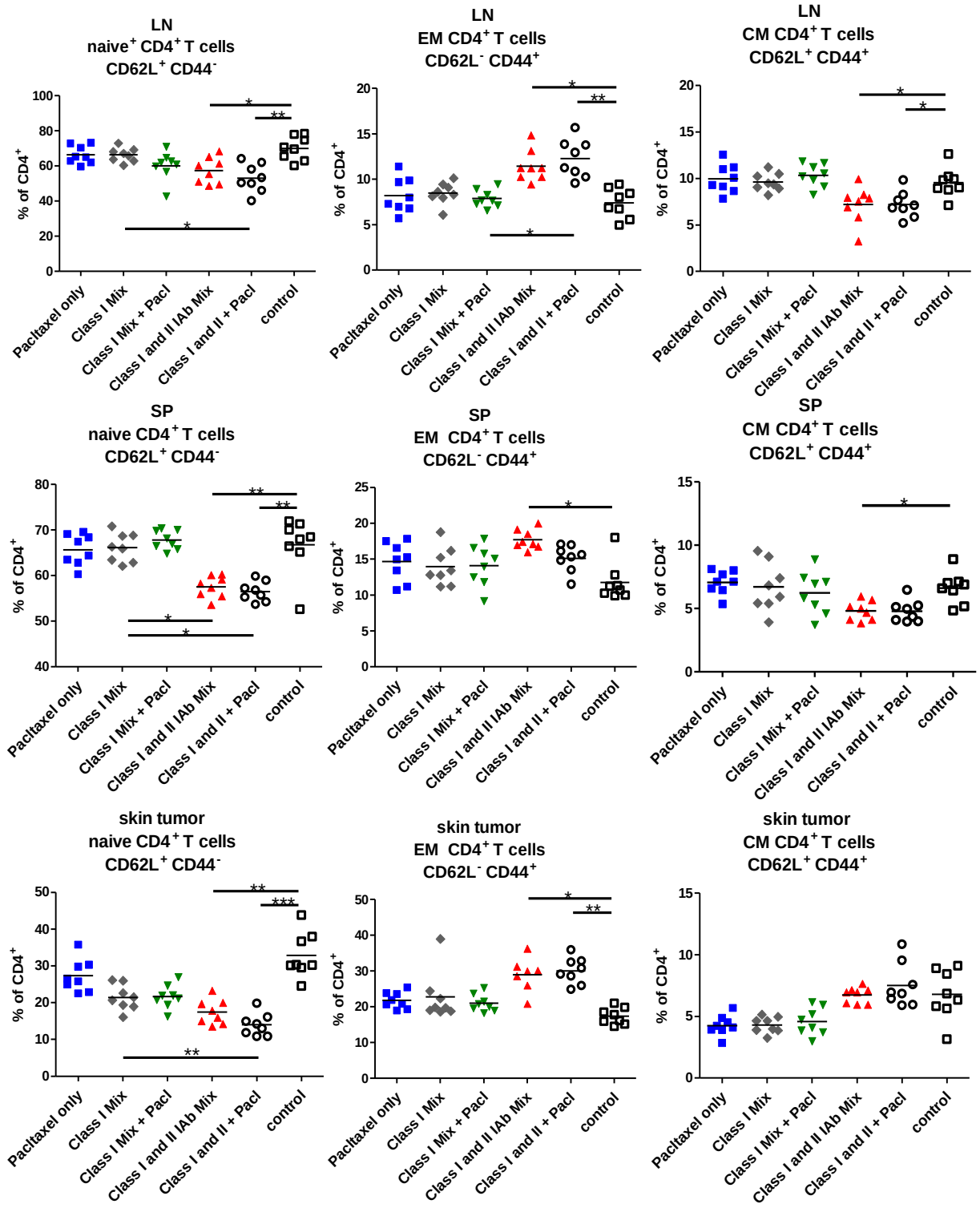

Fig. 44: In combined therapy, paclitaxel increases class I –Mix DC-vaccine effect in diminishing MDSC activity in combined therapy within skin tumors of *ret* tg mice. According to respective treatment group, Melanoma bearing mice were injected with paclitaxel (1mg/kg) and/or vaccinated with class I –Mix or class I –Mix + class II -Mix, respectively. 10 days after last vaccination frequency of naïve, central memory and effector-memory was phenotypically determined on CD4+ and CD8+ T lymphocytes. Graphs represent the percentage of naïve ($CD62L^+$ $CD44^-$) (a, d), central memory (CM; $CD62L^+$ $CD44^+$) (b, e), and effector-memory (EM; $CD62L^-$ $CD44^+$) (c, f) for both $CD8^+$ T cells (a-c) and $CD4^+$ T cells (d-f Results are presented as individual values on scatter plot, mean value of each group is also presented (n= 8; *P ≤ 0.05; **P ≤ 0.01; ***P ≤ 0.001; one-way analysis of variance, the differences were assessed by Bonferroni multiple comparison post-test).

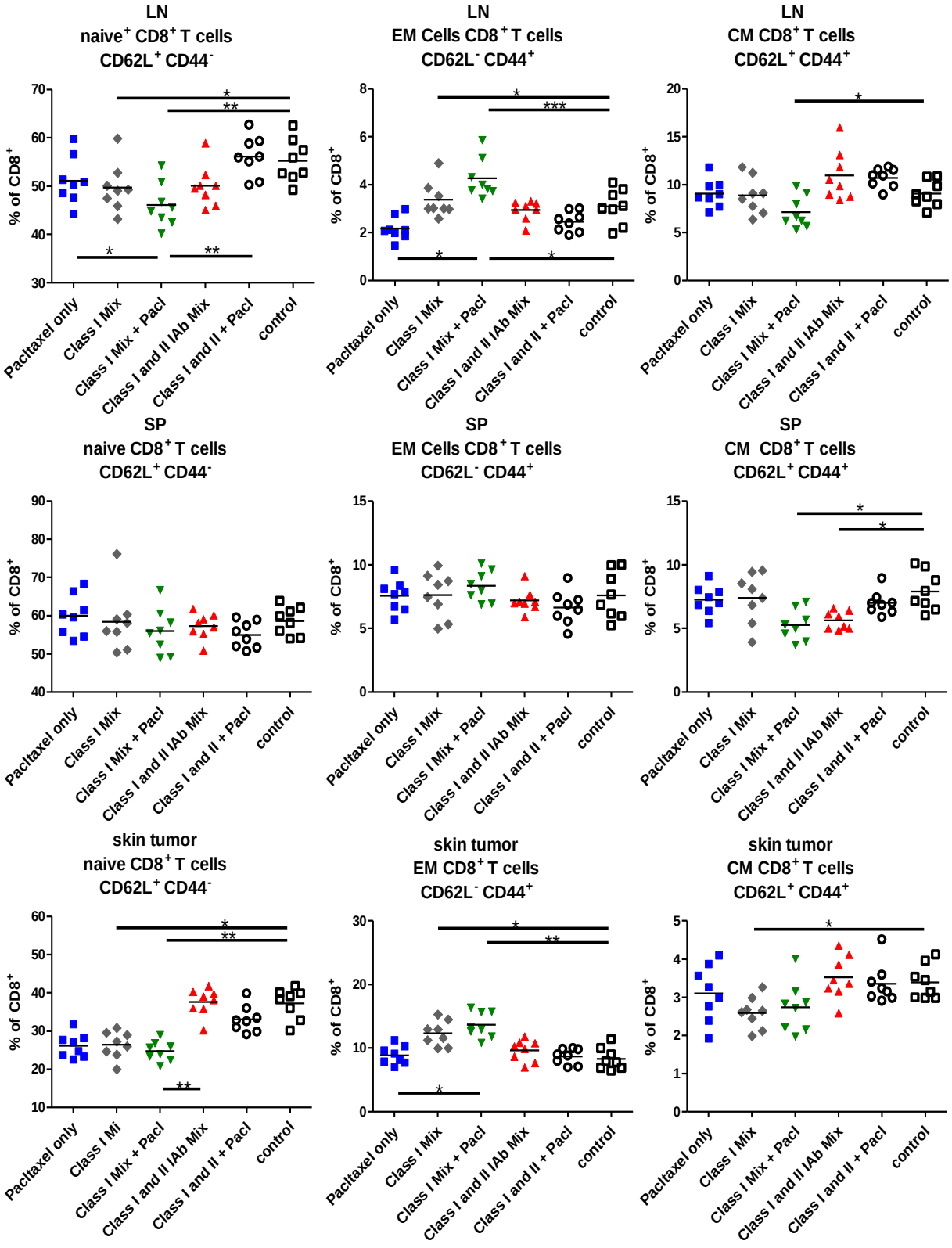

Fig. 45: In combined therapy, paclitaxel increases class I –Mix DC-vaccine effect in diminishing MDSC activity in combined therapy within skin tumors of *ret* tg mice. According to respective treatment group, Melanoma bearing mice were injected with paclitaxel (1mg/kg) and/or vaccinated with class I –Mix or class I –Mix + class II -Mix, respectively. 10 days after last vaccination frequency of naïve, central memory and effector-memory was phenotypically determined on CD4+ and CD8+ T lymphocytes. Graphs represent the percentage of naïve ($CD62L^+$ $CD44^-$) (a, d), central memory (CM; $CD62L^+$ $CD44^+$) (b, e), and effector-memory (EM; $CD62L^-$ $CD44^+$) (c, f) for both $CD8^+$ T cells (a-c) and

$CD4^+$ T cells (d-f). Results are presented as individual values on scatter plot, mean value of each group is also presented (n= 8; *P ≤ 0.05; **P ≤ 0.01; ***P ≤ 0.001; one-way analysis of variance, the differences were assessed by Bonferroni multiple comparison post-test).

Furthermore, the potential of the different DC vaccines to elicit antigen-specific immune responses was assessed. After the treatment, tumors (**Fig. 46**) and metastatic LNs (**Appendix 8**) were analyzed for the induction of peptide-specific $CD4^+$ and $CD8^+$ T cells by ICS for IFN-γ and TNF-α. Our results indicated that vaccination with Class I–Mix s increased the frequency of IFN-γ and TNF-α producing $CD8^+$ T cells (**Fig.46**). These effects were not significantly augmented by Paclitaxel. Furthermore, upon class I mix + Class II mix DC vaccination, increased frequency of IFN-γ and TNF-α producing $CD4^+$ T cells and tendency of increased frequency of CD8+ IFN-γ producing T cells in LNs and skin tumors was detected, indicating an induction of antigen specific CD4+ and CD8+ T cells.

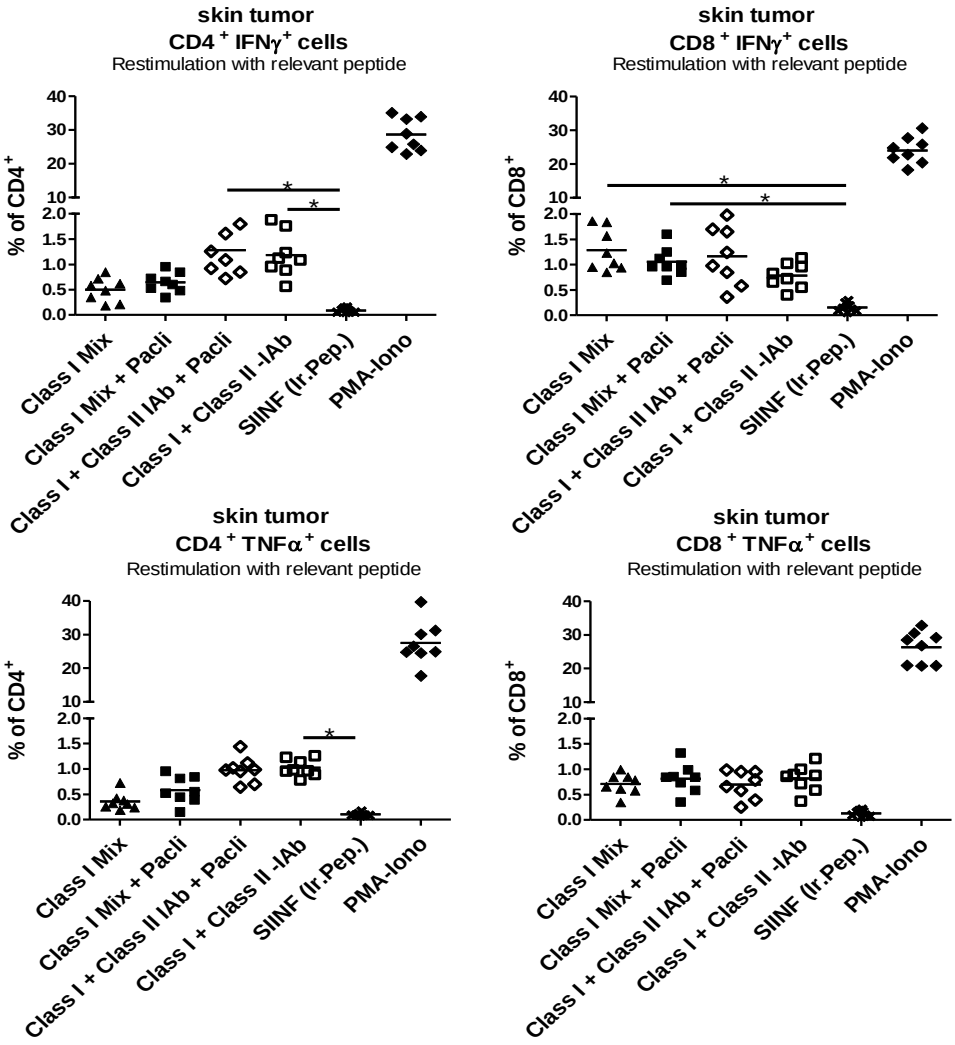

Fig. 46: Analysis of T-cell antigen-specific immune responses in skin tumors of *ret* tg mice following vaccination with class I or class II mRNA-electroporated DCs in combined therapy.

According to respective treatment group, Melanoma bearing mice were injected with Id of paclitaxel (1mg/kg) and/or vaccinated with class I –Mix or class I –Mix + class II -Mix, respectively. 10 days after last vaccination. spleens and lymph nodes were harvested and analyzed for the induction of peptide-specific $CD4^+$ and$CD8^+$ T cells by ICS for IFN-γ and TNF-α, following re-stimulation with the relevant peptide according to the group (ClassI mix: $Trp\text{-}1_{455\text{-}463}$ and $Tyr_{360\text{-}368}$ or their combination with class II peptides: $Trp\text{-}1_{455\text{-}463}$ I-Ab, $Tyr_{99\text{-}117}$ I-Ab). Restimulation with irrelevant peptide (SIINFEKL) was used for as negative control and 50ng/mlPMA-2ug/ml Ionomycine restimulation as positive control. Bar graphs representing the percentages of $CD4^+$ $INF\gamma^+$, $CD4^+$ $TNF\text{-}\alpha^+$ and $CD8^+$ $INF\gamma^+$, $CD8^+$ $TNF\text{-}\alpha^+$ cells. Results are presented as individual values on scatter plot, mean value of each group is also presented, (*P ≤ 0.05; **P ≤ 0.01; ***P ≤ 0.001; one-way analysis of variance, the differences was assessed by Bonferroni multiple comparison post-test).

Next we observed a significant reduction in the frequency of Tregs in tumors SP and LNs upon class I Mix DC vaccination as compared to control ($p<0.05$) or class I mix + class II mix vaccinated group ($p<0.05$) (**Fig. 47**). Treg frequency was even more reduced when class I Mix DC vaccination was combined with paclitaxel treatment ($p<0.01$). When evaluating activation status of Treg, significantly reduced frequencies of $CD39^+$ Tregs and $Ki67^+$ Tregs as compared to control or class I-Mix + Class II-Mix vaccinated groups were detected (**Fig. 47**). These results indicated lower immunosuppressive function and proliferation capacity of Tregs after Class I-Mix vaccination. Interestingly, this inhibitory effect was even more profound after the combination with paclitaxel. Importantly, vaccination with Class I–Mix + Class II–Mix showed increased Treg activity indicated by higher frequencies of $CD39^+$ and $Ki67^+$ Tregs as compared to the control and Class I–Mix vaccinated groups. In addition, Class I–Mix + Class II–Mix vaccination, but not Class I-Mix vaccination, led to a significant reduction of tumor-infiltrating activated Tcons. These results indicated that Class I–Mix + Class II–Mix DC vaccination enhanced functions of tumor-infiltrating Tregs. In agreement with these data, mouse survival could be further improved upon the combination Class I-Mix DC vaccination with low-dose paclitaxel but not upon Class I–Mix + Class II–Mix DC vaccination.

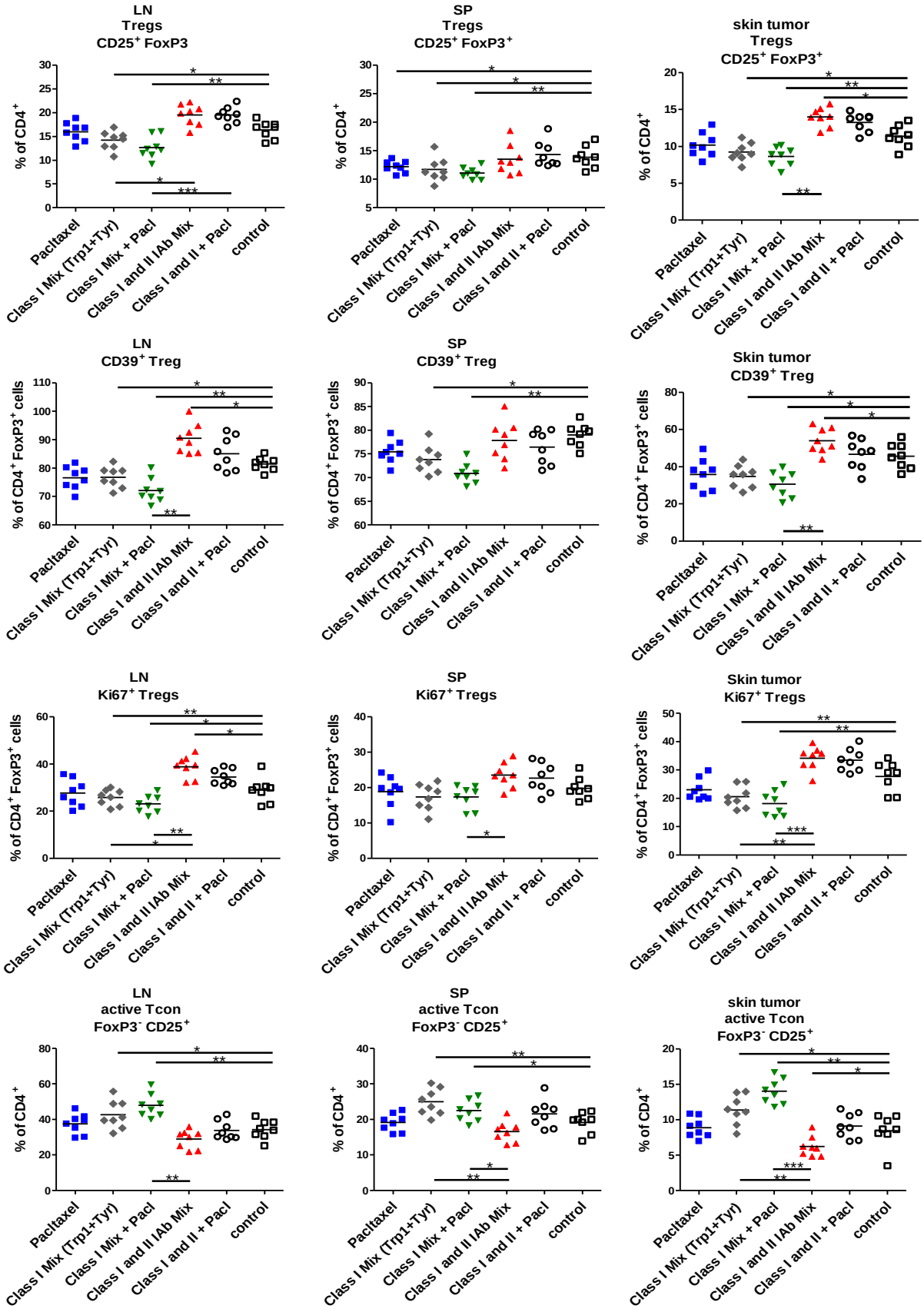

Fig. 47: In combined therapy, paclitaxel significantly influences of activity of Treg and conventional T cells. According to respective treatment group, Melanoma bearing mice were injected with ld of paclitaxel (1mg/kg) and/or vaccinated with class I –Mix or class I –Mix + class II -Mix,

respectively. 10 days after last vaccination.Treg as well as Treg activity was determined by flow cytometry. Graphs represent the percentage of T reg (a) , $CD39^+$ (b), $Ki67^+$ (c) expression on Treg surface. In addition frequency of ($CD4^+CD25^+FoxP3^-$) activated Tcon was assessed. Results are presented as individual values on scatter plot, mean value of each group is also presented (*P ≤ 0.05; **P ≤ 0.01; ***P ≤ 0.001; one-way analysis of variance, the differences were assessed by Bonferroni multiple comparison post-test).

Several mice, which were vaccinated with Class I–Mix DC vaccination, as well as Class I–Mix vaccination in combination with paclitaxel developed treatment-related vitiligo (**Fig.48**).

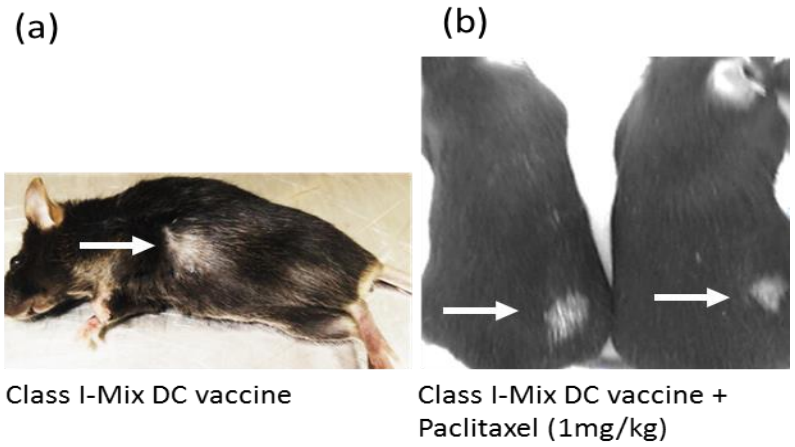

Fig. 48: Treatment-dependent vitiligo after DC vaccination. Class I–Mix DC vaccination, as well as Class I–Mix vaccination in combination with paclitaxel developed treatment related vitiligo. Mice shown were 3-4 months old, approximately 60-80 days after treatment start

4.9.3 Antigen specific $CD4^+$ T cell and Treg induction analyzed by and class II tetramer staining after DC vaccination

Next, we investigated antigen-specific Treg induction upon vaccination with class II mRNA DC vaccine or in combined with class I mRNA DC vaccine, which could partly be responsible for the lack of survival benefits in these groups.

Immature autologous BMDC were harvested and electroporated with respective mRNA construct summarized in **Table 8**. Melanoma bearing mice were vaccinated i.p. with mRNA-electroporated DCs ($0.5x10^6$ cells per mouse) three times in 7 days intervals. Ten days after last vaccination, 3 mice of each treatment group were sacrificed and cell suspensions of LN, SP and skin tumors were restimulated in vitro with specific peptide $TRP1_{(111-128)}$ and $Tyr_{(99-117)}$, or irrelevant control $OVA_{(323-339)}$ for 65-70h. Afterwards, cells were subjected to MHC class II tetramer staining in order to confirm presence of antigen specific CD4 T cells and Treg, respectively.

Table 7: MHC restricted constructs used for immunizations

#	MHC class I -Vaccine Construct's Composition	Designation
1	Variant-Trp-$1_{455-463}$-hβ2m-K^b /TLR4 and $Tyr_{360-368}$-hβ2m-$K^{b/}$ TLR4 -Mix	Class I –Mix
2	Trp-$1_{455-463}$ - H2-I-A^b and TYR_{99-117} - H2-IA^b - Mix	Class II –Mix- I-A^b
3	Class II –Mix- I-A^b + Paclitaxel (1mg/kg)	Class II –Mix- I-A^b + Paclitaxel
4	Trp-$1_{455-463}$ - CLIP and TYR_{99-117} - CLIP - Mix	Class II –Mix- CLIP
5	Class I–Mix (#1) + Class II -I-A^b–Mix (#2)	Class I –Mix + Class II –I-A^b –Mix

As shown in **Fig. 49**, $TRP1_{455-463}$ -I-A^b and Tyr_{99-117} -I-A^b tetramer staining of splenocytes after in- vitro restimulation with relevant peptide showed elevated levels of $CD4^+$ $tetramer^+$ T cells , upon class II vaccination or combination of class II + class I. Importantly, tetramer staining showed elevated levels of antigen specific T reg population upon vaccination in spleen of these groups (**Fig.50**). Remarkably, antigen specific $CD4^+$ T cell and Treg inductionwas not detectable in mice vaccinated with class I vaccine, indicating class II antigen specific CD4 T cell induction (**Fig.** 49 and **Fig**. 50). No CD4+ $tetramer^+$ T cells and Treg were detectable in LNs and skin tumors.

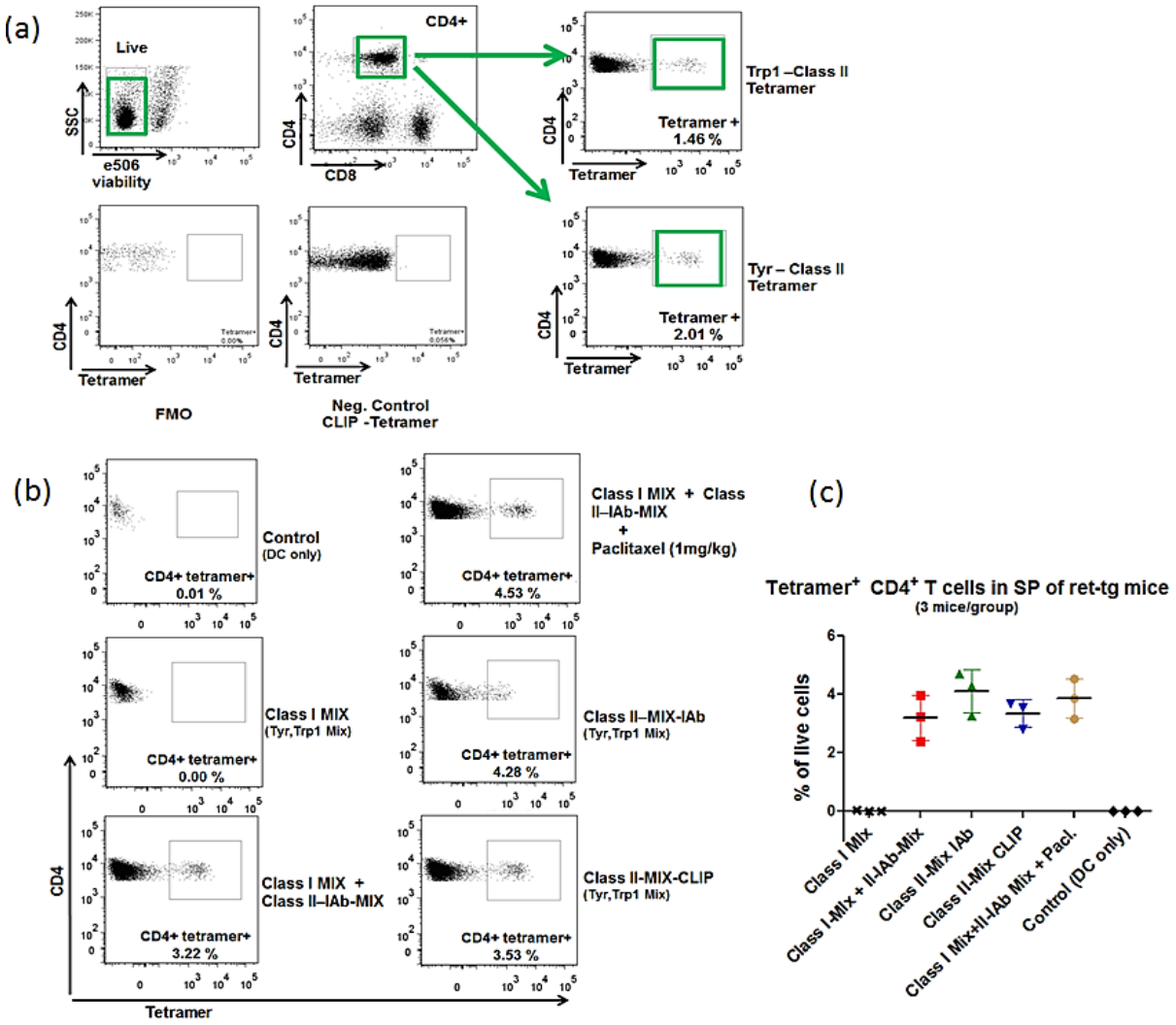

Fig. 49: Detection of Trp-1$_{455-463}$ and TYR$_{99-117}$ specific CD4 T cells by MHC class II tetramer staining. (a) Gating strategy to detect Trp-1$_{455-463}$ and TYR$_{99-117}$ -specific CD4 Tcells in splenocytes upon DC vaccination. Tetramer staining was analyzed in viable CD4+ lymphocytes. (b) Examples of detection of Trp-1$_{455-463}$ and TYR$_{99-117}$ CD4 T cells -specific cells with combined staining with 2 tetramers for each treatment groups. (c) Scatter plot summarizes results of CD4+ tetramer+ T cells of each treatment group (n=3) in percent.

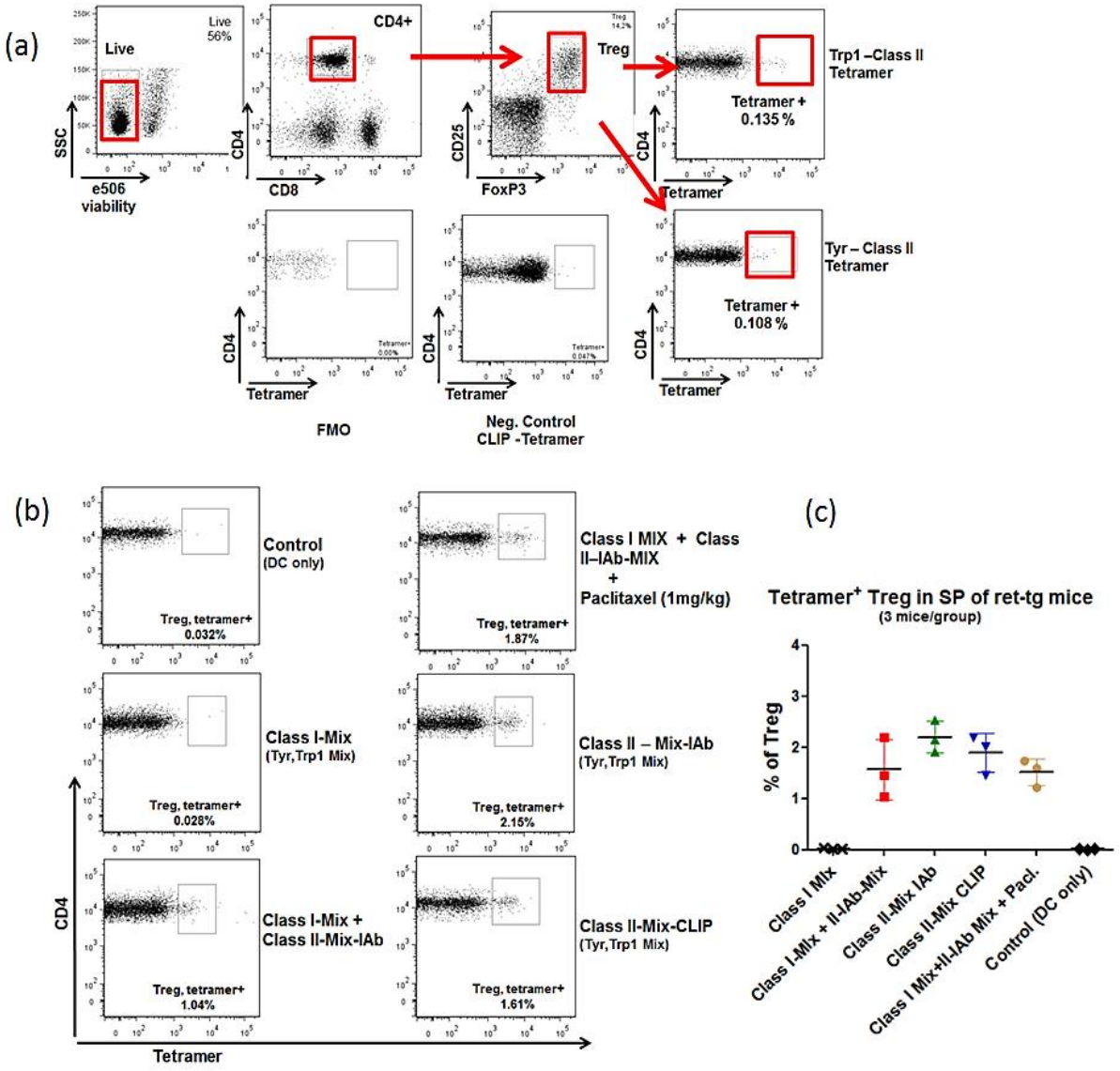

Fig. 50: Detection of Trp-1$_{455-463}$ and TYR$_{99-117}$ specific Treg by MHC class II tetramer staining. (a) Gating strategy to detect Trp-1$_{455-463}$ and TYR$_{99-117}$ -specific Treg in splenocytes upon DC vaccination. Tetramer staining was analyzed in viable CD4+ lymphocytes. (b) Examples of detection of Trp-1$_{455-463}$ and TYR$_{99-117}$ CD4 T cells -specific cells with combined staining with 2 tetramers for each treatment groups. (c) Scatter plot summarizes results of CD4+ tetramer+ T cells of each treatment group in percent (n=3).

4.10 Therapy experiment of class I Mix DC vaccine in *BRAF* mouse model

As mutational activation of *BRAF* is the earliest and most common genetic alteration in human melanoma, Class I-Mix DC vaccine in combination with low-dose paclitaxel was tested in the genetically engineered BRAF^{CA},Tyr:CreER Pten^{lox4-5} mice (BRAF mice). In addition to the BRAF-V600-mutation, all relevant MAAs (e.g. Trp1, Trp2, gp100 and Tyr are overexpressed) in this mouse model. As we could conclude from previous experiments with the ret-tg mice, class II vaccination or combination of class II with class I would not lead to significant improved survival rates of melanoma bearing BRAF mice. Thus, we were focusing on testing the class I mRNA based DC vaccines, expressing simultaneously 4 different constructs on theDC surface, encoded for 4 different MHC class I MAA in combination with paclitaxel. Treatment groups are summarized in **Table 9** and tumor inoculation and treatment strategy are shown in **Figure 51**. 25 days following intracutaneous application of 12.5 mg/mL (32mM) 4-hydroxytamoxifen (4-OHT), 5-8 weeks old BRAF mice developed small palpable BRAF-V600-mutated tumors in the flank. Tumor-bearing mice were then treated i.p. with 1mg/kg paclitaxel 3 times in weekly intervals. In addition, 3-4 days after each paclitaxel treatment, mice were vaccinated i.p. with mRNA-electroporated DCs (0.5x10^6 cells per mouse) three times in 7 days intervals. Ten days after last vaccination, 3 mice of each treatment group were sacrificed and flow cytometry analyses were performed. Remaining mice of each group were retained for survival analysis and tumor growth was monitored in regular intervals for at 80 days.

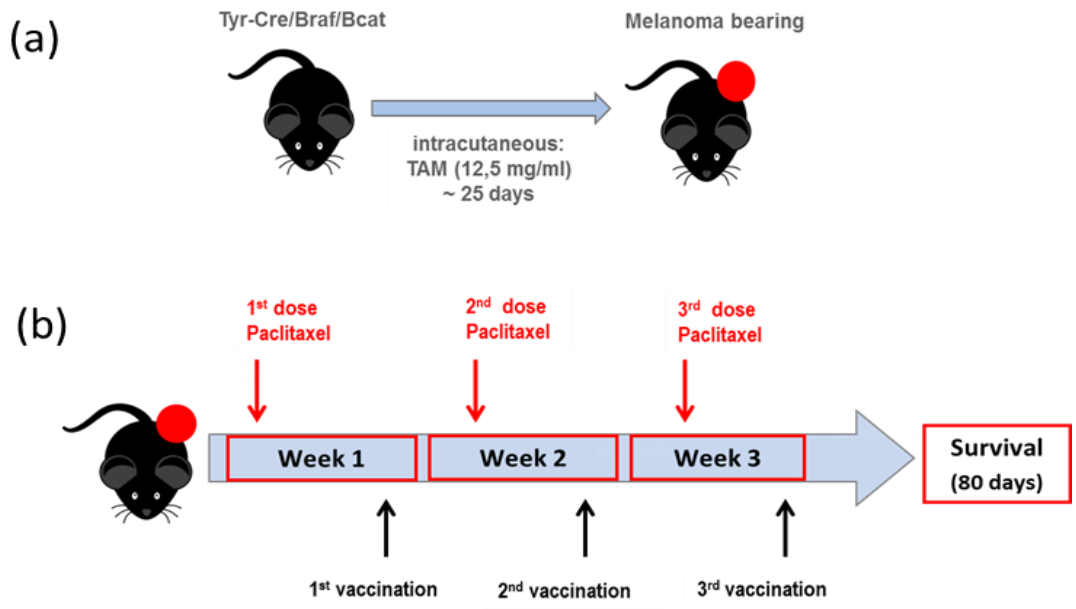

Fig. 51: Combined melanoma treatment strategy for Paclitaxel and dendritic cell vaccination in Braf melanoma mouse model. 5-8 weeks old BRAF^{CA},Tyr:CreER Pten^{lox4-5} mice were subjected to intracuteneous injection with 4-OHT and palpable tumor was developed after 25 days. In order to compare the effects of combined melanoma immunotherapy, melanoma bearing BRAF mice were

treated i.p. with ultra-low dose of Paclitaxel (1mg/kg) three times in 7 days intervals. 3-4 days later respective mice were vaccinated i.p. with mRNA-electroporated DCs ($0.5X10^6$ cells per mouse) three times in 7 days intervals. Ten days after last vaccination, 3 mice of each treatment group were sacrificed and flow cytometry analyses, was performed. Remaining mice of each group were kept for survival analysis and monitored for at least 80 days in regular intervals

Table 8: Treatment groups for immunotherapy experiment combined with paclitaxel of braf-mutated melanoma bearing mice

#	**Treatment**
1	Class I –Mix (Trp-$1_{455-463}$/ mTRP$2_{180-188}$/ hgp100_{25-33}/mTyr$_{360-368}$-hβ2m-K^b / TLR4 (1:1)
2	Class I –Mix + Paclitaxel (1mg/kg)
6	Paclitaxel (1mg/kg)
7	Control (DC only)

4.10.1 Tumor growth and survival analyses of BRAF mice following DC vaccination

Quadruple class I mRNA –DC vaccination resulted in a potent anti-tumor response indicated by the reduced tumor growth (**Fig 52a**) and significantly prolonged survival (**Fig 52b**) as compared to untreated or treated with paclitaxel only mice. This effect was even more profound when class I mRNA –DC vaccination was combined with low dose paclitaxel treatment.

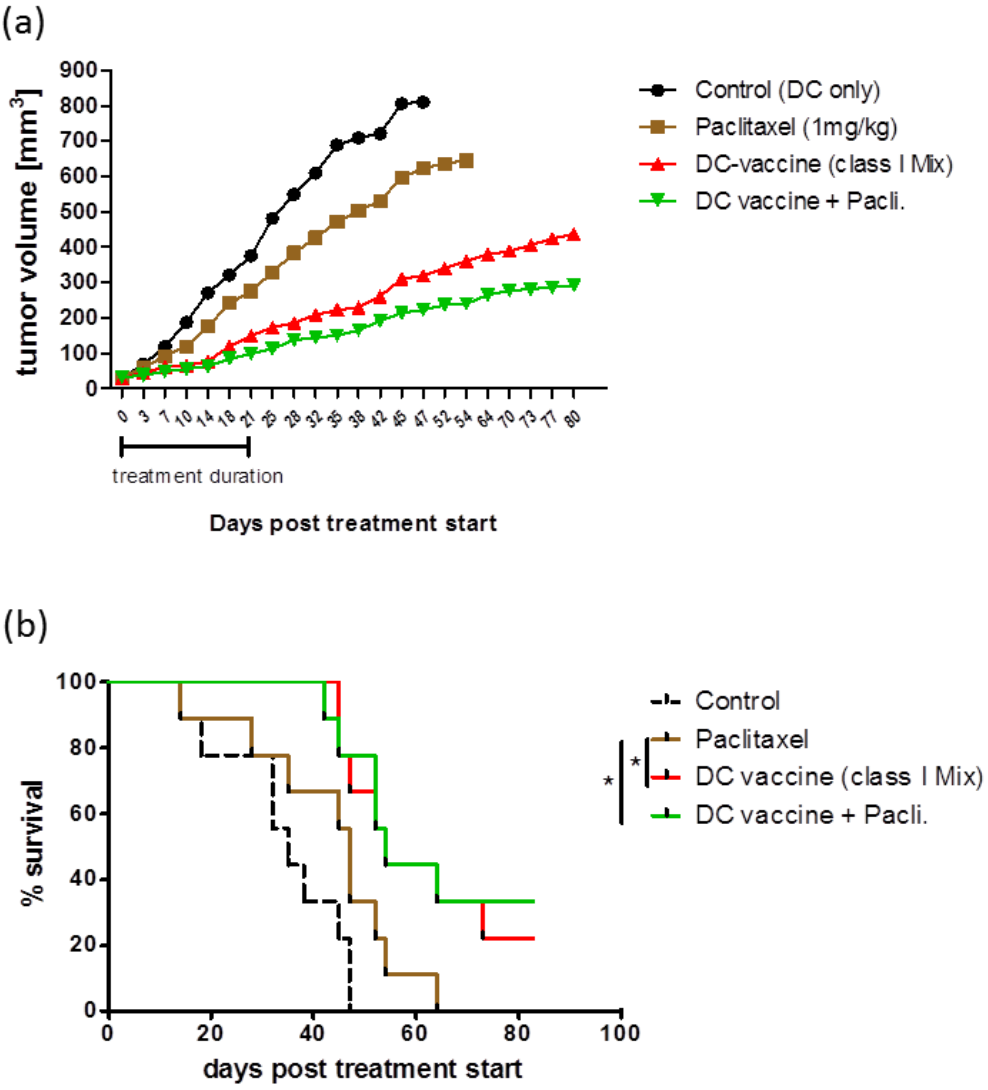

Fig. 52: Effect of vaccination with class I mRNA-electroporated DCs in combination with low dose of Paclitaxel on survival of BRAF mutated melanoma bearing mice. Mean values of tumor growth (a) and survival curves (b) in Braf mice bearing BRAF-V600-mutated melanomas established for 25 days in different treatment groups. Tumor growth and survival of Braf melanoma bearing mice upon treatment were monitored for 80 days post treatment start (b) Survival proportions of BRAF melanoma bearing mice following vaccination with class Mix of class I mRNA electroporated DCs in combination with Paclitaxel, monitored for 80 days post treatment start (n = 9; *P < 0.05; **P < 0.01). Results are presented as percent of surviving mice (*P ≤ 0.05; **P ≤ 0.01; ***P ≤0.001; generated using product limit (Kaplan-Meier) method, comparison of survival curves; Log-rank (Mantel-Cox) test)

4.10.2 **Mechanistic analysis of immune cell subsets in BRAF mice**

In combined therapy, paclitaxel with Class I-DC vaccine decreased the frequency of MDSC in LNs, SP and tumors as compared to untreated control group (**Fig. 53**). In addition, the activity of MDSC from LNs, SP and tumors was significantly diminished upon Class I–Mix DC vaccination as compared to control. This effect was even more profound after the combination with paclitaxel indicated by a significant decrease of arginase-1 and PD-L1 expression, as well as NO production.

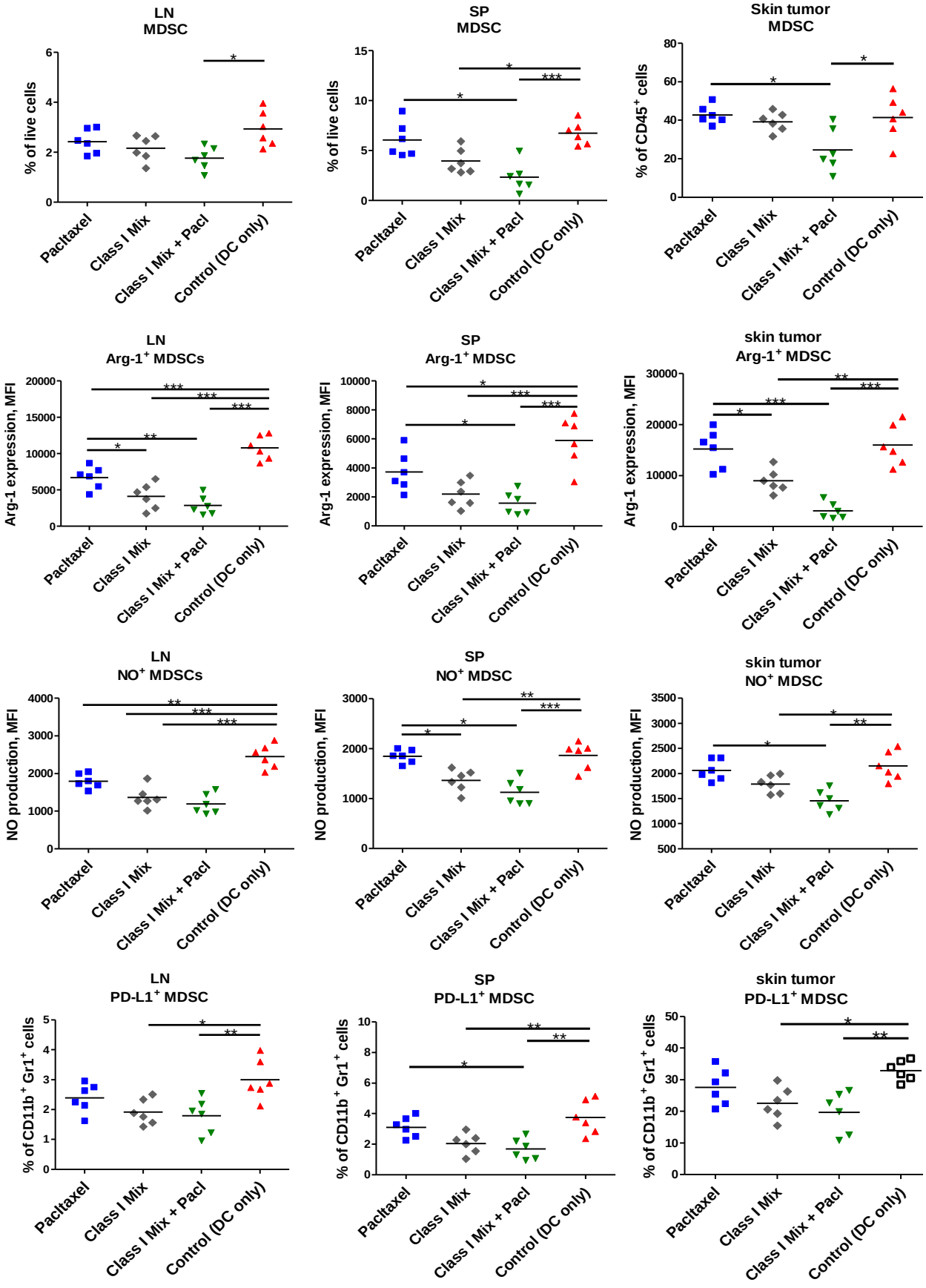

Fig. 53: In combined therapy, paclitaxel increases class I –Mix DC-vaccine effect in diminishing MDSC activity in combined therapy of melanoma bearing BRAF mice. Braf mice bearing BRAF-

V600-mutated melanomas, tumours were induced intracutaneously by 4-OHT and established for at least 25 days prior to treatment start. 10 days following last DC vaccination MDSC frequency within LN, Sp and tumor was phenotypically analyzed by flow cytometry (a). MDSC activity was assessed by their Arginase-1 production (b), NO-production (c) and PD-L1 surface expression (d) upon vaccination with respective DC vaccine. Results are presented as individual values on scatter plot, mean value of each group is also presented (*P ≤ 0.05; **P ≤ 0.01; ***P ≤0.001; one-way analysis of variance, the differences were assessed by Bonferroni multiple comparison post-test).

In addition, the vaccination with Class I–Mix DC vaccine significantly reduced the frequency of naive $CD8^+$ T cells and elevated the frequency of EM and CM $CD8^+$ T cells in all tested organs (**Fig.55**). Importantly, combination with paclitaxel further augmented this effect indicated by an increased frequency of EM $CD8^+$ T cells as compared to Class I–Mix DC vaccination alone or untreated or paclitaxel only treated mice. These results showed that combinatorial treatment could enhance memory T cell induction in the BRAF mouse model.

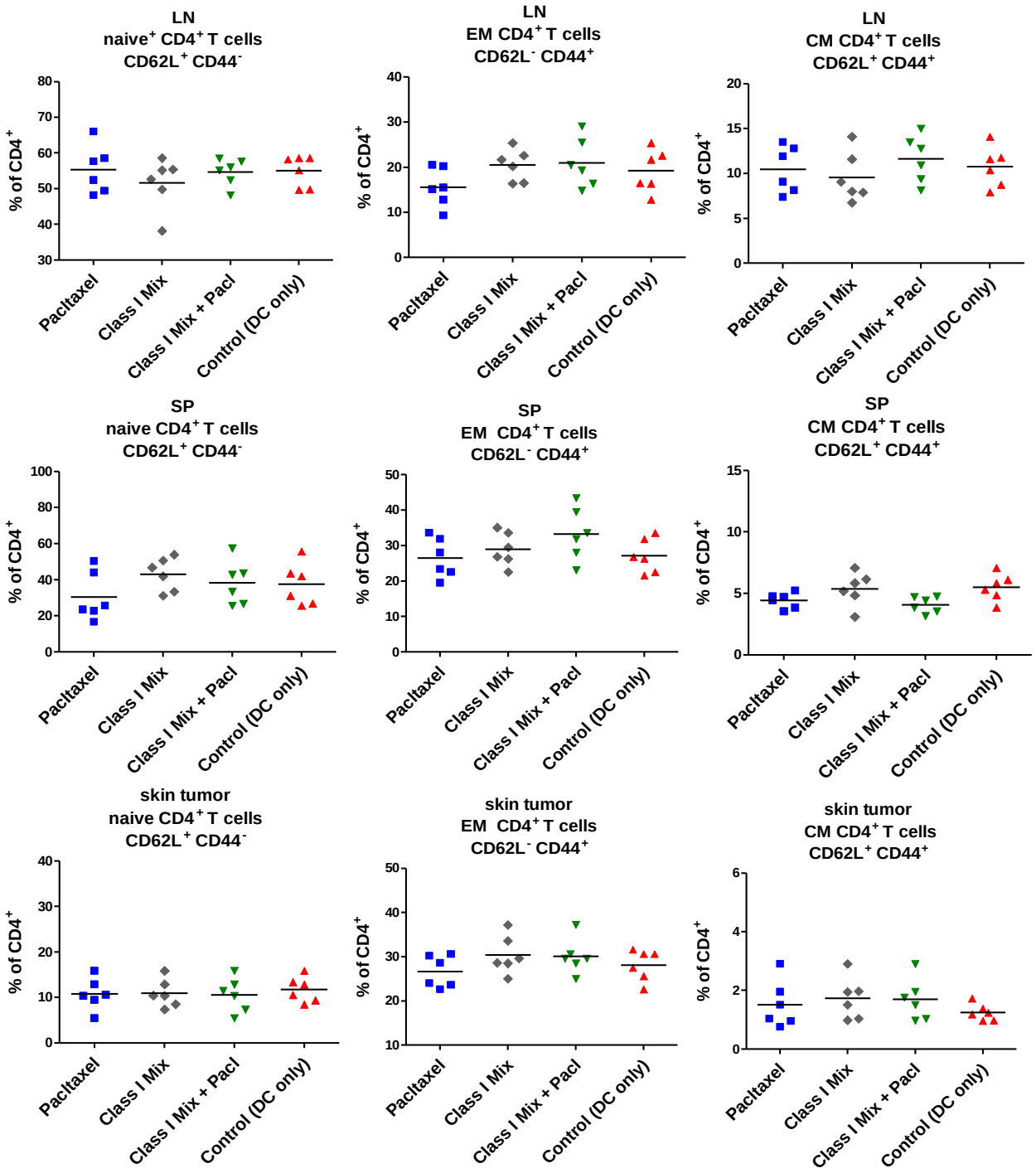

Fig. 54: **Influences of class I–Mix DC-vaccine in combination with paclitaxel on memory T cells in melanoma bearing BRAF mice**. Braf mice bearing BRAF-V600-mutated melanomas, tumours were induced intracutaneously by 4-OHT and established for at least 25 days prior to treatment start. Mmice were injected with paclitaxel (1mg/kg) and/or vaccinated with class I –Mix. 10 days after last vaccination frequency of naive, CM and EM CD4+ T lymphocytes were measured. Graphs represent the percentage of naive ($CD62L^+$ $CD44^-$) (a, d), central memory (CM; $CD62L^+$ $CD44^+$) (b, e), and effector-memory (EM; $CD62L^-$ $CD44^+$) (c, f) for both $CD8^+$ T cells (a-c) and $CD4^+$ T cells (d-f). Results are presented as individual values on scatter plot, mean value of each group is also presented (*P ≤ 0.05; **P ≤ 0.01; ***P ≤ 0.001; one-way analysis of variance, the differences were assessed by Bonferroni multiple comparison post-test).

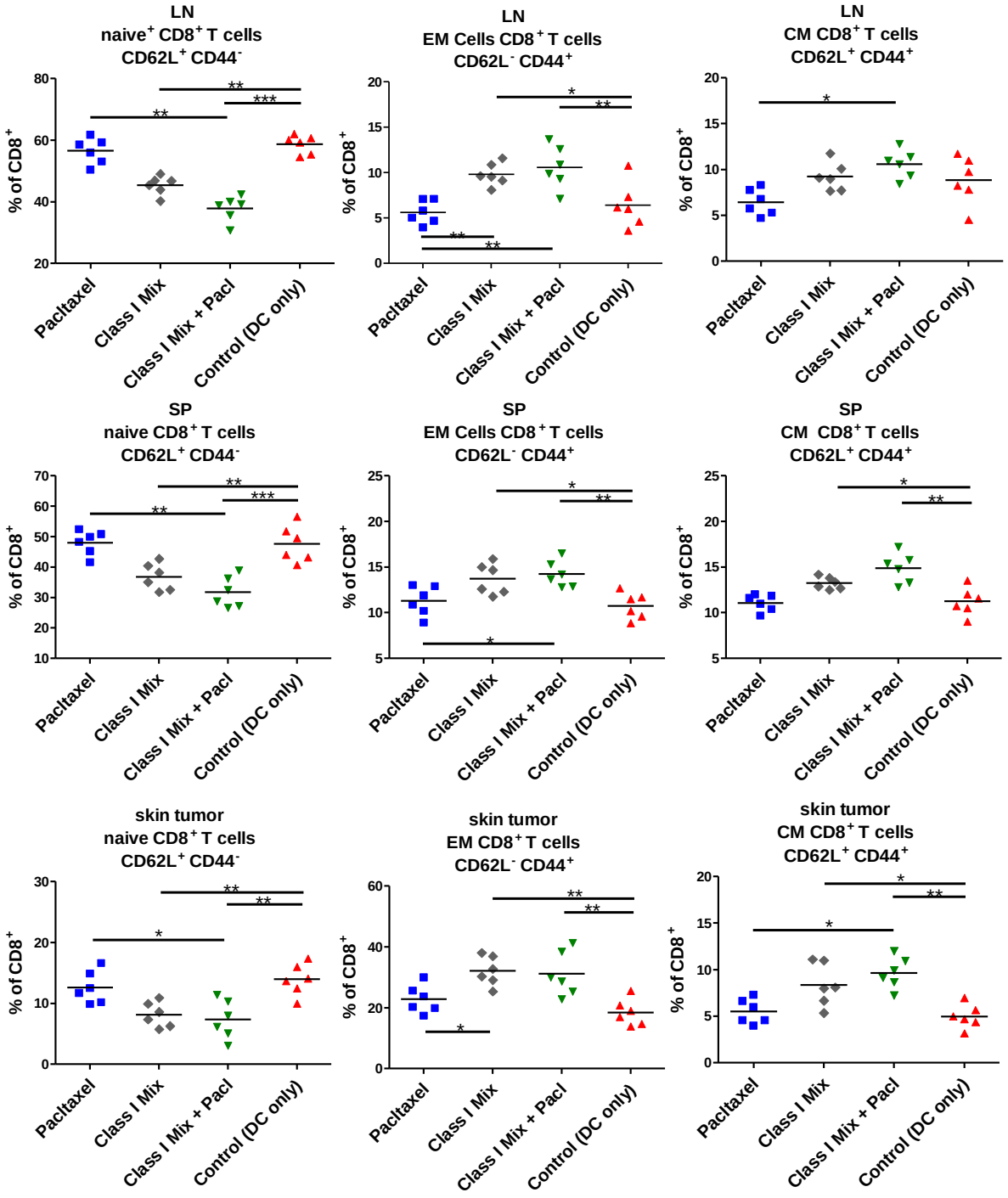

Fig. 55: Influences of class I–Mix DC-vaccine in combination with paclitaxel on memory T cells in melanoma bearing BRAF mice. Braf mice bearing BRAF-V600-mutated melanomas, tumours were induced intracutaneously by 4-OHT and established for at least 25 days prior to treatment start. According to respective treatment group, mice were injected with ld of paclitaxel (1mg/kg) and/or vaccinated with class I –Mix, respectively. 10 days after last vaccination frequency of naive, central memory and effector-memory was phenotypically determined on CD8+ T lymphocytes. Graphs represent the percentage of naive ($CD62L^+$ $CD44^-$) (a, d), central memory (CM; $CD62L^+$ $CD44^+$) (b, e), and effector-memory (EM; $CD62L^-$ $CD44^+$) (c, f) for both $CD8^+$ T cells (a-c) and $CD4^+$ T cells (d-f). Results are presented as individual values on scatter plot, mean value of each group is also presented (*P ≤ 0.05; **P ≤ 0.01; ***P ≤ 0.001; one-way analysis of variance, the differences were assessed by Bonferroni multiple comparison post-test).

Furthermore, vaccination with DC vaccines only did not significantly alter frequency $CD4^+$ T cells in LN, SP and skin tumors (**Appendix 9**). In addition, we did not observe altered intensities of TCR ζ-chain and PD-1 expression on $CD4^+$ T cells after Class I–Mix DC vaccination (**Appendix 9**). Class I-Mix vaccination resulted in significantly increased TCR ζ-chain expression in $CD8^+$ T cells as well as frequency of $PD\text{-}1^+$ $CD8^+$ T cells in LNs, SP and skin tumors (**Fig. 56**) as compared to control or paclitaxel only treated group. Moreover, TCR ζ-chain expression and frequency of $PD\text{-}1^+$ $CD8^+$ T cells were even more elevated after combination with paclitaxel particularly in $CD8^+$ T cells infiltrating metastatic LNs and tumors. These results showed that paclitaxel increased DC vaccine effect by restoring the activity of $CD8^+$ T cells in tumors, LN and SP of melanoma bearing BRAF mice.

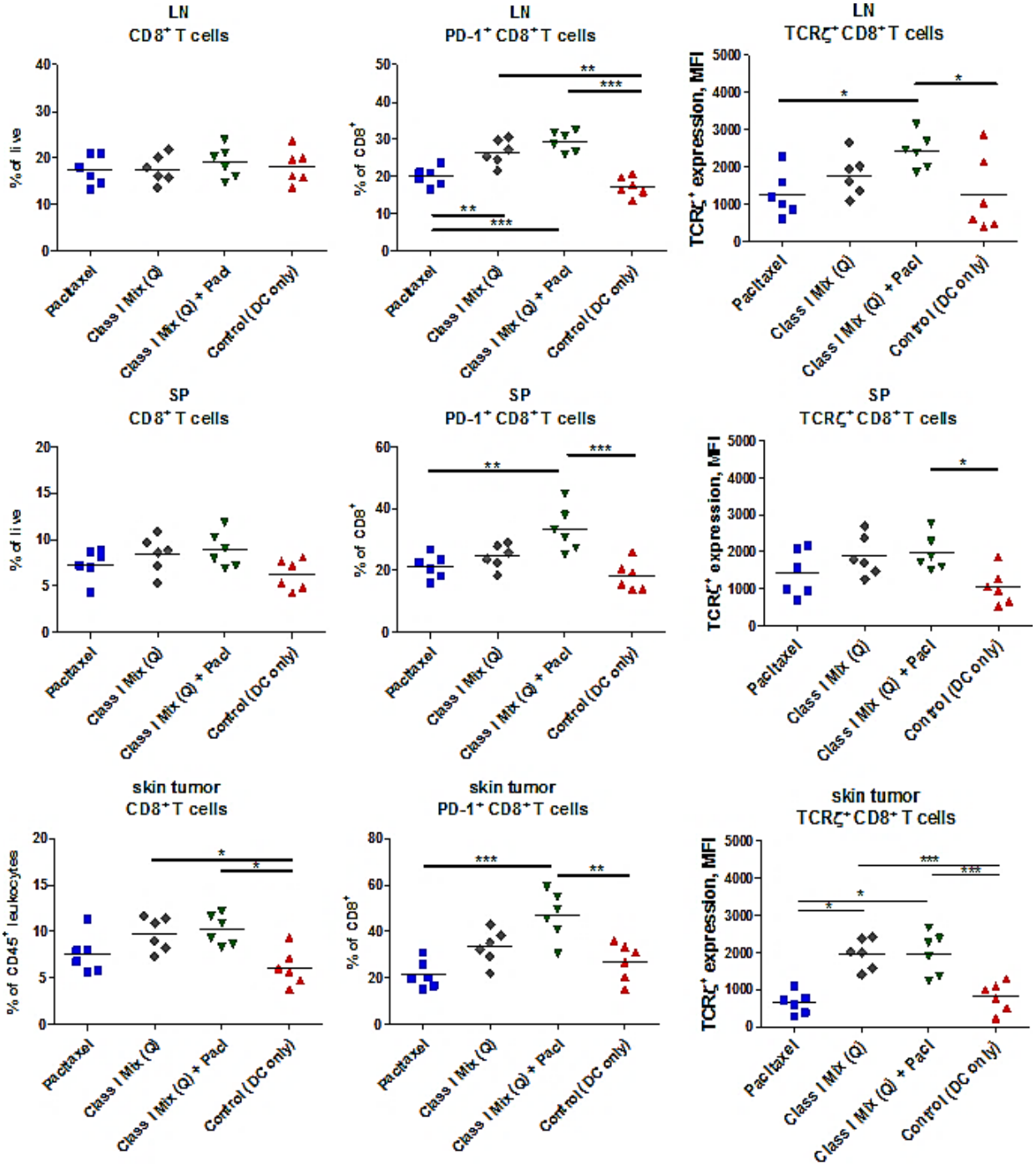

Fig. 56: Restored CD8$^+$ T cells activity upon class I–Mix DC-vaccine in combination with paclitaxel. Braf mice bearing BRAF-V600-mutated melanomas, tumours were induced intracutaneously by 4-OHT and established for at least 25 days prior to treatment start. According to respective treatment group, mice were injected with ld of paclitaxel (1mg/kg) and/or vaccinated with class I –Mix, respectively. 10 days after last vaccination, CD4+ and CD8+ T cell frequency within the tumor was phenotypically analyzed by flow cytometry (a, d). T cell activity was assessed by intensity of TCRζ-chain expression (b, e), and the percentage of PD-1$^+$ T cells (c, f) upon respective treatment. Results are presented as individual values on scatter plot, mean value of each group is also presented (*P ≤ 0.05; **P ≤ 0.01; ***P ≤0.001; one-way analysis of variance, the differences were assessed by Bonferroni multiple comparison post-test).

To further characterize the T cell populations following DC vaccination combined with paclitaxel, we tested the frequency and activity of Tregs in treated melanoma bearing BRAF mice. Furthermore, the frequency of activated Tcons was measured. No statistically significant differences in the frequency of Tregs within LN, SP or skin tumor were detected (**Fig. 57**). However, when evaluating their activation status, significantly reduced frequencies of $CD39^+$ Tregs and $Ki67^+$ Tregs were detected in all three analyzed organs. These results indicated lower immunosuppressive function and proliferation capacity of Tregs after Class I-Mix vaccination. Interestingly, this inhibitory effect was even more profound after the combination with paclitaxel compared to control or paclitaxel only treated group. In addition, Class I–Mix vaccination, and combinatorial treatment with paclitaxel resulted in a significant reduction of activated Tconsin tumors LNs and SP. In summary, the results clearly indicated that Class I–Mix DC vaccination hampered activity of tumor-infiltrating Tregs and further increased activated Tcons upon vaccination. Combinatorial treatment with paclitaxel further augmented these effects.

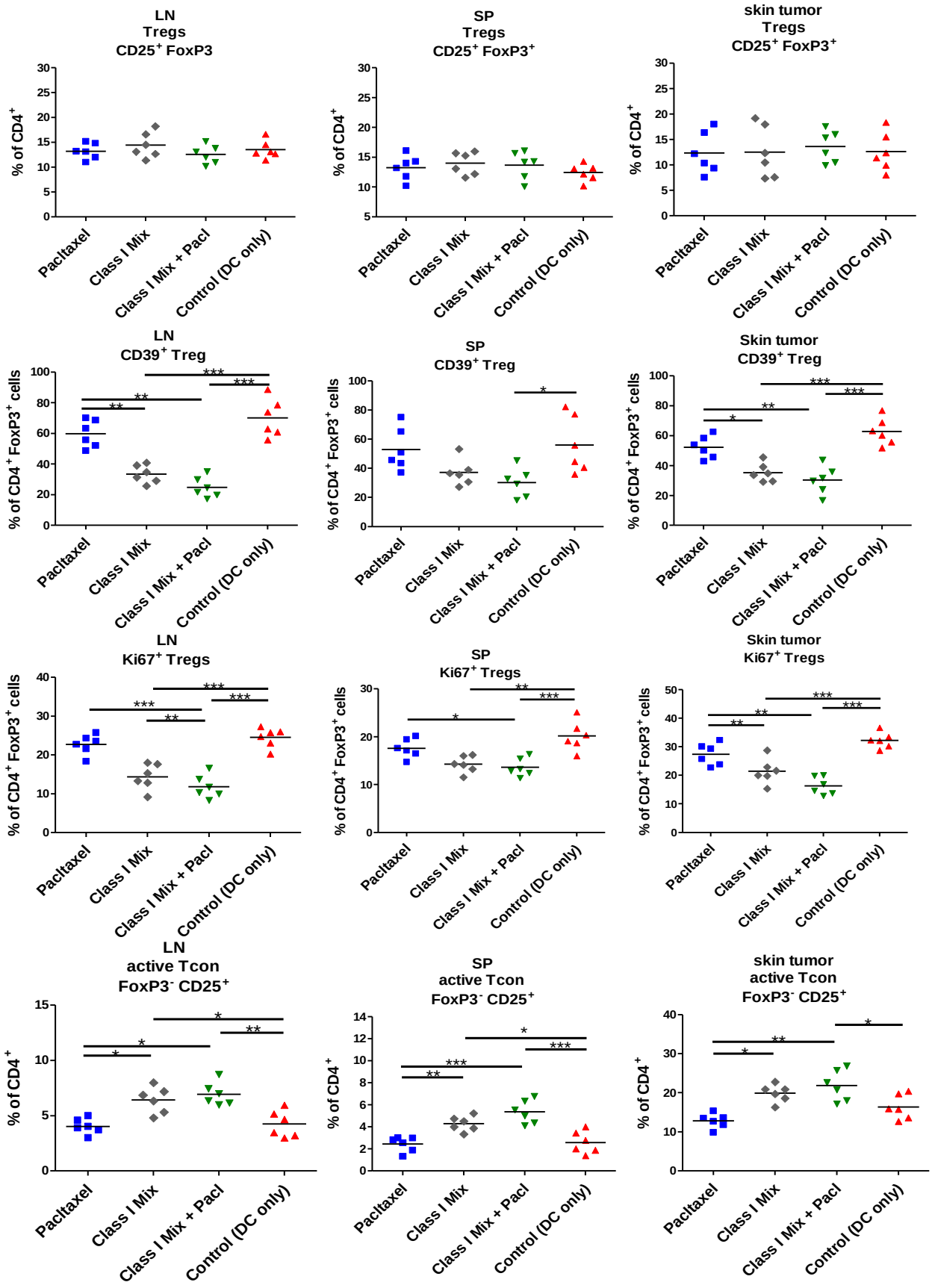

Fig. 57: In combined therapy, Class I –mix DC vaccination and paclitaxel significantly influenced activity of Treg and conventional T cells. Braf mice bearing BRAF-V600-mutated

melanomas, tumours were induced intracutaneously by 4-OHT and established for at least 25 days prior to treatment start. According to respective treatment group, mice were injected with Id of paclitaxel (1mg/kg) and/or vaccinated with class I –Mix, respectively. 10 days after last vaccination, Treg frequencies as well as Treg activity was determined by flow cytometry. Graphs represent the percentage of T reg (a) , $CD39^+$ (b), $Ki67^+$ (c) expression on Treg surface. In addition frequency of ($CD4^+CD25^+FoxP3^-$) activated Tcon was assessed. Results are presented as individual values on scatter plot, mean value of each group is also presented (*P ≤ 0.05; **P ≤ 0.01; ***P ≤ 0.001; one-way analysis of variance, the differences were assessed by Bonferroni multiple comparison post-test).

Furthermore, the potential of the Class I-Mix vaccine to elicit antigen-specific immune responses in melanoma bearing BRAF mice was assessed. We found an elevated tendency of IFN-γ and TNF-α producing $CD8^+$ T cells in LNs and SP upon vaccination with Class I–Mix. (**Fig. 58**).

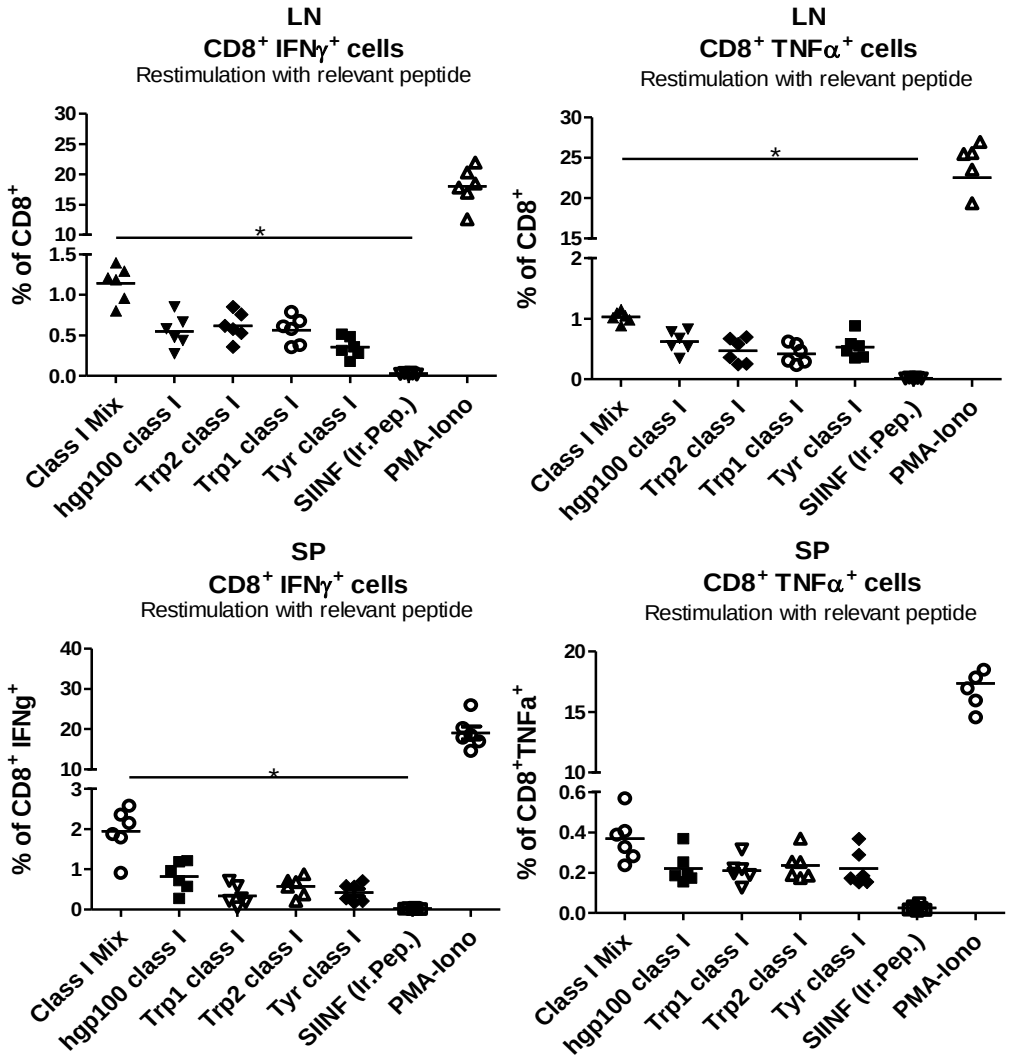

Fig. 58: Antigen-specific CD8+ T cells responses in LN and SP following vaccination with class I Mix DC vaccination in melanoma bearing BRAF mice. Braf mice bearing BRAF-V600-mutated melanomas, tumours were induced intracutaneously by 4-OHT and established for at least 25 days prior to treatment start. According to respective treatment group, mice were injected with Id of paclitaxel (1mg/kg) and/or vaccinated with class I –Mix, respectively. 10 days after last vaccination spleens and lymph nodes were harvested and analyzed for the induction of antigen-specific $CD8^+$ T cells by ICS for IFN-γ and TNF-α, following re-stimulation with the relevant peptide according to the group (ClassI mix: Trp-$1_{455-463}$/ mTRP$2_{180-188}$/ hgp100_{25-33}/mTyr$_{360-368}$ or their combination as class I –

Mix). Restimulation with irrelevant peptide (SIINFEKL) was used for as negative control and 50ng/mlPMA-2ug/ml Ionomycine restimulation as positive control for unspecific T cell proliferation. Scatter plot represents the percentages $CD8^+$ $INF\gamma^+$ (c), $CD8^+$ $TNF\text{-}\alpha^+$ (d) and $INF\gamma^+/TNF\text{-}\alpha^+$ double positive cells. Results are presented as individual values on scatter plot, mean value of each group is also presented (*P ≤ 0.05; **P ≤ 0.01; ***P ≤ 0.001; one-way analysis of variance, the differences was assessed by Bonferroni multiple comparison post-test).

To summarize, similarly to therapy experiments conducted in ret tg mice, the treatment of melanoma bearing BRAF mice with multivalent DC expressing chimeric class I receptors with four different MAAs inhibited tumor growth, leading to a significantly improved survival. Moreover, DC vaccination combined with paclitaxel treatment showed the tendency to be beneficial for anti-tumor immune responses.

5 Discussion

The clinical impact of DC immunotherapy in melanoma and other cancer entities has been limited so far despite the induction of tumor-specific T cell responses in many patients and occasional tumor regressions. Many reasons may explain this lack of success with DC vaccines and requires optimization at several levels. Firstly, the DC maturation stimuli in use; secondly, the type and form of antigen to be loaded on DCs; thirdly, the origin, subset and the number of DCs to inject; and finally the amount, frequency, route and the site of injection[129,134,169,170]. Until today, a large number of methods have been developed to deliver TAAs or their peptide fragments to DCs. Tumor-associated peptides either in cell lysates or as recombinant full proteins have been used to load MHC-I molecules at the surface of DCs. Other methods use gene delivery of target peptides into DCs to maximize their presentation to CTLs. Transfection of DCs with RNA derived from tumors or transcribed in vitro to encode TAAs emerges as an effective and safe genetic resource to elicit MHC-I restricted responses[12,14,122,171–173].

5.1 MHC class I and class II restricted MAA-sequences for designing chimeric DC receptors with improved MHC presentation on BMDC

5.1.1 Chimeric beta-2 microglobulin-TLR4/-Kb platform for CTL induction

Efficient MHC-peptide complex expression on the cell surface determines the degree of T cell responsiveness[14,171,174]. The maximal yield of presented antigenic peptides derived from encoded proteins is thus a key parameter in the design of cancer vaccines. This rationale has prompted attempts to enhance the level of antigenic peptide presentation by APCs through genetic manipulations aimed at elevating the actual number of pre-selected MHC-I-peptide and MHC-II-peptide complexes on the cell surface[14,171,174]. According to the novel method developed by Cafri et al.[145,147], genetic constructs were designed to generate chimeric MCH class I, as well as MHC class II receptors as a platform for $CD8^+$ CTL and $CD4^+$Thelper cell induction, respectively.

We demonstrated that these chimeric receptors enable stable, affinity and TAP-independent MHC-presentation of any antigen of choice on APC, eliciting a much faster and more efficient $CD8^+$ CTL and $CD4^+$Thelper cell induction than other conventional peptide loaded or DNA-transfected DC vaccines.

In this study, we tested several class I and class II restricted MAA candidate peptide-sequences, derived from TRP-1 and Tyr for their capability to elicit a potent $CD8^+$ CTL and

$CD4^+$ Th cell response, respectively (Table.3). Successful candidates were then used for generation of chimeric MHC class I, well as MHC class II receptor constructs. Afterwards, we tested their membrane expression kinetics and ability to stimulate DC maturation ex vivo. Then we further examined their ability to induce specific killing and anti-tumor activity, similar to the chimeric antigen-hβ2m constructs derived from MAA, hgp100 and TRP-2, Cafri and colleagues described in 2013 and 2016.[145,153]

As we aimed to increase the repertoire of chimeric antigen-hβ2m constructs for multivalent melanoma immunotherapy, we tested class I MAA candidate peptides for antigen specific CTL induction in CTL in vivo and CTL in vitro killing assay. Sequence variant-2 of mTRP-$1_{455-463}$ (AAPDNLGYM) showed the best CTL induction (Fig.13) and best, specific tumor cell lysis (Fig.14), followed by moderate effects induced by the native sequence mTRP-$1_{455-463}$ (TAPDNLGYA). This is in line with other study [175], which first described the modifications of the native mTRP-$1_{455-463}$ sequence and to induce stronger CTL responses. Strikingly, class I candidate peptide Tyr $_{360-368}$ (SSMHNALHI) showed also the CTL induction in vivo (Fig.13; Tyr #6) and in vitro killing assay (Fig 14; Tyr #6). This antigenic peptide was predicted to bind to H2-Kb by SYFPEITHI prediction tool and hasn't yet been described in literature to be a potent antigenic peptide for CTL induction.

We further subjected these 3 most promising class I peptides to RF cloning to generate respective TRP1 and Tyr-peptide-ß2m-TLR4 and peptide-hß2m-Kb constructs, according to the method described by Cafri et al.[144].We performed class I construct expression kinetics by flow cytometry and showed elevated expression levels for at least 48h for the hß2m-Kb constructs and 36h for hß2m-TRL4 constructs, respectively (Fig.16), indicating a less stable surface expression of the hß2m-TRL4 constructs. Cafri and colleagues, were describing similar expression surface expressions (unpublished data), however co-transfection of hß2m-Kb + hß2m-TLR4 still lead to sufficient BMDC maturation and durable peptide presentation to elicit a strong antigen-specific CTL as well as effector memory T cell response, superior to peptide-loaded counterparts[144,145,147]. We also observed similar results after comparative analyses of Trp1/Tyr-hß2m-Kb /TLR4 mRNA transfected BMDC versus Trp1/Tyr peptide-loaded, LPS maturated BMDC. Co-transfected Trp1/Tyr-hß2m-Kb /TLR4 mRNA-DC vaccine (class I-Mix-EP) resulted in profound, antigen–specific $CD8^+$ T cell responses indicated by a significantly increased IFN-γ production by $CD8^+$ T cells (Fig.22) and elevated frequency of EM $CD8^+$ T cells in LN and SP of vaccinated mice (Fig.23). Importantly, these elevations were significantly higher than in mice vaccinated with corresponding Trp1/Tyr-peptide-Mix (class I-Mix-PL) loaded BMDC. Comparative survival analyses of melanoma bearing *ret*-tg mice further confirmed superior anti-tumor effects in mice that were vaccinated with mRNA-transfected BMDC (Fig. 29; class I-Mix-EP) .Our date are consistent with survival rates

obtained previously in B16F10.6 transplantable melanoma model[144] and in ret-tg mouse model[153], in which gp100/Trp2-mRNA-transfected BMDC showed superior tumor protection, survival benefits and delayed tumor growth compared to respective hpg100/Trp2-peptide loaded BMDC.

5.1.2 **Chimeric MHC-II platform for CD4 T cells induction**

To address the challenge of inducing a significant immune response to specific antigens by $CD4^+$ T cells, the group of Prof. Lea Eisenbach designed a single chain chimeric MHC-II-IAb receptor. It comprises a class II-H2-IAb restricted antigenic peptide of choice, covalently attached through a linker sequence to the complete MHC-II-I-Ab alpha, beta chain and additional CD40-anchor sequence, stabilizing class II-peptide presentation on the DC surface. Profound $OVA_{323-339}^+$ CD4+ T cells responses were observed upon vaccination of OT-II mice with BMDC presenting chimeric $OVA_{323-339}$ H2-IAb receptors (*personal communication and unpunished data by Gal Cafri and colleagues of Prof. Lea Eisenbach's lab in February 2015*). As this platform does not have universal application perspectives, the group of Prof. Lea Eisenbach developed a class-II associated invariant chain-peptide (CLIP) construct, in which the CLIP coding sequence was exchanged for a class II restricted antigenic-peptide sequence of choice presented on the native MHC class II receptor through the intrinsic class II loading and presenting pathway. Thus, the chimeric CLIP-construct represents the preferable universal class II counterpart to the universal chimeric class I-hß2m constructs.

In this study we examined five MHC class II –H2-IAb restricted peptides for their ability to elicit a specific $CD4^+$ T cell response (Table 3). We found 2 peptides, $mTRP1_{111-128}$ (GTCRPGWRGAACNQKILT) and $mTYR_{99-117}$ (NCGNCKFGFGGPNCTEKRV) that were able to induce a specific T cell proliferation *in vitro*. Specific proliferation was detected by ^3H-labelled thymidine uptake, resulting in strong elevation of CPMs compared to control (Fig.15 #122 and #130). These two peptides were then further subjected to the RF cloning to produce the respective I-Ab and CLIP constructs. Respective class II construct expression kinetics upon electroporation into DC2.4 cells revealed that both constructs showed elevated I-Ab expression for at least 36h (Fig.17). Moreover, following electroporation of BMDC and vaccination of BL/6 mice, an increased proliferation rate in CD4+ T cells subsets, but not in CD8+ T cell subsets were detected by *in vitro* proliferation assay (Fig. 20). Furthermore, presence of antigen specific CD4+ T cells was confirmed by class II-tetramer staining for $mTRP1_{111-128}$ construct, as well as for $mTYR_{99-117}$ constructs (Fig.21).

With regards to the mTRP1$_{111-128}$ class II-constructs, our results are partly in line with data of Muranski et al.[176], who first identified the mTRP1$_{111-128}$ peptide sequence as a minimal epitope for of TRP-1-specific CD4+ T cell in a TRP-1 transgenic mice. Although they could show, that these TRP-1–specific CD4+T cells fail to protect transgenic mice against B16melanoma cell challenge, they showed the development of autoimmunity after adoptive transfer. Further functional characterization of Th0-, Th1-, or Th17-polarized cells from TRP-1 TCR transgenic mice, could show that only Th17-polarized TRP-1–specific T cells mediate highly efficient treatment of large established tumor, leading to a complete cure and the long-term survival[176].

The murine TYR$_{99-117}$ sequence was selected and further investigated by us after IEDB database MHC Class II-IAb binding prediction and was not yet described in the literature to be a potent MHC class II restricted peptide for CD4+ T cell induction in BL/6 mice. We could here describe and characterize murine TYR$_{99-117}$ peptide sequence to be a potent candidate for CD4$^+$ T cell induction upon *in vitro* re-challenge in *in vitro* proliferation assay. Although we did not further characterize the induced CD4$^+$ immune response upon DC vaccination for Th0-, Th1-, or Th17-polarization as Muranski et al.[176], we were encouraged by our results to further examine, if our Trp1/Tyr class II-chimeric constructs mediate efficient treatment of established melanoma tumors in *ret*-tg mice in comparison to untreated or class II–peptide loaded, LPS maturated DC vaccine.

To summarize, we were able to successfully design and characterize in total five class I and class II chimeric receptors, respectively, which upon mRNA transfection enable autologous BMDC to become a potent, multivalent DC vaccine by elongated, and simultaneous presentation of Trp1 and Tyr class I, as well as class II epitopes on BMDC surface. The duration of MAA presentation by DC vaccine is highly important for efficient antigen-specific CD8+ and CD4+ T cell responses and thus for its clinical success. By allowing DC-presentation up to 2 days the chimeric-MHC receptor platform improves the prospects of peptide-presenting DC to enter the lymph nodes and to encounter antigen specific naïve T cells. We could characterize and design two chimeric mTRP-1$_{455-463}$ antigen-hß2m constructs and one Tyr $_{360-368}$ chimeric antigen-hß2m constructs, which has not yet been described in the literature. Trp1/Tyr-hß2m-Kb /TLR4 mRNA transfected BMDC showed superior antigen-specific CTL induction, as wells as anti-tumorigenic properties *in vivo* upon vaccination of melanoma bearing *ret*-tg mice, versus Trp1 mTRP-1$_{455-463}$ /Tyr $_{360-368}$ peptide-loaded, LPS maturated BMDC. In order to complement our construct repertoire with CD4$^+$ T cell inducing chimeric receptors we identified and characterized mTRP1$_{111-128}$ to class II constructs, as well as mTYR$_{99-117}$ constructs and their capacity to induce a strong CD4$^+$ T cell response *in vivo* upon vaccination and subsequent analysis of tetramer$^+$ antigen specific CD4$^+$T cell in LN

of vaccinated of BL/6 mice and detected by *in vitro* $CD4^+$ T cell proliferation assay. In contrast to class I chimeric ß2m-receptors, exclusive class II chimeric receptor mRNA DC vaccination did not lead to improved survival of melanoma bearing *ret*-tg mice.

5.2 Immunotherapy of melanoma bearing ret-transgenic mice

In this study, we applied our chimeric mRNA constructs in *ret* transgenic (ret-tg) mice that develop spontaneously skin tumors and metastases in the BM, lungs, liver and brain, resembling the human situation better than conventional B16-transplantable tumor models[150,152]. Moreover, melanoma lesions express several MAAs such as tyrosinase, gp100, TRP-1 and TRP-2[152]. It has been also reported that *ret* transgenic mice could develop specific T-cell responses against TRP-2 upon vaccination[151,152] Here, melanoma bearing *ret* tg mice were vaccinated with DCs electroporated with class I mRNAs constructs for TRP1 and Tyr, as well as with class I mRNA constructs. We used chimeric vaccines in single treatment and in combination for comparative analyses.

With regards to chimeric class I-β2m-receptors, we appreciated a significant improved survival rate in mice treated with either chimeric class I-β2m-DC vaccine. However the most efficient treatment was the class-I-Mix (Fig.26). We observed 25% increased survival in this group compared to control. This can be partly explained due to the dual functionality of the Class I Mix DC vaccine, which was also reflected in exclusively increased $CD8^+$ T cell dependent immune responses but almost no $CD4^+$ T cells response, indicating $CD8^+$ specific T cell induction (Fig. 32 and Fig 33). We observed significant elevated frequency in LN and skin tumor of $CD8^+$ effector memory T cells in the Mix group as compared to the control group or class II vaccinated group. $CD8^+$ effector memory T cells were also accumulated in mice vaccinated with Tyr construct as compared to the control. Moreover, these results were correlating with reduced levels of naïve $CD8^+$ T cells in respective groups, suggesting a conversion of naive T cells to central memory and further to effector memory state upon repeated boost of DC vaccination. These data are consistent with our previous results, showing that the Mix treatment, expressing gp100 and Trp-2 antigens, induced the most effective $CD8^+$ response in *ret*-tg mouse model [153], and with previous study in a B16 transplantable melanoma model owing to its dual functionality, which allowed long-lasting peptide presentation through Kb in conjunction with DCs maturation driven by TLR4[144].

Studying activity of CD8 T cells upon chimeric class I-ß2m-DC vaccine, we detected, elevated levels of IFN-γ producing CD8 T cells upon *in vitro* restimuation, indicating antigen specific CTL induction upon vaccination. Furthermore, an increased TCR ζ-chain expression, as well increased frequencies of $CD69^+$ T cells in LN, skin tumor as well as in SP were detected (Fig. 34), suggesting a profound and systemic $CD8^+$ T cell activation upon class I Mix vaccination. Interestingly, these results were accompanied with significantly increased PD-1 levels in LN, SP and skin tumors, suggesting T cell exhausting due to persistent antigen stimulation, described in chronic infections and cancer[177]. However, since elevated

PD-1 expression was simultaneously detected with elevated CD69 early marker for T cell activation, we assume that there might be a steady state of activation not yet reached exhaustion state at the time point of our T cell assessment. Interestingly, Restoring of effector functions of exhausted CD8 T cells, expressing high levels of PD-1 during chronic infections was described already several times [178–180]. and PD-1 high expressing CD8 Tcells were proposed to be a prospective marker for treatment response to anti-PD-1 treatment in cancer patients[179,181]. We did not measure CD69, Ki 67, or PD-1 in treated mice at later time points in this study. So the PD-1 contributions to abrogate immune responses after stopping vaccination and thus leading to incomplete tumor rejection and reduced overall survival of *ret*-tg mice, needs to be further investigated.

Regarding $CD4^+$ memory T cells, as well as $CD4^+$ T cell activity we observed significant elevated levels exclusively upon chimeric class II-IAb DC vaccination compared to control (Fig.33 and Fig.35). We detected reduced naïve $CD4^+$ T cells and elevated $CD4^+$ T effector cells in SP, LN and tumor. Furthermore, we measured elevated TCRζ- chain expression, CD69 as well as PD-1 expression; similar to the $CD8^+$ T cells responses induced upon the class I restricted DC-counterpart, suggesting a profound and systemic $CD4^+$ T cell response. However, to our surprise, exclusive class II DC vaccination did not lead to an improved survival in any treated group compared to control group. This might be explained by the fact that the contribution of $CD4^+$ T cells to antitumor immunity is contradictory due to their heterogeneity[182]. For instance, it was described that IL-4 cytokine, secreted by $CD4^+$ T cells, may exert antitumor effect[183] However, the frequency of antigen-specific $CD4^+$ cells that produce IL-5 has been correlated with progressive growth of melanoma[183]

Further investigations of different $CD4^+$ T-cell subsets are required to determine their function and contribution to the tumor progression. In addition Treg induction was described leading in overall immune tolerance[184], associated with tumor progression as they hamper effective antitumor immune response in cancer patients and tumor-bearing mice[185,186]. Moreover, several studies described MDSC as another crucial immunosuppressive cell population that hamper T cell immunity in lymphoid organs and at the tumor site. In addition some evidence suggests that MDSC can induce an expansion of Tregs[68]. Moreover, a transient elevation of MDSCs in mice following immunization was demonstrated[187,188]. In our previous studies with chimeric class I gp100 and TRP-2 vaccination in *ret*-tg mice we did not find statistically significant changes in MDSC [153], however the immunosuppressive activity of these cells was not investigated.

In this study we monitored Treg activity and MDSC activity upon Trp1/Tyr class I as well as class II vaccination in *ret*-tg mice. Similar to our previous studies we did not observe

significant changes of MDSC, as well as Tregs in LN and skin tumors after vaccination but significant differences in their activity. We detected a tremendous decrease in Arg-1 and NO expression levels in MDSC of SP and LN, as well as skin tumor; particularly upon class I-Mix vaccination, compared to control or class II vaccinated groups. In addition PD-L1 expression on MDSC in LN, SP and particularly in skin cancer of ret-tg mice were significantly reduced. Interestingly, in contrast to these results, upon class II vaccination we could only observe a reduced tenancy of respective MDSC activity markers, which was significantly less profound than class I-Mix DC vaccination. These results suggest a persistent, immunosuppressive MDSC activity in class II-Mix vaccinated ret-tg mice that may partly explain the less profound anti-tumorigenic immune response, which resulted in constant tumor growth. More evidence for this hypothesis was found upon monitoring of Treg activity upon class I and class II DC vaccination. We detected a great reduction of $CD39^+$ Treg as well as decreased expression levels of Ki 67-proliferation marker in these cells, clearly indicating reduced activity of Tregs upon class-I-Mix DC vaccination. Interestingly, we saw increased Treg activity solely upon class II DC vaccination, by increased CD39 expression on Tregs in metastatic LN and skin lesions and increased Ki67 proliferation marker in LN and SP of vaccinated ret-tg mice. Our observations are in line with previous studies describing CD73 and CD39 ectonucleotidases in controlling naive T-cell homeostasis and memory cell survival through adenosine production through ATP hydrolysis and accumulated adenosin was found to tilt the balance towards immunosuppressive microenvironments[54,189].

To summarize we have demonstrated that DC vaccination with chimeric TRP-1 and Tyr class I-ß2m DC vaccine and in particular the TRP-1/Tyr-Mix-ß2m DC vaccine, mainly due to its multivalent properties, can significantly improve survival of melanoma bearing *ret*-tg mice. These findings are consistent with our previous results obtained by gp100/TRP-Mix-ß2m DC vaccination[153]. In this recent study, we demonstrated increased frequency of IFNγ producing CD8+ T cells, complemented by increased, systemic CD 8^+ T cell activity as well as an increase of CD8+ effector memory T cells. Importantly, these immune-stimulatory effects were found without any stimulatory effects on immunosuppressive Tregs and MDSC. Finally, we could detect signs of autoimmunity (vitiligo) in two *ret*-tg mice treated with TRP-1/Tyr class I-Mix DC vaccine, providing further evidence of increased immune stimulation (Fig. 48). Furthermore, we could demonstrated that DC vaccination with chimeric TRP-1 and Tyr class II DC vaccine induced a profound $CD4^+$ specific immune response in healthy mice, as well as in *ret*-tg mice. Unexpectedly, exclusive class II vaccination did not improve survival rate of melanoma bearing *ret*-tg mice. Skin lesions continued to grow and mice had to be sacrificed upon massive tumor growth, similarly to the control group. This might be explained due to the lack of concomitant antigen-specific $CD8^+$ CTL induction on the one hand, and furthermore

by the heterogeneity of $CD4^+$ cell subsets, which would need to be characterized in more detail in future experiments. Indeed, some evidence in our results showed significant induction of Treg activity upon class II vaccination, which could abrogate effective antitumor immunity.

5.3 Combined melanoma treatment with dendritic cell vaccination and low-dose paclitaxel

Recent studies suggest combining immunotherapy with chemotherapeutic agents, which for instance can abrogate the suppressive influence of Tregs and allow effective antitumor immunity to emerge[124]. For instance, immunoregulatory properties were discovered in melanoma, as well as in other cancer entities upon low-dose application of paclitaxel, to promote T helper 1 and type 17 immunity, enhance DC function, as well as decreasing Treg and MDSC function number and function [124102]. Indeed, newer combined regiments, including paclitaxel, cisplatin, temozolomide combined with IL-2 and IFN-α are currently studied in patients with metastatic melanoma[190].

We further hypothesize that combining of all our chimeric class I-β2m constructs enable simultaneous presentation of quadrupled MAA-Mix (TRP1, Tyr, gp100, TRP2) on the DC surface. This modality would provide a potent multivalent DC vaccine, which can further increase anti-tumor immunity and survival rate of melanoma bearing *ret*-tg mice. In addition, as exclusive class II vaccination did not improve survival of melanoma bearing *ret*-tg mice, we would like to test our theory that simultaneous CD8 and CD4 T cell stimulation in cancer immunotherapy can markedly improve the anti-tumor response. In that way we can overcome current limitations of class II vaccination to elicit a durable antitumor response with significant improved survival. Furthermore, we combined our DC vaccine with chemo-modulating non-cytotoxic doses of paclitaxel in order to further promote $CD8^+$ T cell function and decrease MDSC activity as well as decreasing levels of pro-inflammatory chemo- and cytokines as previously shown in our group by Sevko and colleagues in 2012[123].

In combined therapy, class I-Mix-β2m- and class I-Mix-IAb-DC vaccination did significantly increase survival rates of melanoma bearing *ret*-tg mice compared to control. Surprisingly, survival was not improved compared to paclitaxel only treated group. And further combination of paclitaxel with class I-Mix- β2m-DC and class I-Mix-IAb-DC vaccine also did not further improve the survival. These results were quite surprising to because on cellular level, combined class I-Mix- β2m- and class I-Mix-IAb-DC vaccination induced a mixed CD8 and CD4 dependent immune response in LN, SP and skin lesions of vaccinated *ret*-tg mice. Firstly, we detected a mixed antigen-specific IFNγ induction in $CD8^+$ as well as $CD4^+$ T cells in LN and skin tumors. Secondly, a profound reduction of naïve $CD4^+$ and $CD8^+$ T cells, associated with $CD4^+$ and $CD8^+$ effector memory induction was detected in SP, LN and skin tumor. Furthermore, induced CD8 and $CD4^+$ T cell activity was shown, by increase TCRζ-chain and PD-1 expression in tumor infiltrating T cells, clearly indicating efficient Ag-presentation of our multivalent DC vaccine to $CD8^+$ and $CD4^+$ T cells and subsequent

antigen specific activation of T cells, especially in the tumor of vaccinated mice. However, we could also appreciate, that class I-Mix- β2m- and class I-Mix-IAb-DC vaccination did not influence MDSC activity markers as strong as class I-Mix- β2m –DC vaccination alone. For instance, we saw only a tendency of reduced Arg-1, NO as well as PD-L1 expression compared to control. In contrast, class I-Mix- β2m-DC vaccination tremendously reduced all respective MDSC markers more profound than class I and II Mix vaccine. These results suggest that, although a solid $CD8^+$ and $CD4^+$ T cell response was induced, an additional stimulation of MDSC occurred. Interestingly, combined treatment with low-doses of paclitaxel seemed not to abrogate these immunosuppressive effects. This would be partly in line with previous studies suggesting a transient MDSC elevation and thus increased immunosuppression upon immunization[187,188]. Furthermore, some studies showed than MDSC can expand Tregs[68]. Indeed, we measured systemically increased Treg frequencies in LN, SP and skin tumor, which was associated with increased Treg activity, by increased levels of CD39 and Ki 67 proliferation. Further evidence was provided by significant reduced levels of tumor-infiltrating active T cons as well as in LN and SP, which was in contrast highly increased in class I-Mix-ß2m-DC vaccinated group in respective organs. In fact, upon further investigations with class II tetramer staining, we could detect elevated levels of $tetramer^+$ Tregs amongst $CD4^+$ T cell fraction (Fig. 50), proposing antigen-specific Treg induction exclusively in class-II DC vaccination and class-I and class-II vaccinated groups, which can be responsible for abrogation of antitumor immunity and progressive tumor growth in melanoma bearing *ret*-tg mice. Further experiments need to be performed to carefully explain additional modes of action.

In contrast, class I-Mix- β2m-DC vaccination showed superior $CD8^+$ T cells dependent anti-tumorigenic effects. Combinatorial treatment with low-doses of paclitaxel promoted survival rates of melanoma bearing mice up to 40% compared to only DC vaccinated group (35%). Improved survival was associated with two mice developing vitiligo, due to autoimmune reactive T cells attacking MAAs overexpressed in melanocytes of *ret*-tg mice (Fig. 48). Improved survival was associated with increased PD-1 and TCRζ-chain expression on $CD8^+$ T cell subsets and increased frequency of IFNγ-producing $CD8^+$ T cells, clearly indicating antigen specific CTL activation compared to control or paclitaxel only treated group to control subsets compared to paclitaxel only. In addition, profound, systemic effector memory T cells induction was measured. Furthermore, significantly reduced MDSC activity as well as Treg activity was detected, which was more profound upon combined treatment with paclitaxel.

Finally we tested our class I-Mix- β2m-DC vaccination in the BRAF-mouse model to further proof anti-tumor immunity in an additional melanoma bearing mouse model. This would show potential treatment benefits in BRAF-mutated tumors which are additionally are

overexpressing MAAs. We applied the same class I-Mix- β2m-DC vaccination regime with and without combinatorial paclitaxel treatment once palpable tumors of at least 0.1 mm^3 were established. Strikingly, class I-Mix- β2m-DC vaccination inhibited tumor growth which resulted in slower growing tumor burden and significantly improved survival compared to control or paclitaxel only treated group. As class I-Mix- β2m-DC vaccination combined with paclitaxel did not lead to a complete tumor regression, but to a much lower tumor growth rate in BRAF mice, we investigated immune cell subsets in LN, SP and skin tumor upon respective treatment, similarly to the experiments we performed in the melanoma bearing *ret*-tg mice.

We observed significant changes of MDSC frequencies, in combined treatment of paclitaxel with chimeric class I-Mix- β2m-DC vaccine in LN,SP and skin lesions, associated with a great decrease in Arg-1 and NO and PD-L1 expression levels, particularly upon class I-Mix vaccination combined with paclitaxel (Fig.53), indicating reduced immunosuppression. These results are in line with reduced Treg activity, detected by decreased CD39 and Ki 67 expression (Fig.57). Studying activity of CD8 T cells upon chimeric class I-Mix- β2m-DC vaccination in BRAF mice, we detected elevated levels of IFNγ producing CD8 T cells upon *in vitro* restimuation, indicating antigen specific CTL induction upon vaccination (Fig.58). Furthermore an intense reduction of naïve $CD8^+$ T cells, associated with $CD8^+$ effector memory induction was detected in SP, LN and skin tumor (Fig.55). Finally, increased frequency of tumor infiltrating $CD8^+$ T cells upon combined treatment of paclitaxel with chimeric class I-Mix-ß2m-DC vaccine was observed which was associated with an increased TCRζ- chain expression (Fig. 56), suggesting a profound and systemic $CD8^+$ T cell activation upon class I Mix vaccination. Interestingly, these results were accompanied with significantly increased PD-1 levels in LN, SP and skin tumors, similar to observed levels in ret-tg mice upon vaccination, suggesting T cell exhausting state. Overall, results observed in BRAF mice are in line with previous studies performed by us in the *ret*-tg mice, further providing rational for advantages in combined immunotherapy with our improved DC vaccine. Novel treatment regimens of BRAF-mutated tumors which occur in about 40 -60% of melanoma lesions are urgently needed due to frequently occurring BRAFi or MEKi resistance[102,191]. Indeed, there are currently several clinical trials ongoing in patients with metastatic melanoma, beneficial combined treatment regimes, such as targeted therapies with check-point inhibitors and chemotherapeutics to overcome current resistance-limitations of BRAF mutated melanoma treatment[114].

6 Abbreviations

A

APC	allophycocyanin
APC	antigen-presenting cell
ARG-1	arginase-1
Ab	antibody

B

BM	bone marrow
BSA	bovine serum albumine
BL/6	mice on C57BL/6 background
BMDC	bone marrow derived dendritic cell

C

CCL	C-C chemokine ligand
CCR	C-C chemokine receptor
CD	cluster of differentiation
Cy5 or Cy7	cyanine-5 or -7
CFSE	carboxyfluorescein succinimidyl ester
CTL	cytotoxic lymphocytes
CTLA-4	cytotoxic T lymphocyte antigen 4
Class I	major histocompatibility complex class I
Class II	major histocompatibility complex class II

D

DC2.4	immortalized dendritic cell line
DC	dendritic cell
DNA	desoxyribonucleic acid
dH_2O	distilled water
DMSO	dimethylsulfoxide

E

EDTA	ethylenediamine-tetra-acetic acid
Et al.	et alteri

F

FACS	fluorescence activated cell sorting
FBS	fetal bovine serum
FITC	fluorescein-isothiocyanat
FMO	fluorescence minus one
FoxP3	forkhead box P3
FSC	forward scatter

G

GM-CSF	granulocyte-macrophage colony-stimulating factor

H

HLA-DR	human leucocyte antigen-DR
Hß2-m	human-beta2 microglibulin

I

IFN	interferon
iNOS	inducible nitric oxide synthase
IL	interleukine
i.p.	intraperitoneal injection
i.v.	Intravenous injection
i.d.	intradermal
i.f.p	Intra foodpad

L

LN	lymph nodes

M

MACS	magnetic-activated cell sorting
MDSC	myeloid-derived suppressor cells
MHC	major histocompartibility complex
Mo-MDSC	Monocytic MDSC
mM	Micromolar

N

NO	nitric oxide
Nf-κB	nuclear factor-kappa B

P

PBMC	peripheral blood mononuclear cells
PBS	phosphate buffered saline
PD-1	programmed death 1
PD-L1	programmed death ligand 1
PE	phycoerythrin
PerCp	peridinin-chlorophyll-protein complex
PAMPS	Pathogen-associated molecular patterns
PRR	Pattern recognition receptors
PMN-MDSC	Polymorphonuclear MDSC

R

RBC	red blood cell
ret	human *ret* proto-oncogene
ret tg	*ret* transgenic mice
ret tu	*ret* transgenic tumor-bearing mice

ROS	reactive oxygen species
RPMI	Roswell Park Memorial Institute medium
RT	room temperature
rpm	rounds per minute
RF-	restriction free -
mRNA	messenger ribonucleic acid

S

SSC	side scatter
SP6	SP6 promotor
s.c.	Subcutaneous injection

T

T cell	T lymphocyte
Tcon	conventional $CD4^+$ T cells ($FoxP3^-$)
Teff	effector T cells
T_{EM}	effector memory Tcells
T_{CM}	central memory T cells
T_{naive}	Naive T cells
TCR	T cell receptor
TGF-β	transforming growth factor beta
Treg	regulator $CD4^+$ T cells ($CD25^+FoxP3^+$)
TRP	tyrosinase related protein
TAM	Tumor associated macrophages
Th	T helper lymphocyte
Tyr	Tyrosinase
TIL	Tumor-infiltrating lymphocytes
TLR	Toll-like receptor
T7	T7 promotor of bacteriophage

V

VEGF	vascular endothelial growth factor

7 List of Tables

8 List of Figures

9 References

1. Janeway, C. a & Medzhitov, R. Innate immune recognition. *Annu. Rev. Immunol.* **20,** 197–216 (2002).
2. Medzhitov, R. & Janeway, C. A. Innate immunity: impact on the adaptive immune response. *Curr. Opin. Immunol.* **9,** 4–9 (1997).
3. Blander, J. M. & Medzhitov, R. Toll-dependent selection of microbial antigens for presentation by dendritic cells. *Nature* **440,** 808–12 (2006).
4. Re, F. & Strominger, J. L. Toll-like Receptor 2 (TLR2) and TLR4 Differentially Activate Human Dendritic Cells. *J. Biol. Chem.* **276,** 37692–37699 (2001).
5. Kawai, T. & Akira, S. The role of pattern-recognition receptors in innate immunity: update on Toll-like receptors. *Nat. Immunol.* **11,** 373–84 (2010).
6. Granucci, F., Foti, M. & Ricciardi-Castagnoli, P. Dendritic cell biology. *Adv. Immunol.* **88,** 193–233 (2005).
7. Acton, S. E. & Reis e Sousa, C. Dendritic cells in remodeling of lymph nodes during immune responses. *Immunol. Rev.* **271,** 221–229 (2016).
8. McBlane, J. F. *et al.* Cleavage at a V(D)J recombination signal requires only RAG1 and RAG2 proteins and occurs in two steps. *Cell* **83,** 387–95 (1995).
9. Watanabe, R. Resident memory T cells in mouse and human. *Nihon Rinsho Meneki. Gakkai Kaishi* **39,** 505–512 (2016).
10. Ardavin, C., Amigorena, S. & Reis e Sousa, C. Dendritic Cells : Immunobiology and Cancer Immunotherapy. *Immunity* **20,** 17–23 (2004).
11. Collin, M., McGovern, N. & Haniffa, M. Human dendritic cell subsets. *Immunology* **140,** 22–30 (2013).
12. Radford, K. J. & Caminschi, I. New generation of dendritic cell vaccines. *Hum. Vaccines Immunother.* **9,** 259–264 (2013).
13. Whiteside, T. L. & Odoux, C. Dendritic cell biology and cancer therapy. *Cancer Immunol. Immunother.* **53,** 240–248 (2004).
14. Benteyn, D., Heirman, C., Bonehill, A., Thielemans, K. & Breckpot, K. mRNA-based dendritic cell vaccines. *Expert Rev. Vaccines* **16,** 1–16 (2014).
15. Adams, S., O'Neill, D. W. & Bhardwaj, N. Recent advances in dendritic cell biology. *J. Clin. Immunol.* **25,** 87–98 (2005).
16. Netea, M. G., Meer, J. W. M. Van Der, Sutmuller, R. P., Adema, G. J. & Kullberg, B. From the Th1 / Th2 Paradigm towards a Toll-Like Receptr/T-Helper Bias. *Antimicrob. Agents Chemother.* **49,** 3991–3996 (2005).
17. Melief, C. J. M. *et al.* Dendritic cells, new tools for vaccination. *Immunity* **20,** 193–233 (2008).
18. Neill, D. W. O. *et al.* Review in translational hematology Manipulating dendritic cell biology for the active immunotherapy of cancer. *Blood J.* **104,** 2235–2247 (2015).
19. Lesterhuis, W. J. *et al.* Dendritic cell vaccines in melanoma: From promise to proof? *Crit. Rev. Oncol. Hematol.* **66,** 118–134 (2008).
20. Xu, H. & Cao, X. Dendritic cell vaccines in cancer immunotherapy: from biology to translational medicine. *Front. Med.* **5,** 323–332 (2011).
21. Siegel, R. L., Miller, K. D. & Jemal, A. Cancer statistics, 2016. *CA. Cancer J. Clin.* **66,** 7–30 (2016).

22. Garbe, C. *et al.* Diagnosis and treatment of melanoma: European consensus-based interdisciplinary guideline. *Eur. J. Cancer* **46,** 270–83 (2010).

23. MacKie, R. M., Hauschild, A. & Eggermont, A. M. M. Epidemiology of invasive cutaneous melanoma. *Ann. Oncol. Off. J. Eur. Soc. Med. Oncol.* **20 Suppl 6,** vi1-7 (2009).

24. Miller, A. J. & Mihm, M. C. Melanoma. *N. Engl. J. Med.* **355,** 51–65 (2006).

25. Tronnier, M., Semkova, K., Wollina, U. & Tchernev, G. Malignant melanoma: epidemiologic aspects, diagnostic and therapeutic approach. *Wien Med Wochenschr* **163,** 354–358 (2013).

26. Bertolotto, C. Melanoma: from melanocyte to genetic alterations and clinical options. *Scientifica (Cairo).* **2013,** 635203 (2013).

27. Ortenberg, R. *et al.* Novel Immunotherapy for Malignant Melanoma with a Monoclonal Antibody That Blocks CEACAM1 Homophilic Interactions. *Mol. Cancer Ther.* **11,** 1300–1310 (2012).

28. Vesely, M. D., Kershaw, M. H., Schreiber, R. D. & Smyth, M. J. Natural innate and adaptive immunity to cancer. *Annu. Rev. Immunol.* **29,** 235–71 (2011).

29. Atherton, M. J., Morris, J. S., McDermott, M. R. & Lichty, B. D. Cancer immunology and canine malignant melanoma: A comparative review. *Vet. Immunol. Immunopathol.* **169,** 15–26 (2016).

30. Maslin, B., Alexandrescu, D. T., Ichim, T. E. & Dasanu, C. a. Newer developments in the immunotherapy of malignant melanoma. *J. Oncol. Pharm. Pract.* **20,** 3–10 (2014).

31. Mukherji, B. Immunology of melanoma. *Clin. Dermatol.* **31,** 156–65 (2013).

32. Umansky, V. & Sevko, A. Melanoma-induced immunosuppression and its neutralization. *Semin. Cancer Biol.* **22,** 319–26 (2012).

33. Lizée, G., Radvanyi, L. G., Overwijk, W. W. & Hwu, P. Immunosuppression in melanoma immunotherapy: potential opportunities for intervention. *Clin. Cancer Res.* **12,** 2359s–2365s (2006).

34. Malmberg, K.-J. & Ljunggren, H.-G. Escape from immune- and nonimmune-mediated tumor surveillance. *Semin. Cancer Biol.* **16,** 16–31 (2006).

35. Whiteside, T. L. Immune suppression in cancer: effects on immune cells, mechanisms and future therapeutic intervention. *Semin. Cancer Biol.* **16,** 3–15 (2006).

36. Wherry, E. J. & Kurachi, M. Molecular and cellular insights into T cell exhaustion. *Nat. Rev. Immunol.* **15,** 486–499 (2015).

37. Hanahan, D. & Weinberg, R. A. Hallmarks of cancer: The next generation. *Cell* **144,** 646–674 (2011).

38. Dunn, G. P., Old, L. J. & Schreiber, R. D. The three Es of cancer immunoediting. *Annu. Rev. Immunol.* **22,** 329–60 (2004).

39. Reddy, S. M. *et al.* Oncology meets immunology: The cancer-immunity cycle. *Oncoimmunology* **37,** 1–10 (2016).

40. Campoli, M. & Ferrone, S. Tumor escape mechanisms: potential role of soluble HLA antigens and NK cells activating ligands. *Tissue Antigens* **72,** 321–34 (2008).

41. Farber, D. L., Yudanin, N. a & Restifo, N. P. Human memory T cells: generation, compartmentalization and homeostasis. *Nat. Rev. Immunol.* **14,** 24–35 (2013).

42. Nicolette, C. A. *et al.* Dendritic cells for active immunotherapy: Optimizing design and manufacture in order to develop commercially and clinically viable products. *Vaccine*

25, (2007).

43. Nagaraj, S., Youn, J.-I. & Gabrilovich, D. I. Reciprocal relationship between myeloid-derived suppressor cells and T cells. *J. Immunol.* **191,** 17–23 (2013).

44. Hargadon, K. M. The extent to which melanoma alters tissue-resident dendritic cell function correlates with tumorigenicity. *Oncoimmunology* **5,** e1069462 (2016).

45. Gabrilovich, D. I. & Nagaraj, S. Myeloid-derived suppressor cells as regulators of the immune system. *Nat. Rev. Immunol.* **9,** 162–74 (2009).

46. Gabrilovich, D. I., Ostrand-Rosenberg, S. & Bronte, V. Coordinated regulation of myeloid cells by tumours. *Nat. Rev. Immunol.* **12,** 253–68 (2012).

47. Umansky, V. & Sevko, A. Tumor microenvironment and myeloid-derived suppressor cells. *Cancer Microenviron.* **6,** 169–77 (2013).

48. Melief, C. J. M. Cancer Immunotherapy by Dendritic Cells. *Immunity* **29,** 372–383 (2008).

49. Nencioni, A. *et al.* The use of dendritic cells in cancer immunotherapy. *Crit. Rev. Oncol. Hematol.* **65,** 191–199 (2008).

50. Chen, X. *et al.* CD4 + CD25 + regulatory T cells in tumor immunity. *Int. Immunopharmacol.* **34,** 244–249 (2016).

51. Josefowicz, S. Z., Lu, L.-F. & Rudensky, A. Y. Regulatory T cells: mechanisms of differentiation and function. *Annu. Rev. Immunol.* **30,** 531–64 (2012).

52. Vignali, D. A. A., Collison, L. W. & Workman, C. J. How regulatory T cells work. *Nat. Rev. Immunol.* **8,** 523–32 (2008).

53. Ouyang, Z. *et al.* Regulatory T cells in the immunotherapy of melanoma. *Tumor Biol.* **37,** 77–85 (2016).

54. Bono, M. R., Fernández, D., Flores-Santibáñez, F., Rosemblatt, M. & Sauma, D. CD73 and CD39 ectonucleotidases in T cell differentiation: Beyond immunosuppression. *FEBS Lett.* **589,** 3454–60 (2015).

55. Liu, L. *et al.* Low intratumoral regulatory T cells and high peritumoral CD8(+) T cells relate to long-term survival in patients with pancreatic ductal adenocarcinoma after pancreatectomy. *Cancer Immunol. Immunother.* **65,** 73–82 (2016).

56. Preston, C. C. *et al.* The ratios of CD8+ T cells to CD4+CD25+ FOXP3+ and FOXP3- T cells correlate with poor clinical outcome in human serous ovarian cancer. *PLoS One* **8,** (2013).

57. Chen, X. & Oppenheim, J. J. Resolving the identity myth: Key markers of functional CD4 +FoxP3 + regulatory T cells. *Int. Immunopharmacol.* **11,** 1489–1496 (2011).

58. Jablonski, K. A. *et al.* Novel markers to delineate murine M1 and M2 macrophages. *PLoS One* **10,** 5–11 (2015).

59. Pardoll, D. Cancer and Immune System: Basic Concepts and Targets for Intervention. *Semin. Oncol.* **42,** 523–538 (2015).

60. Mosser, D. M. & Edwards, J. P. Exploring the full spectrum of macrophage activation. *Nat. Rev. Immunol.* **8,** 958–69 (2008).

61. Nadella, V., Singh, S. & Prakash, H. Macrophages directed approaches are paramount for effective cancer immunotherapies. *Integr. Cancer Sci. Ther.* **3,** 465–472 (2016).

62. Quatromoni, J. G. & Eruslanov, E. Tumor-associated macrophages: function, phenotype, and link to prognosis in human lung cancer. *Am. J. Transl. Res.* **4,** 376–89

(2012).

63. Ugel, S., De Sanctis, F., Mandruzzato, S. & Bronte, V. Tumor-induced myeloid deviation: when myeloid-derived suppressor cells meet tumor-associated macrophages. *J. Clin. Invest.* **125,** 3365–76 (2015).

64. Gwak, J. M., Jang, M. H., Kim, D. Il, Seo, A. N. & Park, S. Y. Prognostic value of tumor-associated macrophages according to histologic locations and hormone receptor status in breast cancer. *PLoS One* **10,** e0125728 (2015).

65. Zhang, Y. *et al.* ROS play a critical role in the differentiation of alternatively activated macrophages and the occurrence of tumor-associated macrophages. *Cell Res.* **23,** 898–914 (2013).

66. Chavez-Galan, L., Olleros, M. L., Vesin, D. & Garcia, I. Much more than M1 and M2 macrophages, there are also $CD169^+$ and TCR^+ macrophages. *Front. Immunol.* **6,** 1–15 (2015).

67. Italiani, P. & Boraschi, D. From monocytes to M1/M2 macrophages: Phenotypical vs. functional differentiation. *Front. Immunol.* **5,** 1–22 (2014).

68. Gabrilovich, D. & Nagaraj, S. Myeloid-derived-suppressor cells as regulators of the immune system. *Nat Rev Immunol* **9,** 162–174 (2009).

69. Marvel, D. & Gabrilovich, D. I. Myeloid-derived suppressor cells in the tumor microenvironment: expect the unexpected. *J. Clin. Invest.* **125,** 3356–3364 (2015).

70. Umansky, V., Sevko, A., Gebhardt, C. & Utikal, J. Myeloid-derived suppressor cells in malignant melanoma. *J. Dtsch. Dermatol. Ges.* **12,** 1021–7 (2014).

71. Talmadge, J. E. & Gabrilovich, D. I. History of myeloid-derived suppressor cells. *Nat. Rev. Cancer* **13,** 739–52 (2013).

72. Stromnes, I. M., Greenberg, P. D. & Hingorani, S. R. Molecular pathways: myeloid complicity in cancer. *Clin. Cancer Res.* **20,** 5157–70 (2014).

73. Bronte, V. *et al.* Recommendations for myeloid-derived suppressor cell nomenclature and characterization standards. *Nat. Commun.* **7,** 12150 (2016).

74. Youn, J.-I., Nagaraj, S., Collazo, M. & Gabrilovich, D. I. Subsets of myeloid-derived suppressor cells in tumor-bearing mice. *J. Immunol.* **181,** 5791–802 (2008).

75. Zhou, Z. *et al.* Development and function of myeloid-derived suppressor cells generated from mouse embryonic and hematopoietic stem cells. *Stem Cells* **28,** 620–32 (2010).

76. Meyer, C. *et al.* Chronic inflammation promotes myeloid-derived suppressor cell activation blocking antitumor immunity in transgenic mouse melanoma model. *Proc. Natl. Acad. Sci. U. S. A.* **108,** 17111–6 (2011).

77. Meyer, C. *et al.* Chronic inflammation promotes myeloid-derived suppressor cell activation blocking antitumor immunity in transgenic mouse melanoma model. *Proc. Natl. Acad. Sci. U. S. A.* **108,** 17111–6 (2011).

78. Kumar, V., Patel, S., Tcyganov, E. & Gabrilovich, D. I. The Nature of Myeloid-Derived Suppressor Cells in the Tumor Microenvironment. *Trends Immunol.* **37,** 208–220 (2016).

79. Cheng, P. *et al.* Inhibition of dendritic cell differentiation and accumulation of myeloid-derived suppressor cells in cancer is regulated by S100A9 protein. *J. Exp. Med.* **205,** 2235–49 (2008).

80. Condamine, T. & Gabrilovich, D. I. Molecular mechanisms regulating myeloid-derived suppressor cell differentiation and function. *Trends Immunol.* **32,** 19–25 (2011).

81. Kusmartsev, S. & Gabrilovich, D. I. Role of immature myeloid cells in mechanisms of immune evasion in cancer. *Cancer Immunol. Immunother.* **55,** 237–245 (2006).

82. Schouppe, E., De Baetselier, P., Van Ginderachter, J. A. & Sarukhan, A. Instruction of myeloid cells by the tumor microenvironment: Open questions on the dynamics and plasticity of different tumor-associated myeloid cell populations. *Oncoimmunology* **1,** 1135–1145 (2012).

83. Solito, S. *et al.* A human promyelocytic-like population is responsible for the immune suppression mediated by myeloid-derived suppressor cells. *Blood* **118,** 2254–65 (2011).

84. Sinha, P., Clements, V. K., Bunt, S. K., Albelda, S. M. & Ostrand-Rosenberg, S. Cross-talk between myeloid-derived suppressor cells and macrophages subverts tumor immunity toward a type 2 response. *J. Immunol.* **179,** 977–83 (2007).

85. Wang, H. *et al.* High numbers of CD68+ tumor-associated macrophages correlate with poor prognosis in extranodal NK/T-cell lymphoma, nasal type. *Ann. Hematol.* **94,** 1535–44 (2015).

86. Quail, D. F. & Joyce, J. a. Microenvironmental regulation of tumor progression and metastasis. *Nat. Med.* **19,** 1423–37 (2013).

87. Meyer, C. *et al.* Chronic inflammation promotes myeloid-derived suppressor cell activation blocking antitumor immunity in transgenic mouse melanoma model. *PNAS* 6–11 (2011). doi:10.1073/pnas.1108121108

88. Baniyash, M. TCR zeta-chain downregulation: curtailing an excessive inflammatory immune response. *Nat. Rev. Immunol.* **4,** 675–87 (2004).

89. Meirow, Y., Kanterman, J. & Baniyash, M. Paving the Road to Tumor Development and Spreading: Myeloid-Derived Suppressor Cells are Ruling the Fate. *Front. Immunol.* **6,** 523 (2015).

90. Weide, B. *et al.* Myeloid-derived suppressor cells predict survival of patients with advanced melanoma: comparison with regulatory T cells and NY-ESO-1- or melan-A-specific T cells. *Clin. Cancer Res.* **20,** 1601–9 (2014).

91. Noman, M. Z. *et al.* PD-L1 is a novel direct target of HIF-1α, and its blockade under hypoxia enhanced MDSC-mediated T cell activation. *J. Exp. Med.* **211,** 781–90 (2014).

92. Srivastava, M. K., Sinha, P., Clements, V. K., Rodriguez, P. & Ostrand-Rosenberg, S. Myeloid-derived suppressor cells inhibit T-cell activation by depleting cystine and cysteine. *Cancer Res.* **70,** 68–77 (2010).

93. Cipponi, A., Wieers, G., van Baren, N. & Coulie, P. G. Tumor-infiltrating lymphocytes: apparently good for melanoma patients. But why? *Cancer Immunol. Immunother.* **60,** 1153–60 (2011).

94. Koshenkov, V. P., Broucek, J. & Kaufman, H. L. Surgical Management of Melanoma. *Cancer Treat. Res.* **167,** 149–79 (2016).

95. Davar, D. & Kirkwood, J. M. Adjuvant Therapy of Melanoma. *Cancer Treat. Res.* **167,** 181–208 (2016).

96. Bajetta, E. *et al.* Metastatic melanoma: chemotherapy. *Semin. Oncol.* **29,** 427–45 (2002).

97. Arrangoiz, R. Melanoma Review: Epidemiology, Risk Factors, Diagnosis and Staging. *J. Cancer Treat. Res.* **4,** 1 (2016).

98. Harries, M. *et al.* Treatment patterns of advanced malignant melanoma (stage III-IV) - A review of current standards in Europe. *Eur. J. Cancer* **60,** 179–189 (2016).

99. Spagnolo, F., Ghiorzo, P. & Queirolo, P. Overcoming resistance to BRAF inhibition in BRAF-mutated metastatic melanoma. (2014).

100. Bajetta, E. *et al.* Metastatic melanoma: chemotherapy. *Semin. Oncol.* **29,** 427–45 (2002).

101. Polkowska, M., Czepielewska, E. & Kozłowska-Wojciechowska, M. Drug Combinations as the New Standard for Melanoma Treatment. *Curr. Treat. Options Oncol.* **17,** 61 (2016).

102. Wargo, J. A., Reuben, A., Cooper, Z. A., Oh, K. S. & Sullivan, R. J. Immune Effects of Chemotherapy, Radiation, and Targeted Therapy and Opportunities for Combination With Immunotherapy. *Semin. Oncol.* **42,** 601–16 (2015).

103. Hersh, E. M. *et al.* A phase II multicenter study of ipilimumab with or without dacarbazine in chemotherapy-naïve patients with advanced melanoma. *Invest. New Drugs* **29,** 489–98 (2011).

104. Wolchok, J. D. *et al.* Ipilimumab efficacy and safety in patients with advanced melanoma: a retrospective analysis of HLA subtype from four trials. *Cancer Immun.* **10,** 9 (2010).

105. Hodi, F. S. *et al.* Ipilimumab plus sargramostim vs ipilimumab alone for treatment of metastatic melanoma: a randomized clinical trial. *JAMA* **312,** 1744–53 (2014).

106. Weber, J. Immune checkpoint proteins: A new therapeutic paradigm for cancerpreclinical background: CTLA-4 and PD-1 blockade. *Semin. Oncol.* **37,** 430–439 (2010).

107. Postow, M. A., Callahan, M. K. & Wolchok, J. D. Immune Checkpoint Blockade in Cancer Therapy. *J. Clin. Oncol.* (2015). doi:10.1200/JCO.2014.59.4358

108. Kalinski, P., Muthuswamy, R. & Urban, J. Dendritic cells in cancer immunotherapy: vaccines and combination immunotherapies. *Expert Rev. Vaccines* **12,** 285–95 (2013).

109. Palucka, K. & Banchereau, J. Dendritic-Cell-Based Therapeutic Cancer Vaccines. *Immunity* **39,** 38–48 (2013).

110. Nestle, F. O. *et al.* Vaccination of melanoma patients with peptide- or tumor lysate-pulsed dendritic cells. *Nat. Med.* **4,** 328–32 (1998).

111. Zaks, T. Z. & Rosenberg, S. A. Immunization with a peptide epitope (p369-377) from HER-2/neu leads to peptide-specific cytotoxic T lymphocytes that fail to recognize HER-2/neu+ tumors. *Cancer Res.* **58,** 4902–8 (1998).

112. Kyte, J. A. *et al.* Immune response and long-term clinical outcome in advanced melanoma patients vaccinated with tumor-mRNA-transfected dendritic cells. *Oncoimmunology* **5,** e1232237 (2016).

113. Pujol, J.-L. *et al.* Safety and Immunogenicity of MAGE-A3 Cancer Immunotherapeutic with or without Adjuvant Chemotherapy in Patients with Resected Stage IB to III MAGE-A3-Positive Non-Small-Cell Lung Cancer. *J. Thorac. Oncol.* **10,** 1458–67 (2015).

114. Polkowska, M., Czepielewska, E. & Kozłowska-Wojciechowska, M. Drug Combinations as the New Standard for Melanoma Treatment. *Curr. Treat. Options Oncol.* **17,** 61 (2016).

115. Bender, C., Hassel, J. C. & Enk, A. Immunotherapy of Melanoma. *Oncol. Res. Treat.* **39,** 369–76 (2016).

116. Gotwals, P. *et al.* Prospects for combining targeted and conventional cancer therapy with immunotherapy. *Nat. Rev. Cancer* (2017). doi:10.1038/nrc.2017.17

117. Hu-Lieskovan, S., Homet Moreno, B. & Ribas, A. Excluding T Cells: Is β-Catenin the Full Story? *Cancer Cell* **27,** 749–50 (2015).

118. Cook, A. M., McDonnell, A. M., Lake, R. A. & Nowak, A. K. Dexamethasone co-medication in cancer patients undergoing chemotherapy causes substantial immunomodulatory effects with implications for chemo-immunotherapy strategies. *Oncoimmunology* **5,** e1066062 (2016).

119. Lake, R. A. & Robinson, B. W. S. Immunotherapy and chemotherapy--a practical partnership. *Nat. Rev. Cancer* **5,** 397–405 (2005).

120. Shurin, G. V, Tourkova, I. L. & Shurin, M. R. Low-dose chemotherapeutic agents regulate small Rho GTPase activity in dendritic cells. *J. Immunother.* **31,** 491–9 (2008).

121. Shurin, G. V, Tourkova, I. L., Kaneno, R. & Shurin, M. R. Chemotherapeutic agents in noncytotoxic concentrations increase antigen presentation by dendritic cells via an IL-12-dependent mechanism. *J. Immunol.* **183,** 137–44 (2009).

122. Michels, T. *et al.* Paclitaxel promotes differentiation of myeloid-derived suppressor cells into dendritic cells in vitro in a TLR4-independent manner. *J. Immunotoxicol.* **9,** 292–300 (2012).

123. Sevko, A. *et al.* Application of paclitaxel in low non-cytotoxic doses supports vaccination with melanoma antigens in normal mice. *J. Immunotoxicol.* **9,** 275–81 (2012).

124. Chen, G. & Emens, L. A. Chemoimmunotherapy: reengineering tumor immunity. *Cancer Immunol. Immunother.* **62,** 203–16 (2013).

125. Curiel, T. J. Tregs and rethinking cancer immunotherapy. *J. Clin. Invest.* **117,** 1167–1174 (2007).

126. Breckpot, K. & Escors, D. Dendritic cells for active anti-cancer immunotherapy: targeting activation pathways through genetic modification. *Endocr. Metab. Immune Disord. Drug Targets* **9,** 328–43 (2009).

127. Bonehill, A., Heirman, C. & Thielemans, K. Genetic approaches for the induction of a CD4+ T cell response in cancer immunotherapy. *J. Gene Med.* **7,** 686–95 (2005).

128. Hsu, F. J. *et al.* Vaccination of patients with B-cell lymphoma using autologous antigen-pulsed dendritic cells. *Nat. Med.* **2,** 52–8 (1996).

129. Palucka, K. & Banchereau, J. Cancer immunotherapy via dendritic cells. *Nat. Rev. Cancer* **12,** 265–277 (2012).

130. Anguille, S., Smits, E. L., Lion, E., Van Tendeloo, V. F. & Berneman, Z. N. Clinical use of dendritic cells for cancer therapy. *The Lancet Oncology* **15,** (2014).

131. Anguille, S. *et al.* Dendritic Cells as Pharmacological Tools for Cancer Immunotherapy. *Pharmacol. Rev.* **67,** 731–53 (2015).

132. Oshita, C. *et al.* Dendritic cell-based vaccination in metastatic melanoma patients: Phase II clinical trial. *Oncol. Rep.* **28,** 1131–1138 (2012).

133. Nasi, A. *et al.* Immunogenicity is preferentially induced in sparse dendritic cell cultures. *Sci. Rep.* **7,** 43989 (2017).

134. Frankenberger, B. & Schendel, D. J. Third generation dendritic cell vaccines for tumor immunotherapy. *Eur. J. Cell Biol.* **91,** 53–58 (2012).

135. Nestle, F. O., Farkas, A. & Conrad, C. Dendritic-cell-based therapeutic vaccination against cancer. *Curr. Opin. Immunol.* **17,** 163–169 (2005).

136. Schuler, G., Schuler-Thurner, B. & Steinman, R. M. The use of dendritic cells in

cancer immunotherapy. *Curr. Opin. Immunol.* **15,** 138–147 (2003).

137. Mitchell, D. A. & Nair, S. K. RNA-transfected dendritic cells in cancer immunotherapy. *J. Clin. Invest.* **106,** 1065–9 (2000).

138. Zhong, L., Granelli-Piperno, A., Choi, Y. & Steinman, R. M. Recombinant adenovirus is an efficient and non-perturbing genetic vector for human dendritic cells. *Eur. J. Immunol.* **29,** 964–72 (1999).

139. Gashev, A. a *et al.* Methods for lymphatic vessel culture and gene transfection. *Microcirculation* **16,** 615–628 (2009).

140. Gilboa, E. & Vieweg, J. Cancer immunotherapy with mRNA-transfected dendritic cells. *Immunol. Rev.* **199,** 251–263 (2004).

141. Kyte, J. a *et al.* Phase I/II trial of melanoma therapy with dendritic cells transfected with autologous tumor-mRNA. *Cancer Gene Ther.* **13,** 905–18 (2006).

142. Mu, L. J. *et al.* Immunotherapy with allotumour mRNA-transfected dendritic cells in androgen-resistant prostate cancer patients. *Br. J. Cancer* **93,** 749–56 (2005).

143. Javorovic, M., Pohla, H., Frankenberger, B., Wölfel, T. & Schendel, D. J. RNA transfer by electroporation into mature dendritic cells leading to reactivation of effector-memory cytotoxic T lymphocytes: A quantitative analysis. *Mol. Ther.* **12,** 734–743 (2005).

144. Cafri, G. *et al.* mRNA-transfected Dendritic Cells Expressing Polypeptides That Link MHC-I Presentation to Constitutive TLR4 Activation Confer Tumor Immunity. *Mol Ther* **23,** 1391–1400 (2015).

145. Cafri, G., Margalit, A., Tzehoval, E., Eisenbach, L. & Gross, G. Development of novel genetic cancer vaccines based on membrane-attached β2 microglobulin. *Ann. N. Y. Acad. Sci.* **1283,** 87–90 (2013).

146. Berko, D. *et al.* Membrane-Anchored 2-Microglobulin Stabilizes a Highly Receptive State of MHC Class I Molecules. *J. Immunol.* **174,** 2116–2123 (2005).

147. Cafri, G. *et al.* Coupling presentation of MHC class I peptides to constitutive activation of antigen-presenting cells through the product of a single gene. *Int. Immunol.* **23,** 453–61 (2011).

148. Margalit, a. *et al.* Induction of Antitumor Immunity by CTL Epitopes Genetically Linked to Membrane-Anchored 2-Microglobulin. *J. Immunol.* **176,** 217–224 (2005).

149. Sharbi-Yunger, A. *et al.* mRNA-based dendritic cell immunization improves survival in ret transgenic mouse melanoma model. *Oncoimmunology* **5,** e1160183 (2016).

150. Kato, M. *et al.* Transgenic mouse model for skin malignant melanoma. *Oncogene* **17,** 1885–8 (1998).

151. Umansky, V. *et al.* Melanoma-specific memory T cells are functionally active in Ret transgenic mice without macroscopic tumors. *Cancer Res.* **68,** 9451–8 (2008).

152. Abschuetz, O. *et al.* T-Cell Mediated Immune Responses Induced in ret Transgenic Mouse Model of Malignant Melanoma. *Cancers (Basel).* **4,** 490–503 (2012).

153. Sharbi-Yunger, A. *et al.* mRNA based dendritic cell immunization improves survival in ret transgenic mouse melanoma model. *Oncoimmunology* **5,** 1–7 (2016).

154. Seliger, B., Kloor, M. & Ferrone, S. HLA class II antigen-processing pathway in tumors: Molecular defects and clinical relevance. *Oncoimmunology* **6,** e1171447 (2017).

155. Borghese, F. & Clanchy, F. I. L. CD74: an emerging opportunity as a therapeutic target in cancer and autoimmune disease. *Expert Opin. Ther. Targets* **15,** 237–51 (2011).

156. Vander Lugt, B. *et al.* Transcriptional programming of dendritic cells for enhanced MHC class II antigen presentation. *Nat. Immunol.* **15,** 161–7 (2014).

157. Day, C. P., Merlino, G. & Van Dyke, T. Preclinical Mouse Cancer Models: A Maze of Opportunities and Challenges. *Cell* **163,** 39–53 (2015).

158. Dankort, D. *et al.* Braf(V600E) cooperates with Pten loss to induce metastatic melanoma. *Nat. Genet.* **41,** 544–52 (2009).

159. Damsky, W. E. *et al.* β-catenin signaling controls metastasis in Braf-activated Pten-deficient melanomas. *Cancer Cell* **20,** 741–54 (2011).

160. Houghton, A. N. & Polsky, D. Focus on melanoma. *Cancer Cell* **2,** 275–278 (2002).

161. Sevko, A. *et al.* Cyclophosphamide promotes chronic inflammation-dependent immunosuppression and prevents antitumor response in melanoma. *J. Invest. Dermatol.* **133,** 1610–9 (2013).

162. Kimpfler, S. *et al.* Skin Melanoma Development in ret Transgenic Mice Despite the Depletion of CD25 + Foxp3 + Regulatory T Cells in Lymphoid Organs. *J. Immunol.* **183,** 6330–6337 (2009).

163. Peleg, Y. & Unger, T. DNA Cloning and Assembly Methods. **1116,** (2014).

164. van den Ent, F. & Löwe, J. RF cloning: a restriction-free method for inserting target genes into plasmids. *J. Biochem. Biophys. Methods* **67,** 67–74 (2006).

165. Unger, T., Jacobovitch, Y., Dantes, A., Bernheim, R. & Peleg, Y. Applications of the Restriction Free (RF) cloning procedure for molecular manipulations and protein expression. *J. Struct. Biol.* **172,** 34–44 (2010).

166. Lutz, M. B. & Rössner, S. Factors influencing the generation of murine dendritic cells from bone marrow: the special role of fetal calf serum. *Immunobiology* **212,** 855–62 (2007).

167. Lutz, M. B. IL-3 in dendritic cell development and function: a comparison with GM-CSF and IL-4. *Immunobiology* **209,** 79–87 (2004).

168. Sevko, A. *et al.* Antitumor effect of paclitaxel is mediated by inhibition of myeloid-derived suppressor cells and chronic inflammation in the spontaneous melanoma model. *J. Immunol.* **190,** 2464–71 (2013).

169. Topalian, S. L., Weiner, G. J. & Pardoll, D. M. Cancer immunotherapy comes of age. *J. Clin. Oncol.* **29,** 4828–4836 (2011).

170. Xu, H. & Cao, X. Dendritic cell vaccines in cancer immunotherapy: From biology to translational medicine. *Front. Med. China* **5,** 323–332 (2011).

171. Shen, Z., Reznikoff, G., Dranoff, G. & Rock, K. . Cloned dendritic cells can present exogenous antigens on both MHC class I and class II molecules. *J. Immunol.* **158,** 2723–2730 (1997).

172. Zong, J., Keskinov, A. A., Shurin, G. V. & Shurin, M. R. Tumor-derived factors modulating dendritic cell function. *Cancer Immunology, Immunotherapy* **65,** (2016).

173. Michiels, a *et al.* Electroporation of immature and mature dendritic cells: implications for dendritic cell-based vaccines. *Gene Ther.* **12,** 772–82 (2005).

174. Macri, C., Dumont, C., Johnston, A. P. R. & Mintern, J. D. Targeting dendritic cells: a promising strategy to improve vaccine effectiveness. *Clin Trans Immunol* **5,** e66 (2016).

175. Dougan, S. K. *et al.* Transnuclear TRP1-specific CD8 T cells with high or low affinity TCRs show equivalent antitumor activity. *Cancer Immunol. Res.* **1,** 99–111 (2013).

176. Muranski, P. *et al.* Tumor-specific Th17-polarized cells eradicate large established melanoma. *Blood* **112,** 362–73 (2008).

177. Wherry, E. J. T cell exhaustion. *Nat. Immunol.* **12,** 492–9 (2011).

178. Barber, D. L. *et al.* Restoring function in exhausted CD8 T cells during chronic viral infection. *Nature* **439,** 682–687 (2006).

179. Badoual, C. *et al.* PD-1-expressing tumor-infiltrating T cells are a favorable prognostic biomarker in HPV-Associated head and neck cancer. *Cancer Res.* **73,** 128–138 (2013).

180. Im, S. J. *et al.* Defining CD8(+) T cells that provide the proliferative burst after PD-1 therapy. *Nature* **537,** 417–421 (2016).

181. Kamphorst, A. O. *et al.* Proliferation of PD-1+ CD8 T cells in peripheral blood after PD-1–targeted therapy in lung cancer patients. *Proc. Natl. Acad. Sci.* 4–9 (2017). doi:10.1073/pnas.1705327114

182. Kim, H.-J. & Cantor, H. CD4 T-cell subsets and tumor immunity: the helpful and the not-so-helpful. *Cancer Immunol. Res.* **2,** 91–8 (2014).

183. Tatsumi, T. *et al.* Disease-associated bias in T helper type 1 (Th1)/Th2 CD4(+) T cell responses against MAGE-6 in HLA-DRB10401(+) patients with renal cell carcinoma or melanoma. *J. Exp. Med.* **196,** 619–28 (2002).

184. Grant, C. R., Liberal, R., Mieli-Vergani, G., Vergani, D. & Longhi, M. S. Regulatory T-cells in autoimmune diseases: challenges, controversies and--yet--unanswered questions. *Autoimmun. Rev.* **14,** 105–16 (2015).

185. Zhang, X., Kelaria, S., Kerstetter, J. & Wang, J. The functional and prognostic implications of regulatory T cells in colorectal carcinoma. *J. Gastrointest. Oncol.* **6,** 307–13 (2015).

186. Jethwa, H., Adami, A. A. & Maher, J. Use of gene-modified regulatory T-cells to control autoimmune and alloimmune pathology: is now the right time? *Clin. Immunol.* **150,** 51–63 (2014).

187. Cauley, L. S., Miller, E. E., Yen, M. & Swain, S. L. Superantigen-induced CD4 T cell tolerance mediated by myeloid cells and IFN-gamma. *J. Immunol.* **165,** 6056–66 (2000).

188. Bronte, V. *et al.* Apoptotic death of CD8+ T lymphocytes after immunization: induction of a suppressive population of Mac-1+/Gr-1+ cells. *J. Immunol.* **161,** 5313–20 (1998).

189. de Oliveira Bravo, M., Carvalho, J. L. & Saldanha-Araujo, F. Adenosine production: a common path for mesenchymal stem-cell and regulatory T-cell-mediated immunosuppression. *Purinergic Signal.* **12,** 595–609 (2016).

190. Alrwas, A. *et al.* Phase I trial of biochemotherapy with cisplatin, temozolomide, and dose escalation of nab-paclitaxel combined with interleukin-2 and interferon-α in patients with metastatic melanoma. *Melanoma Res.* **24,** 342–8 (2014).

191. Vanneman, M. & Dranoff, G. Combining immunotherapy and targeted therapies in cancer treatment. *Nat Rev Cancer* **12,** 237–251 (2012).

10 Appendix

Appendix 1:

MDSC analysis in BM and SP 10 days after last vaccination with class I DC vaccine (solid symbols) and class II DC vaccine (empty symbols)

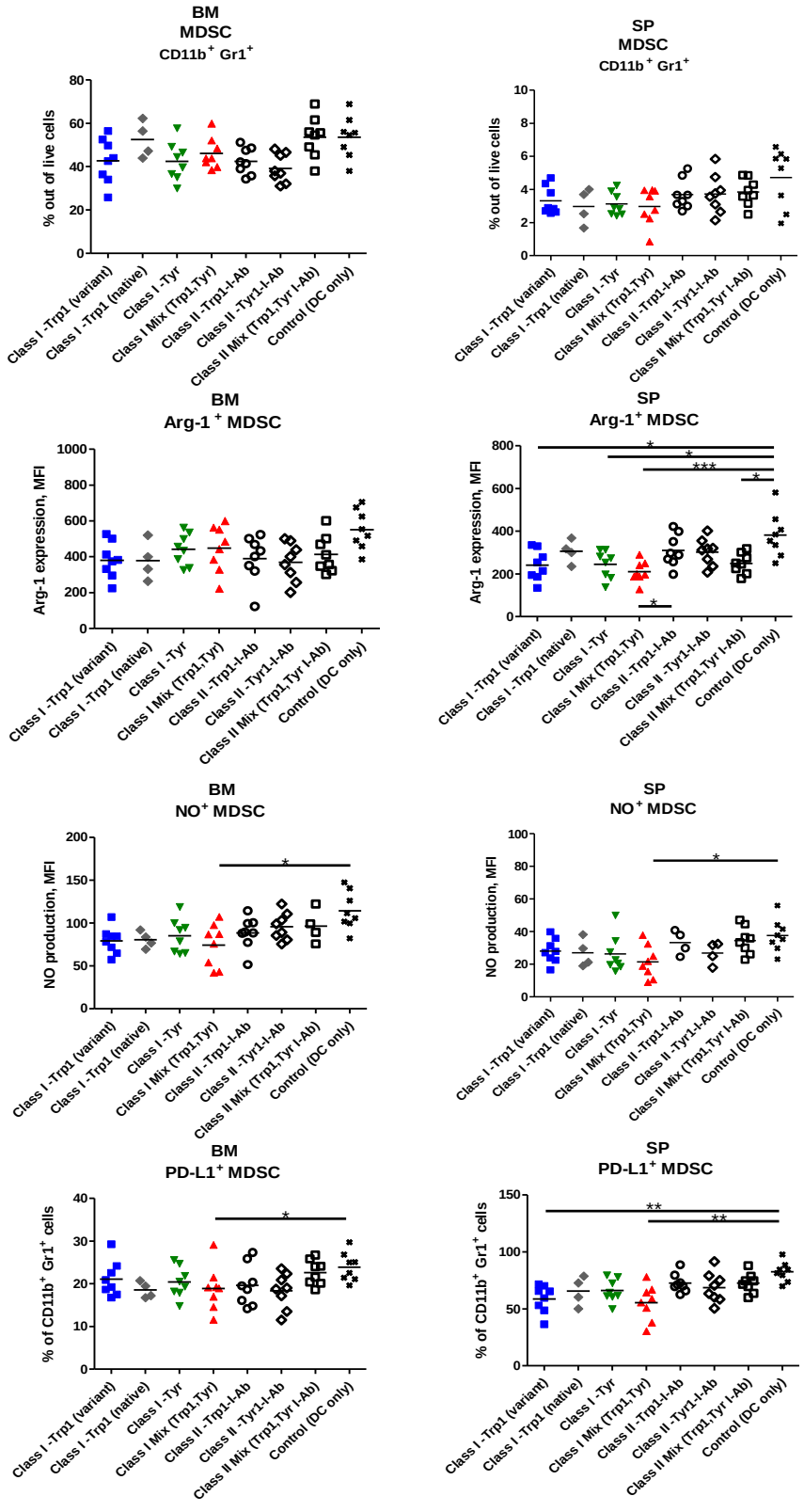

Appendix 2:

CD8+ T memory analysis in BM and SP 10 days after last vaccination with class I DC vaccine (solid symbols) and class II DC vaccine (empty symbols)

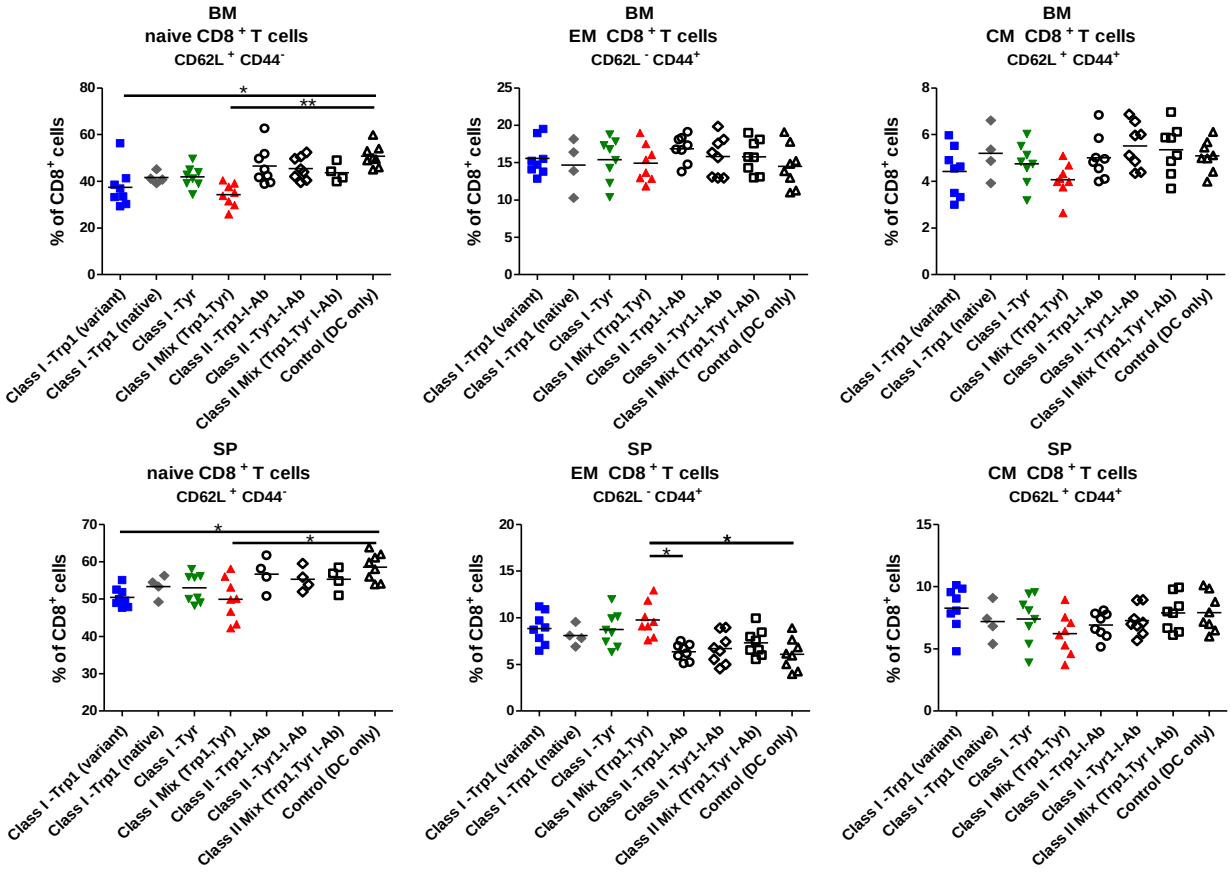

Appendix 3:

CD4+ T memory analysis in BM and SP 10 days after last vaccination with class I DC vaccine (solid symbols) and class II DC vaccine (empty symbols)

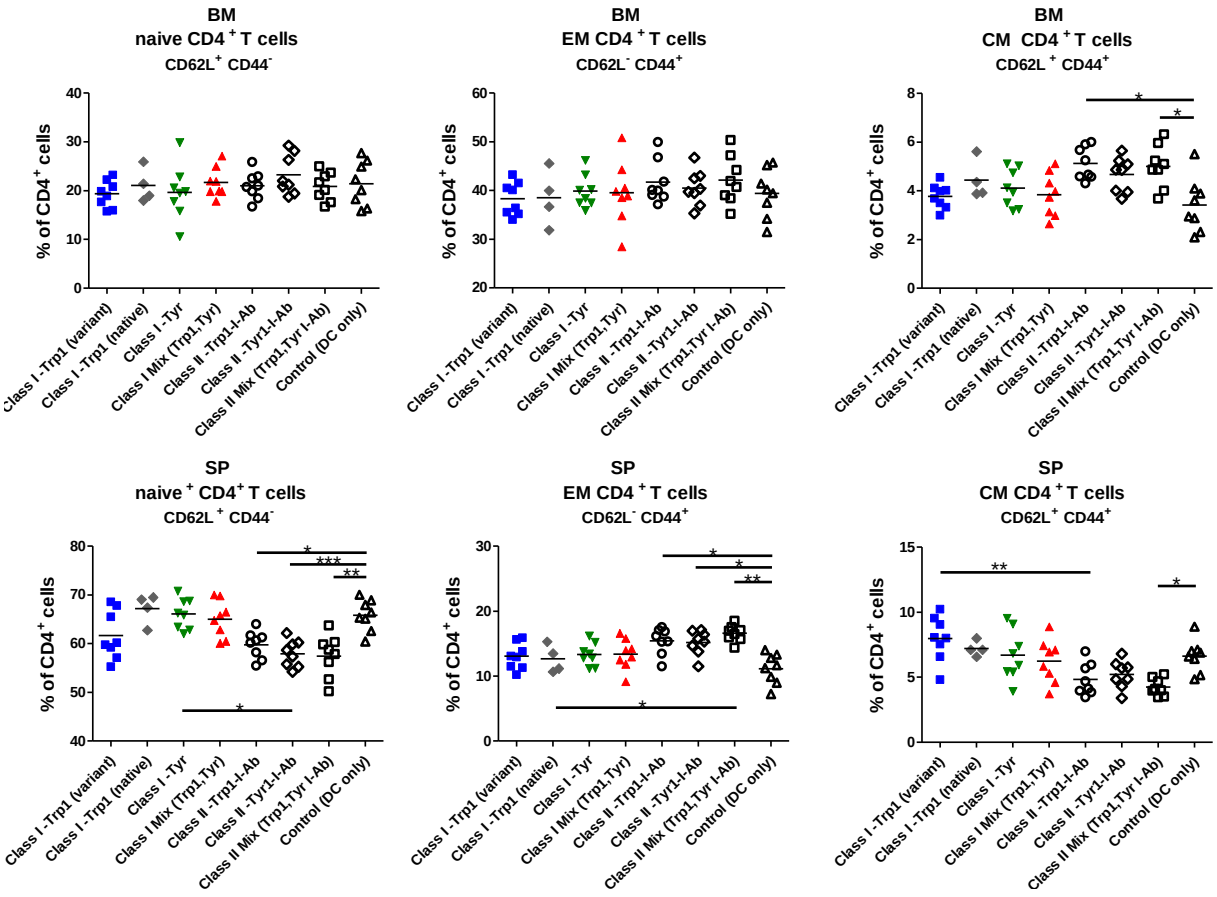

Appendix 4:

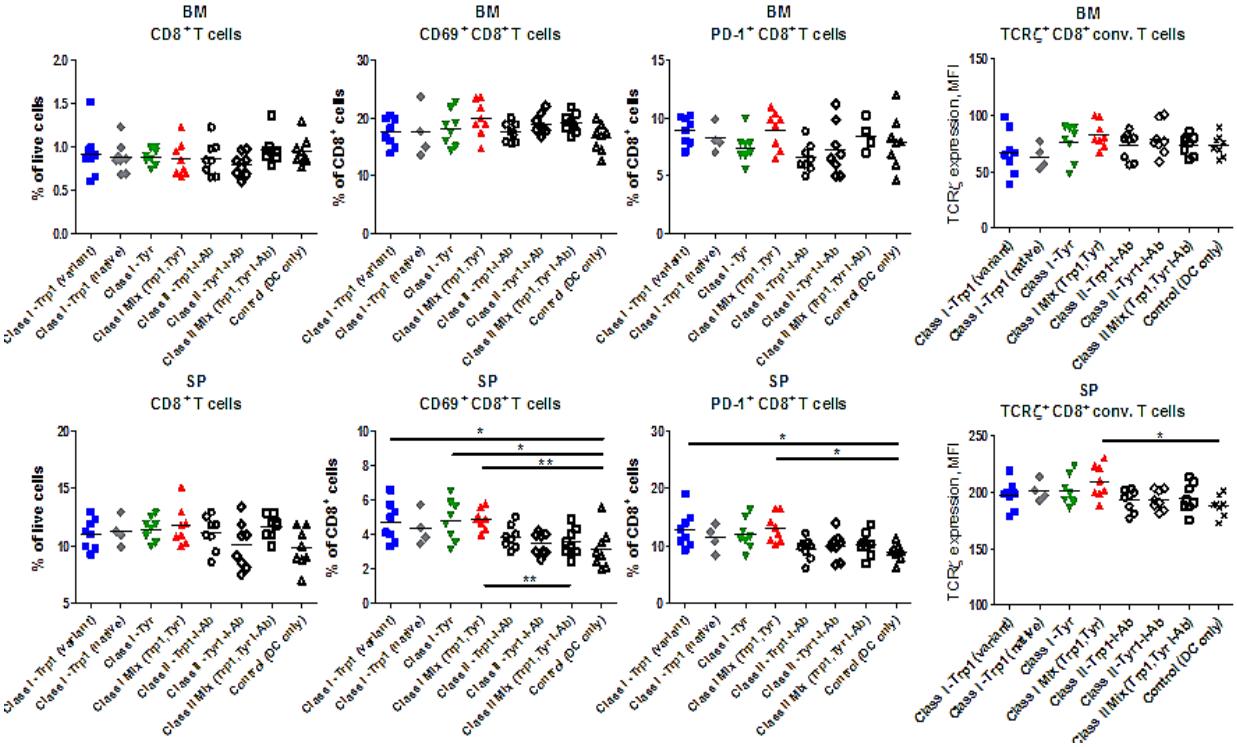

Appendix 5:

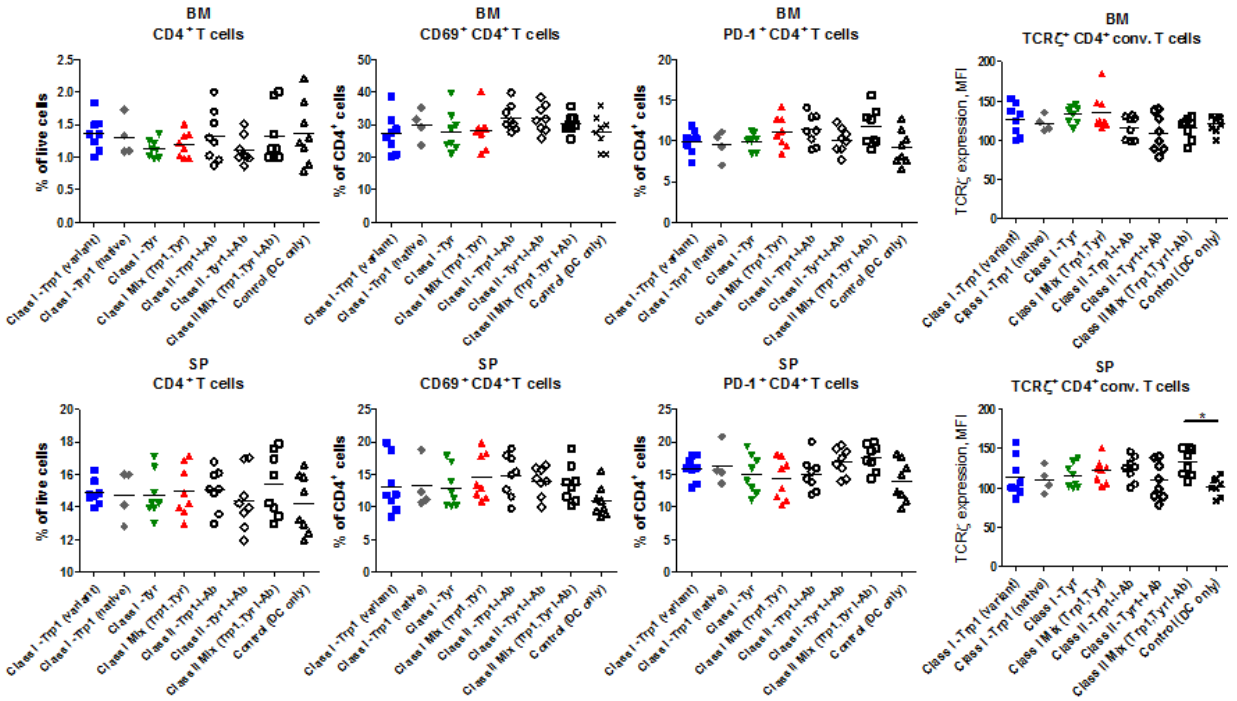

Appendix 6:

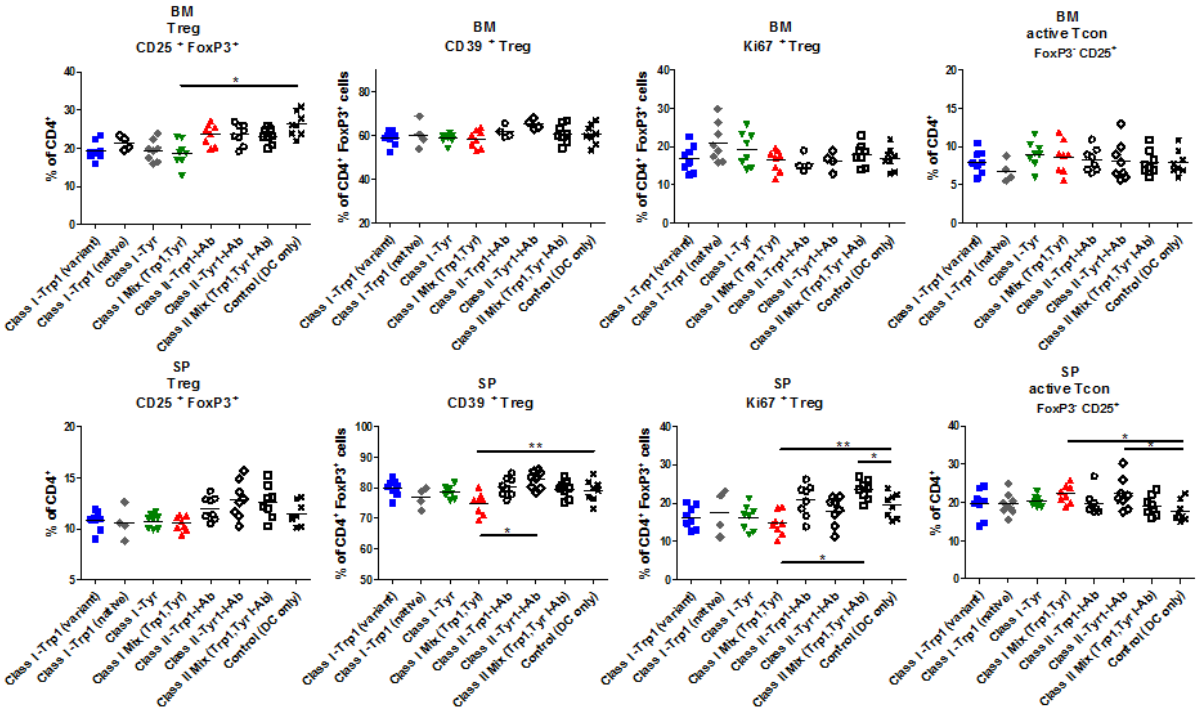
BM
Treg
CD25+FoxP3+
% of CD4+
BM
CD39+Treg
% of CD4+ FoxP3+ cells
BM
Ki67+Treg
% of CD4+ FoxP3+ cells
BM
active Tcon
FoxP3-CD25+
% of CD4+
SP
Treg
CD25+FoxP3+
% of CD4+
SP
CD39+Treg
% of CD4+ FoxP3+ cells
SP
Ki67+Treg
% of CD4+ FoxP3+ cells
SP
active Tcon
FoxP3-CD25+
% of CD4+
Class I-Trp1 (variant)
Class I-Trp1 (native)
Class I-Tyr
Class I Mix (Trp1,Tyr)
Class II-Trp1-I-Ab
Class II-Tyr1-I-Ab
Class II Mix (Trp1,Tyr I-Ab)
Control (DC only)

Appendix 7:

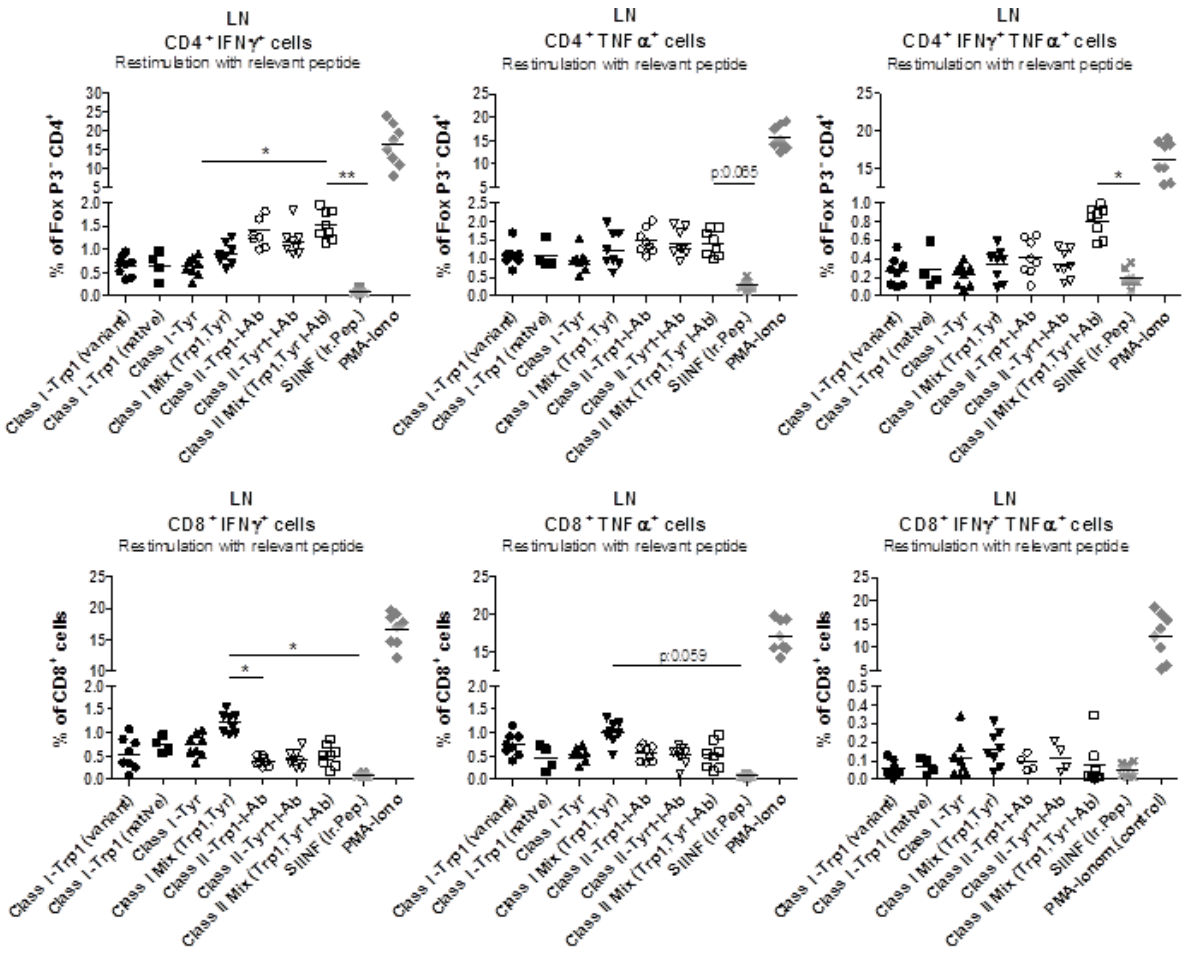
LN
CD4+IFNγ+ cells
Restimulation with relevant peptide
% of Fox P3- CD4+
*
**
Class I-Trp1 (variant)
Class I-Trp1 (native)
Class I-Tyr
Class I Mix (Trp1,Tyr)
Class II-Trp1-I-Ab
Class II-Tyr1-I-Ab
Class II Mix (Trp1,Tyr I-Ab)
SIINF (Ir.Pep.)
PMA-Iono
LN
CD4+TNFα+ cells
Restimulation with relevant peptide
% of Fox P3- CD4+
p:0.065
LN
CD4+IFNγ+TNFα+ cells
Restimulation with relevant peptide
% of Fox P3- CD4+
*
LN
CD8+IFNγ+ cells
Restimulation with relevant peptide
% of CD8+ cells
*
*
LN
CD8+TNFα+ cells
Restimulation with relevant peptide
% of CD8+ cells
p:0.059
LN
CD8+IFNγ+TNFα+ cells
Restimulation with relevant peptide
% of CD8+ cells
PMA-Ionom.(control)

Appendix 8:

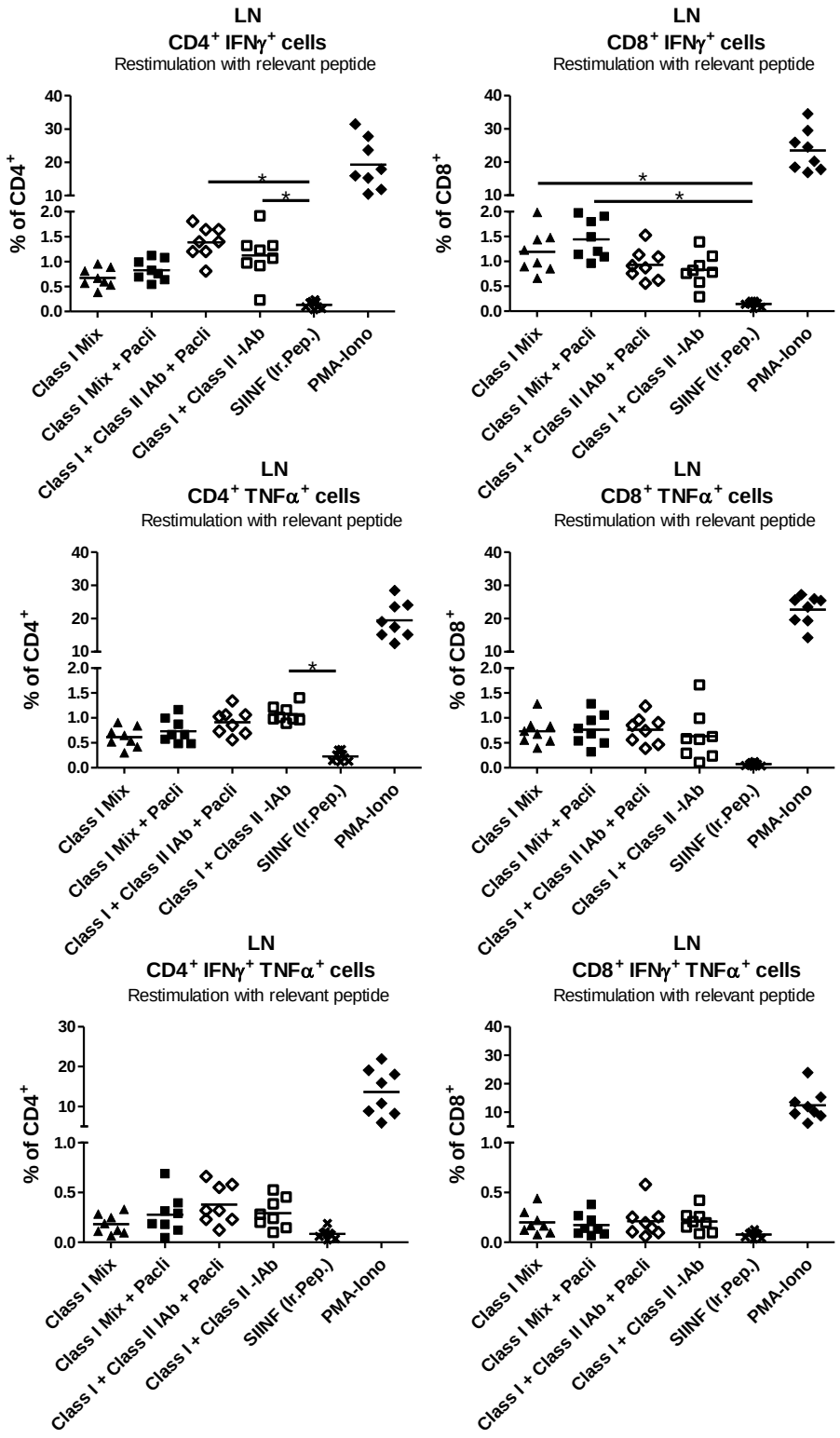
LN
CD4+ IFNγ+ cells
Restimulation with relevant peptide
% of CD4+
LN
CD8+ IFNγ+ cells
Restimulation with relevant peptide
% of CD8+
LN
CD4+ TNFα+ cells
Restimulation with relevant peptide
% of CD4+
LN
CD8+ TNFα+ cells
Restimulation with relevant peptide
% of CD8+
LN
CD4+ IFNγ+ TNFα+ cells
Restimulation with relevant peptide
% of CD4+
LN
CD8+ IFNγ+ TNFα+ cells
Restimulation with relevant peptide
% of CD8+
Class I Mix
Class I Mix + Pacli
Class I + Class II IAb + Pacli
Class I + Class II -IAb
SIINF (Ir.Pep.)
PMA-Iono

Appendix 9:

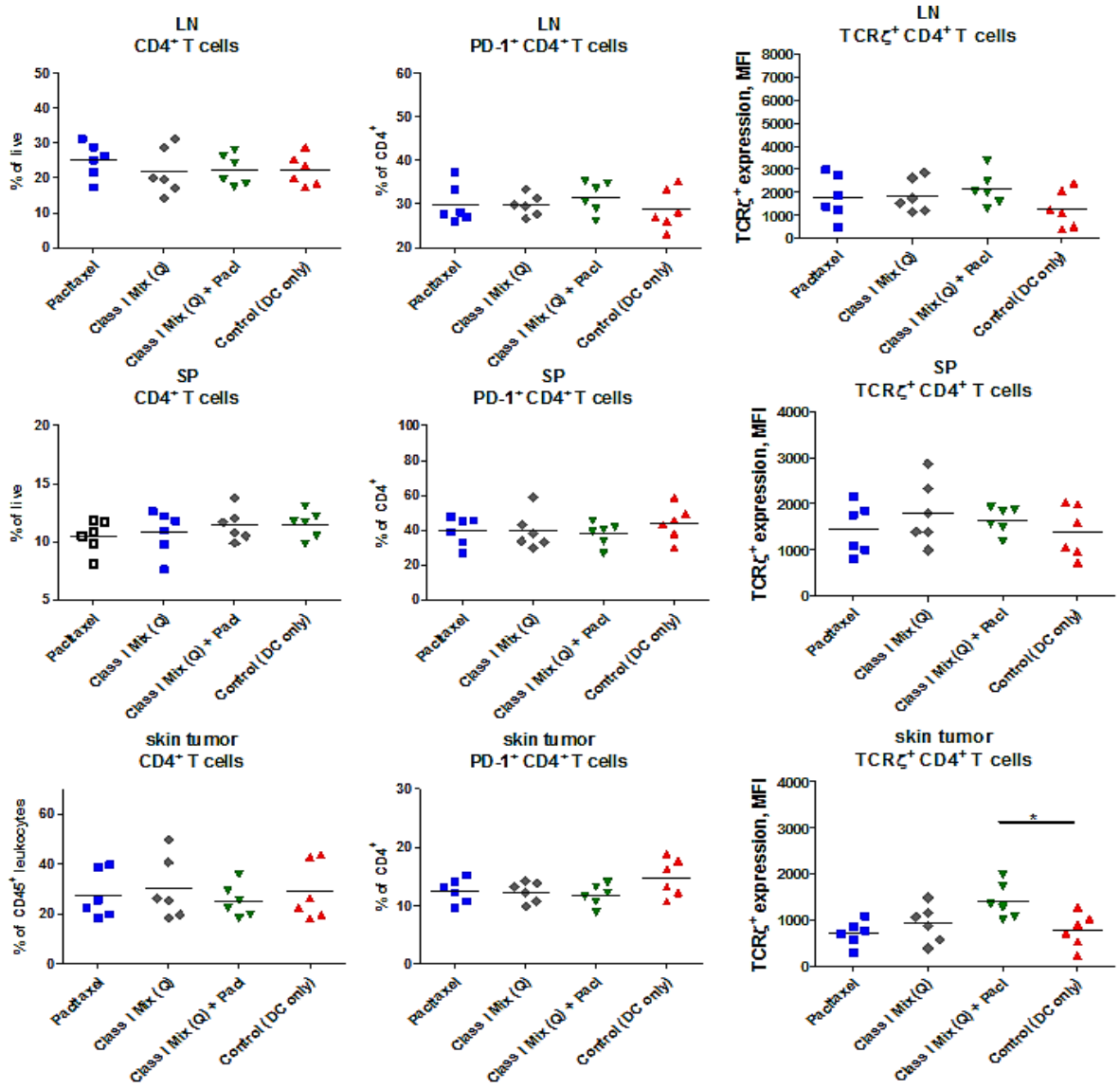
LN
CD4+ T cells
% of live
LN
PD-1+ CD4+ T cells
% of CD4+
LN
TCRζ+ CD4+ T cells
TCRζ+ expression, MFI
SP
CD4+ T cells
% of live
SP
PD-1+ CD4+ T cells
% of CD4+
SP
TCRζ+ CD4+ T cells
TCRζ+ expression, MFI
skin tumor
CD4+ T cells
% of CD45+ leukocytes
skin tumor
PD-1+ CD4+ T cells
% of CD4+
skin tumor
TCRζ+ CD4+ T cells
TCRζ+ expression, MFI
*
Paclitaxel
Class I Mix (Q)
Class I Mix (Q) + Pacl
Control (DC only)

11 Acknowledgement

While my name may be alone on the front cover of this PhD thesis, I am by no means its only contributor. Rather, there are a number of people behind this piece of work who deserve to be both acknowledged and thanked here: kind participants; committed supervisors; generous research advisory group members, colleagues and collaborators; beloved, supportive, and inspiring friends and family.

I would like to thank my primary supervisor Prof. Dr. Viktor Umansky for giving me the opportunity to perform my thesis in his group and supporting me throughout my PhD studies. Moreover, many thanks to Prof. Dr. Jochen Utikal and Dr. Christoffer Gebhardt for their clinical input.

Besides my primary supervisor, I would like to thank the rest of my thesis advisory committee PD Dr. Adelheid Cerwenka, Dr. Niels Halama and Prof Lea Eisenbach. I am grateful for their valuable input and critical advice. Moreover, I also want to acknowledge Dr. Markus Feuerer and Prof. Dr. Ana Martin-Villalba for enrolling as examiners in my disputation.

My sincere thanks also goes to our collaborators, Prof Lea Eisenbach and her group members Esther Tzehoval and Adi Sharbi-Yunger of the Weizmann institute of Science, Rehovot, Israel, for providing me the opportunity to join their team for my research stay. This piece of research looks very different because of their precious support, expert knowledge and constructive scientific discussions.

A very special gratitude goes out to all the members of the Offringa group at the DKFZ and Daniel Baumann for our collaboration on the BRAF-mouse studies. I appreciate all of your help and support!

I would like to thank Christos Evangelou and Daniel Thomas for their great help with my project during their Master/Bachelor studies.

Thanks to all my lab colleagues of the Clinical Cooperation Unit Dermato-Oncology for the great atmosphere, their helpful advices, support and their friendship.

Finally I would like to thank my family and friends. They all have been so supportive and have given me unconditional encouragement throughout; I would not have been able to complete the PhD without them. Thanks a lot and big hugs ☺.